



HAL
open science

Post-transcriptional control of the timeless mRNA in the *Drosophila* circadian clock

Thierry Cottineau

► **To cite this version:**

Thierry Cottineau. Post-transcriptional control of the timeless mRNA in the *Drosophila* circadian clock. Neurobiology. Université Paris-Saclay, 2024. English. NNT : 2024UPASL037 . tel-04646699

HAL Id: tel-04646699

<https://theses.hal.science/tel-04646699>

Submitted on 12 Jul 2024

HAL is a multi-disciplinary open access archive for the deposit and dissemination of scientific research documents, whether they are published or not. The documents may come from teaching and research institutions in France or abroad, or from public or private research centers.

L'archive ouverte pluridisciplinaire **HAL**, est destinée au dépôt et à la diffusion de documents scientifiques de niveau recherche, publiés ou non, émanant des établissements d'enseignement et de recherche français ou étrangers, des laboratoires publics ou privés.

Post-transcriptional control of the *timeless* mRNA in the *Drosophila* circadian clock

Contrôle post-transcriptionnel de l'ARNm timeless dans l'horloge circadienne de la Drosophile

Thèse de doctorat de l'université Paris-Saclay

École doctorale n°577, structure et dynamique des systèmes vivants (SDSV)
Spécialité de doctorat : Neurosciences
Graduate School : Sciences de la vie et santé. Référent : Faculté des sciences d'Orsay

Thèse préparée dans l'unité de recherche **Institut des neurosciences Paris-Saclay (Université Paris-Saclay, CNRS)**, sous la direction de **Brigitte GRIMA**, chargée de recherche

Thèse soutenue à Paris-Saclay, le 02 Juillet 2024, par

Thierry COTTINEAU

Composition du Jury

Membres du Jury avec voix délibérative

Laurent THEODORE Professeur, NeuroPSI, Université Paris-Saclay	Président
Florence BESSE Directrice de recherche, IBV, Université Côte d'Azur	Rapporteur & Examinatrice
Ouria DKHISSI-BENYAHYA Chargée de recherche, HDR, SBRI, Université Lyon 1	Rapporteur & Examinatrice
Clément CHAPAT Chargé de recherche, CBI, Université Toulouse 3	Examineur

Titre : Contrôle post-transcriptionnel de l'ARNm *timeless* dans l'horloge circadienne de la Drosophile

Mots clés : rythmes circadiens, gènes d'horloge, CCR4-NOT, traduction, ARNm, queue poly(A)

Résumé : La vie sur Terre est régie par des cycles jour/nuit causés par la rotation de celle-ci autour de son axe. Des horloges circadiennes ont évolué dans la majorité des organismes vivants, permettant l'anticipation de ces cycles, apportant ainsi un avantage conséquent au travers de l'organisation temporelle de leurs processus biologiques. Les rythmes circadiens (du latin *circa* : environ, et *diem* : jour) sont contrôlés génétiquement par des horloges endogènes, que l'on retrouve à l'échelle cellulaire. Des boucles de rétrocontrôles ciblant la transcription, traduction ou régulations post-traductionnelles de produits de gènes d'horloges, qui sont alternativement activées ou réprimées en respectant des intervalles précis, génèrent des oscillations à une période proche de 24 heures. *Drosophila melanogaster* est un organisme modèle essentiel dans la compréhension du fonctionnement de l'horloge circadienne. En effet, la disponibilité de nombreux outils génétiques ont permis de mieux comprendre les mécanismes moléculaires régissant l'horloge. Il a ainsi été découvert que les protéines PERIOD (PER) et TIMELESS (TIM) exercent un rétrocontrôle sur leur propre expression en réprimant l'activité des deux facteurs de transcription CLOCK (CLK) et CYCLE (CYC), qui contrôlent leur niveau d'expression ainsi que celui d'autres gènes régulés par l'horloge. Les contrôles transcriptionnels et post-traductionnels impliqués dans l'horloge ont été largement étudiés ces dernières 40 années. En revanche, les contrôles post-transcriptionnels et traductionnels sont moins bien compris, bien que ces régulations soient des éléments importants afin de générer des oscillations. Des travaux précédemment publiés par l'équipe ont mis en évidence l'existence d'un contrôle post-transcriptionnel de l'ARNm *timeless* par sa déadénylation par la déadénylase du complexe CCR4-NOT, POP2, où,

la déplétion de cette déadénylase altère le comportement circadien des mouches en modifiant les niveaux d'ARNm *tim* et de protéines TIM. Cette régulation intervient de manière circadienne, dépendante de PER, et spécifique pour *tim*, puisque l'ARNm *per* n'est pas impacté par POP2. L'objectif de mon travail était de mieux comprendre le contrôle de POP2 sur *tim*. En utilisant à la fois des techniques d'analyses comportementales et de biologie moléculaires, comme le TRAP (Purification Affine de Ribosomes en cours de Traduction), et le RNA-seq, nous avons découvert de nouvelles formes de contrôle de l'horloge circadienne. Tout d'abord, nos résultats montrent un contrôle traductionnel oscillant des ARNm *per* et *tim*, en phase avec l'oscillation de leur niveau protéique, suggérant une contribution nouvelle à l'oscillation des protéines d'horloges. Ensuite, nos résultats indiquent que POP2 contrôle la déadénylation de *tim* principalement en fonction de l'abondance de ce dernier, avec un effet réduit lorsque les niveaux d'ARNm *tim* sont élevés, comme c'est le cas en absence de PER. Cela s'applique également à l'échelle du transcriptome, où les transcrits régulés par POP2 le sont en fonction de leur abondance aussi. Puisque le complexe CCR4-NOT est connu pour réguler à la fois la stabilité des ARNm et leur traduction, nous avons cherché un rôle potentiel de POP2 sur la traduction dans l'horloge. Nous avons trouvé que POP2 régule la traduction de l'ARNm *tim* ainsi que celle de *vrille*, un répresseur transcriptionnel qui contrôle la transcription du gène *Clock*. Nos analyses transcriptomiques suggèrent que la déadénylase POP2 contribue fortement au contrôle de l'oscillation de nombreux gènes régulés de manière circadienne.

Title : Post-transcriptional control of the *timeless* mRNA in the *Drosophila* circadian clock

Keywords : circadian rhythms, clock genes, CCR4-NOT, translation, mRNA, poly(A) tail

Abstract : Life is submitted to day-night cycles caused by the rotation of the Earth around its axis. Circadian clocks evolved in most living organisms to allow for the anticipation of these cycles, hence providing a considerable advantage through the temporal organization of their biological processes. The circadian (from the latin circa: about, and diem: day) rhythms are genetically controlled by endogenous clocks, that can be found down to the cellular level. Feedback loops that include transcription, translation, or post-translational regulations of clock gene products that are alternatively activated/repressed with precise delays, generate oscillations with a period close to 24 hours. *Drosophila melanogaster* is an essential model organism in the understanding of the functioning of the circadian clock. Indeed, the many genetic tools available allowed to better understand the molecular mechanisms governing the clock. This led to the discovery that the protein PERIOD (PER) and TIMELESS (TIM) feedback on their own expressions through the repression of the activity of the two transcription factors CLOCK (CLK) and CYCLE (CYC), that control their levels of expression as well as other clock regulated genes. The transcriptional and post-translational controls involved in the clock have been extensively studied in the past 40 years. However, less is known of the post-transcriptional and translational controls of the clock, although these regulations are of importance for generating the oscillations. Previous work from the laboratory reported evidence of a post-transcriptional control of *tim* mRNA through its deadenylation by the deadenylase POP2 of the CCR4-NOT complex, where depletion of this deadenylase altered the circadian behavior of the flies as well as the cycling of *tim* mRNA and TIM protein levels.

This regulation was found to be circadian, PER-dependent, and specific for *tim*, as *per* mRNA is not impacted by POP2. The aim of my work was to further understand the control of POP2 on *tim*. Using combined behavioral assays and molecular biology techniques, such as TRAP (Translating Ribosome Affinity Purification) and RNA-seq, we discovered new layers of control of the circadian clock. First of all, our results show that the translational control of *tim* and *per* is circadianly-regulated and in phase with the cycling of protein levels, suggesting a new contribution to clock protein oscillations. Then, we revealed that POP2-controlled *tim* mRNA deadenylation largely depends on *tim* mRNA abundance, with small effects when *tim* mRNA levels are high as it is the case in the absence of PER. This also applies at the transcriptome scale, where we see that POP2-regulated transcripts are impacted in function of their abundance. Since the CCR4-NOT complex is known to regulate both mRNA stability and translation, we investigated the role of POP2 on translation in the clock. We found that POP2 regulates *tim* mRNA translation as well as the translation of *vriille*, a transcriptional repressor that controls the transcription of the Clock gene. Transcriptome-wide analysis suggest that the POP2 deadenylase has strong contribution to the control of the oscillations of many circadianly-regulated transcripts.

Acknowledgments/Remerciements

Avant tout, je tiens à remercier Brigitte, ma directrice de thèse, pour m'avoir tant appris pendant ces 4 ans et demi. Je te remercie pour ta dévotion au projet, ta ferveur, ton encadrement dont j'avais tellement besoin pour pouvoir m'épanouir professionnellement et surtout, ton incroyable patience face à mes incessantes idées saugrenues et à mon esprit obtus. Merci aussi François, pour m'avoir accueilli au sein de ton équipe, d'avoir fait preuve d'énormément de bienveillance et de pédagogie et d'avoir su être disponible pour me coacher et me préparer quand j'étais en difficulté. Je veux aussi remercier mon jury de thèse, qui a accepté d'évaluer mon travail malgré des délais très serrés, Laurent Théodore qui s'est rendu disponible, Clément Chapat qui nous a aidé avec son expertise à exploiter nos données avec succès, Florence Besse et Ouria Dkhissi-Benyahya pour avoir accepté d'être rapporteur de cette thèse.

Merci aux membres de mon comité de suivi de thèse, Mohammed Taouis et Marc Graille, qui, en plus de leurs apports scientifiques constructifs ont aussi été extrêmement fiables et à l'écoute afin de médier à tous problèmes potentiels pendant mon doctorat et qui m'ont donné des conseils précieux que j'ai essayés de suivre du mieux que je pouvais et qui s'avéraient payants à chaque fois.

Je remercie l'Agence Nationale de la Recherche pour avoir financé mon projet.

How sad would these years have been without the dream team ? I would like to thank all my colleagues from the FR team for all the laughs and rich discussions we had in the evenings when flipping our flies. I thank Abhishek for his brilliant inputs and his jokes. Georges for always being kind and supportive. Christine pour avoir créé une atmosphère détendue là où tu te trouvais. Élisabeth pour ton rire communicatif et ta maîtrise exceptionnelle de la dissection. Enzo pour m'avoir suivi et aidé autant que tu le pouvais. Theja for being so funny and making every day less boring. Ajay for your smile and for always being curious about my project. Ping for being so supportive and have such a strong team spirit. Elara pour m'avoir aidé à la relecture de ma synthèse et pour toutes les astuces que tu m'as fait découvrir. Jérémie pour tes questions qui m'ont beaucoup fait réfléchir et pour l'ambiance chaleureuse que tu créer autour de toi. Zéphyr pour avoir pris la relève des responsabilités que je n'avais plus le temps d'assumer et pour être aussi proche de moi. Letizia for supporting me with the best of your capacities and for your incredible team spirit and enthusiasm. Béatrice pour ton soutien, ta pédagogie et toutes les discussions passionnantes qu'on a eu. Chiara for being the person who probably knows me the best in this team, thank you for your attentive ear and genuine care.

Christian, je suis heureux d'écrire ces lignes car cela veut dire qu'on se reverra bientôt, à ma soutenance, je te remercie de m'avoir transmis une partie de ton savoir-faire, notamment de ton organisation et ton éthique de travail et aussi de ton savoir-être. J'ai adoré travailler avec toi et je suis très reconnaissant d'avoir pu passer ce temps avec toi avant ton départ à la retraite, après lequel tu m'as tant manqué.

Je te remercie, Naïma, d'avoir été aussi bienveillante et gentille avec moi, de m'avoir autant aidé et de m'avoir accueilli à bras ouverts à la plateforme, mon havre de paix, où j'ai passé de très bons moments avec vous.

Éric, je n'ai pas les mots pour exprimer toute ma gratitude à ton égard, je te remercie de m'avoir ouvert les portes de ta plateforme, de m'avoir tant appris, à tous les niveaux. Je suis fier d'avoir travaillé avec toi, tu représentes ce à quoi j'aspire pour ma vie professionnelle et je te remercie de toujours avoir fait tout ton possible pour mon projet, pour lequel tu as été essentiel.

Je remercie ma famille, pour avoir toujours cru en moi, pour m'avoir toujours soutenu, pour toujours être là quand j'en ai besoin, vous êtes ce que j'ai de plus précieux au monde et je vous chéris de tout mon être.

Finally, I thank you, Yijiao, for being more supportive than I could ever dream of, for listening to me when the times are hard, for making me laugh, for believing in me and supporting me as much as my family does, for your patience, your care, for knowing me the best, maybe even more than I know myself, for being everything I need, for being my best friend, my confidant, and my love.

Table of Contents

Acknowledgments/Remerciements.....	4
Abbreviations	8
Figures list	9
Introduction.....	12
I. Presentation of the circadian rhythms.....	12
II. The <i>Drosophila melanogaster</i> model.....	12
1. <i>Drosophila</i> circadian behavior	13
III. Central clock	14
1. Clock neurons network	15
IV. Molecular clock	16
1. Core feedback loop in LD condition.....	17
a. Overview.....	17
b. Light mediated degradation of TIM	18
2. Feedback loop in DD condition.....	20
3. Accessory feedback loop	21
4. The mammalian molecular clock	22
5. Should we expect post-transcriptional control of <i>per</i> and <i>tim</i> mRNAs ?	23
V. Co- and Post-transcriptional control of mRNAs.....	23
1. Generalities about messenger RNAs.....	24
a. Translation	25
b. Localization	27
c. Modifications.....	27
d. Deadenylation.....	27
e. Decay	28
2. The CCR4-NOT complex.....	29
3. Co- & post-transcriptional controls in the clock.....	31
a. Alternative splicing and seasonal adaptation	31
b. Translation around the clock	32
c. Poly(A) tail length rhythms	33
d. Tim mRNA undergoes post-transcriptional control by the deadenylase POP2	34
VI. Questions to answer during my PhD	35
Results.....	36
I. Pop2 gene products cycling analysis	36
1. Exogenous POP2 oscillates in the heads and clock cells in <i>Drosophila</i>	36
2. Endogenous POP2 does not show any oscillations.....	37
a. Knock-In of an HA-tag in the endogenous Pop2 gene.....	37
b. POP2-HA levels do not cycle in the <i>Drosophila</i> heads and are not influenced by PER	37
c. POP2-HA levels do not cycle in the s-LNvs and are not influenced by PER	41
3. Discussion	43

II. Study of POP2 specificity for <i>tim</i>	44
1. Screening of RNA Binding Proteins related to POP2	45
a. identifying the POP2 interactome with mass spectrometry	45
b. POP2 interactors screening shows several RBPs impacting the flies' behavior	47
c. LIG regulates the clock via TIM protein but not <i>tim</i> mRNA	50
2. Analysis of <i>tim</i> mRNA modifications machinery components	52
a. Mettl3 mutant flies are short period in constant darkness	52
b. Mettl3 Δ 1.7 does not resume the effect of POP2 depletion on <i>tim</i> mRNA	52
3. Discussion	53
III. Exploring the role of POP2 on the translation of circadianly-regulated genes	56
1. Article	56
2. Unpublished data	89
a. PER does not bind <i>tim</i> mRNA	89
b. POP2 isoform-specificity for <i>tim</i>	91
c. POP2-downregulated genes also seem less regulated when highly abundant	92
d. Many differentially-regulated genes between CT3 and CT15 are not known cyclers	93
3. Discussion	94
Concluding remarks	95
Material and methods	96
I. Fly genetics and behavioral assay	96
1. Balancer chromosomes	96
2. UAS-GAL4 system	97
3. <i>Drosophila</i> circadian behavior assays	98
4. Pop2-HA K.I design and screening workflow	99
II. Immunofluorescence of POP2-HA	102
III. POP2-HA IP followed by mass spec	104
IV. Molecular biology techniques	105
1. Poly(A) Tail Length assay (PATassay)	105
2. Translating Ribosome Affinity Purification (TRAP)	106
3. TRAP followed by PATassay	106
V. dryR	107
Annexes	108
Synthèse en français	113
I. Introduction	113
1. Introduction générale à l'horloge circadienne	113
2. Résultats antérieurs à la thèse	116
3. Objectifs de ma thèse	117
II. Résultats	118
1. Action circadienne de POP2 sur <i>tim</i>	118
2. Spécificité de POP2 pour <i>tim</i>	119
3. Régulation de la traduction par POP2	120
a. Approches spécifiques d'un gène	120
b. Approche transcriptomique	125

Abbreviations

18S : 18S ribosomal RNA	K.D : Knock Down (RNAi)
BICW : Bayesian information criterion weight	K.I : Knock In (sequence insertion)
bp : base pair	K.O : Knock Out (Null allele)
cDNA : complementary DNA (reverse transcribed from RNA)	LD : Light-Dark
CDS : Coding sequence	LL : Light-Light (constant light)
CLK : clock protein	ILNvs : large ventral lateral neurons
COMD : Codon optimality-mediated decay	LNds : dorsal latera neurons
CT : Circadian time	LPNs : lateral posterior neurons
Ct : RT-qPCR cycle threshold	m6A : N6-methyladenosine
CT0 : Time of light-on in previous entrainment phase	Mass spec : Mass spectrometry
CTRL : Control	miRNA : micro-RNA
CYC : cycle protein	mRNA : Messenger RNA
DAM system : Drosophila Activity Monitoring System	MS : Mass spectrometry
DD : Dark-Dark (constant darkness)	n = : Number of individual or biological replicates tested
DN1as : dorsal anterior nerons1	NMD : Nonsense-mediated decay
DN1ps : dorsal posterior neurons 1	ORF : Open reading frame
DN2s : dorsal neurons 2	P-bodies : Processsing bodies
DN3s : dorsal neurons 3	P1/P2 : Parent 1/Parent 2
DNA : Deoxyribonucleic acid	PABP : Poly(A) binding protein
F1 : First generation of offsprings	PATassay : Poly(A) Tail length assay
FC : Fold change	PCR : Polymerase Chain Reaction
FDR : False discovery rate	PDF : Pigment-Dispersing Factor protein
FLAG : FLAG antigen tag	PDP1 : PAR-domain protein 1 protein
FRET : Förster resonance energy transfer	PER : period protein
Gene name ⁻ : Mutant allele	per : period gene/mRNA
Gene name ⁺ : Wild type allele	per ⁰ : aka per ⁰¹ , period gene null mutant
GFP : Green fluorescent protein	poly(A) tail : poly adenylic acid tail
gRNA : guide RNA	POP2 : Pop2 protein
HA : Hemagglutinin antigen tag	pre-mRNA : precursor mRNA
HB-eyelet : Hofbauer-Buchner eyelet	R ² : Correlation coefficient
IF : Immunofluoresnce staining	RBP : RNA binding protein
IP : Immunoprecipitation	RNA : Ribonucleic acid
	RNAi : RNA interference
	ROI : Region of interest
	RPL : Large ribosomal subunit protein
	RT-qPCR : Reverse Transcription

quantitative PCR	tRNA : Transfer RNA
SD : standard deviation	UAS : Upstream activating sequence
SEM : Standard error of the mean	uORF : upstream open reading frame
Seq : DNA/cDNA sequencing	UTR : Untranslated region
sLNvs : small ventral lateral neurons	VRI : vrille protein
Spe : Specific	WB : Western Blot
TIM : timeless protein	WT : Wild type
tim : timeless gene/mRNA	ZT : Zietgeber time
TRAP : Translating Ribosome Affinity Purification	ZT0 : Light-on time

Figures list

Figure 1 : Figures used to study the *Drosophila* locomotor behavior

Figure 2 : *Drosophila* clock neurons network

Figure 3 : Representation of *tim* and *per* gene products' oscillations in LD cycle

Figure 4 : Simplified representation of the molecular feedback loop in the *Drosophila* clock

Figure 5 : Light-mediated pathway of the degradation of TIM

Figure 6 : Scheme of the uORF coding for the TIM-L protein in *ls-tim* flies

Figure 7 : The two-loop molecular clock model

Figure 8 : Representation of the closed loop model

Table 1 : The standard genetic code in eukaryotes

Figure 9 : PAN2-PAN3 complex targets preferentially long poly(A) tailed transcripts

Table 2 : Main components of the CCR4-NOT complex in different species

Figure 10 : Codon Optimality Mediated Decay (COMD) mechanism of action

Figure 11 : Summary of the results from (Grima et al., 2019)

Figure 12 : Quantification of Western Blot analysis of exogenous POP2-HA protein

Table 3 : Summary of the cycle_p analysis of male endogenous *Pop2-HA* flies

Figure 13 : Western Blot analysis of endogenous *Pop2-HA*

Figure 14 : Western Blot of anti-HA IP fractions

Figure 15 : Representation of the sequencing results obtained for *Pop2-HA*

Figure 16 : Phos-tag analysis using anti-HA antibodies

Figure 17 : Western Blot analysis of endogenous *Pop2-HA* in *Drosophila* heads in *per*⁺ or *per*⁰ context

Figure 18 : IF picture of LNvs clock neurons marked with anti-PDF, HA, PDP1 antibodies of *Pop2-HA* flies

Figure 19 : Quantification of IF experiment following POP2-HA levels in endogenous *Pop2-HA* flies

Figure 20 : Comparison of POP2-HA signal in the sLNvs of endogenous *Pop2-HA* flies

Figure 21 : RT-qPCR quantification of *Pop2-HA* and *GFP* mRNA levels

Figure 22 : Interaction network of proteins being enriched proteins in POP2-HA IP

Table 4 : Genes significantly found enriched with POP2-HA in IP

Table 5 : Summary of the cycle_p analysis of male flies depleted or mutated for endogenous POP2 interactors

Figure 23 : Western Blot analysis of TIM levels of proportion of dephosphorylated TIM in *Drosophila* heads in presence or absence of *UAS-lig-RNAi*

Figure 24 : IF quantification of TIM levels in the sLNvs during 4CTs, in *UAS-lig-RNAi* and control flies

Figure 25 : RT-qPCR quantification of *per* & *tim* mRNAs at 8 circadian times in presence or absence of *lig-RNAi*

Table 6 : Behavior analysis of flies mutated for mRNA modification machinery components

Figure 26 : RT-qPCR quantification of *per* & *tim* mRNA at 8 circadian times in presence or absence of *Mettl3 Delta1.7* null mutant

Article figure 1 : *timeless* and *period* mRNAs show cycling translatability

Article figure 2 : POP2 specifically controls *tim* total mRNA levels in a PER dependent manner and its translation in a PER independent manner via its poly(A) tail

Article figure 3 : POP2 controls *tim* mRNA stability according to its levels

Article figure 4 : POP2 controls many circadianly regulated genes

Article figure 5 : *vri* is also a target of POP2

Article figure 6 : *vri* is regulated by POP2 similarly than *tim*

Article figure 7 : POP2's effect strength is tuned by the expression level of its targets in accordance with their codon usage

Article supplementary figure 1 : Cycling translatability is specific of *tim* and *per*

Article supplementary figure 2 : POP2 regulates *tim* mRNA stability independently of PER

Article supplementary figure 3 : Total and ribosome-bound fractions present similar impact of circadian times and POP2

Article supplementary figure 4 : POP2 regulates *vri* mRNA stability independently of PER

Figure 27 : RT-qPCR quantification of the enrichment of mRNAs bound to PER compared to control background noise

Figure 28 : Representation of the different *tim* isoforms from (Martin Anduaga et al., 2019)

Figure 29 : RT-qPCR quantification of *tim* isoforms at 2 circadian times in *Pop2* K.D context and in presence or absence of PER

Figure 30 : Scatter plot showing the correlation between POP2-targeted genes abundance and *Pop2* K.D effect for downregulated genes

Table 7 : Summary of the RNA-seq results in the ribosome-bound RNA fractions of genes significantly modified between CT15 vs CT3 and between *Pop2* K.D vs *Pop2*+ at CT3 or CT15, all in *per*+ context

Material and methods table 1 : Balancer chromosomes used in my experiments

Material and methods figure 1 : Scheme of the UAS-GAL4 system in *Drosophila*

Material and methods figure 2 : Presentation of the *Drosophila* Activity Monitoring System (DAM System, from TriKinetics) setup.

Material and methods table 2 : Incubator parameters.

Material and methods figure 3 : *Pop2-HA* K.I design.

Material and methods figure 4 : Specific PCR design.

Material and methods figure 5 : Flanking PCR design.

Material and methods figure 6 : Family tree leading to the isolation of the K.I *Pop2-HA* flies.

Material and methods figure 7 : IF picture of LNvs clock neurons marked with anti-PDF (LNvs marker), HA (POP2), PDP1 (clock cells marker)

Material and methods figure 8 : IF image from confocal microscope showing HA signal

Material and methods figure 9 : Workflow of the quantification process using Weka segmentation algorithm

Material and methods figure 10 : Comparison between Fiji thresholding function (Thresholding) and Weka segmentation algorithm (TWS)

Material and methods figure 11 : ROC curves showing the false positive proportion of cycling protein identification

Material and methods figure 12 : PATassay protocol from Affymetrix kit.

Material and methods figure 13 : TRAP protocol

Material and methods figure 14 : TRAP fractions used together with PATassay protocol

Material and methods figure 15 : dryR models presentations

Figure S1 : Quantification of Western Blot analysis of GFP protein

Figure S2 : *Pop2-HA* isoforms PCR investigations

Figure S3 : IF image from showing HA and PDF signal of exogenous *UAS-Pop2-HA* flies

Figure S4 : IF image from confocal microscope showing HA signal only in magenta from endogenous *Pop2-HA* flies

Figure S5 : RT-qPCR quantification of *pre-per*; *pre-tim*; *lig* mRNA at 8 circadian times in presence or absence of *lig-RNAi*

Table S1 : Mutant lines screened for effect on circadian rhythms

Figure S6 : RT-qPCR quantification of *pre-per* & *pre-tim* mRNA at 8 circadian times in presence or absence of *Mettl3Δ1.7* null mutant

Figure S7 : Log2 ribosome-bound mRNA levels relative to respective total mRNA levels

Introduction

I. Presentation of the circadian rhythms

Circadian rhythms are biological processes oscillating over a ~24h period. Found in most organisms, circadian rhythms reflect the adaptation of life to the day-night cycles on Earth, since temporal regulation of behavior, physiology, cell biology, metabolism, and many other processes, is often advantageous (Edery, 2000).

An example is the preferential eclosion of fruit flies from their pupae in the morning, when humidity levels tend to be at the highest, thus limiting desiccation of newly emerged flies (Pittendrigh, 1954).

These circadian rhythms are controlled by internal oscillators, integrating environmental inputs, also called Zeitgebers (German for time givers), such as light and temperature. These oscillators control virtually all biological processes through their outputs. These internal oscillators are referred to as the circadian clocks, are studied down to the molecular level, and often, but not always (Nakajima *et al.*, 2005; O'Neill and Reddy, 2011), consist in autoregulatory transcriptional feedback loops of clock genes, that will be presented in detail later in this introduction.

The existence of circadian clocks allows organisms to anticipate changes in their environment, such as light and temperature.

Currently, circadian rhythms are recognized as such if following 3 criteria (Edery, 2000) :

1. The capacity to free-run : maintenance of rhythms with a ~24h period in the absence of environmental inputs.
2. The ability to be entrained : re-alignment with a change of environmental inputs.
3. The presence of temperature compensation mechanisms : maintenance of a ~24h period over a wide range of temperatures.

These circadian clocks are present as "central" pacemakers in the nervous system or as "peripheral" pacemakers in other tissues in animals (Mohawk, Green and Takahashi, 2012).

II. The *Drosophila melanogaster* model

We owe the use of *Drosophila melanogaster* as an invertebrate model organism in genetic research to Thomas Hunt Morgan, with his discovery of the *white* mutation on the X chromosome, causing white eyes on mutant flies in a sex-limited manner, thus providing the first argument confirming the chromosome theory of inheritance (Morgan, 1910).

Since then, fruit flies have been extensively used in genetic experiments, linking genes to biological functions, which holds strong relevance in research as ~77% of genes related diseases in human show matches with *Drosophila* genes (Reiter *et al.*, 2001). What's more, the fly genome is of relatively low redundancy (Roote and Prokop, 2013),

unlike in mammals, *Drosophila* tend to have one or few genes encoding for members of one protein class, easing the study of gene functions in loss-of-function contexts.

On a practical point of view too, the fruit fly is an attractive model organism :

- Fly pushing is easy and cheap, enabling us to generate and maintain lots of stocks to carry out large scale screenings.
- One generation only requires 10 days to be obtained if kept at 25°C, granting us the possibility to perform long series of crosses in a relatively short time to build complex genotypes.
- Resources are readily available online on the FlyBase database (Larkin *et al.*, 2021), providing us with thorough genes and genomes information.
- Various genetic tools developed and shared in the *Drosophila* community makes experimenting in the *Drosophila* limited essentially by the experimenter's imagination.

Among the genetic tools used in *Drosophila*, Balancer chromosomes and the UAS-GAL4 system were used extensively in my project and are presented in the material and method section.

1. *Drosophila* circadian behavior

The *Drosophila* model doesn't only represent a valuable tool for molecular biology experiments, as it also grants us the possibility to observe the effect of mutations up to the behavior of the fly. Indeed, the *Drosophila* displays several well characterized circadian behaviors, the most well-known being eclosion and locomotor activity.

Nowadays, locomotor activity assay is the most common way to study the fly's circadian clock and is presented in more details in the material and methods section.

When analyzing the locomotor activity pattern of the fly, we see with male flies 2 peaks of activity in LD conditions (12h-12h light-dark cycles), one at dawn (ZT0), one at dusk (ZT12), that starts before the light-on and light-off time due to their anticipations, we can also observe a resting phase in the middle of the day called siesta (Fig. 1A). This bimodal activity pattern is changed in DD (constant darkness conditions), the morning peak of activity shrinks, leaving only the evening peak of activity, cycling with a ~23,8h period. To note, ZT refers to zeitgeber times, in presence of environmental cues entraining the clock, where ZT0 corresponds to light-on and ZT12 light-off. While in absence of environmental cues (DD), we speak of CT, for circadian times, with CT0 corresponding to the time when the light was switched on during the entrainment phase and CT12 the previous light-off time. In constant darkness (DD) we speak of subjective day and night.

This describes a rhythmic fly, with a properly running circadian clock, but this clock can be accelerated (short period), slew down (long period), or not functional (arrhythmic) (Fig. 1B).

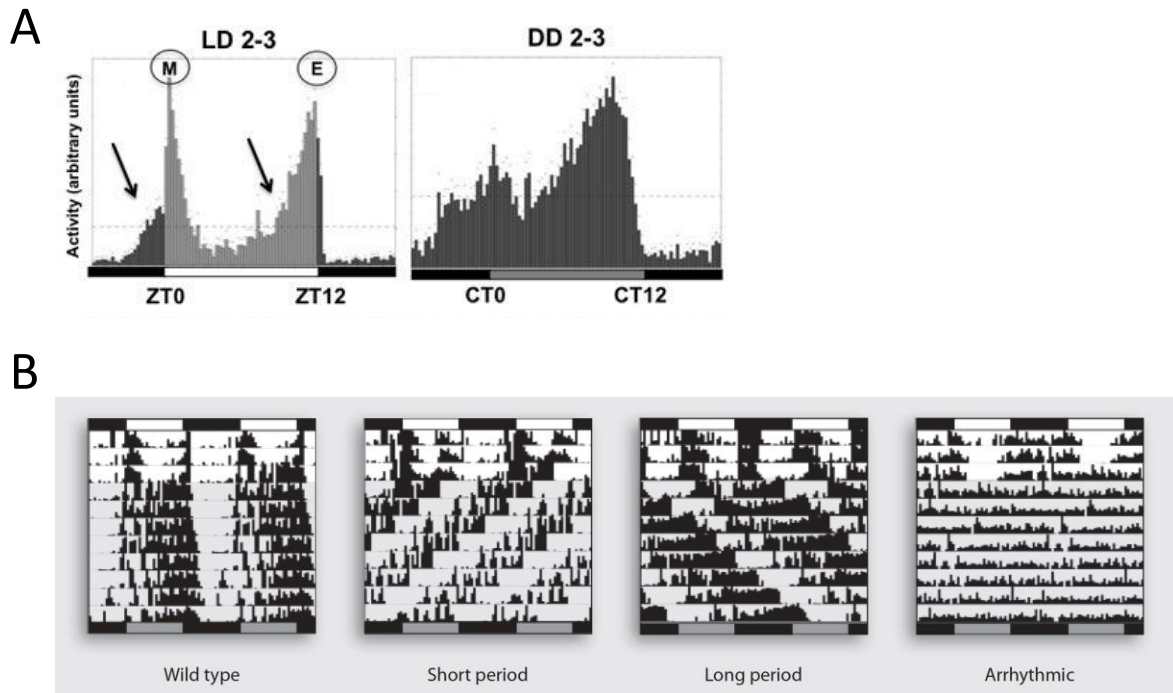


Figure 1 : Figures used to study the *Drosophila* locomotor behavior. (A) Eduction plot showing the average activity of a group of male flies, in 30 minutes intervals, over several days, in LD and DD conditions. This is used to observe the activity peaks, particularly the anticipation of light-on and -off transitions, figure from (Chiu et al., 2010). **(B)** Double plotted actograms showing the averaged activity pattern of flies per 30 minutes intervals, each day is repeated (double plotting), allowing to observe with ease shifts in the period length of the flies' behavior, average activity is represented as histograms, white background corresponds to LD cycles and grey background to DD cycles and the colored bars above and below the actograms represent the time of light transitions in LD, figure from (Muraro and Fernanda Ceriani, 2014).

However, it should be noted, that arrhythmic flies still display peaks of activity during light-on and light-off transitions, this phenomenon is called "startle response", or "light arousal" and can easily be differentiated from proper circadian controlled locomotor activity by the absence of anticipation of the light-on/off transitions. (Wheeler *et al.*, 1993)

III. Central clock

In the fruit fly, light is not only sensed through the compound eyes, Hofbauer-Buchner (HB) eyelet and ocelli, but also directly within the clock cells thanks to a blue-light sensitive photoreceptor named *cryptochrome* (*cry*), which will greatly affect the molecular clock, granting the flies the capacity to integrate light information in virtually all tissues (as light reaches through their cuticles). Still, some peripheral clocks and some circadian rhythms (sleep-wake cycle for example) rely on a central clock based in the nervous system (Handler and Konopka, 1979). Indeed, in 1979, Handler and Konopka grafted brains from short period *per^s* donor flies into the abdomen of arrhythmic *per⁰* (null allele) host flies, the following locomotor activity assay carried out in constant darkness (free-running condition) on these host flies revealed that 4/55 of the surviving *per⁰* host flies showed short period, seemingly coming from a humoral factor released by the grafted *per^s* brain in their abdomen, while only arrhythmic

activities were monitored for the 48 *per*⁰ host flies grafted with *per*⁰ brains. While these results revealed not fully convincing, mainly due to the low proportion of flies showing a behavior in accordance to their transplanted brains, further work done with mosaic flies did support the hypothesis of a predominant role of the nervous system in the timely control of the locomotor activity in *Drosophila* (Konopka, Wells and Lee, 1983; Ewer *et al.*, 1992).

This central clock includes ~150 neurons (for both hemispheres) that co-express the molecular clock components, which will be presented later in this introduction.

These clock neurons form a network with one another as well as non-clock neurons (Fig. 2).

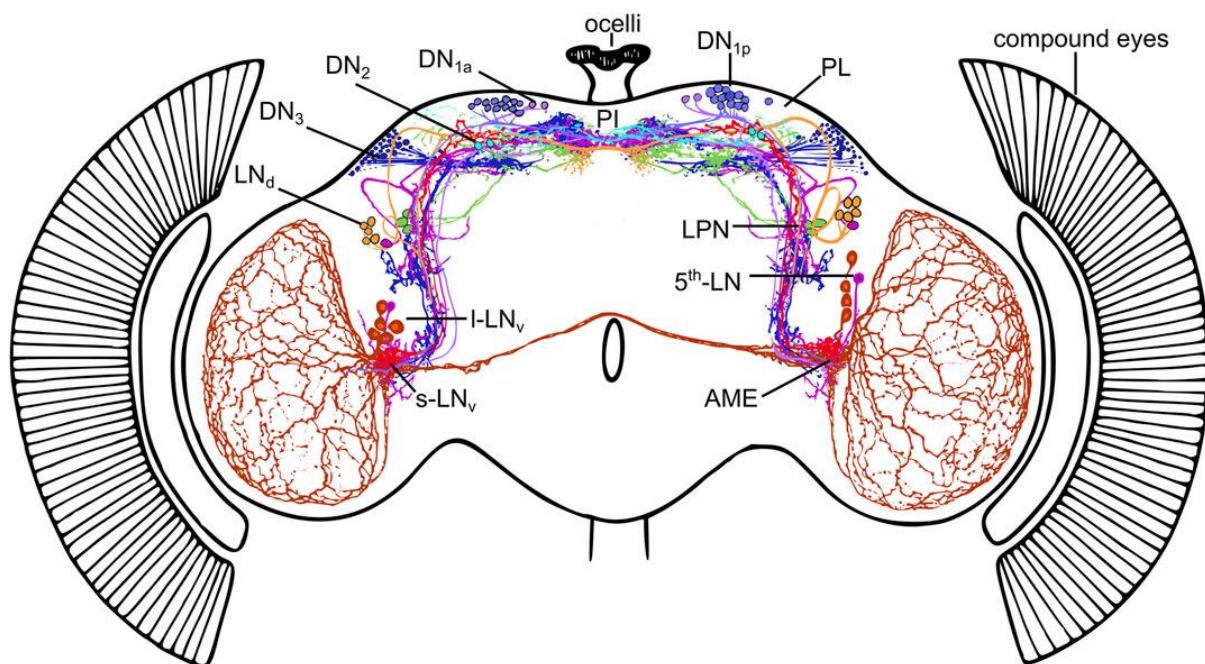


Figure 2 : *Drosophila* clock neurons network. The different anatomical groups of clock neurons are represented in both hemispheres with their projections. AME : Accessory medulla; PL : Pars Lateralis; PI : Pars intercerebralis. Compound eyes and ocelli are part of the visual system, the HB-eyelet is not represented here. Figure from (Reinhard *et al.*, 2022).

1. Clock neurons network

The ~150 neurons that constitutes the core clock in *Drosophila* are classified into groups based on their anatomy, we can find in each hemisphere :

- 5 small ventral lateral neurons (sLNvs)
- 4 large ventral lateral neurons (lLNvs)
- 6 dorsal lateral neurons (LNds)
- 3 lateral posterior neurons (LPNs)
- 15 dorsal posterior neurons 1 (DN1ps)
- 2 dorsal anterior neurons 1 (DN1as)
- 2 dorsal neurons 2 (DN2s)
- 35~40 dorsal neurons 3 (DN3s)

Among the clock neurons, 8 per hemisphere express the neuropeptide *pigment dispersing factor* (PDF), namely 4 sLNvs and 4 ILNvs, the remaining PDF- sLNv is thus often referred to as the 5th sLNv. While CRY is expressed in the 9 LNvs, 3 LNds, and some DN1s and DN3s neurons.

Since, the *Drosophila* and other species display bimodal locomotor activity in LD cycles, scientists hypothesized that the sleep-wake rhythm is controlled by 2 circadian oscillators with different phases (Pittendrigh and Daan, 1974).

In 2004, it was suggested that different subsets of clock neurons drive the different peaks of locomotor activity in *Drosophila* (Grima *et al.*, 2004; Stoleru *et al.*, 2004) in LD cycles, where arrhythmic *per*⁰ flies had a rescue of PER in the PDF+ cells (LNvs) that led to the recovery of morning anticipation of the light-on transition, whereas the recovery of PER in some of the LNds + all sLNvs and few ILNvs was sufficient to restore the evening anticipation of the light-off transition.

These results led to the proposition of a dual oscillator model where the LNvs are the “morning cells” and the LNds + 5th sLNvs are the “evening cells”, in which both groups drive one of the peaks of activity.

Plus, it was similarly shown that the maintenance of rhythmic locomotor activity in DD conditions could be imputed to the morning oscillator of the LNvs, where PDF plays a key role in synchronizing these different oscillators (Lin, Stormo and Taghert, 2004).

Later, this dual oscillator model has been refined (Guo *et al.*, 2014), experiments showed that some E cells output signaling was necessary for the morning and evening peaks of activity in both LD and DD conditions. Plus, M cells firing was showed to impact the phase of the behavioral activity of *Drosophila* likely by regulating the molecular clock of the E cells. These findings offer a view of the dual oscillator model to a lesser degree dualistic than its original formulation.

To note, single-cell transcriptome (Ma and Rosbash, 2020a), connectome datasets (Reinhard *et al.*, 2022; Shafer *et al.*, 2022) and behavioral experiments (Grima *et al.*, 2004; Stoleru *et al.*, 2004) support the idea that this anatomical classifications is rather relevant to predict differential functional activity of these clock neuron groups so far. Nevertheless they revealed a few specificities, such as the non-PDF expressing 5th sLNv that seems in many aspects closer to LNds, or heterogeneity in DN subgroups. Here, I will use anatomical classifications in this thesis, as these emerging new groups do not question (yet?) the affiliation of the members of the group I mainly focus on (*i.e.* the PDF+ sLNvs).

IV. Molecular clock

The molecular clock, as stated previously, often consists in negative transcriptional feedback loops, where, in *Drosophila* and for the core loop, the gene products of *period* (*per*) and *timeless* (*tim*) will accumulate in the course of the day due to the activation of their transcription promoted by the transcription factors CLOCK (CLK) and CYCLE (CYC), followed by the nuclear entry of the heterodimer PER/TIM at night, where PER will sequester CLK-CYC complex, thus interrupting the promotion of its own expression as well as TIM's. In the early morning, light will induce the degradation of TIM via its

binding by the photoreceptor CRY triggering its ubiquitination by JET and ultimately, their degradation by the proteasome. The loss of TIM, which stabilizes PER, will initiate the decline of PER levels, withdrawing its inhibitory effect towards CLK-CYC complex, and therefore, allow a new cycle to begin. More details of the mechanisms of the feedback loops, reviewed in (Edery, 2000; Hardin, 2011; Rouyer, 2013; Muraro and Fernanda Ceriani, 2014; Dubowy and Sehgal, 2017; Mendoza-Viveros *et al.*, 2017), are presented below.

1. Core feedback loop in LD condition

a. Overview

From ~ZT9, which could be seen as the late afternoon, CLK and CYC promote the expression of *tim* and *per* mRNAs (Allada *et al.*, 1998) by activating their transcription through binding to the E-box elements of their promoter regions (Darlington *et al.*, 1998). Then, *tim* and *per* mRNAs will accumulate to peak at ~ZT13 in the evening (Sehgal *et al.*, 1995), where the PER and TIM protein levels will start accumulating to reach their peak levels at ~ZT19 for TIM (Hunter-Ensor, Ousley and Sehgal, 1996a; Zeng *et al.*, 1996), and ~ZT23 for PER (Zeng *et al.*, 1996), corresponding to the late night (Fig. 3).

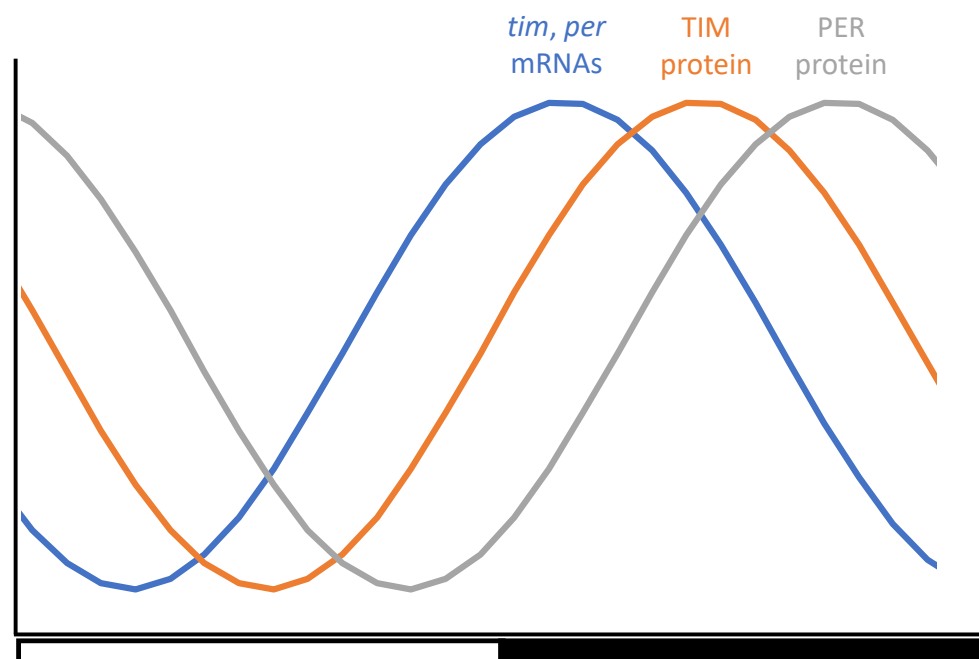


Figure 3 : Representation of *tim* and *per* gene products' oscillations in LD cycle.

This delayed expression of PER and TIM is under the control of well-studied post-translational mechanisms. Among which, the kinase coding genes *discs overgrown* (*dco*), also known as *double-time* (*dbt*), and *nemo* (*nmo*) were found to be clock components as they target PER, impacting its stability and thus participating in the delay between mRNA and protein level peaks (Price *et al.*, 1998; Chiu, Ko and Edery, 2011). As for TIM, the kinases *shaggy* (*sgg*) and *Casein kinase II β subunit* (*CklII β*) target it as well as PER and control their nuclear entry (Martinek *et al.*, 2001; Top *et al.*, 2016).

From ~ZT19, PER is found localized in the nucleus (Curtin, Huang and Rosbash, 1995), this nuclear entry of PER is dependent on PER-TIM heterodimer formation (Gekakis *et al.*, 1995; Saez and Young, 1996). Interestingly, FRET analysis revealed that PER-TIM heterodimers dissociate upon nuclear entry (Meyer, Saez and Young, 2006). Once in the nucleus, PER will repress the activity of CLK and CYC, which will lead to repression of its own transcription as well as for *tim* and other CLK-CYC regulated genes (Darlington *et al.*, 1998; Chang and Reppert, 2003). Noteworthy, this repression of PER on CLK-CYC activity is independent of TIM (Rothenfluh, Young and Saez, 2000; Chang and Reppert, 2003), but necessitates DCO (Nawathean and Rosbash, 2004; Kim *et al.*, 2007), although DCO does not require its catalytic activity to promote CLK phosphorylation (Yu *et al.*, 2009), suggesting that intermediate factors, related to DCO, target CLK to phosphorylate it. In the morning, light induces the quick degradation of TIM (Hunter-Ensor, Ousley and Sehgal, 1996b; Myers *et al.*, 1996; Zeng *et al.*, 1996), which will ultimately lead to the destabilization of PER as well (Fig. 4) (Price *et al.*, 1995; Lee *et al.*, 1996).

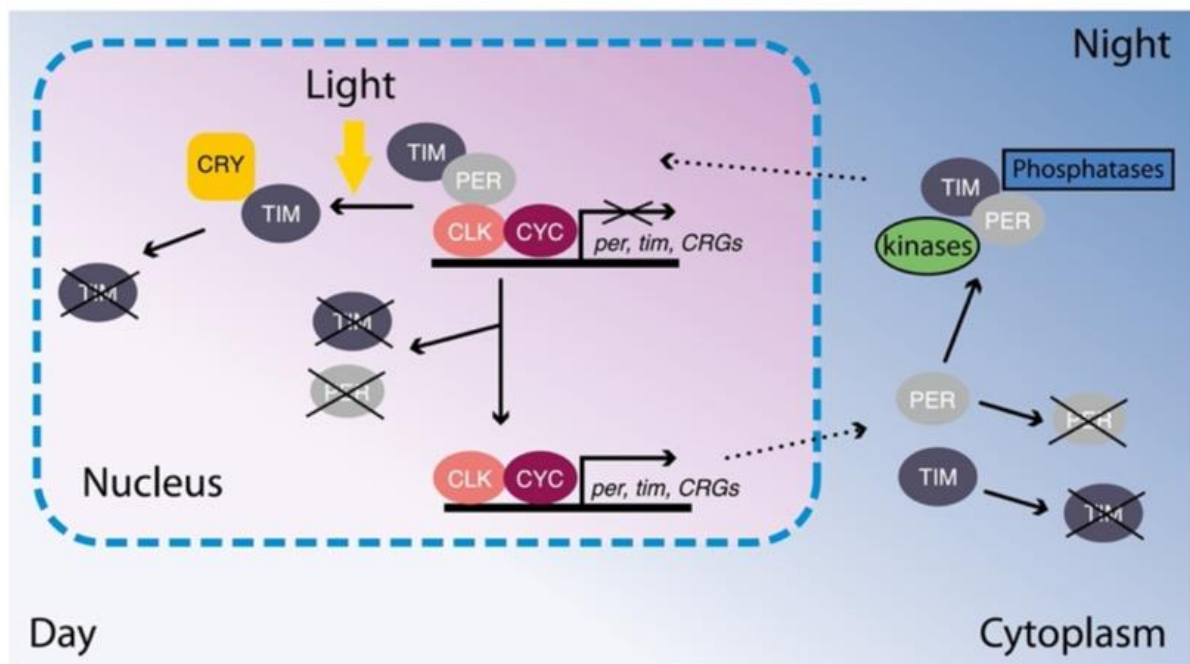


Figure 4 : Simplified representation of the molecular feedback loop in the *Drosophila* clock. CRGs stands for circadianly-regulated genes. Figure from (Rouyer, 2013).

b. Light mediated degradation of TIM

In LD cycles, light serves as a resetting signal by causing the quick degradation of TIM. Yet, TIM is not a photoreceptor and cannot sense light directly. *Cryptochrome* (*cry*) encodes for a blue light receptor that was discovered as a clock component thanks to a screening of mutants causing loss of rhythmicity in *per-luciferase* bioluminescence cycling in LD conditions but not in temperature entrainment conditions (Emery *et al.*, 1998; Stanewsky *et al.*, 1998). CRY is expressed in the eyes, the 9 LNvs, half of the LNDs, and some DNs. The rescue of *cry^b* mutant in the LNvs only

can rescue behavioral rhythms, proving that CRY plays a role in the clock in a cell autonomous manner (Emery *et al.*, 2000). As CRY acts on the clock cell-autonomously, it was hypothesized that it could be the factor at the origin of TIM light-mediated degradation. This is the case, Immunoprecipitation (IP) experiments in *Drosophila* using *tagged-cry* overexpressing flies showed a clear binding between TIM and CRY, as well as an indirect binding between CRY and PER through TIM, which was lost in *tim0* condition (Busza *et al.*, 2004). Most interestingly, this binding between CRY and TIM was mainly visible after a light pulse, showing that CRY binds to TIM upon light exposure, which leads to the quick degradation of TIM (half-life after ~20minutes following a light pulse). The CRY-dependent degradation of TIM after a light pulse requires *jetlag* (*jet*), which codes for a ubiquitin ligase which, upon binding of CRY on TIM, will interact with high affinity with TIM (Peschel, Veleri and Stanewsky, 2006; Peschel *et al.*, 2009), causing its targeting to the proteasome to induce its degradation (Koh, Zheng and Sehgal, 2006). Once TIM degraded, JET will induce the degradation of CRY next (Fig. 5), as its affinity for CRY is lower than for TIM (Peschel *et al.*, 2009).

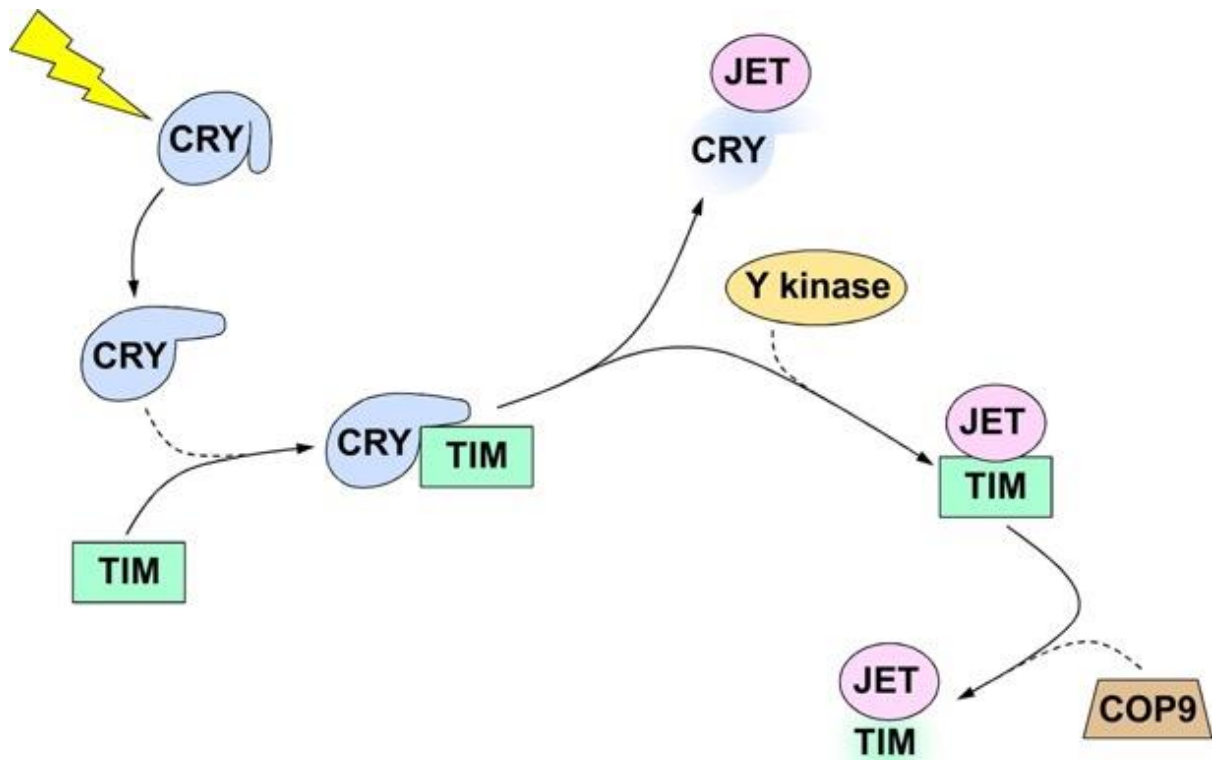


Figure 5 : Light-mediated pathway of the degradation of TIM. Upon exposure to light, CRY binds TIM, leading to high affinity recruitment of JET on TIM that will target TIM to the proteasome, CRY is also bound by JET although less preferentially. Additionally, pharmacological studies suggest the importance of an unknown tyrosine kinase in this pathway in addition to the ubiquitination of TIM (Naidoo *et al.*, 1999), the COP9 signalosome components CSN4 and 5 as well (Knowles *et al.*, 2009). Figure from (Hardin, 2011).

This light-mediated degradation of TIM allows the phase resetting of the clock, and explains why in constant light (LL) conditions flies become arrhythmic, as the TIM

protein is constitutively degraded, thus keeping its levels low and stable (Marrus, Zeng and Rosbash, 1996).

Interestingly, a natural allele of *tim* was found to be more resistant to light (Sandrelli *et al.*, 2007; Tauber *et al.*, 2007; Peschel *et al.*, 2009). The *ls-tim* allele is believed to have emerged ~300 to 3 000 years ago in Europe (Zonato *et al.*, 2018), it allows the translation of an additional slightly longer TIM protein showing diminished interaction with CRY (Fig. 6), hence a higher light resistance (Peschel *et al.*, 2009). This higher-light resistance is believed to play a role in the adaptation to long days at higher latitudes, as *ls-tim* flies show better synchronization to temperature entrainment in constant light conditions than *s-tim* flies (Lamaze *et al.*, 2022).

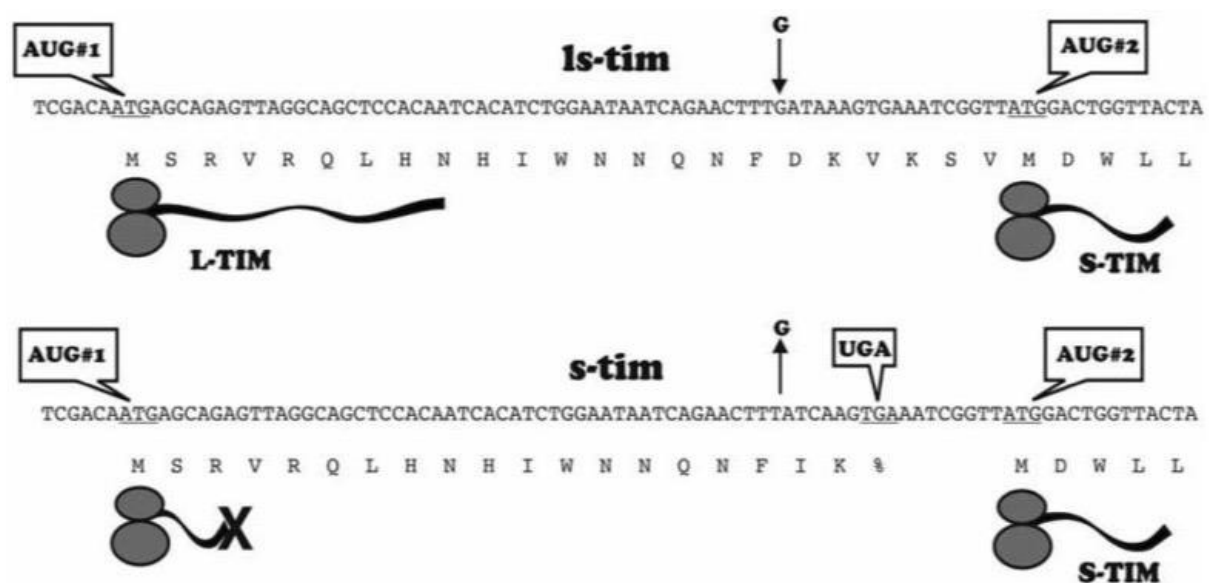


Figure 6 : Scheme of the uORF coding for the TIM-L protein in *ls-tim* flies. *ls-tim* flies possess an insertion in the 5'UTR region of the "canonical" allele *s-tim* that allows the translation of an uORF starting 23 codons upstream of the canonical one. In the *s-tim* allele, the translation of this longer isoform is made impossible by the presence of a stop codon within these 23 codons. In the *ls-tim* allele, an insertion of a G nucleotide changes the subsequent frame, getting rid of the stop codon and allowing the translation of both TIM-L and TIM-S in *ls-tim* flies.

2. Feedback loop in DD condition

In LD cycles, light resets the phase of the clock by inducing the quick degradation of TIM followed by the destabilization of PER in the absence of TIM. Yet, in constant darkness, flies remain rhythmic and maintain *tim* and *per* mRNAs and protein oscillations. Moreover, in LD cycles, TIM protein levels start to decrease before the light-on transition, hinting the presence of other mechanisms controlling the oscillation of clock components.

The kinase DCO has been shown to impact *tim* and *per* mRNA and protein levels in constant darkness conditions (Price *et al.*, 1998), several DCO mutants either shortening the period of the flies, increasing it, or causing arrhythmicity. With these short and long period mutants, the LD cycling of TIM and PER was already affected, although this effect was much more visible in DD, with the period of the proteins

cycling affected similarly to the one of the behaviors, suggesting a role of DCO on TIM and PER stability, ultimately impacting the mRNA levels of *tim* and *per* as well. Nevertheless, the impact of DCO on TIM is expected to be indirect, and PER is its main target (Kloss *et al.*, 1998; Price *et al.*, 1998; Suri, Hall and Rosbash, 2000), as PER and DCO co-localize very well in the head and DCO null mutant leads to high levels of PER and impacts *tim* mRNA and protein less. Hence DCO plays a role in the ticking of the molecular clock, as its mutations will affect the speed of the molecular clock oscillation in constant darkness.

Yet, in control conditions, TIM protein levels start decreasing before the ones of PER, and this is probably a strong cue to entrain the decrease of PER levels in the subjective morning. Shaggy, a kinase phosphorylating TIM, was shown to decrease TIM levels during the subjective night (Martinek *et al.*, 2001).

Additionally, the F-box protein SLMB, a component of the E3 ubiquitin-ligase complex, has been shown to regulated post-translationally the protein levels of TIM and PER in constant darkness (Grima *et al.*, 2002). Interestingly, *slmb^m* mutant flies displayed stable and high levels of phosphorylated PER in DD, suggesting a role of SLMB in the degradation PER. Later, another ubiquitin ligase, CULLIN-3 (CUL-3) was found to regulate TIM and PER levels in LD and DD as well, but while SLMB was important for PER degradation, CUL-3 was necessary for TIM proper accumulation (Grima *et al.*, 2012). These results highlight the importance of post-translational mechanisms in the timekeeping of the clock in free-running conditions.

3. Accessory feedback loop

Vrille (*vri*) is a transcription factor whose expression is cycling and under the control of CLK and CYC (Blau and Young, 1999). CLK and CYC promote the expression of *vri* through an E-box present in its promoter region, its mRNA levels oscillate similarly to *tim* and *per*. Interestingly, mutations in *vri* can decrease or increase the period of the mutant flies. *Vri* mutant flies also present altered PDF expression patterns (Blau and Young, 1999; Gunawardhana and Hardin, 2017). In fact, VRI can repress the expression of *Clk* mRNA by binding to the Vri/PDP1 box (V/P box) in its promoter region (Glossop *et al.*, 2003). This explains the invert oscillation patterns observed for VRI and CLK expressions.

In addition, another transcription factor, PDP1 ϵ , is also induced by CLK-CYC, with an mRNA peak a few hours after *vri*. And while VRI represses *Clk* transcription, PDP1 ϵ activates it (Cyran *et al.*, 2003). This activation occurs after VRI-mediated repression though, as VRI levels peak before the ones of PDP1 ϵ , thanks to the lack of delay between *vri* mRNA and protein levels peaks reported in LD.

This secondary feedback loop is believed to bring more robustness to the core one by controlling the cycling of *Clk* transcription (Fig. 7).

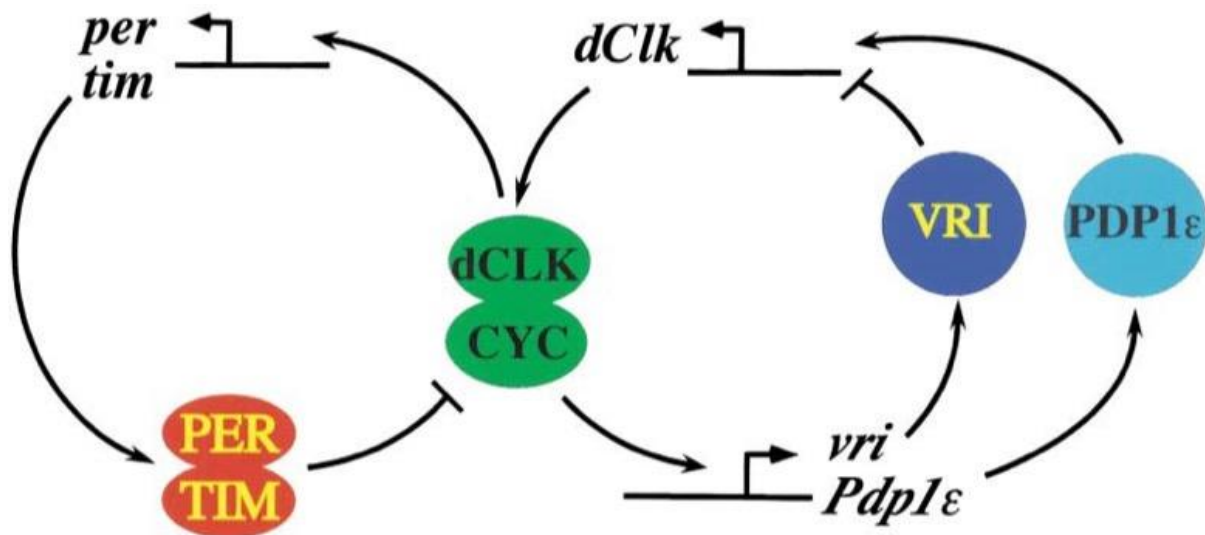


Figure 7 : The two-loop molecular clock model. During the day, CLK-CYC activate the transcription of *per*, *tim*, *vri* and *Pdp1ε* mRNAs. VRI protein represses the transcription of *Clk*, reaching its minimum in the early night. When PER and TIM repress the activity of CLK and CYC in the middle of the night, VRI levels start decreasing, allowing PDP1ε to start activating *Clk* transcription at late night. Figure from (Cyran et al., 2003).

4. The mammalian molecular clock

In mammals, the central clock is located in the suprachiasmatic nuclei of the hypothalamus, where each nucleus counts ~10 000 cells in the mouse (Abrahamson and Moore, 2001). These cells co-express the main components of the molecular clock, which functions generally like the fruit fly clock. The two transcription factors CLOCK and BMAL1 (ortholog of *Drosophila* CYC) activate the transcription of their target genes, among which, *per* and *cry* (Gekakis et al., 1998; Kume et al., 1999; Zheng et al., 2001; Yoo et al., 2005). Upon translation, PER-CRY heterodimers form in the cytoplasm, later joined by other proteins, like CK1ε (ortholog of DCO), to form a complex that will then enter the nucleus to inhibit the activity of the CLOCK/BMAL1 heterodimer (Lee et al., 2009). Followed by the degradation of PER/CRY, allowing a new cycle to begin.

To note, unlike in *Drosophila*, mammals tend to have several clock gene homologs, in mice we count 3 *per* genes, and 2 *cry* genes for example. Among these homologs, *per3* doesn't seem important for preserving normal clock function (Shearman et al., 2000), and instead seems related to development (Noda et al., 2019). Although these homologs can partially rescue each others, they will tend to show functional diversity to bring more complexity to the integration of clock inputs and fine regulation of its outputs (Zheng et al., 2001).

Moreover, in mammals, the partner of PER1/2 is CRY1/2 and not TIM, where CRY proteins lost their photoreceptor activities. The putative role of mammalian TIM in the circadian clock is still debated, as, on one hand, mammalian TIM seems to be related to DNA replication and cell cycle arrest, linking it to cancer (Mao et al., 2013; Yoshida et al., 2013), making it a good potential ortholog of *timeout*, the fly paralog of *tim*, involved in development and chromosome stability (Benna et al., 2010). Nevertheless in *Drosophila*, *timeout* also plays a role on the circadian clock, and similarly in

mammals, *mTim* is required for circadian rhythmicity and some of its isoforms show daily oscillations (Barnes *et al.*, 2003). This suggests a role for *mTim* in the clock, but closer to one attributed to *timeout* in *Drosophila* rather than *timeless*.

5. Should we expect post-transcriptional control of *per* and *tim* mRNAs ?

The delayed accumulation of TIM and PER proteins compared to their mRNA level peaks is a key feature of the clock (Fig. 3), as the absence of delays between RNA rising phase and protein repressive action on transcription was predicted to dampen circadian cycling of *per* gene product (Goldbeter, 1995). Organizing such delays in expressions of clock components requires strong and accurate control mechanisms. So far, post-translational controls in the clock have been extensively studied. And while I only presented the action of phosphorylation and ubiquitination of TIM and PER, dephosphorylation and O-GlcNacylation are also post-translationally affecting clock components (Sathyanarayanan *et al.*, 2004; Fang, Sathyanarayanan and Sehgal, 2007; Kim *et al.*, 2012; Li *et al.*, 2019).

Furthermore, PER protein expression in *per0* flies can be rescued by the use of a *per* transgene constitutively expressed in non-clock, Rh1+ cells, which yields mild cycling of PER protein levels in constant darkness (Cheng and Hardin, 1998). Indicating that PER translational/post-translational controls are sufficient to induce some oscillations of its protein levels. It has been confirmed by showing that *per0* flies' arrhythmic behaviors can be rescued by overexpression of the *UAS-per* transgene in clock neurons, which is believed to be expressed constitutively as well (Grima *et al.*, 2004; Stoleru *et al.*, 2004). This is however less certain regarding *tim0* flies' arrhythmic behavior rescue using *UAS-tim* in neurons (Yang and Sehgal, 2001; Hara *et al.*, 2011), indicating that transcripts oscillations are necessary for *tim* and not for *per* to obtain a functional clock.

Although the importance of post-translational regulations in the control of the free-running molecular clock is not to prove, inappropriate levels of transcripts should affect the clock as well. For example, upon TIM and PER degradation, concomitant low levels of their transcripts will ensure that the recently degraded pool of protein will not immediately be replenished by translation of their transcripts. It is therefore important that the clock mRNA levels are controlled as well to ensure the coordination in the clock feedback loops. Additionally, comparing transcription and transcript levels oscillations clearly shows a delay between *per* transcription and *per* mRNA levels peak, while contradictory results were obtained for *tim* (So, 1997; Rodriguez *et al.*, 2013; Yu and Rosbash, 2023). Regardless, the existence of such delay for *per* at least suggests the existence of post-transcriptional controls allowing delayed *per* mRNA level peaks. These mechanisms will be described later in this introduction.

V. Co- and Post-transcriptional control of mRNAs

1. Generalities about messenger RNAs

Messenger RNAs were discovered in 1961 (Brenner, Jacob and Meselson, 1961; Gros *et al.*, 1961), in pulsed ribosome gradients experiments carried out on E.coli infecting by phages, leading to the discovery of newly translated unstable RNAs corresponding to the phages DNA. Importantly, this was found to occur without synthesis of new ribosomes, as at the time, ribosomes were proposed to be the intermediate between DNA and proteins. This discovery followed the first formal formulation by Crick in 1958 of the Sequence Hypothesis stating that the nucleotide sequence found in nucleic acid codes for the sequence of amino acids in corresponding proteins, as well as the Central Dogma Hypothesis stating that the information encoded into proteins cannot get out again in the nucleic acid sequences (Crick, 1958, 1970).

Messenger RNAs are produced through the transcription of genes found in the DNA by the RNA polymerase II, this process starts at the transcription start site (TSS) which itself is located in promoter regions upstream of a gene (Haberle and Stark, 2018). Transcription can be tuned by chromatin state and enhancer sequences.

For instance, the E-box present in the promoter regions of *tim*, *per* as well as other clock-regulated genes in *Drosophila* leads to increased transcription of the downstream genes upon binding by CLK-CYC heterodimers (Darlington *et al.*, 1998). Transcription of a gene leads to the creation of a precursor messenger RNA molecule (pre-mRNA), consisting in a complementary sequence of the template strand and similar to the coding strand of DNA, with the exception of replacing thymine bases by uracil bases. This pre-mRNA sequence undergoes maturation steps occurring co- and post-transcriptionally to form a mature mRNA molecule that can then be exported out of the nucleus and translated by ribosomes.

Early in the transcription process, m⁷G capping occurs at the 5' extremity of the transcribed eukaryotic pre-mRNA, protecting it from degradation by 5'-3' exonucleases, and playing a stimulating role in translation and nuclear export of the capped mRNAs, it can also affect splicing of the pre-mRNA (Furuichi, 2015).

Nuclear pre-mRNA splicing occurs thanks to the spliceosome complex that will remove intronic regions of the pre-mRNA and bind the exons together. This process can occur co-transcriptionally and can be modulated by regulatory proteins and structural features of the RNA to splice or retain introns differentially in some conditions, which is referred to as alternative splicing, and brings more diversity in the proteome (Will and Luhrmann, 2011). The role of alternative splicing on clock genes and circadian rhythms will be developed later in this introduction.

Close before the transcription termination, the Cleavage and Polyadenylation Specificity Factor complex (CPSF in human and fly) is bound to the RNA pol II and monitors nascent RNA. Upon detection of the Poly-Adenylation Sequence (PAS), the CPSF cleaves the pre-mRNA slightly downstream of the PAS. Then, the poly(A) polymerase, *hüragi* in flies, adds the poly(A) tail at the 3' end of the RNA (Rodríguez-Molina, West and Passmore, 2023). To note, polyadenylation of RNAs is also possible in the cytoplasm on mature RNAs (Juge *et al.*, 2002). Following transcription of the

PAS, the transcription is terminated, and the mature mRNA is exported out of the nucleus through the Nuclear Pore Complexes (NPCs).

Once in the cytoplasm, mRNAs undergo post-transcriptional regulations affecting their stability, localization, and translation.

a. Translation

Once in the cytoplasm, mRNAs can be translated by the ribosomes, translation can be separated into 3 phases :

- Initiation, where, for the canonical “closed loop” model (Fig. 8), the small ribosome subunit (40S in eukaryotes), the eukaryotic initiation factors (eIFs) and the initiator tRNA loaded with a methionine (encoded by the first coding codon of a transcript) assemble at the cap of the mRNA that is forming a loop with its 3' end poly(A) tail through interactions between poly(A) binding proteins (PABP) and the eIFs proteins bound to the m⁷G cap on the 5' end. The 40S subunit will then scan the transcript until reaching the first methionine-coding codon, where it will assemble with the 60S large ribosomal subunit, forming the 80S ribosome that can start the elongation (Shirokikh and Preiss, 2018).

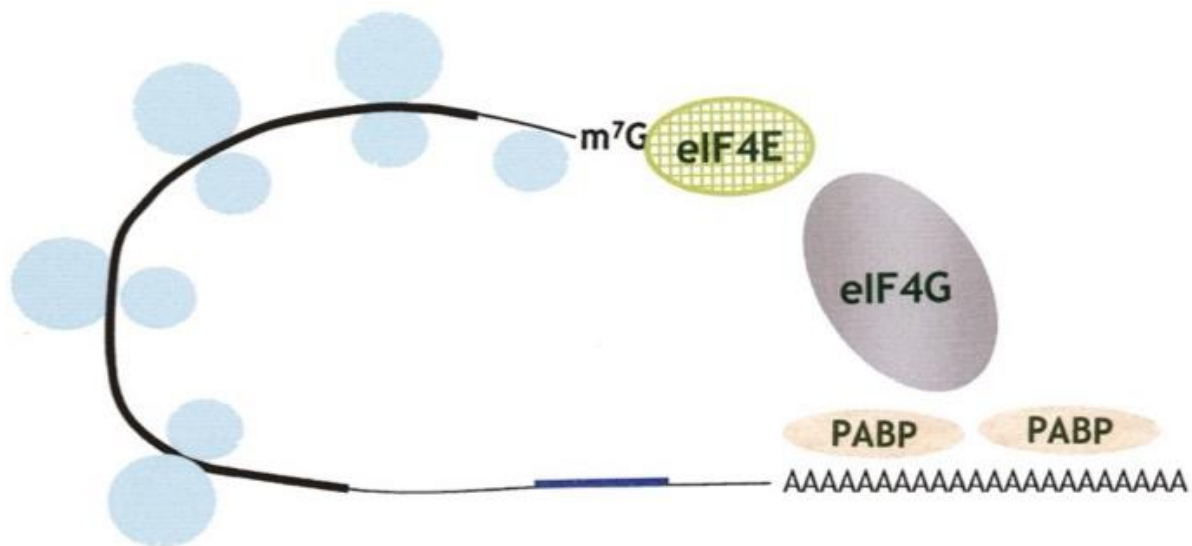


Figure 8 : Representation of the closed loop model. This conformation of the mRNA is proposed to allow faster ribosome recycling.

- Elongation, consisting in the creation of a chain of amino acids that were previously attached to transfer RNAs (tRNAs). These tRNAs bind specific amino acids according to the sequence of their anticodons that will match the mRNA's three nucleotide triplets called codons through complementarity base pairing (Wu and Bazzini, 2023). The ribosome moves along the mRNA, codon after codon. The codons correspondence with an amino acid is redundant, we speak of degeneracy of the genetic code (Table. 1).

First base position	Second base position				Third base position				
	U	C	A	G					
U	UUU	¹ F	UCU	S	UAU	Y	UGU	C	U
	UUC	F	UCC	S	UAC	Y	UGC	C	C
	UUA	L	UCA	S	UAA	Stop	UGA	Stop	A
	UUG	L	UCG	S	UAG	Stop	UGG	W	G
C	CUU	L	CCU	P	CAU	H	CGU	R	U
	CUC	L	CCC	P	CAC	H	CGC	R	C
	CUA	L	CCA	P	CAA	Q	CGA	R	A
	CUG	L	CCG	P	CAG	Q	CGG	R	G
A	AUU	I	ACU	T	AAU	N	AGU	S	U
	AUC	I	ACC	T	AAC	N	AGC	S	C
	AUA	I	ACA	T	AAA	K	AGA	R	A
	AUG	M	ACG	T	AAG	K	AGG	R	G
G	GUU	V	GCU	A	GAU	D	GGU	G	U
	GUC	V	GCC	A	GAC	D	GGC	G	C
	GUA	V	GCA	A	GAA	E	GGA	G	A
	GUG	V	GCG	A	GAG	E	GGG	G	G

¹The one letter symbol of amino acids.

Table 1: The standard genetic code in eukaryotes. Where several codons code for a same amino acid (redundancy). Table from (Sanchez and Grau, 2005).

The codon composition (codon usage) of a transcript will directly impact its stability through its translation, this occurs via the tuning of the ribosome elongation speed, and is referred to as codon optimality. The codon optimality is related to the rarity of a tRNA, that can slow down or accelerate the elongation, which can yield positive or negative effects. If the elongation is slow down too much by the presence of non-optimal codons, translation will be interrupted and the transcript degraded. Similarly, the use of highly optimal codons can also have deleterious effects, as high elongation speeds unallow the nascent proteins to fold correctly co-translationally (Komar, Lesnik and Reiss, 1999; Fu *et al.*, 2016). It is however important to bare in mind that codon optimality can reveal challenging to define, as it directly depends on the mix of available tRNAs at a given time and localization. Usually, the determination of codon optimality will be assessed using the codon usage of transcriptome-wide datasets associated with half-life of corresponding transcripts in order to extrapolate the impact of each codon on transcript stability, hence the codon optimality (Presnyak *et al.*, 2015).

- Termination, upon reaching a stop codon (Table. 1), the ribosome is joined by termination factors eRF1 and 3 recognizing the stop codon, they trigger the release of the nascent protein. The ribosome is then recycled by splitting its two subunits, tRNA and mRNAs are dissociated from the ribosomal subunits. New rounds of translation can be carried out on the same mRNA molecule and the ribosomal subunits can be recycled (Hellen, 2018).

b. Localization

mRNAs are often found in condensates together with RNA binding proteins, forming messenger ribonucleoprotein (mRNP) granules that will regulate many aspects of their life (Buchan, 2014). For instance translationally repressed mRNAs can be found in processing bodies (P-bodies) together with decapping and decay factors (Sheth and Parker, 2003). Alternatively, translated mRNAs can be found clustered in translational factories (Pichon *et al.*, 2016; Dufourt *et al.*, 2021). The formation of these granules has been shown to be dynamic, where signaling pathways can trigger their reversible decondensation (Formicola *et al.*, 2021), and different types of granules even seem to have the ability to interact (Kedersha *et al.*, 2005). Furthermore, granules also permit transport of mRNA, allowing local protein synthesis in remote compartments of the cells (Kiebler and Bassell, 2006).

c. Modifications

mRNAs bases can be modified chemically, so far 100 modifications of RNA were reported, most of them target tRNAs and other non-coding RNAs (ncRNAs) (Gilbert, Bell and Schaening, 2016). These modifications are added by writers, recognized by readers, and removed by erasers. The most abundant modification of mRNA is the N6-methyladenosine (m6A) modification. It is added by the methyltransferase enzyme METTL3 and can be read by different proteins of the YTH family. The presence of mRNA modifications on transcripts can impact virtually all steps of the life of a transcript. In mammals, m6A is predominant in the 3'UTR regions of their transcripts, while in *Drosophila*, most m6A modifications were found in the 5'UTR (Kan *et al.*, 2021), suggesting a distinct role of m6A in *Drosophila* compared to mammals.

d. Deadenylation

Deadenylation constitutes the major pathway leading to mRNA decay (Chen and Shyu, 2011). Once the transcript deadenylated, decapping enzymes (DCP1 & 2 in *Drosophila*) will be recruited on the mRNA to induce decapping, preceding mRNA 3' to 5' degradation by the exonuclease XRN1. Nevertheless, the length of a poly(A) is not a good predictor of the stability of its mRNA. Indeed (Subtelny *et al.*, 2014), used PAL-seq to follow the poly(A) tail length of mRNAs at the transcriptome scale, when comparing the length of poly(A) tails to mRNA half-life in yeast, and mammalian cell lines extracted from other datasets, the correlation was very low between these 2 factors, which was confirmed with other mTAIL-seq analysis later (Lima *et al.*, 2017). Although one similar study did find one weak correlation between mRNA half-life and poly(A) tails in mammalian cells (Chang *et al.*, 2014).

Several deadenylases can be found in eukaryotic cells, among which the main one in flies being the CCR4-NOT complex, we also find the PAN2-PAN3 complex, PARN can also be found in mammals but has no equivalent in flies. PAN2-PAN3 has been proposed in yeast and mammals to deadenylate preferentially long poly(A) tails, containing multiple PABP proteins (Fig. 9) (Yi *et al.*, 2018; Schäfer *et al.*, 2019).

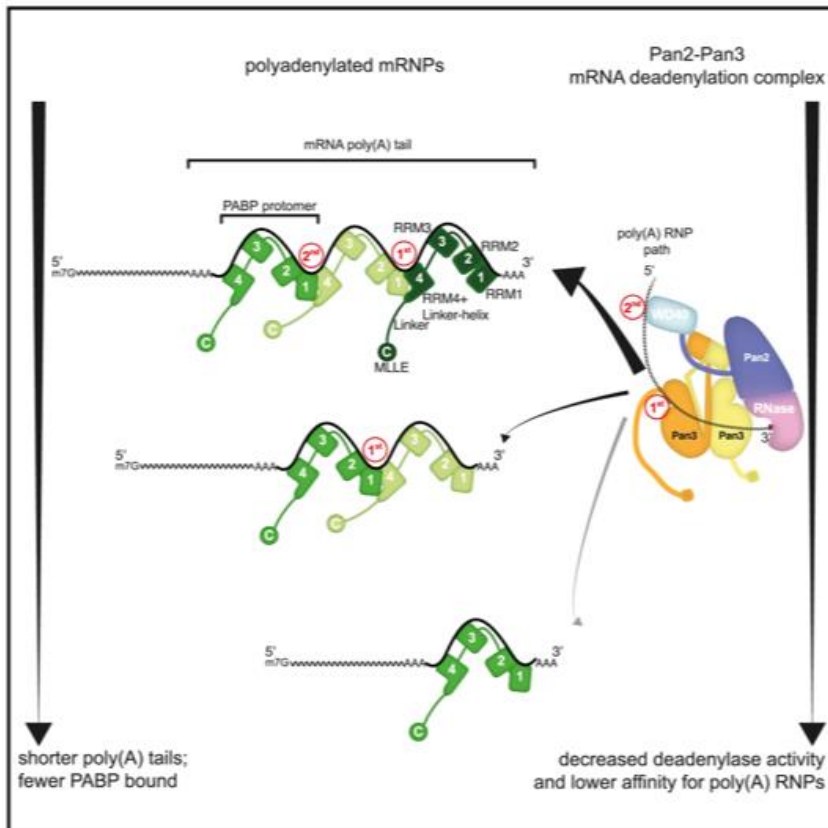


Figure 9 : PAN2-PAN3 complex targets preferentially long poly(A) tailed transcripts, in relation to their PABP number. Figure from (Schäfer et al., 2019).

e. Decay

Several paths can lead to mRNA decay, here is a brief overview of some of them :

- Ribosome-associated quality control. These decays are triggered by aberrant mRNAs detected during translation. It includes the no-go decay (NGD), where ribosome stalls on the mRNA sequence, due to secondary structures of the mRNA for example. Non-stop mRNA decay (NSD), when the transcripts lack a stop codon. Nonsense-mediated decay (NMD), when a premature stop codon is detected during translation. The latter corresponding to the *per0* mutation. These decays aim at avoiding the expression of aberrant proteins (Monaghan, Longman and Cáceres, 2023).
- "Canonical" decay. This one can take 2 forms, depending on the direction of the degradation. First the 5'-3' pathway, where the transcript will be decapped by DCP2, in a deadenylation-dependent or independent manner, followed by XRN1-mediated degradation by 5'-3' exonucleolytic activity. Second, the 3'-5' pathway with deadenylation of the poly(A) tail followed by exosome-mediated degradation by 3'-5' exonucleolytic activity (Li and Kiledjian, 2010).
- miRNA-mediated decay. Micro-RNAs are short RNAs complementary for the sequence of the target transcripts, they bind to it together with the RISC complex, inducing translational repression or deadenylation-dependent decay

through the recruitment of CCR4-NOT by GW182, a member of the RISC complex (Chekulaeva *et al.*, 2011; Fabian *et al.*, 2011).

- Codon optimality-mediated decay (COMD) has been recently characterized and consists in the recruitment of the CCR4-NOT complex to trigger the decay of mRNAs presenting non-optimal codons, causing ribosome slowing/stalling (Bae and Collier, 2022).

In all these pathways, deadenylation is often involved as an initial/intermediate step of the degradation, supporting a key role of deadenylases in controlling mRNA stability.

2. The CCR4-NOT complex

The CCR4-NOT complex is a complex regulating gene expression at all stages, from transcription to post-translational control. The main components of this complex are well conserved through evolution and counts several NOT proteins among which NOT1 is the scaffold protein of the complex, NOT4 is a ubiquitin ligase in yeast and mammals, and POP2 & TWIN are poly(A)-specific ribonucleases (Table. 2) (Collart, 2016). While CCR4-NOT seems to play a more “terminal” role in yeast than PAN2-PAN3 by causing the deadenylation of short poly(A) tails (Webster *et al.*, 2018; Yi *et al.*, 2018), where CCR4 (TWIN) deadenylates slowly tails protected by PAB1 (PABP), while CAF1 (POP2) is more efficient to deadenylate tails lacking PAB1.

Core Name	<i>Drosophila</i> Gene Name	<i>Saccharomyces cerevisiae</i> Gene Name	<i>Homo sapiens</i> Gene Name
Not1	<i>Not1</i>	<i>NOT1/CDC39</i>	<i>CNOT1</i>
Not2	<i>Regena (Rga)</i>	<i>NOT2/CDC36</i>	<i>CNOT2</i>
Not5	<i>Not3</i>	<i>NOT5</i>	<i>CNOT3</i>
Caf1	<i>Pop2</i>	<i>CAF1/POP2</i>	<i>Caf1a/CNOT7/CAF1 and Caf1b/CNOT8/POP2/CALIF</i>
Ccr4	<i>twin</i>	<i>CCR4</i>	<i>CCR4a/CNOT6C and CCR4b/CNOT6L</i>
Caf40	<i>Rcd1</i>	<i>CAF40</i>	<i>CNOT9/Rcd1/CAF40/RQCD1</i>
Not4	<i>Not4</i>	<i>NOT4/MOT2/SIG1</i>	<i>CNOT4</i>
Not10	<i>Not10</i>		<i>CNOT10</i>
Not11	<i>Not11</i>		<i>CNOT11/C2orf29</i>
Caf130		<i>CAF130</i>	
Not3		<i>NOT3</i>	
TAB182			<i>TAB182</i>

I chose Not5 as the core name for fly *Not3*, human *CNOT3*, and yeast *NOT5* because yeast *Not5* rather than *Not3* is certainly the yeast functional ortholog of the fly and human proteins.

Table 2 : Main components of the CCR4-NOT complex in different species. Table from (Collart, 2016).

POP2 and TWIN deadenylase catalytic activities were discovered in flies in 2004 and 2013 respectively (Temme *et al.*, 2004, 2010; Joly *et al.*, 2013). This later confirmation for TWIN specific role is probably due to the fact that POP2 interacts with NOT1 directly to join the complex while TWIN binds POP2 (Raisch and Valkov, 2022). Hence *Pop2* depletion also alters TWIN joining the CCR4-NOT complex, but the opposite is not true.

Although the CCR4-NOT complex regulates the transcription of RNAs (Collart, 2016), I will focus on post-transcriptional and translational roles here.

- Interestingly, CCR4-NOT was shown in human cell lines to regulate mRNA half-life differentially in function of the codon usage of transcripts (Gillen *et al.*, 2021). More precisely, higher proportions of codons ending in A/U in a transcript is linked with low effects of CCR4-NOT on a transcript's half-life. And reversely, high proportions of G/C ending codons correlate with high control of CCR4-NOT on the transcript half-life (CCR4-NOT destabilizes those transcripts more). This feature of the transcript sequences was predicted to explain a major part of CCR4-NOT's effect on the half-life of a transcript, and being related to codon usage, it is likely related to their translations.
- Translation efficiency and poly(A) tail length are well correlated in *Drosophila* embryonic cells (Lim *et al.*, 2016), yet Subtelny *et al.*, 2014 showed that later in development, these correlations are not retrieved in several model organisms, among which *Zebrafish*, *Xenopus*, yeast and mammalian cells. However, this comparison has not been carried out for *Drosophila* so far to my knowledge. The closest we have is the comparison between poly(A) tail length and translation rates in *Drosophila* S2 cell lines (Lima *et al.*, 2017), that shows no correlation. Although others have reported the absence of correlation between translation efficiency and poly(A) tail length in somatic cells, Park *et al.*, 2016 suggests instead a correlation present for short poly(A) tailed RNAs only. Similarly Lima *et al.*, 2017 proposed that short poly(A) tailed transcripts present higher abundance and ribosome association in *C.elegans*, yeast and mice. Hence, the role of the poly(A) tail length in translation remains to be understood.

What is clear however, is that the CCR4-NOT complex does play a role in it. A direct physical interaction has been found between yeast NOT5 (flies NOT3) protein and the ribosome presenting vacant A- and E- sites (Buschauer *et al.*, 2020), which happens on non-optimal codons-rich portions of a transcript due to the absence of corresponding tRNAs. This suggests that CCR4-NOT monitors the ribosome elongation dynamic and can intervene if decoding is slowed down due to non-optimal codons, leading to CCR4-NOT-mediated deadenylation that triggers transcripts degradation through COMD (Fig. 10). Similarly in human, CCR4-NOT has been implicated in ribosome pausing and was even shown to regulate some transcripts' translation independently of its impact on their stability (Gillen *et al.*, 2021). This hints towards a decoupling between CCR4-NOT effect on stability and translatability. This hypothesis is further supported by reported translational repression of transcripts by CCR4-NOT even if they missed a poly(A) tail, and this, in several model organisms (*Drosophila* included) (Jeske *et al.*, 2006; Cooke, Prigge and Wickens, 2010; Van Etten *et al.*, 2012).

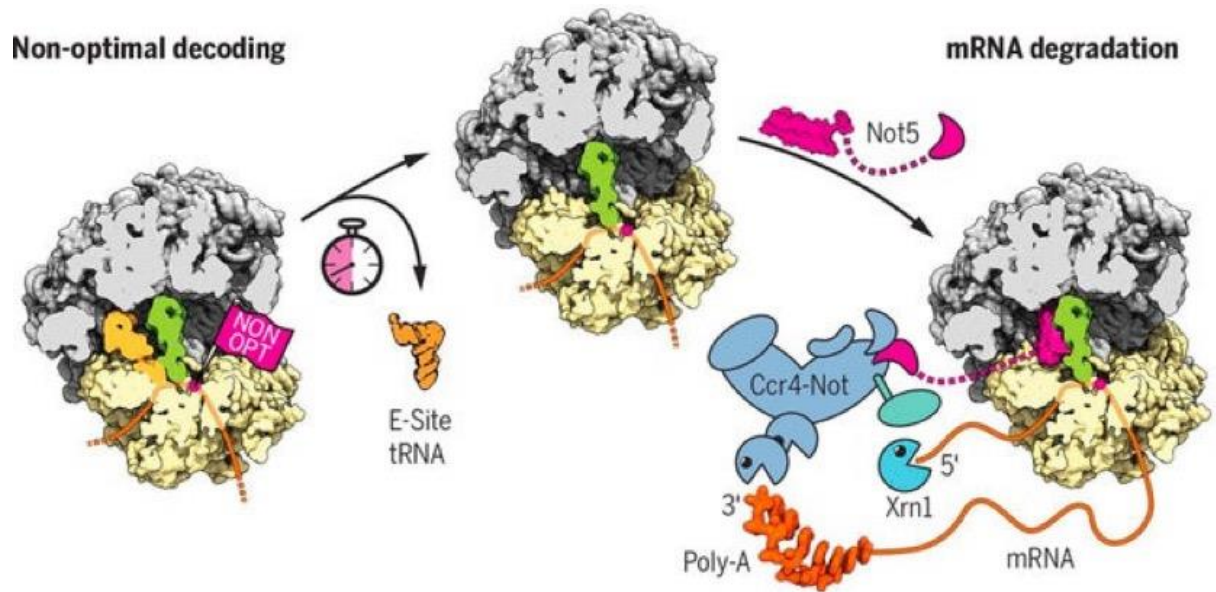


Figure 10 : Codon optimality mediated decay (COMD) mechanism of action. Non-optimal codon slows the ribosome down, leading to the emptying of the ribosome E-site while the A-site is also vacant due to the absence of tRNA complementary for non-optimal codon. This vacancy of A + E sites of the ribosomes entrains a conformational change in the ribosome structure, leading to the recruitment of CCR4-NOT complex through NOT5, triggering mRNA decay. Graphical abstract from (Buschauer et al., 2020).

3. Co- & post-transcriptional controls in the clock

Given the importance of controlling the delays between clock genes transcripts and protein levels, we expect post-transcriptional regulations in addition to the already described post-translational controls in the clock. Additionally, the many regulatory pathways involved in mRNA stability and translation described above support this idea.

a. Alternative splicing and seasonal adaptation

The ability of the clock to compensate temperature represents a challenge, as the clock must maintain a ~24h period at several temperatures but also adapt to them in entrainment, as temperature cycles can entrain the clock in constant darkness. The first discovery regarding the molecular clock adaptation to temperature was an alternative splicing of an intron in the *per* 3'UTR region that was responsible for a phase advance in constant darkness at low temperatures. Later, *tim* also showed a temperature dependent isoform, giving a protein with lower molecular weight that is expressed at low temperature (Boothroyd et al., 2007). This was followed by the finding of splicing factors as regulators of *tim* mRNA splicing, where K.D of these proteins modified the flies' behavioral periods and the levels of *tim* mRNA isoforms, where each isoform is impacted differently according to the environmental condition (Shakhmantsir et al., 2018; Foley et al., 2019). RNA-seq experiments allowed to understand clearly the impact of temperature on circadian alternative splicing (Martin Anduaga et al., 2019). Indeed, overall *tim* mRNA levels are rather stable at different temperatures, but the proportion of each isoform varies according to the temperature. Four main isoforms were described in that study, two that are abundant at low temperatures, *tim-C*

(described in [Boothroyd *et al.*, 2007](#)) and *tim-SC*, where *tim-SC* seems particularly relevant for causing phase advance at low temperature and increased activity during the day. Interestingly, *tim-M*, another isoform that makes up most of *tim* isoforms mix at temperatures above 25°C, does not seem to be translated, suggesting an effect restricted at the mRNA state. The authors propose it as a potential buffer to control the levels of the canonical TIM isoform TIM-L. These discoveries, together with the light-mediated degradation of TIM reveals this clock component as an essential integrator of the clock inputs.

Interestingly, alternative splicing has also been suggested to play a role in *Drosophila* clock neuron identity ([Wang *et al.*, 2018](#)). In this article, clock neurons were dissected and RNA-seq was carried out on clock neurons subsets (namely DN1, LNd, and LNv) and a set of non-clock neurons as control. Then RNA-seq was carried out on these cell subsets, followed by alternative splicing analysis. The results revealed not only the presence of numerous alternative splicing events taking place specifically in some cell subsets, but also that tens of genes showed cycling alternative splicing in clock neurons, while few were detected in non-clock cells. Furthermore, 85% of these cycling alternatively spliced isoforms do not cycle at the mRNA level, revealing a new mechanism that can create rhythm in the clock.

b. Translation around the clock

Comparisons between protein transcript levels oscillations in mice liver estimated that up to half of the cycling proteome does not present cycling transcript levels ([Reddy *et al.*, 2006](#)). The generation of cycling protein levels can be expected to be due to translational and/or post-translational regulations. Therefore, comparing mRNA levels and translation cycling of mRNAs can unveil the proportion of proteins owing, at least partially, their cycling to translational controls. In human cell lines, ribosome profiling was carried out around the clock, allowing to quantitatively determine RNA translation ([Jang *et al.*, 2015](#)). Briefly, ribosome profiling consists in sequencing the ribosome protected fragments (RPF) of mRNAs being translated, allowing not only to know which mRNA is undergoing translation, but also to account for multiple ribosomes translating the same mRNA molecule at the same time (polysomes).

For 266 genes detected as significantly cycling in their total RNA fraction only, they could detect 82 genes that were cycling at the translational level only, and 132 genes cycled in both fractions. Although they failed at detecting translational control of the core clock genes, these results supported the existence of a meaningful role of translation on mRNA cycling at the transcriptome scale.

Furthermore, comparisons between translational and mRNA levels in mice revealed strong differential controls between tissues, where kidney and liver results were compared, revealing hundreds of RNAs cycling specifically at the abundance or translational level, in the kidney or the liver ([Castelo-Szekely *et al.*, 2017](#)). Where core clock components did present differential translational regulations according to their expression localization.

As for *Drosophila*, TRAP-seq experiments (see material and methods section) were carried out at different circadian times, allowing to quantify the amount of mRNAs bound by ribosomes. While losing the information regarding the number of ribosomes bound per mRNA molecules (Huang *et al.*, 2013). This technique has however the advantage to permit the enrichment of ribosome-bound RNAs in a tissue of interest. These analyses displayed 1255 mRNAs presenting cycling ribosome-bound mRNA levels through 2 days in constant darkness in the *tim* positive cells of *Drosophila* heads. This cycling took place with 2 different major phases peaks, one at CT8, and the other closer to CT16, suggesting bimodal regulation of translation. A limit of this study though is lack of comparison with total mRNA levels, as the enrichment of ribosome-bound mRNAs in *tim*+ cells unallows the systematic comparisons of total mRNA levels for mRNAs expressed in other cells. Yet, this approach allowed the discovery of new genes impacting circadian rhythms and sleep probably by a combination of translation-specific and tissue-specific cycling of their mRNA levels (You *et al.*, 2021). Additionally, the genes *tyf*, *atx2* affecting the flies' locomotor rhythms impacted *per* translation in in vitro experiments, supported with reported binding of ATX2 on core clock component mRNAs (Lim *et al.*, 2011; Lim and Allada, 2013; Zhang *et al.*, 2013; Lee *et al.*, 2017).

As stated previously, codon optimality regulates the translation elongation dynamic, as well as the stability of mRNAs. Furthermore, it was found that optimizing part of the codons in *per* CDS causes diminution of rhythmicity in flies' locomotor behavior due to altered oscillations of PER protein and phosphorylation oscillations (Fu *et al.*, 2016). Thermal shift assays of this optimized PER protein indicated structural change in the PER protein, although the amino acid sequence was the same as in WT *per*+ flies. Altogether, these experiments support the existence of another layer of control of the oscillation of core clock components as well as clock-regulated genes between the mRNA and protein levels.

c. Poly(A) tail length rhythms

Poly(A) tail length has been reported to present rhythms in mammals (Kojima, Sher-Chen and Green, 2012). Mouse liver RNAs were extracted around the clock and RNAs were separated according to the size of their poly(A) using oligodT chromatography with varying salt concentrations, the different groups of mRNAs were then quantified by microarray. Normalizing the quantity of long vs short poly(A) tailed mRNA levels by the total mRNA levels around the clock allowed the identification of 237 mRNAs presenting roughly cycling levels (as 2 groups of poly(A) tail lengths only are considered), yet gene-specific approach confirmed the oscillations of the poly(A) tail lengths for several of these genes. Interestingly, the cycling phase of the poly(A) tail length of several genes matched the one of corresponding protein level cycling, while some genes didn't originally show RNA cycling. These results have shown a circadian poly(A) tail length rhythm in mammals, at the transcriptome scale, that can also generate rhythmicity independently of transcription rhythms.

d. *Tim* mRNA undergoes post-transcriptional control by the deadenylase POP2

Several years ago, a screening was carried out in the laboratory, looking for new clock components. The screening was carried out using an RNAi collection of flies from the NIG fly stock center of Ryu Ueda (Japan). The flies used from this collection, carried UAS-RNAi transgenes targeting ~6000 genes altogether. The UAS-RNAi were crossed with a clock neuron specific driver (*gal1118*) to target the K.D of the RNAi-targeted genes in this cell subset. Locomotor behavior of the offspring was then monitored in DD conditions to identify genes potentially affecting the clock.

Among the hits, the gene *Pop2* was identified, as flies with downregulated *Pop2* showed arrhythmic locomotor activities. The impact of *Pop2* on the clock was confirmed, where *Pop2* K.D caused an increase in TIM protein levels in the heads and in DD conditions, but only during the subjective day. On the other hand, PER was unaffected in its protein levels. POP2 being a deadenylase of the CCR4-NOT complex, this circadian change of TIM levels has been attributed to mRNA levels change. Indeed, *tim* mRNA levels, and not *pre-tim* levels were increase in DD conditions during the subjective day upon *Pop2* K.D, while also being slightly reduced at night, suggesting a post-transcriptional regulation of *tim* mRNA. Additionally, *per* mRNA levels were not affected.

This specific and circadian control of POP2 for *tim* mRNA was investigated further by monitoring the poly(A) tail length of *tim*, as POP2 is a deadenylase, this is how it might act on *tim*. PATassay experiments (See material and methods) revealed that in control conditions, *tim* has a short poly(A) tail (<50 nucleotide long) at all timepoints. However, upon K.D of *Pop2*, *tim*'s poly(A) length was increased, particularly during the subjective day, in line with its mRNA stabilization and protein levels increase.

The CCR4-NOT complex is known to be frequently recruited by RBPs binding the 3'UTR sequence of the target RNA. The lab thus took advantage of the *tim-yfp* transgene which possesses the 3'UTR sequence from the *white* gene to investigate whether the recruitment of POP2 on *tim* occurs specifically thanks to its 3'UTR region. Unexpectedly, POP2 also deadenylated *tim-yfp*, suggesting that the recruitment of POP2 on *tim-yfp* happens through a different way.

Finally, it was shown that in the absence of PER (*per0* flies), the effect of POP2 was lost, indeed the high levels of *tim* mRNA observed normally in *per0* context were not modified by *Pop2* K.D, and similarly the poly(A) tail of *tim* was rather short in this context too.

The lab published an article reporting a PER-controlled, specific and circadian deadenylation of *tim* mRNA by POP2 in the clock (Grima *et al.*, 2019). The results are summarized below (Fig. 11).



Figure 11 : Summary of the results from (Grima et al., 2019). In control condition (*tim-gal4*), POP2 deadenylates *tim* at all times, leading to oscillating levels of *tim* mRNA, proteins and the behavior being rhythmic with a 24h period. Upon Pop2 K.D, the poly(A) tail of *tim* is longer, causing increased length of *tim* poly(A), levels of mRNA and protein during the subjective day and flies becoming arrhythmic. In absence of PER, *tim* is deadenylated again, and its levels of mRNA and proteins are not impacted by POP2 anymore, the flies are arrhythmic as they are expected to be in *per0* context.

VI. Questions to answer during my PhD

The objective of my project was to get a better understanding of the control of POP2 on *tim* mRNA.

We see the effect of POP2 on *tim* during the subjective day, but not the subjective night, supporting a circadian regulation of the activity of POP2. Additionally, PER seems to control this activity. Therefore, it is possible that POP2 levels oscillate, although its mRNA levels do not (Grima *et al.*, 2019), which would then be generated at the translational/post-translational level. The first chapter of my thesis results will thus be dedicated to the assessment of POP2 levels oscillations.

Next, POP2 was shown to deadenylate specifically *tim*, but not *per*, and this specificity was not linked to the 3'UTR region of *tim*. The search for the factor that directs specifically POP2 to *tim* will constitute the second results chapter.

Last, the CCR4-NOT complex is known to regulate not only the stability of mRNAs, but also their translations, in relation or not with its deadenylation activity. We thus employed the TRAP method in a gene-specific (RT-qPCR) and transcriptome-wide manner (RNA-seq). This double approach allowed us, on one hand, to study in great details, the circadian translational control of *tim* expression and POP2's impact on it. And on the other hand, to investigate the possibility that POP2 regulate other

circadianly-regulated genes. Additionally, the role of PER on POP2's activity will be further dissected in this third and last results chapter as well.

Results

I. Pop2 gene products cycling analysis

POP2 affects *tim* mRNA stability, poly(A) tail and protein levels during the subjective day, but neither during the subjective night in *per*⁺ conditions, nor in *per0* context (Grima *et al.*, 2019), suggesting that POP2 could act in both, a circadian, and PER-dependent manner to regulate *tim*. Suggesting a potential cycling of *Pop2* gene products. Yet RT-qPCR analysis revealed that *Pop2* mRNA does not oscillate in constant darkness in *Drosophila* heads (Grima *et al.*, 2019). Although *Pop2* mRNA doesn't oscillate, its protein could display daily oscillation in levels, phosphorylation or subcellular localization, as many cycling proteins do not necessarily show cycling transcript levels (Reddy *et al.*, 2006). Following POP2 protein revealed challenging, as the anti-POP2 antibodies available in *Drosophila* displayed numerous aspecific signals. Two strategies were adopted to follow the POP2 protein over the circadian time.

1. Exogenous POP2 oscillates in the heads and clock cells in *Drosophila*

Previous my arrival in the team, a UAS-*Pop2*-HA fly line was used in order to follow the levels of an exogenously expressed POP2 through its HA tag. Western Blot (WB) (Fig. 12) experiments displayed oscillating levels of POP2 in the fly heads, supporting the existence of a strong circadian post-translational control of POP2 expression, in line with our expectations from the lack of oscillation of *Pop2* mRNA. Although these results were promising, the overexpression of *Pop2*-HA is not physiological.

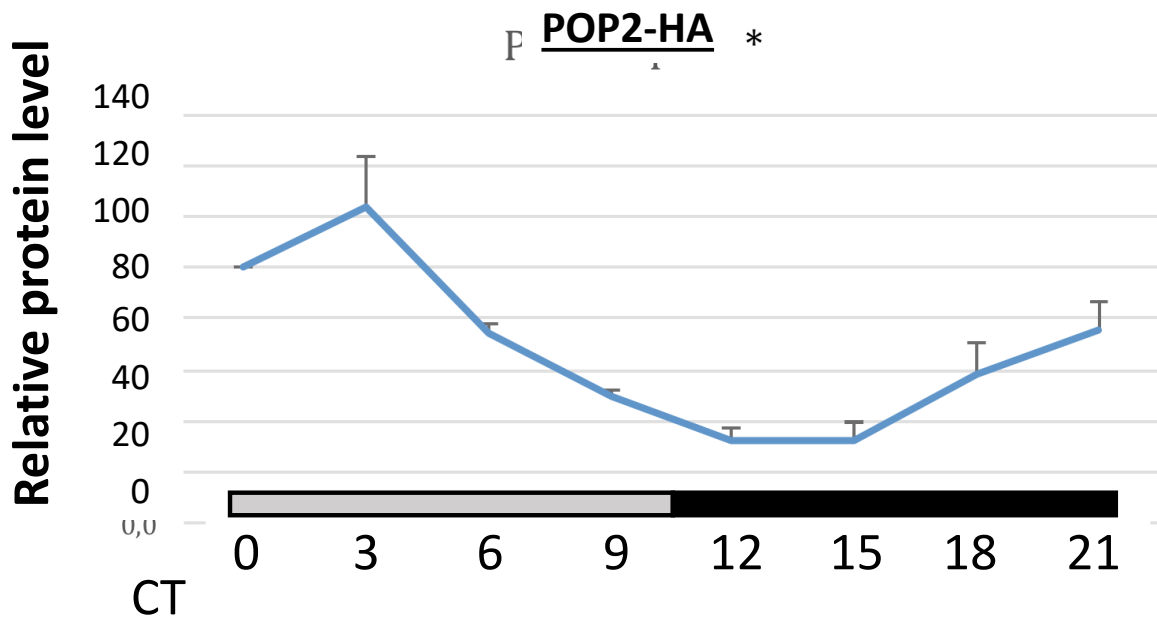


Figure 12 : Quantification of Western Blot analysis of exogenous POP2-HA protein. WB done using anti-HA antibodies from UAS-Pop2-HA expressing flies under the control of the *tim-gal4* driver in drosophila heads. N= 3 replicates for all CTs except CT21 n=2. Experiment realized by Christian Papin.

2. Endogenous POP2 does not show any oscillations

a. Knock-In of an HA-tag in the endogenous *Pop2* gene

To go further, we decided to follow the cycling of endogenous POP2 levels in WB by creating an endogenously HA-tagged *Pop2* fly line taking advantage of the CRISPR-Cas9 technology. The K.I design as well as the screening method is explained in the material and methods section.

- *Pop2*-HA flies behavioral assessment

Once the transformant flies acquired, they were checked for proper circadian locomotor activity rhythms to ensure that the integration of the HA-tag in *Pop2* (or potential off-target genes) does not alter the behavior of the flies (Table. 3). The behavior of the flies in DD condition was not affected.

Genotype	NumTotal	NumAlive	%Rhythmic	Tau (period)	sem	Power	sem
w;+/Sp;Pop2-HA	23	22	95.5	24.4	0.08	307.2	24.43
w;stj+	16	13	92.3	24.6	1.00	251.6	37.76

Table 3 : Summary of the cycle_p analysis of male endogenous Pop2-HA outcrossed flies analyzed in DD condition at 25°C after 4 days of entrainment in LD condition. w;stj+ as controls.

b. POP2-HA levels do not cycle in the Drosophila heads and are not influenced by PER

Next, we used our anti-HA antibodies to carry out WB analysis on our endogenous *Pop2*-HA flies at several circadian timepoints (Fig. 13). Surprisingly, we could detect 2 signals in the heads for only one in the body, with the upper one corresponding to our expected POP2-HA signal, as it was present in UAS-*Pop2*-HA condition, found only in

the heads and not the bodies. The lower signal is present everywhere and could be POP2 signal as well, although the size does not match with expected POP2 protein sizes predicted in FlyBase. Additionally, the expression of endogenous POP2-HA in the head does not seem to oscillate through the circadian times in our 2 replicates.

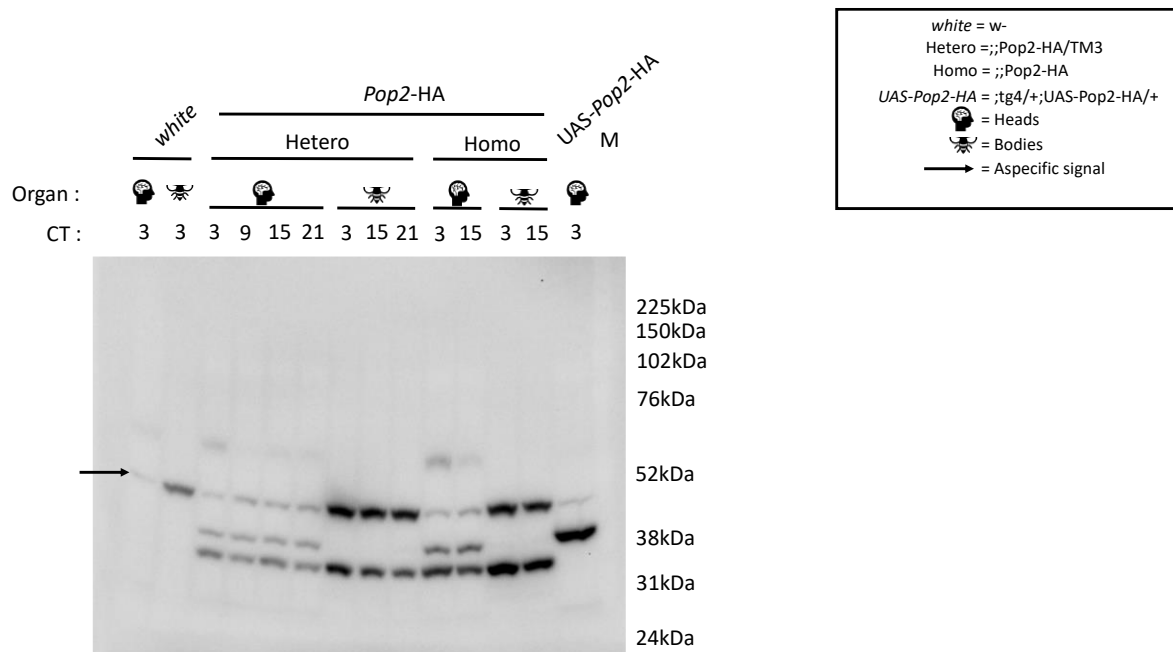


Figure 13 : Western Blot analysis of endogenous Pop2-HA. Experiment realized in *Drosophila* heads or bodies (thorax + abdomen), on non-Pop2-HA *white*-flies as a control for aspecific signals, aspecific signal pointed by black arrow. Flies were heterozygous or homozygous Pop2-HA, overexpressing UAS-Pop2-HA under the control of the *timgal4* driver used as a positive control. M stands for molecular weight markers lane. Representative WB out of the 2 made.

We yet wanted to confirm that the 2 bands observed in the heads both corresponded to POP2 signals. We thus took advantage of our anti-POP2 antibodies that previously presented numerous aspecific signal to carry out Immuno-Precipitation (IP) experiments for POP2. Briefly, we immunoprecipitated POP2-HA from *Drosophila* heads using our anti-HA antibody, followed by Western Blotting of the inputs and eluates of the IP using our anti-POP2 antibodies (Fig. 14). We could indeed find both upper and lower signals with the rabbit anti-POP2 antibody from anti-HA IP eluates, at both CT3 and CT15 in *Pop2*-HA flies, but not *white* controls, strongly supporting that these 2 bands both correspond to POP2, suggesting that there could be an isoform of *Pop2* specific of the head.

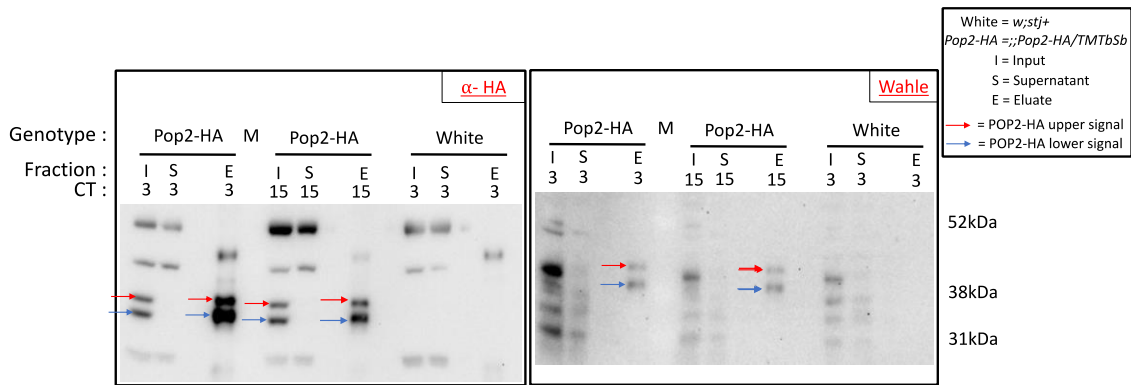


Figure 14 : Western Blot of anti-HA IP fractions. Left WB using anti-HA antibodies for staining, as a control. Right WB using rabbit anti-POP2 antibody from Wahle lab for staining. Input (I) shows the proteins present before IP. Supernatant (S) the ones that do not bind to anti-HA conjugated beads. Eluate (E) the proteins found bound to the anti-HA beads, and revealed on the WB. White- flies without Pop2-HA were used a negative control of apsecific signals.

We tried to characterize these 2 *Pop2* isoforms by sending them to mass spectrometry after acrylamide gel electrophoresis and separation of the upper and lower bands, the bands were analyzed at the proteomics facility (SiCaPS) in I2BC, Gif-sur-Yvette. Unfortunately, the Amino Acid coverage mapped on the POP2 sequence was of approximately 30%, and no differences could be found between lower and upper band amino acid sequences. As an alternative, we explored the profile of *Pop2* transcripts by conducting PCR analysis using *Pop2*-HA cDNAs extracted from heads or bodies that were amplified using different sets of primers to localize any differences at the transcript level (Fig. S2) This revealed a difference between head and body *Pop2* signal located from the first to second exon of the *Pop2*-RA isoform, the bands obtained after electrophoresis were cut, purified, and sequenced (Fig. 15).

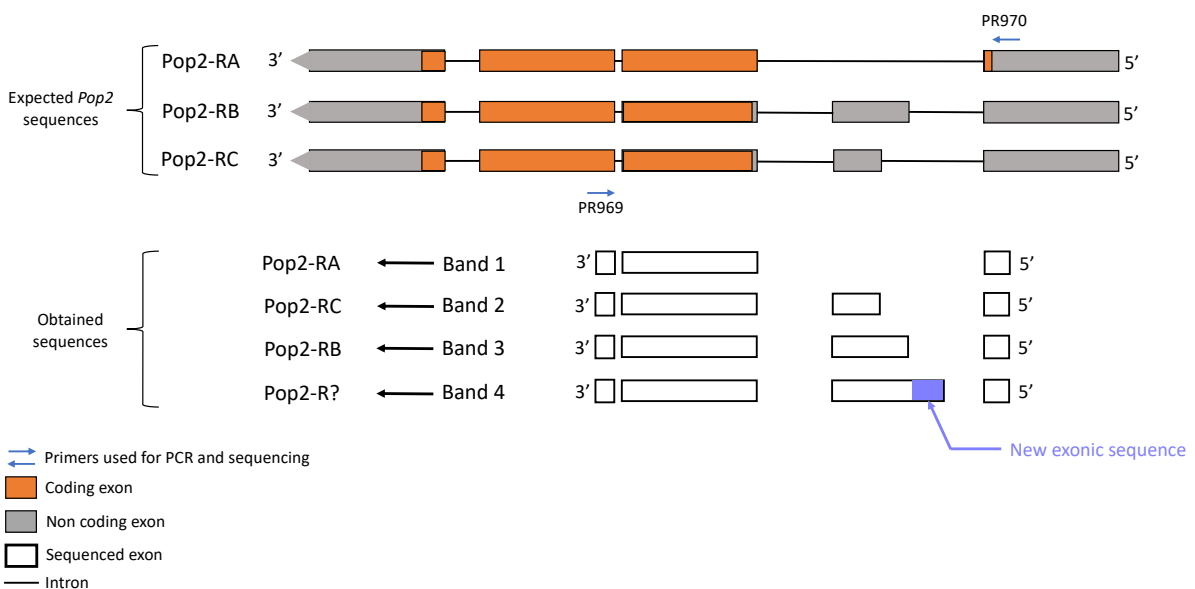


Figure 15 : Representation of the sequencing results obtained for Pop2-HA. Only the band corresponding to *Pop2*-RA was found in the flies' bodies.

We indeed sequenced a 5' extension of a non-coding exon that was not previously described for *Pop2*. This could give rise to a new coding exon, which would increase the length of POP2-HA protein, thus explaining the presence of the upper signal seen in WB.

A possibility in explaining the circadian control of POP2 on *tim* could be in its phosphorylation status, as several kinases and phosphatases have been linked to the functioning of the molecular clock (Mendoza-Viveros *et al.*, 2017). Yet, we could not detect any changes in the size of POP2 protein in WB at different timepoints (Fig. 13), we thus used the Supersep Phos-tag gels allowing separation of phosphorylated and dephosphorylated protein signals during polyacrylamide electrophoresis through the use of zinc and manganese ions added to precast gels (Kinoshita *et al.*, 2006). Using Phos-tag gels did not reveal any phosphorylations of endogenous POP2-HA in heads or body (Fig. 16).

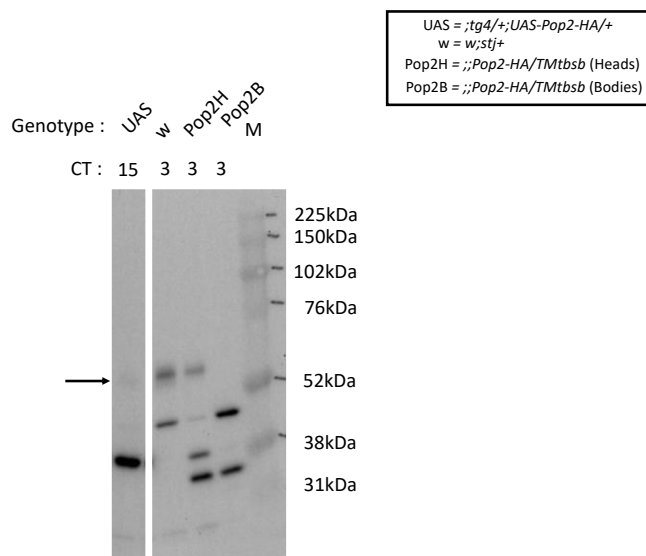


Figure 16 : Phos-tag analysis using anti-HA antibodies. *UAS* is a positive control of *UAS-Pop2-HA* expression under the control of the *tim-gal4* driver. *W* is a negative control of non-*Pop2-HA* expressing flies to detect aspecific bands, *Pop2H* and *B* refers to endogenously tagged *Pop2-HA* flies' heads or bodies. Black arrow for aspecific signal. Representative WB analysis of 2 replicates.

Furthermore, we wanted to test whether the presence or absence of PER would impact the levels of POP2, as it does impact its activity on *tim* mRNA (Grima *et al.*, 2019). We realized WB in *per+* and *per0* contexts at 4 CTs and quantified the levels of POP2-HA upper and lower bands (Fig. 17).

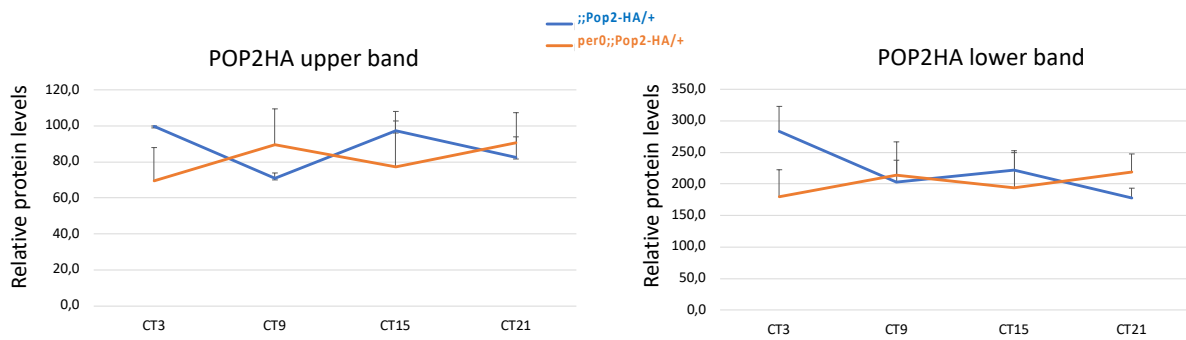


Figure 17 : Western Blot analysis of endogenous Pop2-HA in *Drosophila* heads in *per+* or *per0* context. Quantification averaged from 3 replicates. Experiment realized by Christian Papin.

We did not observe any difference in POP2-HA levels in *per0* vs *per+* context.

Here we found no evidence of circadian regulation of endogenous POP2 in the head, neither at the protein level, or phosphorylation, in presence or absence of PER. The difference between exogenous and endogenous cycling of POP2 protein could be due to the lack of tissue specificity of our WB experiments, indeed the endogenously tagged POP2 is found in a ubiquitous manner in the heads, where non-clock cells could express POP2 in a stable manner, thus masking oscillations of this protein in the clock cells. To investigate this possibility, we performed immunofluorescence experiments.

c. POP2-HA levels do not cycle in the s-LNvs and are not influenced by PER

Following the expression of endogenous POP2-HA in the clock neurons will allow us to estimate the presence of cyclic expression of POP2 while avoiding the bias caused by *Pop2*'s ubiquitous expression. The more detailed procedure developed to quantify POP2-HA in clock neurons is developed in the material and methods section. Briefly, we dissected the heads of POP2-HA flies to carry out IF experiment following POP2 using an anti-HA antibody in the s-LNvs, the clock neurons implicated in the maintenance of rhythmicity of the flies in constant darkness conditions (Grima *et al.*, 2004) (Fig. 18).

Interestingly, we could see the POP2-HA signal only in homozygous *Pop2-HA* flies, meaning that 2 copies of the tagged *Pop2-HA* gene are needed to allow enough expression to detect it. Additionally, we see the signal localizing in the cytosol of the cells, but not in the nucleus, similar to what was found previously by others (Temme *et al.*, 2004, 2010), but unlike what was found in our lab using the UAS-*Pop2-HA* with the *gal1118* driver (Fig. S3) where exogenous POP2 also seemed to localize in the nucleus. Highlighting the lack of physiology in the use of overexpressing *Pop2-HA* flies.

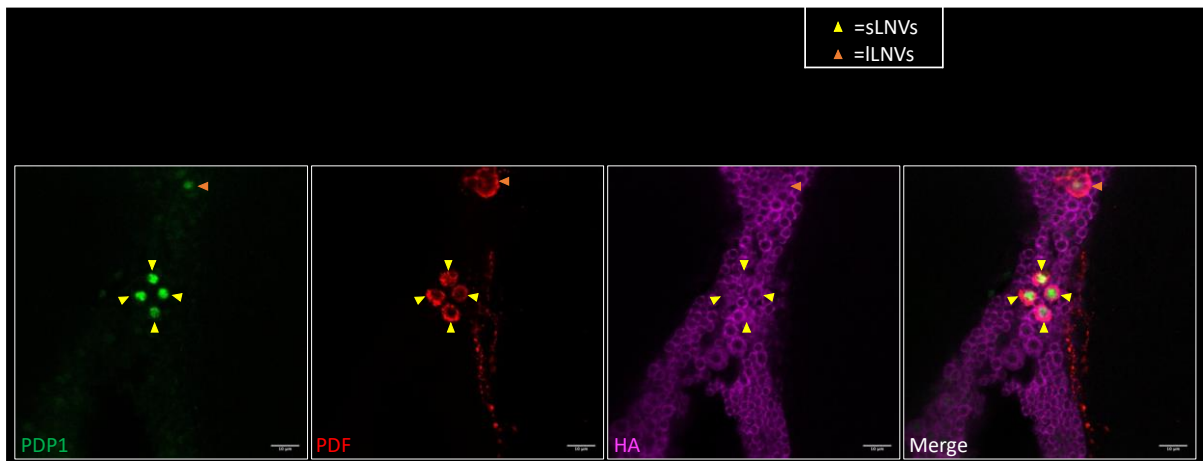


Figure 18 : IF picture of LNvs clock neurons marked with anti-PDF (LNvs marker), HA (POP2), PDP1 (clock cells marker) antibodies of *Pop2-HA* flies. Images taken using a Leica SP8 confocal microscope. Realized with help from Élisabeth Chélot.

We proceeded to dissect endogenous *Pop2-HA* fly heads (~10 brains per conditions), with a first replicate of 4 CTs showing a potential very mild oscillation (data not shown) and another one at 8 circadian timepoints (Fig. 19) to quantify the POP2-HA signal in the sLNvs around the clock. We could not see any oscillations of POP2, similarly to what we observed in WB analysis. Additionally, the localization of POP2 in the sLNvs as well as the neighboring cells was found only in the cytoplasm at all timepoints, as expected from previous work in S2 cells (Temme *et al.*, 2010) and *Drosophila* embryos (Temme *et al.*, 2004).

Ratio of mean POP2-HA signal in sLNvs compared to control cells.

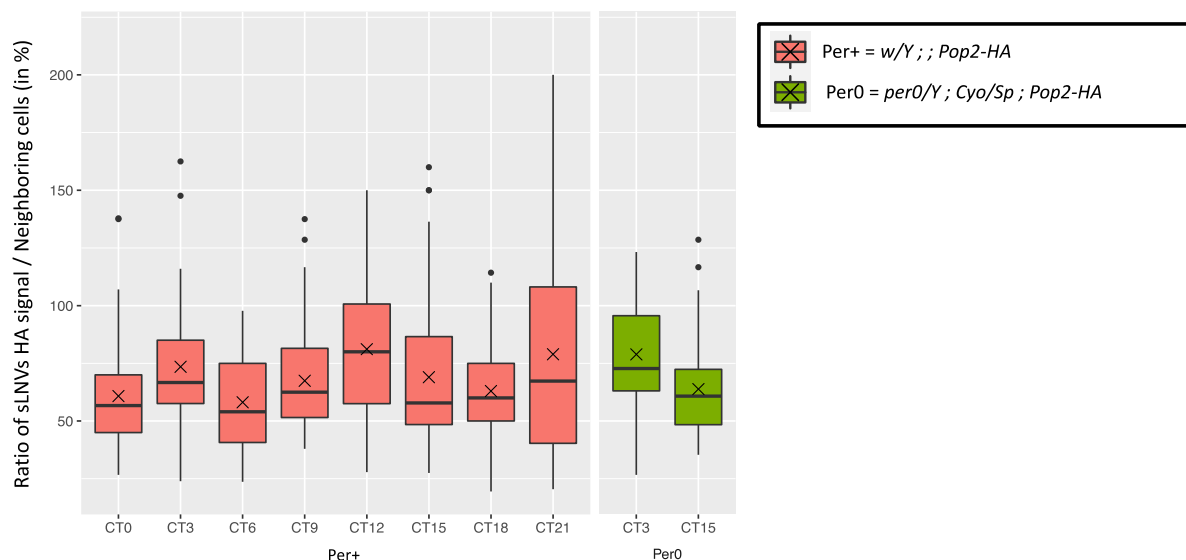


Figure 19: Quantification of IF experiment following POP2-HA levels in endogenous *Pop2-HA* flies entrained in LD at 25°C for 3 days and dissected on the first day of constant darkness at 8 CTs pour *per+* *Pop2-HA* flies and 2 CTs for *per0* *Pop2-HA* flies. The results are represented in the form of boxplots of the ratios between each sLNv HA signal intensity and neighboring cells HA signal intensity. The cross represents the average and the middle bar the median. Dissections realized with Élisabeth Chélot.

For both replicates, we also followed the levels of POP2 in *per0* context, to see whether POP2 levels or localization would be altered in absence of PER (Fig. 20) Comparisons

were made by pooling the timepoints together, no significant differences were found in POP2-HA levels in the sLNvs between *per+* and *per0* context.

Pooled ratio of mean POP2-HA signal in sLNvs compared to control cells.

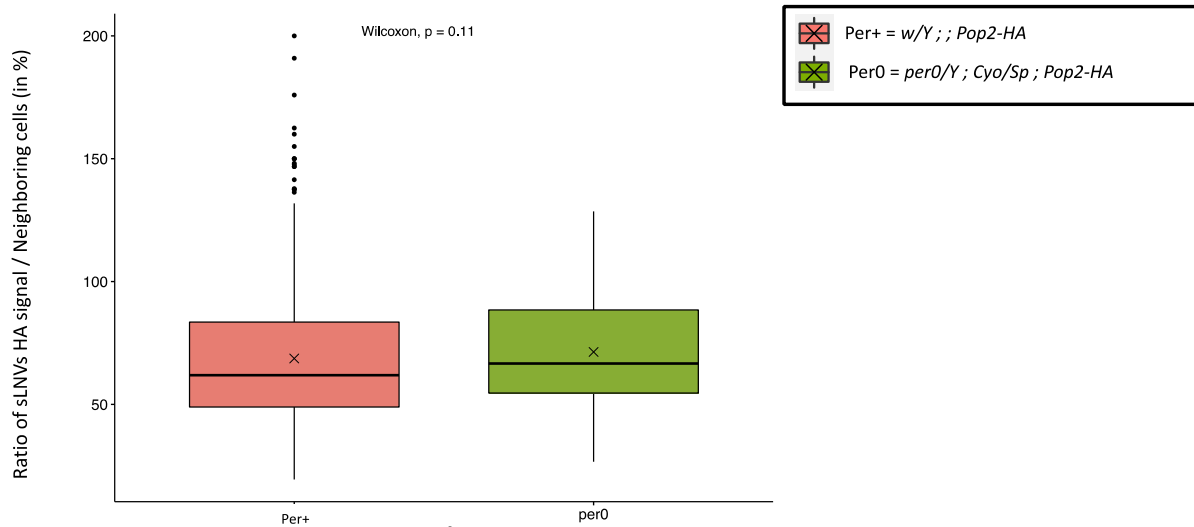


Figure 20 : Comparison of POP2-HA signal in the sLNvs of endogenous Pop2-HA flies in *per+* or *per0* context, the results from 8CTs were pooled for *per+* and 2 CTs for *per0*. Statistical analysis carried out with Wilcoxon signed rank test.

3. Discussion

We have contradictory results regarding the cycling of POP2 between UAS-*Pop2*-HA and *Pop2*-HA flies where POP2 oscillates in WB experiments with UAS-*Pop2*-HA flies, but does not oscillate with *Pop2*-HA ones, even in the sLNv clock neurons. To clarify these results, we looked at the RNA oscillations of exogenous *Pop2*-HA and *GFP* mRNAs under the control of *tim-gal4* (Fig. 21), as we already knew that endogenous *Pop2* mRNA did not oscillate (Grima *et al.*, 2019) and GFP protein neither (Fig. S1).

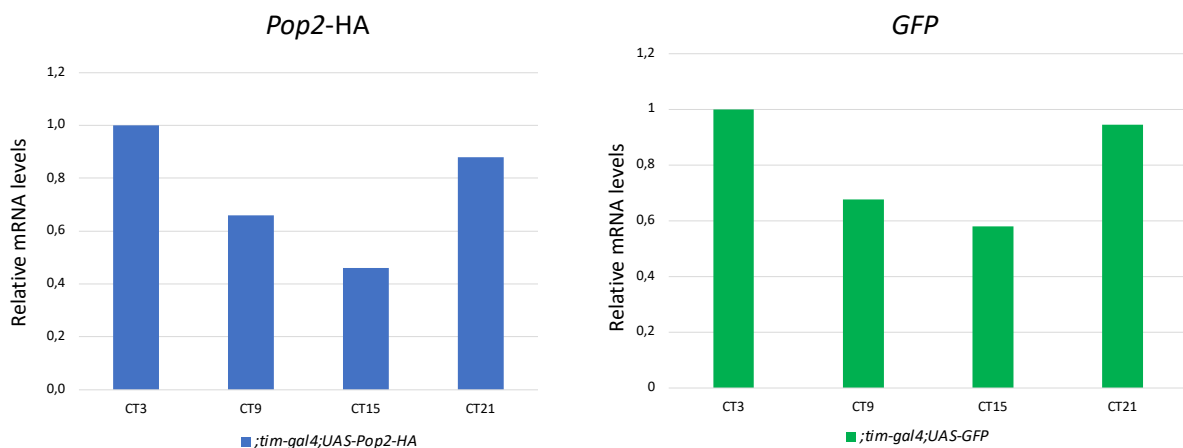


Figure 21 : RT-qPCR quantification of *Pop2*-HA and *GFP* mRNA levels (left) *Pop2*-HA mRNA levels in ; *tim-gal4* ; UAS-*Pop2*-HA flies using primers specific to the *Pop2*-HA sequence, eliminating PCR amplification of endogenous *Pop2* mRNA; (right) *GFP* mRNA levels in ; *tim-gal4* ; UAS-*GFP* flies at 4 circadian times. N=1 replicate. Experiment done with Christian Papin, as well as Éric Jacquet & Naima Nhiri (QPCR facility, ICSN, Gif-sur-Yvette, France).

We could unexpectedly see similar low oscillations between *Pop2*-HA and *GFP* mRNAs, that corresponded to the ones observed for the POP2 protein in UAS-*Pop2*-HA flies

(Fig. 12), while in the same conditions, the GFP protein does not oscillate, probably due to a stronger stability. These results suggest that the expression of *Gal4* under the control of the *tim* promoter cycles and consequently leads to cycling of the targeted transgenes downstream of the UAS element. This was previously unknown, since the GAL4 protein is expected to be stable and control the expression of its target in a constitutive manner, this can lead to numerous biased experiments.

All in all, it seems that POP2 is not acting circadianly on *tim* through its mRNA or protein levels, phosphorylation, or localization. Additionally, the impact of PER on POP2's activity does not seem to be linked to any of these elements. We also brought evidence of potential remnant cyclic action of the UAS-GAL4 system when used with some cycling drivers, here *tim-gal4*. This discovery should encourage caution regarding the use of the UAS-GAL4 system that should be accompanied with verifications of absence of cycling of downstream transgenes.

Interestingly, the acquisition of our endogenous *Pop2*-HA fly line led to the discovery of a new *Pop2* isoform, expressed specifically in the head, which could play a specific role in the regulation of transcripts. Although this was not known in *Drosophila*, previous work had been published in human showing that *CNOT7* (human ortholog of *Pop2*) could be alternatively spliced, generating an isoform that would not act as a deadenylase, but instead localize in the cell nucleus and regulate alternative splicing (Chapat *et al.*, 2017). This is probably not our case though, as we could not detect POP2-HA signals from the endogenous POP2 in the nucleus of any cells in our IF experiments (Fig. S4), but this other isoform specific of the head could play a functional role specific to a cell population of the head, such as neurons, glial cells or photoreceptor cells. For example, in *Drosophila*, *elav* and *fne* were found to be necessary for the generation of neuronal transcript signature, consisting in the choice of neuronal specific alternative polyadenylation signals on transcripts expressed in neurons (Carrasco *et al.*, 2020).

To summarize, we successfully generated an endogenously tagged *Pop2*-HA fly line but could not detect any oscillations in the levels of *Pop2* mRNA, protein, or any phosphorylated forms of POP2. Nevertheless, we discovered a new isoform of *Pop2* that is specifically expressed in the head and could play a unique role in this tissue.

II. Study of POP2 specificity for *tim*

Although POP2 expression, phosphorylation and localization themselves are not impacted by circadian times, it is possible that a circadianly regulated partner of POP2 links this one to *tim* mRNA. Additionally, the existence of a specific POP2 partners that would also be specific of the *tim* mRNA could explain why POP2 regulates *tim* but not *per*.

1. Screening of RNA Binding Proteins related to POP2

The CCR4-NOT complex has been found to be recruited by several different RNA Binding Proteins (RBPs) (Raisch and Valkov, 2022), hence, immunoprecipitating POP2 with its protein partners followed by mass spectrometry analysis could reveal an RBP partner of POP2 that resumes the UAS-*Pop2*-RNAi phenotype once depleted in the clock cells. Such a screening was carried out previous my arrival in the lab in 2017 using UAS-*Pop2*-HA flies to ImmunoPrecipitate (IP) POP2-HA together with its protein partners, this experiment was realized in triplicates at 4 pooled CTs, CT0-3, 6-9, 12-15, 18-21. I will not describe these results further as they didn't lead to the identification of a potential partner linking POP2 to *tim* mRNA. Thus, we hypothesize that the UAS-*Pop2*-HA expressed under the control of *tim-gal4* presents too many biases to allow the identification of all its partners in a physiological context, as suggested by its abnormal nuclear localization (Fig. S3). This is why Brigitte Grima and Christian Papin proceeded to repeat this experiment, using the endogenous *Pop2*-HA flies newly acquired in the lab.

a. identifying the POP2 interactome with mass spectrometry

Pop2-HA and *w;stj*⁺ control flies were entrained through 4 pools of CTs, 5 replicates were prepared for each timepoints, immunoprecipitation of POP2-HA was carried out with anti-HA antibodies, and eluates were then delivered to the proteomics facility (SiCaPS) in I2BC, Gif-sur-Yvette, for mass spec analysis. CCR4-NOT components, such as NOT1, NOT3, RGA, and TWIN were found highly enriched with POP2, confirming proper IP of POP2 known partners. Additionally, POP2 interactors included many components of the ribosome or factors associated with translation, in line with reported interactions between the CCR4-NOT complex and the ribosomes (Allen *et al.*, 2021) (Fig. 22). Altogether, 69 proteins were found significantly enriched in *Pop2*-HA flies compared to WT control flies (adjusted p-value < 0.15) all timepoints combined (Table. 4). Out of those 69 proteins, 15 were found significantly cycling. Emphasis was put for genes presenting RNA related functions in their Gene Ontology molecular function, biological process or gene snapshot extracted from Flybase.

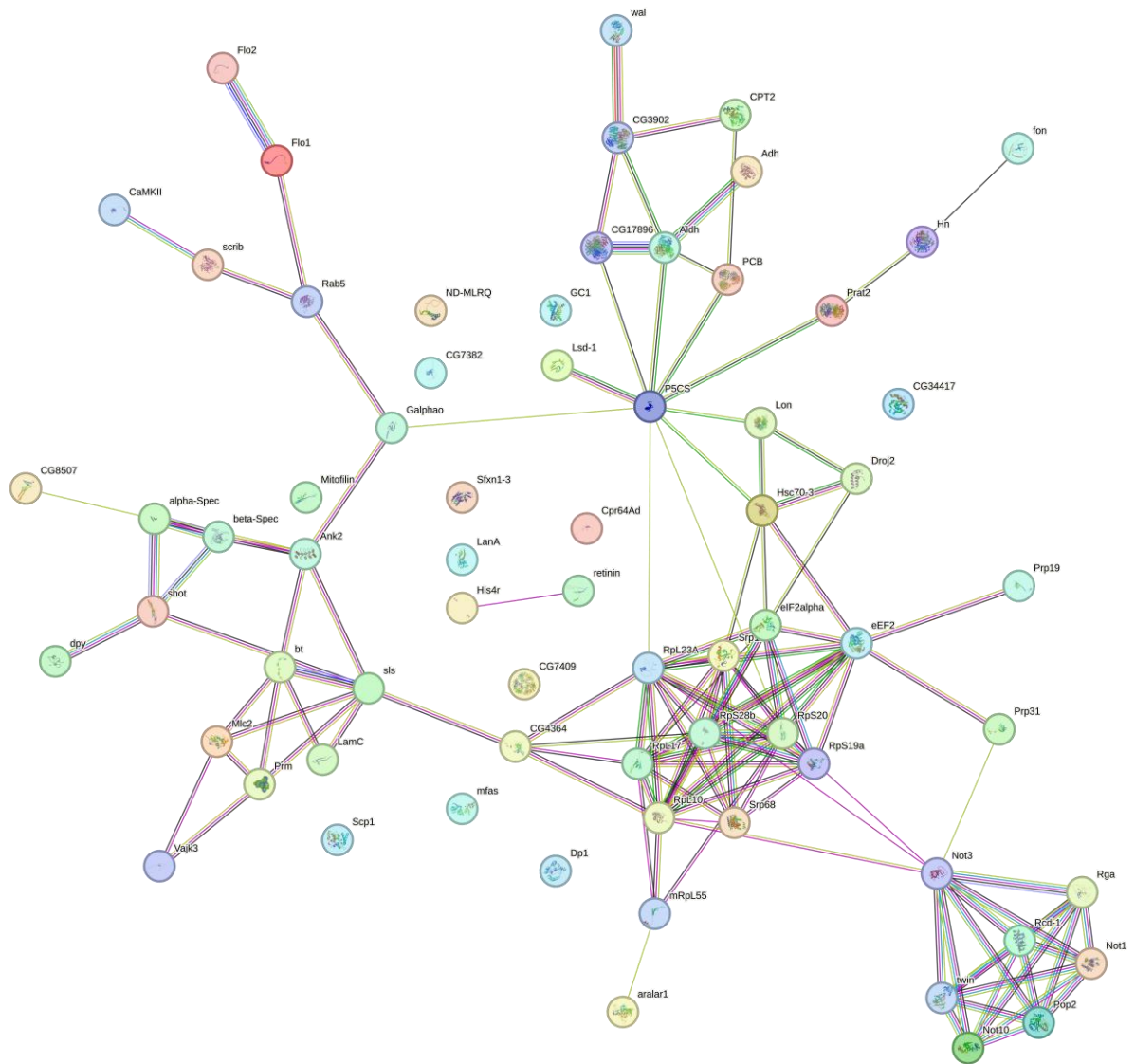


Figure 22 : Interaction network of proteins being enriched proteins in POP2-HA IP, analysed by MS, in at least 1 timepoint. Network realized on the STRING database version 12.0 (Szklarczyk et al., 2023). Cyan lines represent : curated interactions; magenta are experimentally determined; green, red and blue are predicted; yellow are text mined; black are co-expressions and purple are protein homology.

SYMBOL	Flybase ID	CT0-3		CT6-9		CT12-15		CT18-21		Cycling amp	reg p-value	rob-reg p-value
		Log2FC	-Log10 pvalue	Log2FC	-Log10 pvalue	Log2FC	-Log10 pvalue	Log2FC	-Log10 pvalue			
Not1	FBgn0085436	7,99	5,04	7,98	4,46	8,22	7,06	8,12	6,78			
Not3	FBgn0033029	7,29	9,33	7,48	7,13	7,39	7,48	8,14	7,71			
Rga	FBgn0017550	7,16	5,22	7,36	5,77	6,20	4,05	7,42	5,89			
Pop2	FBgn0036239	6,77	6,84	5,82	6,35	5,73	4,88	6,48	5,06			
twin	FBgn0011725	6,34	5,71	7,08	5,72	6,73	8,03	7,23	5,21			
Srp68	FBgn0035947	2,24	1,47	2,60	1,77	2,44	2,47	2,70	2,67			
Rcd-1	FBgn0031047	1,86	3,66			1,24	1,01	1,04	0,82			
P5CS	FBgn0037146	1,08	3,71	1,18	4,11	1,22	3,85	1,34	4,85			
eEF2	FBgn0000559	1,04	0,93							1,57	0,01	0,02
CG3902	FBgn0036824	1,03	1,59	1,92	1,45	1,45	1,94	1,45	3,27	0,45	0,17	0,17
CG8507	FBgn0037756	0,92	1,84									
Ank2	FBgn0261788	0,85	0,83									
His4r	FBgn0013981	0,81	2,77									
mRpL55	FBgn0038678	0,72	0,86									
bt	FBgn0005666	0,70	0,86	1,71	2,14							
Aldh	FBgn0012036	0,67	2,56			1,08	2,44	0,83	2,40			
beta-Spec	FBgn0250788	0,67	1,31									
alpha-Spec	FBgn0250789	0,61	1,16									0,16
Rp519a	FBgn0010412			4,06	1,60							
RpL17	FBgn0029897			3,35	1,22							
RpS28b	FBgn0030136			2,15	1,18					2,77	0,09	0,09
RpL23A	FBgn0026372			2,09	0,98	0,88	1,06	0,63	1,11			
FloZ	FBgn0264078			2,07	2,07							
RpL10	FBgn0024733			2,05	0,87							
Prm	FBgn0003149			1,80	1,33							0,12
CG7409	FBgn0035817			1,69	1,15	1,34	1,09			1,74	0,10	0,10
Not10	FBgn0260444			1,65	1,23	1,79	1,35	0,93	0,97			
Cpr64Ad	FBgn0035513			1,63	1,17			1,66	1,07			
mfas	FBgn0260745			1,57	1,37							
Scp1	FBgn0020908			1,43	1,00							
RpS20	FBgn0019936			1,35	1,02					0,71	0,05	0,05
Sfxn1-3	FBgn0037239			1,34	1,17							
wal	FBgn0010516			1,24	1,06							
dpy	FBgn0053196			1,19	1,33					1,76	0,01	0,05
Galphao	FBgn0001122			1,19	1,02			0,88	0,85			
CaMKII	FBgn0264607			1,18	0,85							
PCB	FBgn0027580			1,16	2,26	1,20	1,90	0,91	2,61			
CG4364	FBgn0032138			1,14	1,11			0,76	0,97			
Adh	FBgn0000055			1,13	0,90	1,19	1,06	1,33	1,11			
Mitofilin	FBgn0019960			1,11	1,58							
Flo1	FBgn0024754			1,10	0,85							
Mlc2	FBgn0002773			1,08	1,16					1,64	0,05	0,11
scrib	FBgn0263289			1,06	0,99					1,89	0,00	0,00
shot	FBgn0013733			1,04	1,22							
Lsd-1	FBgn0039114			1,03	1,02							
Prat2	FBgn0041194			0,97	0,90							
Hn	FBgn0001208			0,97	0,86					1,93	0,09	0,09
Prp19	FBgn0261119			0,96	0,85	0,81	0,89					
LamC	FBgn0010397			0,90	0,87							
CG34417	FBgn0085446			0,89	1,15					0,77	0,15	0,07
sls	FBgn0086906			0,87	0,95							
CG7382	FBgn0031708			0,86	0,98							
aralar1	FBgn0028646			0,76	0,93	0,64	1,52					
LanA	FBgn0002526			0,65	0,97							
Hsc70-3	FBgn0001218			0,65	1,63							
Lon	FBgn0036892			0,64	0,88	0,91	0,87					
Rab5	FBgn0014010			0,61	1,02					0,66	0,15	0,15
CG17896	FBgn0023537					2,42	1,07			2,02	0,04	0,05
ND-MLRQ	FBgn0052230					1,26	2,02					
Srp19	FBgn0015298					0,94	0,90	0,98	1,48			
GC1	FBgn0260743					0,85	1,15					
retinin	FBgn0040074					0,77	0,83					
Prp31	FBgn0036487					0,75	1,07					
Dp1	FBgn0027835					0,71	1,31	0,78	1,07			
fon	FBgn0032773							1,20	1,87	1,00	0,12	0,15
eIF2alpha	FBgn0261609							1,17	0,89			
CPT2	FBgn0035383							1,16	1,69			
Droj2	FBgn0038145							0,82	1,00	0,71	0,10	0,06
Vajk3	FBgn0028544							0,72	0,95	1,43	0,11	0,12

Table 4 : Genes significantly found enriched with POP2-HA in IP in drosophila heads at 4 pools of CTs, cycling amp : cycling amplitude, reg p-value : regression p-value, rob reg p-value : robust regression p-value.

b. POP2 interactors screening shows several RBPs impacting the flies' behavior

Genes presenting RNA related functions or high enrichment were analyzed further through behavioral activity rhythm assessment, TIM/PER protein/mRNA cycling

analysis on flies depleted or mutated for the gene of interest. This strategy aimed at identifying RBPs presenting similar effects than POP2 on the clock upon depletion. In parallel, genes found to regulate or recruit the CCR4-NOT to its targets in the literature were also investigated. From both the literature and the MS results, ~82 genes were tested in behavior with various mutants and RNAi lines. The ones causing robust alterations in the flies' behavior (arrhythmicity, long/short period) in DD were further investigated to see whether these flies presented altered cycling of TIM and/or PER proteins. Here I selected the results of behavioral experiments for 9 genes of interest that were studied in WB analysis (Table. 5). Briefly, no robust differences were found for TIM levels with any of these candidates, except for the gene *lingerer*.

Symbol	Crosses	NumTotal	NumAlive	%Rhythmic	Tau (period)	sem	Power	sem
Controls	dicer-timgal4xw	16	15	100.0	24.2	0.08	78.5	9.40
	dicer-gal1118xw	15	15	100.0	24.1	0.06	319.3	8.68
	timgal4xw	16	14	87.5	24.5	0.21	153.9	19.00
	gal1118xw	16	15	100.0	24.2	0.07	180.2	10.51
CaMKII	dicer-gal1118x38930	16	13	100.0	24.5	0.11	136.9	22.81
	dicer-timgal4x38930	16	15	46.7	24.6	0.20	39.9	5.01
	gal1118x29665	16	15	100.0	24.6	0.05	178.9	16.62
	timgal4x29665	16	14	64.3	25.8	0.30	80.6	14.84
	dicer-gal1118x29401	16	16	100.0	23.8	0.08	93.9	8.80
	dicer-timgal4x29401	16	16	62.5	23.9	0.24	68.0	11.12
	dicer-gal1118x100265	16	15	100.0	23.7	0.07	145.3	7.57
	dicer-timgal4x100265	16	15	66.7	23.5	0.22	72.8	11.75
Flo2	dicer-gal1118x31525	16	15	100.0	24.5	0.03	143.0	17.58
	dicer-timgal4x31525	16	16	50.0	24.6	0.11	64.9	16.21
	13065*	18	18	94.4	23.8	0.07	129.8	12.93
	dicer-timgal4x31525	16	15	66.7	24.2	0.19	89.5	16.08
Prat2	timgal4x51492	16	16	68.8	23.8	0.26	84.6	13.19
	dicer-timgal4x90991	16	14	78.6	23.6	0.15	69.0	
	dicer-gal1118x90991	16	16	100.0	24.5	0.05	210.7	12.61
	gal1118x51492	16	13	100.0	24.4	0.06	143.1	12.31
	dicer-timgal4x90991	16	16	100.0	24.3	0.13	95.0	8.00
	timgal4x90991	16	15	93.3	24.2	0.11	108.9	18.53
Smg6	81034*x81045*	9	9	77.8	26.6	0.20	130.4	17.65
	81045*x81035*	22	18	44.4	26.4	0.57	57.6	11.81
	81045*x24998(df)	15	12	100.0	27.1	0.14	147.3	12.62
ssp3	dicer-gal1118x105858	16	16	25.0	23.1	0.31	64.1	16.55
	dicer-timgal4x105858	8	8	25.0	29.8	5.25	45.8	23.24
	80635*	13	13	76.9	26.2	2.34	100.9	16.76
Rbp	gal1118x29312	16	15	100.0	24.1	0.05	204.6	11.92
	dicer-timgal4x29312	16	16	81.2	23.8	0.15	117.7	16.40
	timgal4x29312	24	24	33.3	25.4	1.27	112.5	
	timgal4x54828	16	16	43.8	34.2	2.70	36.3	5.57
	gal1118x54828	10	10	50.0	29.0	0.45	72.2	13.92
lig	dicer-gal1118x103948	16	16	62.5	24.5	1.22	62.5	7.04
	dicer-timgal4x103948	16	14	28.6	28.0	4.77	29.9	3.91
twin	dicer-gal1118x104442	16	14	100.0	23.8	0.07	165.9	17.14
	dicer-timgal4x104442	16	16	43.8	23.5	0.15	51.2	5.97
	timgal4x104442	16	16	68.8	23.8	0.22	93.1	14.68
	gal1118x104442	16	16	100.0	23.8	0.08	166.7	8.46
Srp68	dicer-gal1118x104867	16	16	31.2	24.0	0.52	55.8	29.19
	dicer-timgal4x104867	6	6	33.3	23.8	0.25	56.7	16.23
	dicergal1118x27351	16	16	87.5	23.7	0.88	120.9	11.70
	dicer-timgal4x27351	8	8	12.5	25.5	0.00	30.9	0.00

Table 5 : Summary of the cycle_p analysis of male flies depleted or mutated for endogenous POP2 interactors analyzed in DD condition at 25°C after a minimum of 3 days of entrainment in LD condition. Dicer was added in some crosses in order to improve RNAi production. Mutant lines are represented followed by an asterisk (*) following their Bloomington or VDRC line numbers, df stands for deficiency. Flies were selected for further experiment when

rhythmicity < 80% and/or period increased or decreased by more than 1h. Example controls were added as reference, w stands for w- flies.

c. LIG regulates the clock via TIM protein but not tim mRNA

Lingerer is a putative RBP that interacts genetically with *Orb2*, *FMR1*, *Capr*, *Rin* and physically with *Orb2* & probably *Rin* that are involved in the regulation of memory formation (Kimura *et al.*, 2015) and of tissue growth (Baumgartner, Stocker and Hafen, 2013), respectively. Most interestingly, *Capr* and *FMR1* human orthologs have been shown in vitro to form condensates that increases deadenylation by CNOT7 (human ortholog of POP2) to repress translation of target transcripts (Kim *et al.*, 2019), making *lig* a promising candidate. *Lig* depletion caused strong arrhythmicity in the fly behavior (Table. 5), and, although *lingerer* depletion did not cause any changes in the overall levels of TIM proteins, it did affect its phosphorylation status (Fig. 23). We see that TIM is mainly dephosphorylated when *lig* is depleted in *tim+* cells, indicating a potential role of *lig* in the post-translational control of TIM. Although the phenotype observed is not the same as the one in *Pop2* depletion, it could still be relevant to investigate this candidate further. Interestingly, when quantifying TIM and PER in the sLNvs doing IF in flies expressing or not *lig*-RNAi (Fig. 24), we could indeed see for TIM an increased level at CT3 and a reduction at CT21 compared to control, looking like a delayed expression of TIM.

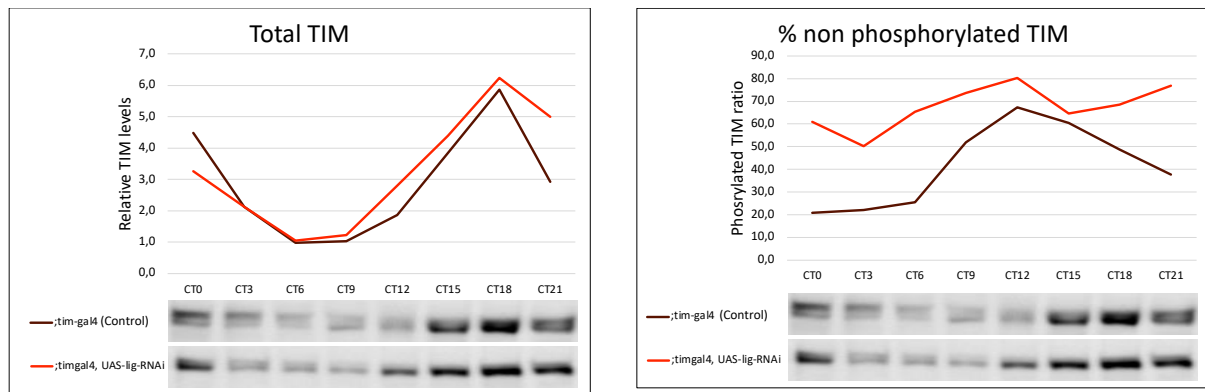


Figure 23 : Western Blot analysis of TIM levels of proportion of dephosphorylated TIM in Drosophila heads in presence or absence of UAS-lig-RNAi under the control of the tim-gal4 driver, experiment realized over 8CTs. Quantification from 1 replicate. Experiment realized by Christian Papin.

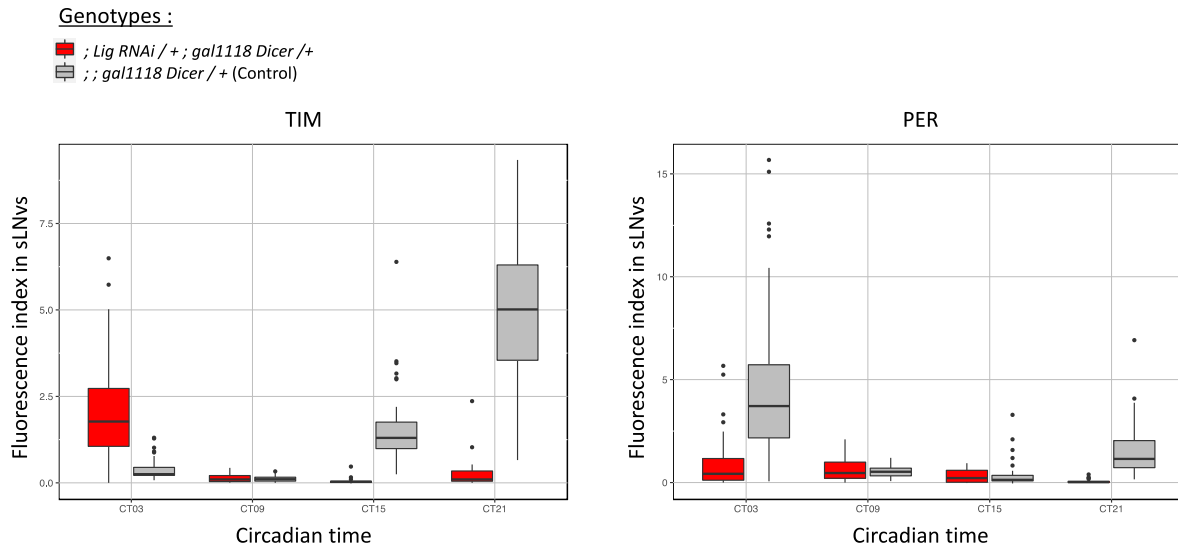


Figure 24 : IF quantification of *TIM* levels in the sLNvs during 4CTs, in *UAS-lig-RNAi* and control flies using the *gal1118 Dicer* driver.

As for *PER*, we could see a reduction of its levels in *lig*-RNAi condition compared to control at CT3 and 21, leading to overall low levels of *PER* in the sLNvs. This exciting discovery was followed with an RT-qPCR experiment in *lig*-RNAi condition for 8 timepoints to investigate whether *lig* could be involved in the post-transcriptional control of *tim*, which would hint towards a link with POP2 (Fig. 25). Unfortunately, no differences were seen between *lig*-RNAi and control conditions for the levels of *tim* and *per* mRNAs as well as for the levels of pre-*tim* and pre-*per*. Yet the depletion of *lig* was confirmed in the RT-qPCR results, where we could also see that *lig* mRNA is expressed in a stable manner through the circadian times (Fig. S5).

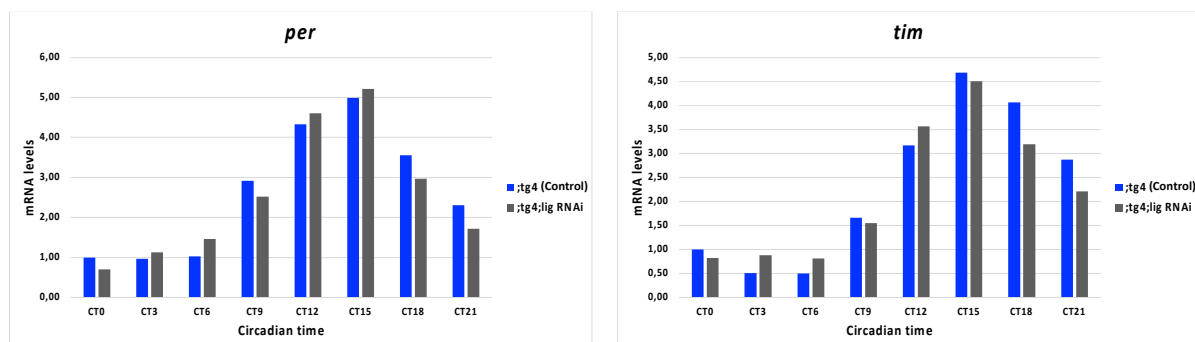


Figure 25 : RT-qPCR quantification of *per* & *tim* mRNAs at 8 circadian times in presence or absence of *lig*-RNAi under the control of *tim-gal4* driver. N=1 replicate. Experiment done with Christian Papin, Éric Jacquet & Naima Nhiri.

To summarize, we tested many partners of POP2 to find an RBP that could link it to *tim*, the most interesting candidate was *LIG*, a putative RBP related to P-bodies components that, upon depletion, caused alterations in the flies' locomotor activity and disturbed the phosphorylation rate of *TIM* in the heads and modified the levels of

TIM and PER in the sLNvs, yet this role seems limited to post-translational mechanisms, as the mRNA levels of both *tim* and *per* were unaltered upon *lig* depletion.

2. Analysis of *tim* mRNA modifications machinery components

We investigated the hypothesis that *tim* but not *per* could be targeted by mRNA modifications, such as m6A, m5C, and pseudouridylation that could trigger its destabilization through the recruitment of CCR4-NOT via reader proteins, as it was suggested in humans (Du *et al.*, 2016). Additionally, *tim* was found with one potential m6A modification in the *Drosophila* heads in a miCLIP dataset (Supplementary data 5 - Ythdf comparisons) (Kan *et al.*, 2021). We thus collaborated with Jean-Yves Roignant and Lina Worpenberg (Unil, Lausanne, Switzerland), using mutant fly lines for mRNA modification writers, readers and erasers (Table. S2).

a. *Mettl3* mutant flies are short period in constant darkness.

The behavioral assay in DD showed a strong arrhythmicity in the *Mettl3Δ6* catalytic mutant, which was not retrieved with the *Mettl3Δ1.7* null mutant, suggesting a gain of function in the catalytic mutant (Table. 6)

Genotype	NumTotal	NumAlive	%Rhythmic	Tau (period)	sem	Power	sem
<i>w;stj+</i> (control)	16	16	100.0	23.6	0.09	112.7	10.97
Δ CG1582	32	32	100.0	23.6	0.06	125.7	7.43
Δ CG1582CTRL	32	28	96.4	23.5	0.06	159.5	9.63
Δ CG6144	32	31	100.0	23.7	0.05	107.2	7.57
Δ CG6144CTRL	32	32	100.0	23.8	0.06	104.8	9.09
<i>Mettl3Δ1.7</i>	28	19	84.2	22.9	0.11	72.3	9.77
<i>Mettl3Δ6</i>	8	6	33.3	22.8	0.25	29.8	0.74
<i>pus3KO</i>	32	31	87.1	24.1	0.03	108.7	10.24
<i>pus7KO</i>	32	29	89.7	24.0	0.09	127.4	7.09
<i>pusL1KO17.2</i>	32	31	100.0	23.1	0.06	99.4	9.29

Table 6 : Behavior analysis of flies mutated for mRNA modification machinery components, details of each line in (Table. S2), measured in constant darkness at 25°C after 3 days of entrainment in LD 12h-12h conditions.

These results suggest a strong effect of the *Mettl3Δ6* catalytic mutant on the rhythmicity of the flies, while the *Mettl3Δ1.7* null mutant displayed a slightly shorter period with a mild decrease of rhythmicity. Yet the *Mettl3Δ6* mutant line had already been investigated previously in the lab and yielded unreproducible results, we thus turned to the *Mettl3Δ1.7* mutant in order to support or not a role of *Mettl3* in *tim* mRNA levels.

b. *Mettl3Δ1.7* does not resume the effect of POP2 depletion on *tim* mRNA

RT-qPCR experiments realized at 8 timepoints in both DD (CT) and LD (ZT) conditions in *Mettl3Δ1.7* and *w;stj+* control flies in presence of absence of PER revealed a reduction of *tim* mRNA levels at ZT12-21 and CT9-15 in *Mettl3* mutant conditions (Fig. 26), while *per* was mainly unaffected. This effect was visible for *tim* in presence of PER

only, and pre-*tim* mRNA levels quantifications showed the same effect (Fig. S6), suggesting that it was caused at the transcriptional level.

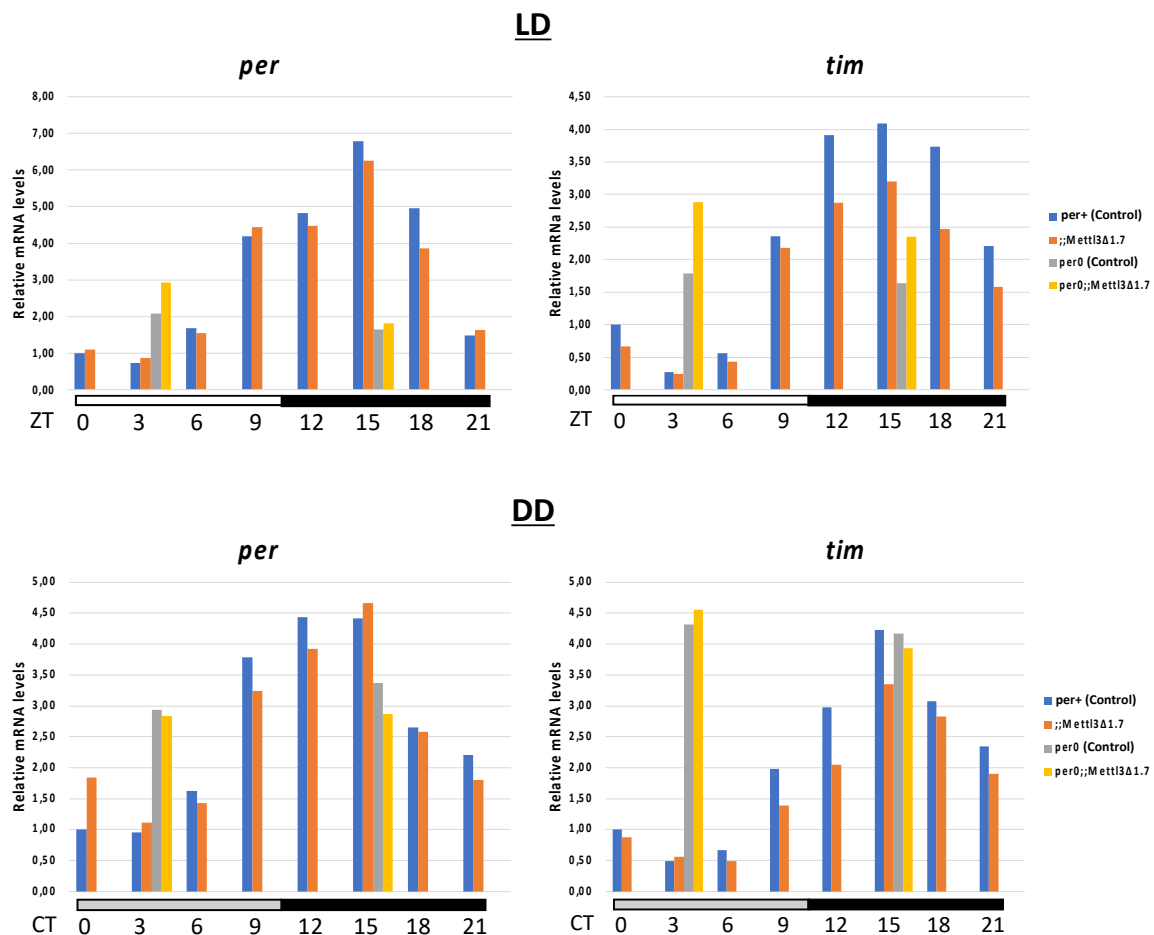


Figure 26 : RT-qPCR quantification of *per* & *tim* mRNA at 8 circadian times in presence or absence of *Mettl3Δ1.7* null mutant. N=1 replicate. Experiment done with Christian Papin, Éric Jacquet & Naima Nhiri.

Although we do see an effect of *Mettl3* on *tim* mRNA, this one does not resume the effect of POP2 on *tim*, behaviorally and molecularly, plus, this shows a transcriptional regulation of *Mettl3* on *tim*, but not necessarily a post-transcriptional one. It seems that *Mettl3*'s action on *tim* cannot link it with POP2.

3. Discussion

- RNA binding proteins

The search of an intermediate between POP2 and *tim*, that might explain both the circadian and specific action of POP2 has not been discovered yet. Indeed the mass spec analysis of co-immunoprecipitated POP2 partners yielded satisfactory results, displaying the components of the CCR4-NOT complex and ribosome-related proteins, with most proteins enriched uniquely in the endogenous POP2-HA IP of 2021 experiment compared to the ones found in the exogenous POP2-HA IP of 2017 (49/69 uniquely enriched proteins in 2021 vs 2017) and 15/69 proteins enriched in a circadian manner, yet the candidates that were screened further only revealed *lingerer* as a

regulator of the clock. *Lingerer* seems to regulate the molecular clock at the post-translational level by affecting the phosphorylation status of TIM in the heads and the levels of TIM and PER in the sLNVs. But no effect of *lingerer* at the mRNA level for *tim* and *per* was found. Hence the screening for a protein intermediate between POP2 and *tim* revealed unfruitful. Several explanations can be formulated, first, although the 2017 experiment was biased by the use of UAS-*Pop2*-HA flies that present abnormal oscillations of *Pop2* mRNA and protein levels and localization (See Fig 21, 12, S2), this fly line still has the advantage of expressing POP2 specifically in *tim*⁺ cells, allowing the analysis of enriched POP2 partners in the cell subset of interest. On the other hand, the 2021 screening relied on the use of endogenously-expressing *Pop2*-HA flies, which, although more physiological, has the flaw of being expressed everywhere in a ubiquitous manner, which could easily mask the detection of POP2 partners that would be bound to POP2 only in *tim* positive cells. Although we hoped that the detection of cycling partners could overcome this limit, it might not have been enough.

Second, it is possible that this intermediate is a ubiquitous factor, found on many other mRNAs, which would then likely make it one of the proteins enriched with POP2 in our experiment, but the screening method employed to identify this protein consisted in depleting it with RNAi lines or using mutants for this gene. This approach is limiting, as we already experienced difficulties working with CCR4-NOT components, indeed, mutants of *Not1* and *Pop2* are lethal in homozygous flies, similarly, using RNAi targeting *Pop2* causes lethality if the crosses are reared at 25°C, due to high depletion of *Pop2*. It is thus possible that the intermediate between POP2 and *tim* reveals essential for the overall cell physiology and causes lethality upon depletion/mutation, while the tested RNAi lines showing flies survival could have been too weak to cause any phenotypes at all.

Third, the intermediate could be rescued by another factor upon depletion.

Fourth, in vitro experiments studying the deadenylation of purified human CCR4-NOT complex components in different conditions, (pH, divalent cations concentrations, RNA substrates, CCR4-NOT complex components) showed that the CCR4-NOT components present RNA affinity (Raisch *et al.*, 2019; Chen *et al.*, 2021), which was also true in yeast (Bhaskar *et al.*, 2013). Although the CCR4-CAF1 deadenylases alone can bind RNAs directly, this binding is much less efficient than the one observed with the full CCR4-NOT complex, which additionally provides substrate specificity, it should thus be considered that the specificity observed between POP2 and *tim* mRNA could be directly due to another component of the CCR4-NOT complex, which would reveal hard to prove, as K.D of any component of the complex could cause overall destabilization of this one, which would ultimately lead to the same phenotype observed in absence of POP2.

Fifth, others showed that RBPs can not only recruit the CCR4-NOT complex to an mRNA, but also compete with it, and particularly the CAF40 subunit (RCD-1 in *Drosophila*), where peptides can bind to its RNA interaction domains in a competitive manner (Raisch *et al.*, 2019). It is thus possible that POP2 is not specific of *tim* mRNA, *per se*, but rather is repelled from some mRNAs, like *per*, thanks to RBPs protecting

them by binding the CCR4-NOT complex. In which case, depletion of these RBPs interacting with the CCR4-NOT complex should not be expected to resume the effect of *Pop2* depletion.

Sixth, the specificity of POP2 for *tim* could be indirect, for example through differential localizations of the mRNAs, for instance, *tim* and *per* mRNAs could localize in different RNP granules where the CCR4-NOT complex would localize only in the ones containing *tim*, but not *per*. This hypothesis is not very likely however, as although CNOT1 (NOT1 in *Drosophila*) forms granules upon cellular stress (using arsenite) (Panasenکو *et al.*, 2019), we did not see clear punctae in our confocal microscopy images of the endogenous POP2-HA protein (Fig. S4), instead our signal seemed diffused in the cytoplasm, unlike what was previously documented in *Drosophila* embryos (Temme *et al.*, 2010).

Another approach we considered was to overlap the proteins partners bound to POP2 identified in our mass spec experiment and the ones bound to *tim* mRNA by carrying out an mRNP capture (Wippich and Ephrussi, 2019), this method consists in hybridizing a transcript of interest, here *tim*, using biotinylated DNA probes, together with its bound proteins, thanks to cross-linking, to then identify the proteins bound to the transcript by mass spec. The limit with this method is the need for massive starting material to be able to identify successfully the RBPome of a transcript. In the article adapting this method in *Drosophila*, 10-15mL of egg-chambers were used per conditions to yield enough RNA recovery to be able to identify their bound proteins in mass spec. While *tim* is relatively highly expressed in the head according to the ModENCODE and FlyAtlas2 RNA-seq datasets available in FlyBase (Graveley *et al.*, 2011; Krause *et al.*, 2022), *oskar*, the transcript used for the mRNP capture protocol, is up to 10 fold more expressed in the ovaries than *tim* in the head, reducing our chances to recover the *tim* mRNA as efficiently. Additionally, collecting 10-15mL of heads probably represents tens of thousands of heads, this project was thus abandoned.

- *Tim* mRNA modifications

Behavioral assessment of mutant fly lines for m6A, m5C, pseudouridylation, but also cap methyltransferases (gift from Matthias Soller) only revealed a short period for *Mettl3* mutant flies, which was probably caused by *tim* mRNA transcriptional decrease in mutant flies. Although this supports the existence of a regulation of *Mettl3* on the clock through *tim*, this role is likely not attributable to post-transcriptional control. This could seem surprising, as mRNA modifications are expected to impact mRNA stability, translation, but not transcription. Yet, a regulation of transcription through m6A modifications of RNAs has been reported in mammals (Patil *et al.*, 2016; Liu *et al.*, 2020) where, for the first article, the transcriptional silencing of the X-chromosome in human cells through the *XIST* lncRNA is impaired upon *Mettl3* depletion, the second article proposed that m6A modification of chromosome-associated regulatory RNAs (carRNAs) can impact neighbor chromatin state, and consequently, the transcription of downstream genes. More recent work proposed that the transcribed RNAs themselves, upon addition of m6A modifications on their transcripts could recruit the

DNA 5-methylcytosine demethylase TET1 via the m6A reader FXR1 leading to modified transcription of the m6A modified transcript's gene (Deng *et al.*, 2022). If similar regulations of transcription exist in *Drosophila*, these could explain the reduction of *tim* transcription in *Mettl3* mutant flies.

III. Exploring the role of POP2 on the translation of circadianly-regulated genes

1. Article

Control of *Drosophila* cycling transcripts' levels and translation by the POP2 deadenylase depends on their abundance

Thierry Cottineau¹, Béatrice Martin¹, Christian Papin¹, Letizia Cybi¹, Jérôme E Roger¹, Naïma Nhiri², Eric Jacquet², François Rouyer^{1*}, and Brigitte Grima^{1*}

¹ Institut des Neurosciences Paris-Saclay (NeuroPSI), Université Paris-Saclay, CNRS, 91400 Saclay, France

² Institut de Chimie des Substances Naturelles (ICSN), Université Paris-Saclay, CNRS, 91190 Gif-sur-Yvette, France

[†] These authors contributed equally

* Corresponding authors

Abstract

In the *Drosophila* circadian clock, a negative feedback loop involves the CLOCK (CLK) and CYCLE (CYC) transcription factors which induce the expression of many cycling transcripts including *period* (*per*) and *timeless* (*tim*). The PER and TIM proteins then inhibit the activity of CLK and CYC, thus generating an oscillation. The delay between the mRNA oscillation and the protein oscillation is a key part of the circadian clockwork, and appears to be mostly contributed by post-translational mechanisms. Here, using TRAP experiments to compare total and ribosome-bound mRNAs, we reveal a translational contribution to the oscillations of the PER, TIM and VRILLE (VRI) clock proteins. We previously reported that the *tim* mRNA was post-transcriptionally regulated by the POP2 deadenylase. We show here that translation of the *tim*, *vri* as well as several other circadianly-regulated genes are under POP2 control. Importantly, POP2-regulated transcripts are more strongly impacted when their abundance is low. We propose that the POP2 deadenylase contributes to protein oscillations by destabilizing mRNAs and inhibing their translation at trough levels.

Keywords : circadian rhythms, clock genes, CCR4-NOT, POP2, translation, mRNA poly(A) tail

Introduction

Circadian clocks have evolved in most living organisms to allow the adaptation of their physiology and behavior to day-night cycles. At the cellular level, the molecular clocks often consist in transcription-translation negative feedback loops of clock genes that will inhibit their own transcription in a circadian manner (Mendoza-Viveros *et al.*, 2017). In *Drosophila*, the core loop includes the *period* (*per*) and *timeless* (*tim*) mRNAs that accumulate in the second part of the day due to the activation of their transcription promoted by CLOCK (CLK) and CYCLE (CYC). PER and TIM proteins accumulate at night, with the heterodimerization of PER/TIM preceding the nuclear entry of the proteins at night. In the nucleus, PER interacts with the CLK-CYC complex to inhibit the expression of the *per* and *tim* genes as well as other clock-controlled-genes (Dubowy and Sehgal, 2017). A secondary feedback loop involves the control of Clk gene expression by the PDP1 and VRI transcriptional regulators (Blau and Young, 1999; Cyran *et al.*, 2003; Glossop *et al.*, 2003). A key step here for the generation of rhythmicity is the delay between the transcription and the accumulation of TIM and PER proteins which, so far, has been largely attributed to post-translational regulations of TIM and PER targeting their stability, nuclear entry, and PER repressor activity (Szabó *et al.*, 2018; Li *et al.*, 2019; Giesecke *et al.*, 2023). Nevertheless, several studies reported a time interval between *per* transcription and mRNA level peaks, likely due to post-transcriptional regulations of *per*, while the existence of such time interval was uncertain for *tim* (So, 1997; Rodriguez *et al.*, 2013; Yu and Rosbash, 2023). Yet, different studies revealed the existence of co-/post-transcriptional regulations of *tim* (Chen and Rosbash, 2016; Shakhmantsir *et al.*, 2018; Foley *et al.*, 2019; Grima *et al.*, 2019; Martin Anduaga *et al.*, 2019). This includes a role for the CCR4-NOT complex, which contains two poly(A)-specific ribonucleases, *twin* (Ccr4 in *S. cerevisiae*) (Joly *et al.*, 2013) and *Pop2* (Caf1 in *S. cerevisiae*) (Temme *et al.*, 2004, 2010) and regulates both mRNA half-life and translation (Collart, 2016; Collart, Audebert and Bushell, 2023). In *Drosophila*, POP2 controls the levels of *tim* mRNA by shortening its polyA tail (Grima *et al.*, 2019). Surprisingly, the absence of PER reduced the destabilization effect of POP2 on *tim* mRNA (Grima *et al.*, 2019).

Here, we present evidence for a POP2-dependent regulation of the *tim* mRNA translation through the control *tim* mRNA poly(A) tail. Furthermore, RNA-seq experiments identified *vri* as another POP2-regulated mRNA. The POP2-dependent control of *tim*, *vri* and its other target mRNAs appears to depend on their levels, suggesting that POP2 regulates the amplitude of the oscillations of cycling transcripts.

Results

***per* and *tim* mRNAs show a circadian control of their translatability.**

To study the translational control of *tim* and *per* mRNAs, we used the TRAP (Translating Ribosome Affinity Purification) followed by RT-qPCR method to quantify total mRNAs as well as ribosome-bound mRNAs from *Drosophila* heads expressing the

flag-tagged RPL13A ribosomal protein in the *tim* positive cells through 8 timepoints in constant darkness (DD). RPL13AF3 expressing flies (Huang *et al.*, 2019) were used rather than RPL10A-GFP (Huang *et al.*, 2013) as they provide high yield of immunoprecipitated RNA, without affecting the circadian rhythms in DD (Fig. S1A) and lead to relatively low aspecific RNA immunoprecipitation (Fig. S1B). The ribosome-bound fraction showed oscillations for *per* and *tim* mRNAs close to the ones observed in the total mRNA fraction (Fig. 1A), as well as to oscillations reported in a previous study (Huang *et al.*, 2013). Interestingly, the phase of *tim* and *per* ribosome-bound mRNAs presented a phase delay of approximately 2-3h compared to total *tim* and *per* mRNAs. However, normalizing the ribosome-bound mRNA levels by the total mRNA levels for *per* and *tim* allowed to define the levels of mRNAs bound to ribosomes independently of their total levels in a given condition, and thus to approximate their translatability levels. Translatability curves of *tim* and *per* mRNAs revealed an oscillation, detected with the dryR Im function (Weger *et al.*, 2021), with an amplitude of approximately 2-fold and a peak at CT0 for *tim* and CT3 for *per* (Fig. 1B), while housekeeping genes did not show such cycling translatability (Fig. S1C). Surprisingly, when comparing *tim* and *per* translatability cycling patterns with the expression levels of their proteins (Fig. 1C), *per* presented a close cycling pattern. For *tim* the pattern of translatability followed only the tendencies of the cycling protein curve profile, particularly the trough of translatability of *tim* at CT9 matching with the delayed increase of TIM protein levels compared to *tim* mRNAs already rising from CT6. These results suggest that the regulation of the translatability of *tim* and *per* could constitute a new layer of control of the cyclic expression of these gene products, that may participate in the delay between mRNA and protein oscillations.

***tim* mRNA shows translational control by the deadenylase POP2 through its polyadenylation status.**

Previous results indicated that POP2 specifically controls *tim* mRNA stability by deadenylating it during subjective morning, in a PER-dependent manner (Grima *et al.*, 2019). Poly(A) tails have been associated with translation (Lim *et al.*, 2016; Park *et al.*, 2016; Lima *et al.*, 2017; Passmore and Coller, 2021) in different organisms including *Drosophila*, and we thus decided to investigate the possibility that POP2 not only regulates *tim* stability, but also its translatability, by following the quantity of mRNAs bound to ribosomes in *Pop2 K.D* flies. We performed TRAP RT-qPCR experiments for *tim* and *per* mRNAs on 8 timepoints in *per*⁺ flies and 4 timepoints in *per*⁰ flies in DD both in presence or absence of UAS-*Pop2*-RNAi (Fig. 2A). *tim* translatability was decreased in *per*⁰ context compared to *per*⁺ (Fig. 2B), suggesting that PER upregulates slightly *tim*'s translatability, we verified a potential interaction between *tim* mRNA and PER protein by RNA-IP and could not detect any enrichment of *tim* with PER compared to housekeeping genes (Data not shown). The translatability of *tim* mRNA in *Pop2 K.D* context was increased at least by one log₂ at all times in *per*⁺ and *per*⁰ conditions (Fig. 2B), as well as delayed in the phase of translatability of *tim* when *Pop2* was depleted. On the other hand, *per* translatability level was not impacted by POP2, as in UAS-*Pop2*-

RNAi flies, only a phase delay of *per* translatability was observed (Fig. 2B). Surprisingly, although the translatability of *tim* still oscillates in UAS-*Pop2*-RNAi context, the quantity of *tim* bound to ribosomes in that condition are very high and stable at all times (Fig. S1D), highlighting the importance of POP2 for *tim*'s circadian binding to ribosomes.

We next followed the poly(A) tail length of *tim* from the total, as well as the ribosome-bound mRNA fractions (Fig. 2C). As previously described (Grima *et al.*, 2019) for the total mRNA fraction in *per*⁺ and *per*⁰ flies, *tim* was deadenylated. However, when *Pop2* was depleted, the poly(A) tail length of *tim* increased, being more polyadenylated during subjective day than night. Conversely, in the ribosome-bound fraction, whereas *tim* was deadenylated in *per*⁺ and *per*⁰ flies, when *Pop2* was depleted, *tim* was mainly in its polyadenylated form, even during subjective night, where this polyadenylated form was dim in the total fraction. The same was observed in *per*⁰ condition, supporting the hypothesis that polyadenylated forms of *tim* mRNA are preferentially bound to the ribosomes, explaining why, even when there is no visible increase in the stability of *tim* in *per*⁰ or *per*⁺ during subjective night in *Pop2* *K.D* context, the translatability of *tim* is still increased, as low levels of polyadenylated *tim* are strongly interacting with ribosomes.

***tim* total mRNA levels define the destabilization effect of POP2.**

Since the effect of POP2 on *tim* total mRNA stability was present only in *per*⁺ condition and during the subjective day (Fig. 2A), the presence or absence of PER itself is not sufficient to explain how POP2 regulates *tim*, as PER is highly expressed during the end of the subjective night (Fig. 1C). In addition, in both *per*⁺ subjective night, and *per*⁰ conditions, the levels of *tim* mRNA were at the highest. This suggested that the control of POP2 on *tim* mRNA stability could depend on *tim* mRNA levels. To test this hypothesis, mutants and environmental conditions known to alter the levels of *tim* mRNA were selected (Allada *et al.*, 1998; Matsumoto *et al.*, 1999). Each condition was made with and without UAS-*Pop2*-RNAi, in order to follow the impact of POP2 according to *tim* mRNA levels for each condition by RT-qPCR. The presence of UAS-*Pop2*-RNAi increased the stability of *tim* mRNA in conditions where *tim* was expressed at low levels, while conditions showing high levels of *tim*, like *per*⁺ CT15, LL2, *per*⁰, showed no/weak changes of *tim* levels (Fig. 3A). Additionally, the poly(A) tail length of *tim* mRNA in *Pop2* *K.D* conditions coincided with the stabilization effect (Fig. 3C): conditions showing stronger polyadenylated signal than deadenylated one also displayed increased stability of *tim* mRNA. In contrast, *per* mRNA levels were mainly unaffected by *Pop2* *K.D*. Importantly, pre-*tim* levels were quantified in all the conditions to confirm that the effect of POP2 on *tim* was impacting its stability, and not its transcription levels (Fig. S2A). The depletion of POP2 was also verified for all these conditions (Fig. S2B). Finally, we plotted the replicates average levels of *tim* in each condition with the delta of average levels of *tim* in presence versus absence of UAS-*Pop2*-RNAi for both *tim* and *per* (Fig. 3B). The correlation was strong for *tim* (R-

squared = 0,78) and not for *per* (R-squared = 0,2), suggesting that the strength of effect of POP2 on *tim* stability correlates with *tim* mRNA levels.

To test the possibility that PER levels or phosphorylation status impact POP2's control on *tim* stability, Western Blot analyses were performed in different conditions where POP2 impacted *tim* or not (Fig. S2C). The *per*⁺, *clk*^{irk} CT3 and *tim*^{tit} conditions showed phosphorylated PER signals, and *clk*^{irk} CT15 and *per*⁺ LL2 showed dephosphorylated signals, while *clk*^{irk} at CT15 presented an impact of *tim* mRNA in UAS-*Pop2*-RNAi but *per*⁺ LL2 did not, supporting an absence of correlation between PER phosphorylation status and the effect of POP2 on *tim* mRNA. Similarly, PER levels could not explain the effect of POP2 either. Altogether, these results indicate that the control of POP2 on *tim* mRNA stability is not directly PER-dependent, but rather seems to depend on *tim* mRNA levels.

Many circadianly-regulated genes are targets of POP2.

To find new circadianly-regulated POP2 targets, RNA-seq was carried out on the TRAP samples, for 2 circadian timepoints, in *per*⁺ and *per*⁰ condition, in presence or absence of UAS-*Pop2*-RNAi for both total, and ribosome-bound RNA fraction. Since both the UAS-*Pop2*-RNAi and the UAS-*RpL13AF3* are expressed under the control of the *tim-gal4* driver, *Pop2* K.D is only affecting the *tim*⁺ cells, and the ribosome-bound RNA fraction is also from the *tim*⁺ cells only. The quantitative data were analyzed separately for each fraction, and a particular emphasis was made for *tim*⁺ ribosome-bound RNA data, for which, significantly regulated genes were selected using False Discovery Rate (FDR) < 0,05 and Log2 Fold Change (FC) > 1 or < -1 as thresholds. Our results thus yielded 41 genes regulated significantly by the circadian time (CT15/CT3); 4278 genes regulated significantly by POP2 (*per*⁺ *Pop2* K.D/*per*⁺) including both CT3 and CT15 timepoints, and 3624 genes regulated significantly by POP2 in a circadian independent manner (*per*⁰ *Pop2* K.D/*per*⁰). Among the circadianly-regulated genes (Fig. 4A), we retrieved canonical clock components: *vri*, *per*, *tim*, *Clk*, as expected, with similar number of genes presenting positive and negative FC between CT15 and CT3 in *per*⁺ conditions, that could correspond to sets of cycling genes with inverse phases. Among the significantly circadianly-regulated genes (Table. 1), *tim* was expectedly upregulated in *Pop2* K.D context at CT3 in *per*⁺ conditions, but not *per*. Surprisingly, out of the numerous genes significantly regulated by POP2 at CT3 (Fig. 4B) and CT15 (Fig. S3A), many genes were downregulated in the absence of POP2 supporting an alternative role of POP2 on mRNA regulation in *Drosophila* compared to human (Zeng *et al.*, 2018; Haugen *et al.*, 2023). Hierarchical clustering of the circadianly-regulated genes (Fig. 4C), allowed to detect genes regulated similarly to *tim* by POP2, such as *vri*, *CG14275* and *Ugt35B1* in ribosome-bound RNA fractions, and to a lesser extent in total RNA (Fig. S3B). This was likely caused by expression of these genes in non-*tim*⁺ cells, highlighting the relevance to focus on *tim*⁺ cells.

We then asked whether the regulation of circadianly-regulated transcripts by POP2 would persist in non-cycling conditions (*per*⁰) (Fig. 4D). 38 out of 41 genes detected as circadianly regulated genes were impacted by POP2, among which 17 genes were

impacted by POP2 only in *per*⁺ conditions only. Cycling genes regulated by POP2 in *per*⁺ condition showed a large overlap between total and ribosome-bound RNAs (Fig. S3C). Overall, these results suggest that POP2 is involved in the transcriptional and post-transcriptional control of a large number circadianly-regulated genes in *tim*⁺ cells.

***vri* mRNA is a target of POP2.**

vri appeared regulated similarly to *tim* in the RNAseq experiments. We thus analyzed *vri* total and ribosome-bound mRNA levels through 8 timepoints in DD in *per*⁺ conditions and 4 timepoints in *per*⁰ conditions, in presence or absence of *Pop2* K.D (Fig. 5A). The total mRNA levels of *vri* were increased in *Pop2* K.D condition during the subjective day,, similarly to *tim* mRNA. *per*⁰ contexts also led to high levels of *vri* mRNA, that were not influenced by *Pop2* K.D anymore. The translatability of *vri* was also increased by POP2 (Fig. 5B), while the *per*⁰ contexts displayed only a small increase of translatability of *vri*, that can be found in the ribosome-bound fraction as well (Fig. S4B), suggesting that unlike *tim*, *vri* might not be translationally controlled by POP2 independently of PER. This reduced action of POP2 on *vri* translational control could be due to lack of translational control of *vri* overall in the clock since there is no delay between *vri* mRNA and protein levels (Cyran *et al.*, 2003; Gunawardhana and Hardin, 2017). When comparing the total and ribosome-bound mRNA cycling pattern for *vri* (Fig. 5C), a slightly delayed ribosome-bound cycling was observed in comparison to total mRNA, although it seems less strong than for *tim* or *per*. Normalization of the ribosome-bound mRNA levels by total mRNA levels showed an oscillation of *vri* translatability with a peak earlier than the *tim* and *per* peak. Thus, *vri* is under circadian translational control.

***Vrille* is deadenylated by POP2.**

We analyzed *vri* mRNA stabilization by UAS-*Pop2*-RNAi in the different conditions tested previously for *tim* total mRNA levels (Fig. 3A). *vri* mRNA levels were affected by the different conditions with *Pop2* K.D affecting *vri* mRNA differentially according to its levels (Fig. 6A), with a strong correlation observed between POP2's effect strength and *vri* original levels (Fig. 6B). A slight effect of POP2 on *vri* transcription was observed in some conditions (Fig. S4C) but could not explain the changes in mRNA levels. To verify the poly(A) tail status of *vri* in presence or absence of POP2, we designed primers that were specific of *vri*-A+E+F isoforms to perform PATassay (Fig. 6C), in which *vri*-F would produce a long PCR amplicon that was not checked as alternative splicing analysis carried out revealed very low expression of this isoform (Data not shown), additionally, *vri*-E has been shown to not oscillate in control conditions (Gunawardhana *et al.*, 2021), leaving *vri*-A as our isoform of interest here. Similar to *tim*, *Vri*-A+E isoforms were polyadenylated in *Pop2* K.D context at CT3 in total mRNA fraction (Fig. 6D), while the ribosome-bound fraction showed a strong increase of *vri* polyadenylation at both CT3 & CT15 in *Pop2* K.D context. In *per*⁰ context, total *vri*-A+E mRNA was not polyadenylated when POP2 was depleted (Fig. 2C). Of the two

remaining *vri* isoforms, *vri-D* is probably a cycling isoform as well (Gunawardhana *et al.*, 2021), another couple was designed to target all isoforms, where *vri-C+D* were the amplicons of interest with which there was not only an effect of POP2 at both CT3 & CT15, for total and ribosome-bound mRNAs, but also in *per⁰* condition (Fig. 6E), showing that these isoforms are more impacted by POP2. These results suggest a post-transcriptional regulation of *vri* by POP2, in an isoform specific manner, although not as strong as the one observed with *tim*.

POP2 targets' expression level tunes the effect strength of POP2.

We asked whether the *per⁺* CT3 normalized expression of POP2 targets correlates with *Pop2 K.D*'s effect for positively-regulated genes only (Fig. 7A). A mild negative correlation (R-squared = -0,38) was found for ribosome-bound RNAs with weakly expressed genes showing stronger effects of POP2. It has been shown that the half-life increase of CCR4-NOT targets upon depletion of Not1 was correlated with the presence of G/C ending codons in the CDS of these targets in human cells (Gillen *et al.*, 2021). The correlation between codon usage and fold change increase of RNAs in *Pop2 K.D* condition at CT3 was opposite (Fig. 7B), with codons ending with A/U being associated with increased levels in *Pop2 K.D* context. this is in agreement with the correlation observed between *per⁺* CT3 normalized expression of POP2 targets and codon usage, where A/U ending codons were associated with weakly expressed genes and G/C ending codons correlated with higher gene expression (see Kanaya *et al.*, 2001; Heger and Ponting, 2007) (Fig. 7C). We thus took advantage of our circadianly regulated genes to test whether the change in expression observed between CT15 and CT3 would correlate with POP2 effect (Fig. 7D). A strong negative correlation was observed between circadian expression levels changes and the effect of POP2, at both CT3, and CT15 (Fig. 7E). We hypothesize that the strength of POP2 effect is at least partially determined by the expression level of its target, which for some genes is related to the codon usage.

Discussion

Cycling expression of the clock proteins is key in the circadian oscillator mechanism. Our results reveal a new layer of control in the cycling of the PER, TIM, and VRI proteins through the regulation of their translation. Translational mechanisms regulating clock protein cycling have been previously reported (Lim *et al.*, 2011; Huang *et al.*, 2013; Lim and Allada, 2013; Zhang *et al.*, 2013; Huang, McNeil and Jackson, 2014; You *et al.*, 2021), but we report for the first time a translatability curve for three key clock genes in *Drosophila*.

Our TRAP experiment showed a 2-3h delay between *tim*, *per* and *vri* cycling total and ribosome-bound mRNA curves. This is similar to the translation curves previously reported (Huang *et al.*, 2013). However, normalizing the ribosome-bound fraction reveals a cycling of translatability with a phase that is close to the phase of protein cycling for PER, and to a lesser extent for TIM. This potential role of translation in the delay of cycling peak is particularly relevant for *per*, which was predicted to undergo

post-transcriptional control in its oscillation (So, 1997; Yu and Rosbash, 2023), while supporting the existence for such control for *tim* as well (Rodriguez *et al.*, 2013). For *vri* however, no delays were previously reported comparing *vri* mRNA and protein levels in the past (Cyran *et al.*, 2003; Gunawardhana and Hardin, 2017). Yet, there seemed to be a translational regulation controlling the expression of *vri*, which would also be consistent with a predicted post-transcriptional control for *vri*'s oscillation in the clock (Rodriguez *et al.*, 2013). Why would *vri* mRNA translation be delayed compared to protein cycling is unclear, but translation and protein stability are likely co-optimized to generate a properly-phased protein oscillation.

For *per*, *tim* and *vri* genes, the trough in translatability observed occurred during the rising phase of the total mRNA levels, this could constitute a way to reduce translation of highly expressed clock genes in order to avoid saturating translational machineries which was predicted as a potential cause of loss of cycling in the molecular clock (Kurosawa and Iwasa, 2002).

POP2, in addition to controlling *tim* and *vri*, but not *per* mRNA stability, regulates their translatability. The downregulation of POP2 affect mRNA stability during day time whereas the translatability is affected around the clock, suggesting that the two functions are independent. Deadenylation-independent translational regulation was previously reported (Jeske *et al.*, 2006; Cooke, Prigge and Wickens, 2010; Van Etten *et al.*, 2012). Nevertheless, given that the effect of POP2 on *tim* and *vri* translatability associates well with a lengthening of the poly(A) tail of these ribosome-bound transcripts, it is likely that the translational regulation of Pop2 on *tim* and *vri* is, at least partially, deadenylation-dependent. A positive correlation between translational efficiency and poly(A) tail length has been shown in *Drosophila* embryos (Lim *et al.*, 2016), but whether this is a common rule in flies is unknown. In other organisms, examples exist where poly(A) tail length does not correlate with translational efficiency in non-embryonic cells (Subtelny *et al.*, 2014), and short poly(A) tails can also be associated with higher expression (Lima *et al.*, 2017). Positive or negative regulation of ribosome-bound transcript levels by POP2 can be observed according to targets, as shown in this study and other studies in flies (Zeng *et al.*, 2018; Haugen *et al.*, 2023). To what extent these functions are deadenylation-dependent or not remains to be precisely defined, but different mechanisms are likely involved for POP2 action. Another explanation for our results could be that ribosome-bound polyadenylated *tim* and *vri* observed in *Pop2* K.D context are not necessarily translationally active, these *tim* and *vri* transcripts could include molecules trapped in stalled ribosomes, as the CCR4-NOT complex has been shown to play a regulatory role in ribosome elongation dynamics (Allen *et al.*, 2021). Therefore, the absence of POP2 could lead to the accumulation of stalling events, yet this should also lead to increased levels of *tim* and *vri* during the subjective night in the total mRNA fraction. We thus propose that the difference in POP2's effect size on translatability versus stability for *tim* and *vri* is due to an enrichment of ribosome-bound polyadenylated transcripts in the absence of POP2 that are diluted in the total mRNA fraction by a pool of transcripts that are

deadenylated. While, the absence of increase of TIM protein levels in *Pop2* K.D context during the subjective night, when *tim* translatability is increased, could be due to post-translational controls, or to this dilution effect as well. This would also explain the effect of PER presence or absence in *Pop2* K.D context that increases *tim* translatability but not stability.

We observe a strong correlation between POP2 mRNA destabilizing function and low levels of transcripts for *tim*, *vri*, as well as other targets of our RNA-seq dataset. This might appear counter-intuitive, as one would expect that highly expressed genes compete more effectively for POP2's control, as it is proposed for miRNA regulations (Tay, Rinn and Pandolfi, 2014). It is possible that POP2 action is limiting, thus regulating constant levels of target transcripts, independently of their relative steady-state levels. This would lead to a stronger relative decrease of low abundance transcripts. In this scenario, POP2 would not regulate its targets in a circadian manner *per se*, but instead increases the amplitude of cycling genes by lowering further their minimum levels, without affecting greatly their peak expression levels. This would also be true for the ribosome-bound RNAs regulated even at their maximum abundance, as enriching our fractions would allow to distinguish the effect of POP2 with greater resolution. However, different mechanisms have been shown to link transcription with the control of mRNA polyadenylation and stability (Nagaike et al., 2011; Trcek et al., 2011; Haimovich et al., 2013; Das et al., 2017), and we cannot exclude a circadian control of POP2 function through transcription. Notably, interactions between the transcription machinery and the CCR4-NOT complex indicate that mRNA deadenylation can be regulated at the transcriptional level (Gupta et al., 2016; Rambout et al., 2016; Sharma et al., 2016; Stupfler et al., 2016; Ukleja et al., 2016; Hicks et al., 2017). In any case, the correlation between low mRNA levels and a strong POP2 action likely explains the loss of POP2 control in the absence of PER (Grima et al., 2019).

Codon usage analysis revealed that POP2-targeted transcripts rich in codons ending in G/C present higher expression levels than transcripts rich in A/U-ending codons. This is in agreement with previous findings on *Drosophila* genes (Kanaya et al., 2001; Heger and Ponting, 2007). POP2 diminished more the levels of transcripts rich in A/U-ending codons, unlike what was found in human cell lines (Gillen et al., 2021), possibly as a consequence of differences in codon optimality between *Homo sapiens* and *Drosophila melanogaster*. Another cause could be that POP2 operates differently between human and *Drosophila* which is probable considering the presence of a large cluster of downregulated genes upon *Pop2* K.D found in our study and others in *Drosophila*, but not in human (Zeng et al., 2018; Gillen et al., 2021; Haugen et al., 2023). The low expression levels associated with these transcripts rich in A/U-ending codons might be the main factor for making them preferential targets of POP2.

The POP2 specificity for *tim* and *vri*, but not *per* is intriguing. Motif enrichment search was carried out in order to reveal RNA motifs but we could not identify a

canonical motif present in *tim* and *vri* but not in *per* mRNA sequences. The CCR4-NOT complex is expected to be recruited on its targets through various pathways involving diverse RNA binding proteins or microRNAs that will each recognize different motifs (Fabian *et al.*, 2011; Joly *et al.*, 2013; Du *et al.*, 2016; Hanet *et al.*, 2019; Wakiyama and Takimoto, 2022; Haugen *et al.*, 2023; Pekovic *et al.*, 2023). It would be interesting to investigate the possibility that shared miRNAs between *tim* and *vri* could trigger the recruitment of POP2, as *per* does not have known miRNAs targeting it so far (Xia *et al.*, 2020), while *tim* and *vri* do. Also, the control operated by POP2 on *tim* and *vri* is necessary for their proper oscillations, as well as for the clock itself, it is thus likely that similar control mechanisms operate on the other clock components and that these mechanisms are somehow conserved through evolution.

Materials and methods

Fly lines : Fly stocks were reared on standard cornmeal-yeast-agar medium under 12h-12h LD conditions at 18°C or 25°C.

crosses were grown at 18°C and transferred at 25°C for 3 days entrainment in LD followed by collection on first day of DD except for the LL2 conditions that were collected on the second day of LL. UAS-*Pop2*-RNAi #30492 were obtained from the TRiP collection (<http://www.flyrnai.org/TRiP-HOME.html>), UAS-*RpL13AF3* #83684 from the Bloomington stock center (<https://bdsc.indiana.edu>) and were described previously (Huang *et al.*, 2019), UAS-*RpL13A* #F001744 from FlyORF (<http://flyorf.ch/>), *per*⁰ (Konopka and Benzer, 1971), *tim-gal4* (Kaneko, 1998), *clk*^{irk} (Allada *et al.*, 1998), *tim*^{rit} (Matsumoto *et al.*, 1999).

TRAP : 1-10 days old adult flies reared at 18°C were entrained in 12h-12h LD cycles for at least 3 days at 25°C and were collected on the subsequent first day of DD at different CT, each timepoint comprised ~250 flies. Flies were quickly frozen in dry ice upon collection. Heads were sorted in dry ice using geological sieves. Frozen heads were homogenized in ice cold extraction buffer (20mM HEPES pH 7,4; 300mM KCl; 0,75% Igepal CA-630; 1mM DTT; 100µg/mL Cycloheximide; 5mM MgCl₂; 250U/mL SUPERase-IN; EDTA-free protease inhibitor (Roche)) for 90 seconds followed by 20 minutes of incubation at 4°C with agitation, debris were removed by centrifugation at 18 000g for 15 minutes at 4°C, supernatant were collected and centrifuged a second time at 18 000g for 10 minutes at 4°C, 100µL of lysate was saved as total mRNA fraction and 1mL TRIzol was added for RNA extraction, the other part underwent protein concentration measurement using Bio-rad protein assay Kit. 1,5mg of protein extracts were added to 50µL of anti-FLAG coupled M2 agarose beads (Sigma) and incubated for 90 minutes at 4°C with agitation. Beads were then washed 5 times in wash buffer (20mM HEPES pH 7,4; 300mM KCl; 0,75% Igepal CA-630; 1mM DTT; 100µg/mL Cycloheximide; 5mM MgCl₂; EDTA-free protease inhibitor (Roche)), ribosome-bound RNAs bound to beads were then extracted using TRIzol followed with Macherey Nagel's NucleoSpin RNA extraction following kit's instructions.

RT-qPCR : RNA amounts were quantified using Qubit 3 fluorometer (Thermo Fisher Scientific) together with RNA BR assay (Broad Range). Genomic DNA contamination was controlled doing a qPCR using pre-*tim* and *18S* primers on RNAs. RNAs were reverse transcribed using High-capacity cDNA reverse transcription kit (Applied Biosystems) with RNase inhibitor and random primers following manufacturer's instructions. Quantitative PCR was performed with a QuantStudio 12K Flex Real-Time PCR System using the SYBR green detection protocol. 3 ng of cDNA were mixed with Fast SYBR® Green Master Mix and 500 nM of each primer. Reaction mix was loaded on 384 well microplates and submitted to 40 cycles of PCR (95°C/20sec;(95°C/1sec; 60°C/20 sec) X40) followed by a fusion cycle in order to analyze the melting curve of the PCR products. All quantitative RT-PCR reactions were carried out in technical duplicates. And each experiment was realized with standard ranges to determine efficiency of PCR for each couple of primers. Primers were: tub-For 5'-TCCAATAAAAACACTCAATATGCGTGA-3' tub-Rev 5'-CAAGCAGTAGAGCTCCCAGCA-3' per-For 5'-GAGCAGCTACAAGGTTCCCG-3' per-Rev 5'-CCACGTGCGATATGATCCC-3' pre-per-For 5' GTCCACGATGCGATTCAATGTA-3' pre-per-Rev 5'-GGTGCTCCATGATCTTGTCTC-3' tim-For 5'-TCAAGAATTTGGGAAGCGGA-3' tim-Rev 5'-GCGACCAAGAGCAAACGGTA-3' pre-tim-For 5'-ACTGCTTTCCAATGCGGTATG-3' pre-tim-Rev 5'-AAGCCTCCGAAAAACATATGAAAA-3' Pop2-For 5'-AAATGCGTGAGATGTTCTTCGAG-3' Pop2-Rev 5'-TTGGTGCCATTGACGATGAA-3' vri-For 5'-CATCGCCATGATGAACAACG-3' vri-Rev 5'-CATGGACAACGGATGCAAGTT-3' pre-vri-For 5' CAAGCAGGATAATCCCAGCAA-3' pre-vri-Rev 5'-ACAGATTTCAAGATCAAACGTGGA-3'.

RT-qPCR data analysis : Ct values obtained from the technical duplicates were averaged and the averaged Ct values were then processed following Taylor *et al.*, 2019 (Taylor *et al.*, 2019) with adjusted efficiency obtained from the average efficiency calculated over several experiments for a given couple of primers (Pfaffl, 2001). Reference genes were *18S*, *Mnf* and *tub* for classic qPCR experiments and *18S* only for TRAP experiments, as it remained stable between total and ribosome-bound RNA fractions.

PAT assay : PAT assay (Affymetrix) analyses were carried out following manufacturer's protocol as previously described (Grima *et al.*, 2019). Briefly, G/I tailing was performed with 100-500ng total RNA, 2µl 5X tail buffer mix, 1µl 10X tail enzyme mix, and water to a total volume of 10 µl, and the reaction mix was incubated at 37°C for 1 hour. Next, 1µl 10X tail stop solution was added to stop the G/I tailing reaction. For reverse transcription, 5µl G/I-tailed RNA sample, 4µl 5X RT buffer mix, and 2µl 10X RT enzyme mix were mixed in a total of 20µl and incubated at 44°C for 1 h and 92°C for 10 min. The reverse transcription sample was then diluted with water to 40µl, and then 5µl diluted RT sample was used in a 25µl PCR mixture containing 5µl 5X PCR buffer mix, 1µl 10µM universal PCR reverse primer (Un-Rev), 1 µl 10µM gene-specific forward primer, and 1,25 units HotStart-IT Taq DNA polymerase. Two-step PCR conditions were

as follows: 94°C for 2 min; 35 cycles of 94°C for 10s, 60°C for 60s; 72°C for 5min; and a hold at 4°C. 12,5µl of the PCR reaction were loaded on a 2% agarose gel and stained with ethidium bromide. The primers used were as follows: tim-For 5'-GCAGAAAGTGAAGAAAAGTGCATTA-3' tim-Rev 5'-GGCTACAGGGAAAGCTTTACTG-3'; riAEF-For 5' CACAGCGCTTCAACTAAATGTTAT-3'; vriAEF-Rev 5'-TTCATTGATCAACACAAACGAGTTA-3'; vriCD-For 5'-GTTTGTAAGCAAACGTTACAAAGTA-3'; vriCD-Rev 5' TTTCTTTCATCTCTCACGTTTTGAA-3'. The poly(A) tail lengths of the gene-of-interest are the sizes of poly(A) PCR-amplified products minus the sum of calculated length of the gene-specific forward primer to the putative polyadenylation start site and the length of Universal Reverse primer (35nt). For each gene, a control of specific amplification was performed with forward and reverse primers and a reaction containing no sample was used to control for gDNA contaminations in our reagents.

RNA-seq of TRAP samples : RNA-seq was carried out by Qiagen genomic services (Hilden – Germany) with n = 2 independent replicates : The library preparation was done using the QIAseq Stranded Total RNA Library Kit with QIAseq FastSelect rRNA and globin depletion. The amount of 100ng starting material was heat fragmented. QIAseq FastSelect Fly was used to reduce the amount of unwanted RNA species. After first and second strand synthesis, the cDNA was end-repaired and 3' adenylated. Sequencing adapters were ligated to the overhangs. Adapted molecules were enriched using by 16 cycles of PCR and purified by a bead based cleanup. Library preparation was quality controlled using capillary electrophoresis (Tape D1000). High quality libraries are pooled based in equimolar concentrations. The library pool(s) were quantified using qPCR and optimal concentration of the library pool used to generate the clusters on the surface of a flowcell before sequencing on a NovaSeq (Illumina Inc.) instrument (2x76, 2x10) according to the manufacturer instructions (Illumina Inc.). Raw data was de-multiplexed and FASTQ files for each sample were generated using the bcl2fastq software v2.20.0.422 (Illumina inc.).

RNA-seq analysis : All primary analysis is carried out using [CLC Genomics Server 23.0.5](#). The workflow "RNA-Seq Analysis" of CLC Genomics Server with standard parameters is used to map reads to the drosophila melanogaster genome (BDGP6.46). The 'Empirical analysis of DGE' algorithm of the CLC Genomics Workbench 23.0.5 was used for differential expression analysis with default settings. It is an implementation of the 'Exact Test' for two-group comparisons (Robinson and Smyth, 2007) and incorporated in the EdgeR Bioconductor package (Robinson, McCarthy and Smyth, 2010). Comparisons with an FDR <0,05 and a $\log_2FC \geq 1$ were considered significant. For the hierarchical clustering analysis, genes showing significant changes between CT3 and CT15 in *per*⁺ condition and a TPM value ≥ 1 in at least one of the two conditions were considered. Analysis of the correlations between expressions of the genes at *per*⁺ CT3 and FC effect of *Pop2* K.D was carried out for significantly regulated genes presenting TPM values in both conditions > 0, in order to avoid biases in FC size

that would be due solely to transcriptional effects of POP2. For the G/C ending codons analyses, significantly positively regulated genes upon *Pop2* K.D at CT3 were filtered, the CDS of these transcripts were obtained from Flybase Batch Download tool (Öztürk-Çolak *et al.*, 2024). The codon usage for each CDS was then calculated using the codon usage analysis tool from Sequence Manipulation Suite website (https://www.bioinformatics.org/sms2/codon_usage.html) (Stothard, 2000). Codon usage for transcripts CDS of a same gene were averaged and averaged codon usage percentage for each codons had Spearman correlation coefficient computed with positive \log_2FC values ≥ 1 upon *Pop2* K.D or TPM values > 0 in *per*⁺ CT3 condition.

Statistical analyses : Oscillation analyses were carried out using dryR package with *lm* function (Weger *et al.*, 2021) using the following thresholds for significance : 4 conditions : Rhythm BICW $\geq 0,4$; Mean BICW $\geq 0,6$; 2 conditions Rhythm : BICW $\geq 0,6$; Mean BICW $\geq 0,95$. Pearson's correlation coefficient was obtained from Excel. All other statistical analyses were carried out in RStudio version 2023.06.2+561 and R version 4.2.2.

Behavioral analysis : Locomotor activity of individual flies was measured using the *Drosophila* activity monitors from Trikinetics at 25°C. Adult males (1-10 days old) were entrained for 3 days in 12h-12h light-dark cycles (LD) followed by dark-dark cycles (DD) to monitor their activity in constant darkness. The locomotor activity analysis was carried out with FaasX 1.3 (<https://neuropsi.cnrs.fr/departements/cnn/equipe-francois-rouyer/>) (Klarsfeld, Leloup and Rouyer, 2003). The actograms presented are double plotted graphs representing the absolute activity levels of the flies in 30min bins, averaged for N flies per genotype. The hash density was set to 15.

Acknowledgments

We thank Élisabeth Chélot for help with preliminary experiments; Jean-Yves Roignant and Lina Worpenberg for helpful discussions; Michel Boudinot for the Faas software; Ralf Stanewsky for anti-PER antibodies; The Bloomington *Drosophila* Stock center, Vienna *Drosophila* Resource Center, NIG-Fly, FlyORF for fly lines. This study was supported by the PostClock grant (Agence Nationale de la Recherche). F.R. is supported by INSERM.

References

- Allada, R. *et al.* (1998) 'A Mutant *Drosophila* Homolog of Mammalian Clock Disrupts Circadian Rhythms and Transcription of period and timeless', *Cell*, 93(5), pp. 791–804. Available at: [https://doi.org/10.1016/S0092-8674\(00\)81440-3](https://doi.org/10.1016/S0092-8674(00)81440-3).
- Allen, G.E. *et al.* (2021) 'Not4 and Not5 modulate translation elongation by Rps7A ubiquitination, Rli1 moonlighting, and condensates that exclude eIF5A', *Cell Reports*, 36(9), p. 109633. Available at: <https://doi.org/10.1016/j.celrep.2021.109633>.

Blau, J. and Young, M.W. (1999) 'Cycling vrilie Expression Is Required for a Functional *Drosophila* Clock', *Cell*, 99(6), pp. 661–671. Available at: [https://doi.org/10.1016/S0092-8674\(00\)81554-8](https://doi.org/10.1016/S0092-8674(00)81554-8).

Burow, D.A. *et al.* (2018) 'Attenuated Codon Optimality Contributes to Neural-Specific mRNA Decay in *Drosophila*', *Cell Reports*, 24(7), pp. 1704–1712. Available at: <https://doi.org/10.1016/j.celrep.2018.07.039>.

Chen, X. and Rosbash, M. (2016) 'mir-276a strengthens *Drosophila* circadian rhythms by regulating *timeless* expression', *Proceedings of the National Academy of Sciences*, 113(21), pp. E2965–E2972. Available at: <https://doi.org/10.1073/pnas.1605837113>.

Collart, M.A. (2016) 'The Ccr4-Not complex is a key regulator of eukaryotic gene expression', *WIREs RNA*, 7(4), pp. 438–454. Available at: <https://doi.org/10.1002/wrna.1332>.

Collart, M.A., Audebert, L. and Bushell, M. (2023) 'Roles of the CCR4-NOT complex in translation and dynamics of co-translation events', *WIREs RNA*, p. e1827. Available at: <https://doi.org/10.1002/wrna.1827>.

Cooke, A., Prigge, A. and Wickens, M. (2010) 'Translational Repression by Deadenylation', *Journal of Biological Chemistry*, 285(37), pp. 28506–28513. Available at: <https://doi.org/10.1074/jbc.M110.150763>.

Cyran, S.A. *et al.* (2003) 'vrille, Pdp1, and dClock Form a Second Feedback Loop in the *Drosophila* Circadian Clock', *Cell*, 112(3), pp. 329–341. Available at: [https://doi.org/10.1016/S0092-8674\(03\)00074-6](https://doi.org/10.1016/S0092-8674(03)00074-6).

Das, D. *et al.* (2017) 'Effect of transcription factor resource sharing on gene expression noise', *PLOS Computational Biology*. Edited by R. Guigo, 13(4), p. e1005491. Available at: <https://doi.org/10.1371/journal.pcbi.1005491>.

Du, H. *et al.* (2016) 'YTHDF2 destabilizes m6A-containing RNA through direct recruitment of the CCR4–NOT deadenylase complex', *Nature Communications*, 7(1), p. 12626. Available at: <https://doi.org/10.1038/ncomms12626>.

Dubowy, C. and Sehgal, A. (2017) 'Circadian Rhythms and Sleep in *Drosophila melanogaster*', *Genetics*, 205(4), pp. 1373–1397. Available at: <https://doi.org/10.1534/genetics.115.185157>.

Fabian, M.R. *et al.* (2011) 'miRNA-mediated deadenylation is orchestrated by GW182 through two conserved motifs that interact with CCR4–NOT', *Nature Structural & Molecular Biology*, 18(11), pp. 1211–1217. Available at: <https://doi.org/10.1038/nsmb.2149>.

Foley, L.E. *et al.* (2019) 'Drosophila PSI controls circadian period and the phase of circadian behavior under temperature cycle via tim splicing', *eLife*, 8, p. e50063. Available at: <https://doi.org/10.7554/eLife.50063>.

Giesecke, A. *et al.* (2023) 'A novel period mutation implicating nuclear export in temperature compensation of the Drosophila circadian clock', *Current Biology*, 33(2), pp. 336-350.e5. Available at: <https://doi.org/10.1016/j.cub.2022.12.011>.

Gillen, S.L. *et al.* (2021) 'Differential regulation of mRNA fate by the human Ccr4-Not complex is driven by coding sequence composition and mRNA localization', *Genome Biology*, 22(1), p. 284. Available at: <https://doi.org/10.1186/s13059-021-02494-w>.

Glossop, N.R.J. *et al.* (2003) 'VRILLE Feeds Back to Control Circadian Transcription of Clock in the Drosophila Circadian Oscillator', *Neuron*, 37(2), pp. 249–261. Available at: [https://doi.org/10.1016/S0896-6273\(03\)00002-3](https://doi.org/10.1016/S0896-6273(03)00002-3).

Grima, B. *et al.* (2019) 'PERIOD-controlled deadenylation of the timeless transcript in the Drosophila circadian clock', *Proceedings of the National Academy of Sciences*, 116(12), pp. 5721–5726. Available at: <https://doi.org/10.1073/pnas.1814418116>.

Gunawardhana, K.L. *et al.* (2021) 'Crosstalk between vrilie transcripts, proteins, and regulatory elements controlling circadian rhythms and development in Drosophila', *iScience*, 24(1), p. 101893. Available at: <https://doi.org/10.1016/j.isci.2020.101893>.

Gunawardhana, K.L. and Hardin, P.E. (2017) 'VRILLE Controls PDF Neuropeptide Accumulation and Arborization Rhythms in Small Ventrolateral Neurons to Drive Rhythmic Behavior in Drosophila', *Current Biology*, 27(22), pp. 3442-3453.e4. Available at: <https://doi.org/10.1016/j.cub.2017.10.010>.

Gupta, I. *et al.* (2016) 'Translational Capacity of a Cell Is Determined during Transcription Elongation via the Ccr4-Not Complex', *Cell Reports*, 15(8), pp. 1782–1794. Available at: <https://doi.org/10.1016/j.celrep.2016.04.055>.

Haimovich, G. *et al.* (2013) 'Gene Expression Is Circular: Factors for mRNA Degradation Also Foster mRNA Synthesis', *Cell*, 153(5), pp. 1000–1011. Available at: <https://doi.org/10.1016/j.cell.2013.05.012>.

Hanet, A. *et al.* (2019) 'HELZ directly interacts with CCR4–NOT and causes decay of bound mRNAs', *Life Science Alliance*, 2(5), p. e201900405. Available at: <https://doi.org/10.26508/lsa.201900405>.

Haugen, R.J. *et al.* (2023) *Regulation of the Drosophila transcriptome by Pumilio and CCR4–NOT deadenylase*. preprint. Molecular Biology. Available at: <https://doi.org/10.1101/2023.08.29.555372>.

Heger, A. and Ponting, C.P. (2007) 'Variable Strength of Translational Selection Among 12 *Drosophila* Species', *Genetics*, 177(3), pp. 1337–1348. Available at: <https://doi.org/10.1534/genetics.107.070466>.

Hicks, J.A. *et al.* (2017) 'Human GW182 Paralogs Are the Central Organizers for RNA-Mediated Control of Transcription', *Cell Reports*, 20(7), pp. 1543–1552. Available at: <https://doi.org/10.1016/j.celrep.2017.07.058>.

Huang, K. *et al.* (2019) 'RiboTag translomic profiling of *Drosophila* oenocytes under aging and induced oxidative stress', *BMC Genomics*, 20(1), p. 50. Available at: <https://doi.org/10.1186/s12864-018-5404-4>.

Huang, Y. *et al.* (2013) 'Translational Profiling of Clock Cells Reveals Circadianly Synchronized Protein Synthesis', *PLOS Biology*, 11(11), p. e1001703. Available at: <https://doi.org/10.1371/journal.pbio.1001703>.

Huang, Y., McNeil, G.P. and Jackson, F.R. (2014) 'Translational Regulation of the DOUBLETIME/CKI δ / ϵ Kinase by LARK Contributes to Circadian Period Modulation', *PLoS Genetics*. Edited by P.H. Taghert, 10(9), p. e1004536. Available at: <https://doi.org/10.1371/journal.pgen.1004536>.

Jeske, M. *et al.* (2006) 'Rapid ATP-dependent Deadenylation of nanos mRNA in a Cell-free System from *Drosophila* Embryos', *Journal of Biological Chemistry*, 281(35), pp. 25124–25133. Available at: <https://doi.org/10.1074/jbc.M604802200>.

Joly, W. *et al.* (2013) 'The CCR4 Deadenylation Acts with Nanos and Pumilio in the Fine-Tuning of Mei-P26 Expression to Promote Germline Stem Cell Self-Renewal', *Stem Cell Reports*, 1(5), pp. 411–424. Available at: <https://doi.org/10.1016/j.stemcr.2013.09.007>.

Kanaya, S. *et al.* (2001) 'Codon Usage and tRNA Genes in Eukaryotes: Correlation of Codon Usage Diversity with Translation Efficiency and with CG-Dinucleotide Usage as Assessed by Multivariate Analysis', *Journal of Molecular Evolution*, 53(4–5), pp. 290–298. Available at: <https://doi.org/10.1007/s002390010219>.

Kaneko, M. (1998) 'Neural substrates of *Drosophila* rhythms revealed by mutants and molecular manipulations', *Current Opinion in Neurobiology*, 8(5), pp. 652–658. Available at: [https://doi.org/10.1016/S0959-4388\(98\)80095-0](https://doi.org/10.1016/S0959-4388(98)80095-0).

Klarsfeld, A., Leloup, J.-C. and Rouyer, F. (2003) 'Circadian rhythms of locomotor activity in *Drosophila*', *Behavioural Processes*, 64(2), pp. 161–175. Available at: [https://doi.org/10.1016/S0376-6357\(03\)00133-5](https://doi.org/10.1016/S0376-6357(03)00133-5).

Konopka, R.J. and Benzer, S. (1971) 'Clock Mutants of *Drosophila melanogaster*', *Proceedings of the National Academy of Sciences*, 68(9), pp. 2112–2116. Available at: <https://doi.org/10.1073/pnas.68.9.2112>.

Kurosawa, G. and Iwasa, Y. (2002) 'Saturation of Enzyme Kinetics in Circadian Clock Models', *Journal of Biological Rhythms*, 17(6), pp. 568–577. Available at: <https://doi.org/10.1177/0748730402238239>.

Li, Y.H. *et al.* (2019) 'O-GlcNAcylation of PERIOD regulates its interaction with CLOCK and timing of circadian transcriptional repression', *PLOS Genetics*. Edited by P.H. Taghert, 15(1), p. e1007953. Available at: <https://doi.org/10.1371/journal.pgen.1007953>.

Lim, C. *et al.* (2011) 'The novel gene twenty-four defines a critical translational step in the *Drosophila* clock', *Nature*, 470(7334), pp. 399–403. Available at: <https://doi.org/10.1038/nature09728>.

Lim, C. and Allada, R. (2013) 'ATAXIN-2 Activates PERIOD Translation to Sustain Circadian Rhythms in *Drosophila*', *Science*, 340(6134), pp. 875–879. Available at: <https://doi.org/10.1126/science.1234785>.

Lim, J. *et al.* (2016) 'mTAIL-seq reveals dynamic poly(A) tail regulation in oocyte-to-embryo development', *Genes & Development*, 30(14), pp. 1671–1682. Available at: <https://doi.org/10.1101/gad.284802.116>.

Lima, S.A. *et al.* (2017) 'Short poly(A) tails are a conserved feature of highly expressed genes', *Nature Structural & Molecular Biology*, 24(12), pp. 1057–1063. Available at: <https://doi.org/10.1038/nsmb.3499>.

Martin Anduaga, A. *et al.* (2019) 'Thermosensitive alternative splicing senses and mediates temperature adaptation in *Drosophila*', *eLife*, 8, p. e44642. Available at: <https://doi.org/10.7554/eLife.44642>.

Matsumoto, A. *et al.* (1999) '*tim^{rit}* Lengthens Circadian Period in a Temperature-Dependent Manner through Suppression of PERIOD Protein Cycling and Nuclear Localization', *Molecular and Cellular Biology*, 19(6), pp. 4343–4354. Available at: <https://doi.org/10.1128/MCB.19.6.4343>.

Mendoza-Viveros, L. *et al.* (2017) 'Molecular modulators of the circadian clock: lessons from flies and mice', *Cellular and Molecular Life Sciences*, 74(6), pp. 1035–1059. Available at: <https://doi.org/10.1007/s00018-016-2378-8>.

Nagaike, T. *et al.* (2011) 'Transcriptional Activators Enhance Polyadenylation of mRNA Precursors', *Molecular Cell*, 41(4), pp. 409–418. Available at: <https://doi.org/10.1016/j.molcel.2011.01.022>.

Öztürk-Çolak, A. *et al.* (2024) 'FlyBase: updates to the *Drosophila* genes and genomes database', *GENETICS*. Edited by V. Wood, 227(1), p. iyad211. Available at: <https://doi.org/10.1093/genetics/iyad211>.

Park, J.-E. *et al.* (2016) 'Regulation of Poly(A) Tail and Translation during the Somatic Cell Cycle', *Molecular Cell*, 62(3), pp. 462–471. Available at: <https://doi.org/10.1016/j.molcel.2016.04.007>.

Passmore, L.A. and Collier, J. (2021) 'Roles of mRNA poly(A) tails in regulation of eukaryotic gene expression', *Nature Reviews Molecular Cell Biology* [Preprint]. Available at: <https://doi.org/10.1038/s41580-021-00417-y>.

Pekovic, F. *et al.* (2023) 'RNA binding proteins Smaug and Cup induce CCR4–NOT-dependent deadenylation of the *nanos* mRNA in a reconstituted system', *Nucleic Acids Research*, p. gkad159. Available at: <https://doi.org/10.1093/nar/gkad159>.

Pfaffl, M.W. (2001) 'A new mathematical model for relative quantification in real-time RT-PCR', *Nucleic Acids Research*, 29(9), pp. 45e–445. Available at: <https://doi.org/10.1093/nar/29.9.e45>.

Rambout, X. *et al.* (2016) 'The transcription factor ERG recruits CCR4–NOT to control mRNA decay and mitotic progression', *Nature Structural & Molecular Biology*, 23(7), pp. 663–672. Available at: <https://doi.org/10.1038/nsmb.3243>.

Robinson, M.D., McCarthy, D.J. and Smyth, G.K. (2010) 'edgeR: a Bioconductor package for differential expression analysis of digital gene expression data', *Bioinformatics*, 26(1), pp. 139–140. Available at: <https://doi.org/10.1093/bioinformatics/btp616>.

Robinson, M.D. and Smyth, G.K. (2007) 'Small-sample estimation of negative binomial dispersion, with applications to SAGE data', *Biostatistics*, 9(2), pp. 321–332. Available at: <https://doi.org/10.1093/biostatistics/kxm030>.

Rodriguez, J. *et al.* (2013) 'Nascent-Seq analysis of *Drosophila* cycling gene expression', *Proceedings of the National Academy of Sciences*, 110(4), pp. E275–E284. Available at: <https://doi.org/10.1073/pnas.1219969110>.

Shakhmantsir, I. *et al.* (2018) 'Spliceosome factors target timeless (*tim*) mRNA to control clock protein accumulation and circadian behavior in *Drosophila*', *eLife*, 7, p. e39821. Available at: <https://doi.org/10.7554/eLife.39821>.

Sharma, N. (2016) 'Regulation of RNA polymerase II-mediated transcriptional elongation: Implications in human disease', *IUBMB Life*, 68(9), pp. 709–716. Available at: <https://doi.org/10.1002/iub.1538>.

So, W.V. (1997) 'Post-transcriptional regulation contributes to *Drosophila* clock gene mRNA cycling', *The EMBO Journal*, 16(23), pp. 7146–7155. Available at: <https://doi.org/10.1093/emboj/16.23.7146>.

Stothard, P. (2000) 'The Sequence Manipulation Suite: JavaScript Programs for Analyzing and Formatting Protein and DNA Sequences', *BioTechniques*, 28(6), pp. 1102–1104. Available at: <https://doi.org/10.2144/00286ir01>.

Stupfler, B. *et al.* (2016) 'BTG2 bridges PABPC1 RNA-binding domains and CAF1 deadenylase to control cell proliferation', *Nature Communications*, 7(1), p. 10811. Available at: <https://doi.org/10.1038/ncomms10811>.

Subtelny, A.O. *et al.* (2014) 'Poly(A)-tail profiling reveals an embryonic switch in translational control', *Nature*, 508(7494), pp. 66–71. Available at: <https://doi.org/10.1038/nature13007>.

Szabó, Á. *et al.* (2018) 'Ubiquitylation Dynamics of the Clock Cell Proteome and TIMELESS during a Circadian Cycle', *Cell Reports*, 23(8), pp. 2273–2282. Available at: <https://doi.org/10.1016/j.celrep.2018.04.064>.

Tay, Y., Rinn, J. and Pandolfi, P.P. (2014) 'The multilayered complexity of ceRNA crosstalk and competition', *Nature*, 505(7483), pp. 344–352. Available at: <https://doi.org/10.1038/nature12986>.

Taylor, S.C. *et al.* (2019) 'The Ultimate qPCR Experiment: Producing Publication Quality, Reproducible Data the First Time', *Trends in Biotechnology*, 37(7), pp. 761–774. Available at: <https://doi.org/10.1016/j.tibtech.2018.12.002>.

Temme, C. *et al.* (2004) 'A complex containing the CCR4 and CAF1 proteins is involved in mRNA deadenylation in *Drosophila*', *The EMBO Journal*, 23(14), pp. 2862–2871. Available at: <https://doi.org/10.1038/sj.emboj.7600273>.

Temme, C. *et al.* (2010) 'Subunits of the *Drosophila* CCR4-NOT complex and their roles in mRNA deadenylation', *RNA*, 16(7), pp. 1356–1370. Available at: <https://doi.org/10.1261/rna.2145110>.

Trcek, T. *et al.* (2011) 'Single-Molecule mRNA Decay Measurements Reveal Promoter-Regulated mRNA Stability in Yeast', *Cell*, 147(7), pp. 1484–1497. Available at: <https://doi.org/10.1016/j.cell.2011.11.051>.

Ukleja, M. *et al.* (2016) 'The architecture of the *Schizosaccharomyces pombe* CCR4-NOT complex', *Nature Communications*, 7(1), p. 10433. Available at: <https://doi.org/10.1038/ncomms10433>.

Van Etten, J. *et al.* (2012) 'Human Pumilio Proteins Recruit Multiple Deadenylases to Efficiently Repress Messenger RNAs', *Journal of Biological Chemistry*, 287(43), pp. 36370–36383. Available at: <https://doi.org/10.1074/jbc.M112.373522>.

Wakiyama, M. and Takimoto, K. (2022) 'N-terminal Ago-binding domain of GW182 contains a tryptophan-rich region that confer binding to the CCR4-NOT complex', *Genes to Cells*, p. gtc.12974. Available at: <https://doi.org/10.1111/gtc.12974>.

Weger, B.D. *et al.* (2021) 'Systematic analysis of differential rhythmic liver gene expression mediated by the circadian clock and feeding rhythms', *Proceedings of the National Academy of Sciences*, 118(3), p. e2015803118. Available at: <https://doi.org/10.1073/pnas.2015803118>.

Xia, X. *et al.* (2020) 'Regulation of circadian rhythm and sleep by *miR-375-timeless* interaction in *Drosophila*', *The FASEB Journal*, p. fj.202001107R. Available at: <https://doi.org/10.1096/fj.202001107R>.

You, S. *et al.* (2021) 'Circadian regulation of the *Drosophila* astrocyte transcriptome', *PLOS Genetics*. Edited by J. Ewer, 17(9), p. e1009790. Available at: <https://doi.org/10.1371/journal.pgen.1009790>.

Yu, A.D. and Rosbash, M. (2023) 'Butt-seq: a new method for facile profiling of transcription', *Genes & Development*, p. genesdev;gad.350434.123v1. Available at: <https://doi.org/10.1101/gad.350434.123>.

Zeng, J. *et al.* (2018) 'The *Drosophila* CCR4-NOT complex is required for cholesterol homeostasis and steroid hormone synthesis', *Developmental Biology*, 443(1), pp. 10–18. Available at: <https://doi.org/10.1016/j.ydbio.2018.08.012>.

Zhang, Y. *et al.* (2013) 'A Role for *Drosophila* ATX2 in Activation of PER Translation and Circadian Behavior', *Science*, 340(6134), pp. 879–882. Available at: <https://doi.org/10.1126/science.1234746>.

Figure legends

Fig 1. *timeless* and *period* mRNAs show cycling translatability. (A) Plain line - Log₂ total mRNA levels of *tim* and *per* quantified by RT-qPCR, Dashed line - Log₂ ribosome-bound mRNA levels. *18S* rRNA used as reference gene, and relative to CT0 condition. **(B)** Log₂ ribosome-bound mRNA levels relative to respective total mRNA level. Error bars indicate SEM of log₂ normalized datapoints, n = 3 biological replicates. **(C)** Quantification of protein levels of TIM and PER measured in Western Blot in Grima *et al.*, 2019.

Fig 2. POP2 specifically controls *tim* total mRNA levels in a PER dependent manner and its translation in a PER independent manner via its poly(A) tail. (A) Log₂ total mRNA levels of *tim* and *per* quantified by RT-qPCR, using *18S* rRNA as reference gene, and relative to CT0 condition. **(B)** Log₂ ribosome-bound mRNA levels

relative to respective total mRNA levels. Error bars indicate SEM of log₂ normalized datapoints, differential oscillation analysis realized with dryR lm function, n = 3 biological replicates, n = 2 biological replicates in *per⁰* conditions CT9 & 21. BICW (Bayesian Information Criterion Weight) indicates the plausibility of the indicated model to represent the data the best among all the tested models : Rhythm indicates the analysis for differential cycling parameters between conditions, where a colored cell means the corresponding condition is cycling, and a differently colored cell means a cycling condition, but with different cycling parameters. Mean indicates the differential average levels between conditions, where differently colored cells indicates differences in mean levels of mRNA between conditions. An "Ambiguous" annotation illustrates a condition where the BICW threshold for the best tested model was not reached. **(C)** Poly(A) tail length assay of *tim* mRNA from TRAP samples.

Fig 3. POP2 controls *tim* mRNA stability according to its levels. **(A)** Left panel - Log₂ total mRNA levels of *tim* mRNA in presence or absence of UAS-*Pop2*-RNAi quantified by RT-qPCR, using *18S* rRNA, *Mnf* and *Tub* as reference genes, and relative to *per⁺* CT3 condition. Error bars indicate SEM of log₂ normalized datapoints, statistical analysis realized with two-way ANOVA type 3 (unbalanced design) followed by pairwise comparisons done with Tukey test. (ns, not significant; *, p<0,05; **, p<0,01; ***, p<0,001; ****, p<0,0001). Right panel - Correlations between *tim* mRNA levels in absence of *Pop2* K.D and delta fold change of mRNA levels in presence vs absence of *Pop2* K.D for each conditions. Vertical error bars indicate SEM of log₂ normalized datapoints in *Pop2* K.D condition, horizontal error bars indicate SEM of log₂ normalized datapoints in non-*Pop2* K.D condition, R-squared determined by Pearson's correlation test, n = 3-4 biological replicates per conditions. **(B)** Poly(A) tail length assay of *tim* mRNA in different conditions in absence or presence of *Pop2* K.D. **(C)** Similar to (A) with *per* mRNA

Fig 4. POP2 controls many circadianly regulated genes. **(A)** Volcano plot representing log₂ fold change in *per⁺* CT15 condition vs *per⁺* CT3 on the x-axis and -log₂ FDR p-value of the fold change. **(B)** Log₂ fold change in *per⁺* CT3 *Pop2* K.D condition vs *per⁺* CT3 on the x-axis and -log₂ FDR p-value of the fold change. Plot realized on ribosome-bound RNA fractions with upregulated genes in red, downregulated in blue, and non significantly regulated genes in grey with a FDR p-value ≥0,05 or -1 ≥ Log₂ FC ≤ 1. **(C)** Hierarchical clustering heatmap representing the expression level change of significantly circadianly regulated genes in presence or absence of *Pop2* K.D and in *per⁺* or *per⁰* contexts, for ribosome-bound RNAs. **(D)** Venn diagram representing the number of genes significantly regulated by circadian time CT15 vs 3 (CT), depletion of *Pop2* at CT3 or CT15 (POP2), depletion of *Pop2* in mutant *per⁰* (*per⁰* POP2).

Fig 5. *vri* is also a target of POP2. **(A)** Log₂ total mRNA levels of *vri* quantified by RT-qPCR, using 18S rRNA as reference gene, and relative to CT0 condition. **(B)** Log₂

ribosome-bound mRNA levels relative to respective total mRNA levels. Error bars indicate SEM of log₂ normalized datapoints, differential oscillation analysis realized with dryR lm function, n ≥ 2 biological replicates. **(C)** Plain line - Log₂ total mRNA levels of *vri* quantified by RT-qPCR, Dashed line - Log₂ ribosome-bound mRNA levels. 18S rRNA used as reference gene, and relative to CT0 condition. **(D)** Log₂ ribosome-bound mRNA levels relative to respective total mRNA level. Error bars indicate SEM of log₂ normalized datapoints, n = 3 biological replicates.

Fig 6. *vri* is regulated by POP2 similarly than *tim*. **(A)** Log₂ total mRNA levels of *vri* in presence or absence of *Pop2* K.D quantified by RT-qPCR, using 18S rRNA, *Mnf* and *Tub* as reference genes, and relative to *per+* CT3 condition. Error bars indicate SEM of log₂ normalized datapoints, statistical analysis realized with two-way ANOVA type 3 (unbalanced design) followed by pairwise comparisons done with Tukey test. (ns, not significant; *, p<0,05; **, p<0,01; ***, p<0,001; ****, p<0,0001). **(B)** Correlations between *vri* mRNA levels in absence of *Pop2* K.D and delta fold change of mRNA levels in presence vs absence of *Pop2* K.D for each conditions. Vertical error bars indicate SEM of log₂ normalized datapoints in *Pop2* K.D condition, horizontal error bars indicate SEM of log₂ normalized datapoints in non-*Pop2* K.D condition, R-squared determined by Pearson's correlation test, n = 3-4 biological replicates per conditions. **(C)** Representation of known *vri* mRNA isoforms, black lines = introns; rectangles = exons; grey rectangles = non-coding; orange rectangles = coding sequence. **(D)** Poly(A) tail length assay of *vri* mRNA in different conditions in absence or presence of *Pop2* K.D, - left panel – on TRAP samples, with Input fraction being total mRNA and Eluate being ribosome-bound, - right panel – on total mRNA only. The primers used target *vri*-A+E isoforms. **(E)** Poly(A) tail length assay of *vri* mRNA in different conditions in absence or presence of *Pop2* K.D. The primers used target *vri*-C+D isoforms.

Fig 7. POP2's effect strength is tuned by the expression level of its targets in accordance with their codon usage. **(A)** Scatter plot showing the correlation between log₂ normalized TPM values >0 for POP2-targeted genes in *per+* CT3 condition (x-axis) and of significant log₂ fold changes between *Pop2* K.D vs *per+* context at CT3 (y-axis), red line shows trendline and R-squared determined by Spearman's correlation test. **(B)** Plot showing the Spearman's R-squared correlation coefficient calculated between average percentage of codons in the transcripts of genes significantly targeted by POP2 at CT3 and the positive log₂ fold change of *Pop2* K.D effect at CT3. **(C)** Plot showing the Spearman's R-squared correlation coefficient calculated between average percentage of codons in the transcripts of genes significantly targeted by POP2 at CT3 and the log₂ normalized TPM values for POP2-targeted genes in *per+* CT3 condition. A/U ending codons are represented in red, G/C ending codons in blue. **(D)** Scatter plot showing the correlation between significant log₂ fold changes between CT15 vs CT3 in *per+* context (x-axis) and of significant log₂ fold changes between *Pop2* K.D vs *per+* context at CT3 (y-axis). **(E)** Scatter plot showing the correlation between significant log₂ fold changes between CT15 vs CT3

in *per+* context (x-axis) and of significant log₂ fold changes between *Pop2* K.D vs *per+* context at CT15 (y-axis), red line shows trendline and R-squared determined by Spearman's correlation test, n = 2 biological replicates per conditions.

Fig S1. (A) Double plotted actograms of average activity of flies, white background corresponds to light on time and grey area to light off time. **(B)** Log₂ ratio of translatability (fraction = T) relative to respective total mRNA condition (fraction = C) measured at CT15 for both flag-tagged ribosomal protein expressing flies and non flag-tagged ribosomal protein expressing flies, to estimate background detection of mRNAs in ribosome-bound/translatability contexts. **(C)** Log₂ ribosome-bound mRNA levels relative to respective total mRNA level. Error bars indicate SEM of log₂ normalized datapoints, n = 3 biological replicates. **(D)** Log₂ ribosome-bound mRNA levels. *18S* rRNA used as reference gene, and relative to CT0 condition. differential oscillation analysis realized with dryR lm function, n = 3 biological replicates, n = 2 biological replicates in *per0* conditions CT9 & 21.

Fig S2. (A) Log₂ total mRNA levels of pre-*tim* in presence or absence of *Pop2* K.D quantified by RT-qPCR. **(B)** Log₂ total mRNA levels of *Pop2* in presence or absence of *Pop2* K.D quantified by RT-qPCR, using *Tub* as reference genes, and relative to *per+* CT3 condition. Error bars indicate SEM of log₂ normalized datapoints, statistical analysis realized with two-way ANOVA type 3 (unbalanced design) followed by pairwise comparisons done with Tukey test. n = 3-4 biological replicates per conditions. **(C)** Protein levels of PER in presence or absence of *Pop2* K.D quantified by Western Blot, using Amido Black as a total protein stain control, and relative to *per+* CT3 condition. Error bars indicate SEM, statistical analysis realized with Welch one-way ANOVA type 1 (balanced design) followed by pairwise comparisons done with Dunnett test for PER n = 3 biological replicates per conditions. *Lower panels* – representative Western blot result (ns, not significant; *, p<0,05; **, p<0,01; ***, p<0,001; ****, p<0,0001). n = 3 biological replicates per conditions. *Lower panels* – representative Western blot result.

Fig S3. (A) Log₂ fold change in *per+* CT15 *Pop2* K.D condition vs *per+* CT15 on the x-axis and $-\log_2$ FDR p-value of the fold change. Plot realized on ribosome-bound RNA fractions with upregulated genes in red, downregulated in blue, and non significantly regulated genes in grey with a FDR p-value $\geq 0,05$ or $-1 \geq \text{Log}_2 \text{FC} \leq 1$. **(B)** Hierarchical clustering heatmap representing the expression level change of significantly circadianly regulated genes in presence or absence of *Pop2* K.D and in *per+* or *per0* contexts, for total RNAs. **(C)** Venn diagram including the number of genes significantly regulated by circadian time CT15 vs 3 (CT), depletion of *Pop2* at CT3 or CT15 (POP2), and excluding genes significantly regulated by depletion of *Pop2* in *per0* condition, for both total and ribosome-bound RNAs, n = 2 biological replicates per conditions.

Fig S4. (A) Log2 total mRNA levels of pre-*vri* quantified by RT-qPCR, using *18S* rRNA as reference gene, and relative to CT0 condition. **(B)** Log2 ribosome-bound mRNA levels. *18S* rRNA used as reference gene, and relative to CT0 condition. differential oscillation analysis realized with dryR lm function, $n \geq 2$ biological replicates. **(C)** Log2 total mRNA levels of pre-*vri* in presence or absence of *Pop2* K.D quantified by RT-qPCR, using *18S* rRNA, *Mnf* and *Tub* as reference genes, and relative to *per+* CT3 condition, error bars indicate SEM of log2 normalized datapoints, statistical analysis realized with two-way ANOVA type 3 (unbalanced design) followed by pairwise comparisons done with Tukey test (ns, not significant; *, $p < 0,05$; **, $p < 0,01$; ***, $p < 0,001$; ****, $p < 0,0001$), $n = 2-3$ biological replicates per condition.

Figures

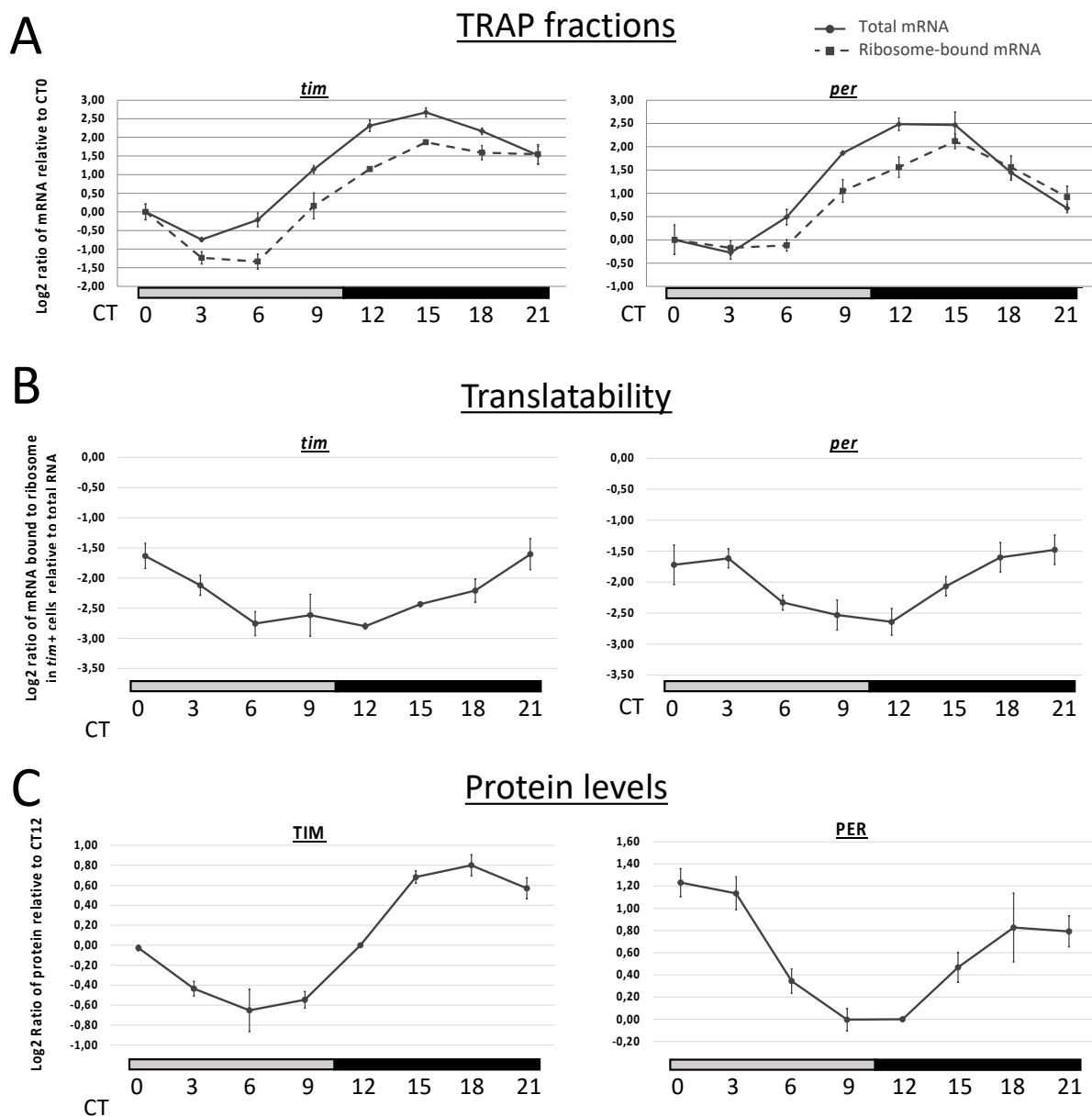
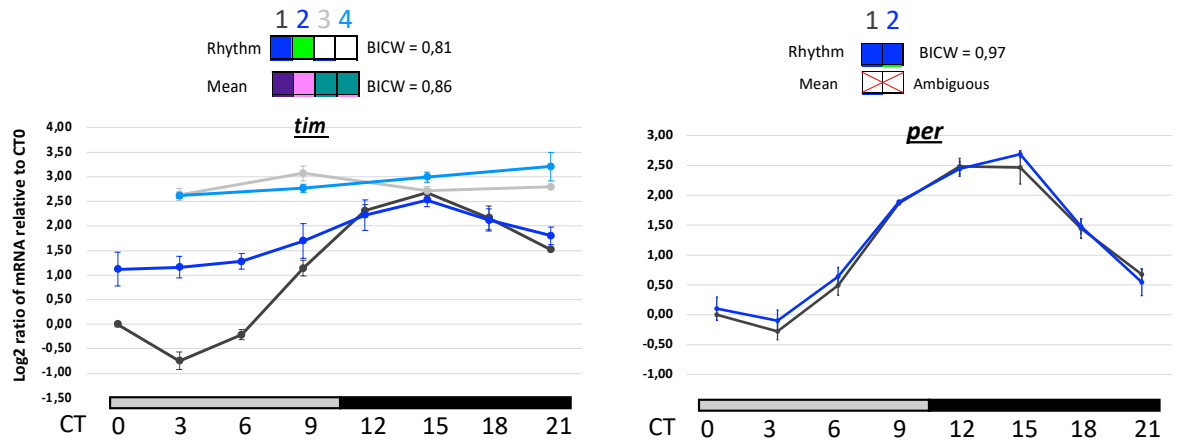


Fig. 1

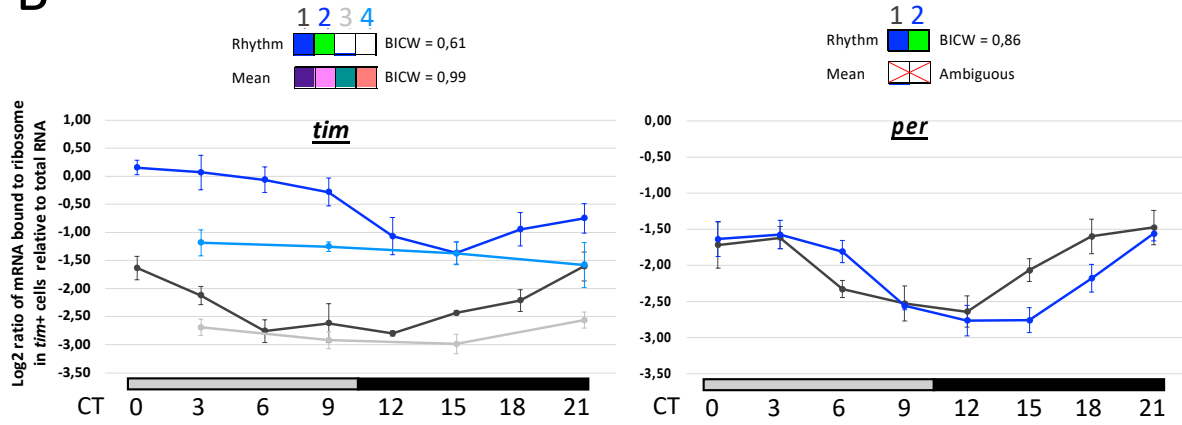
A

Total mRNA



B

Translatability



C

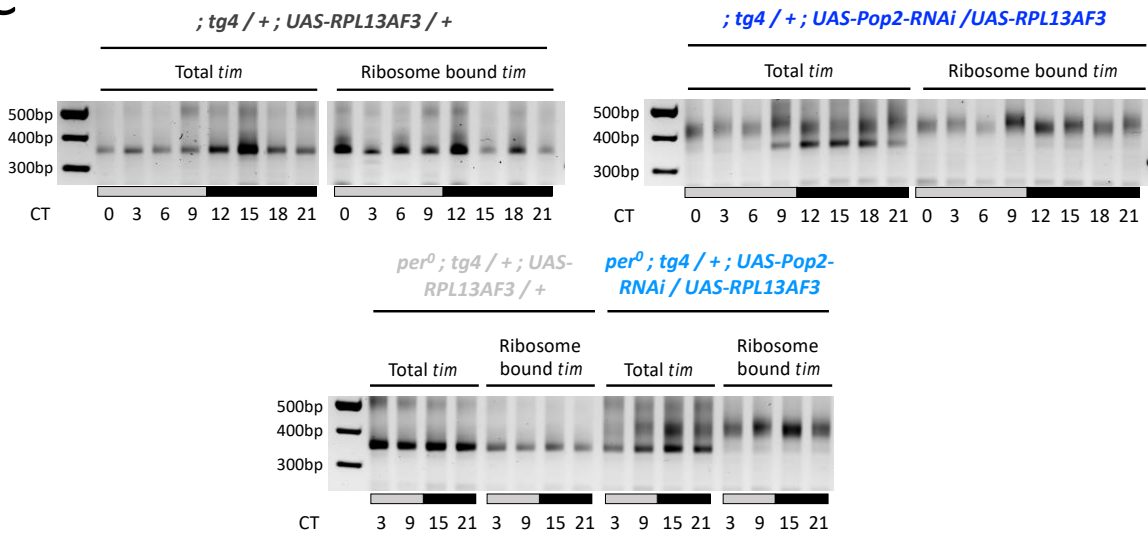
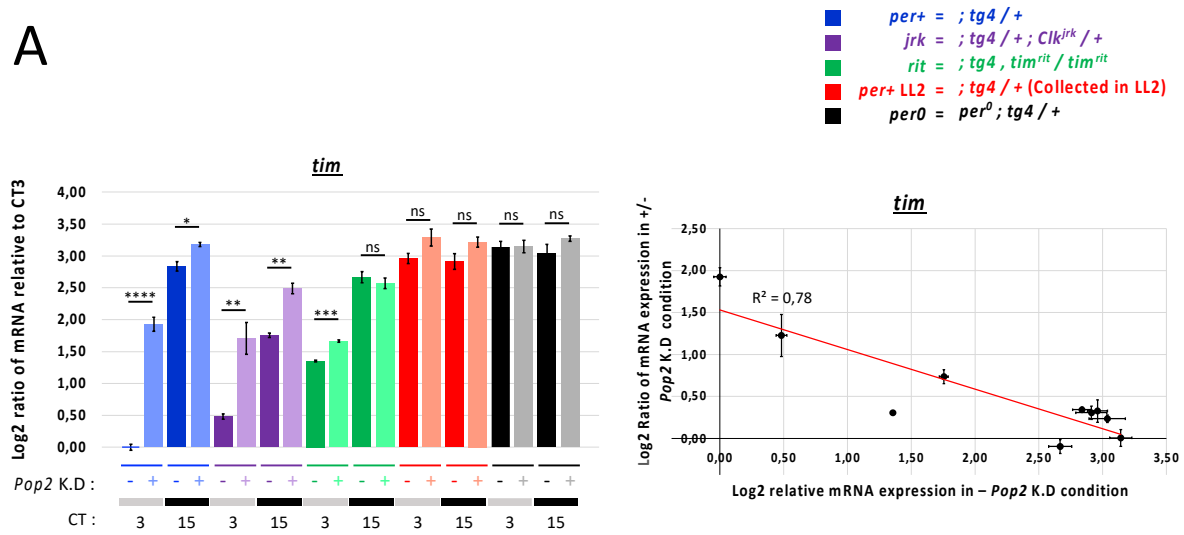
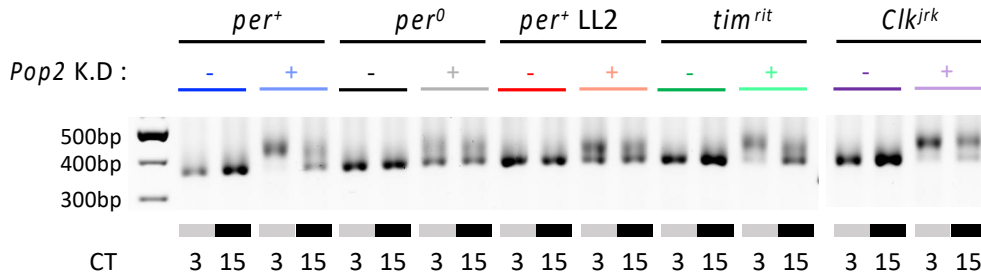


Fig. 2

A



B



C

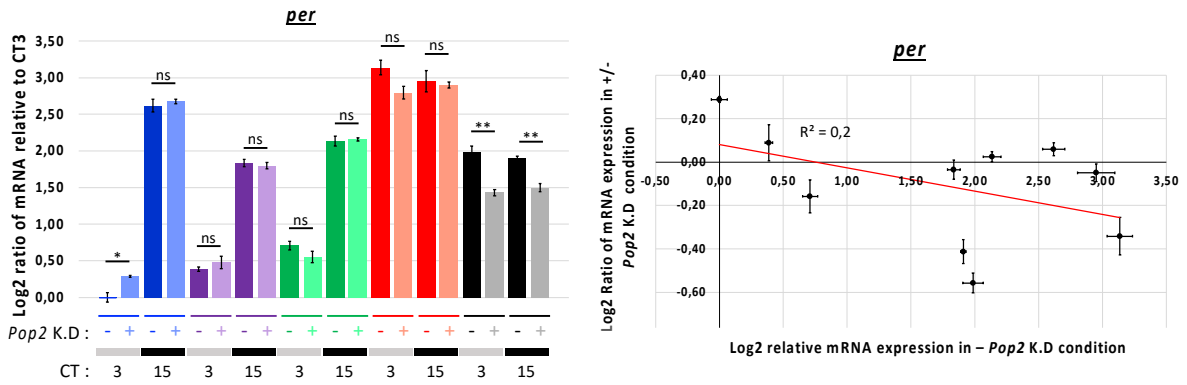
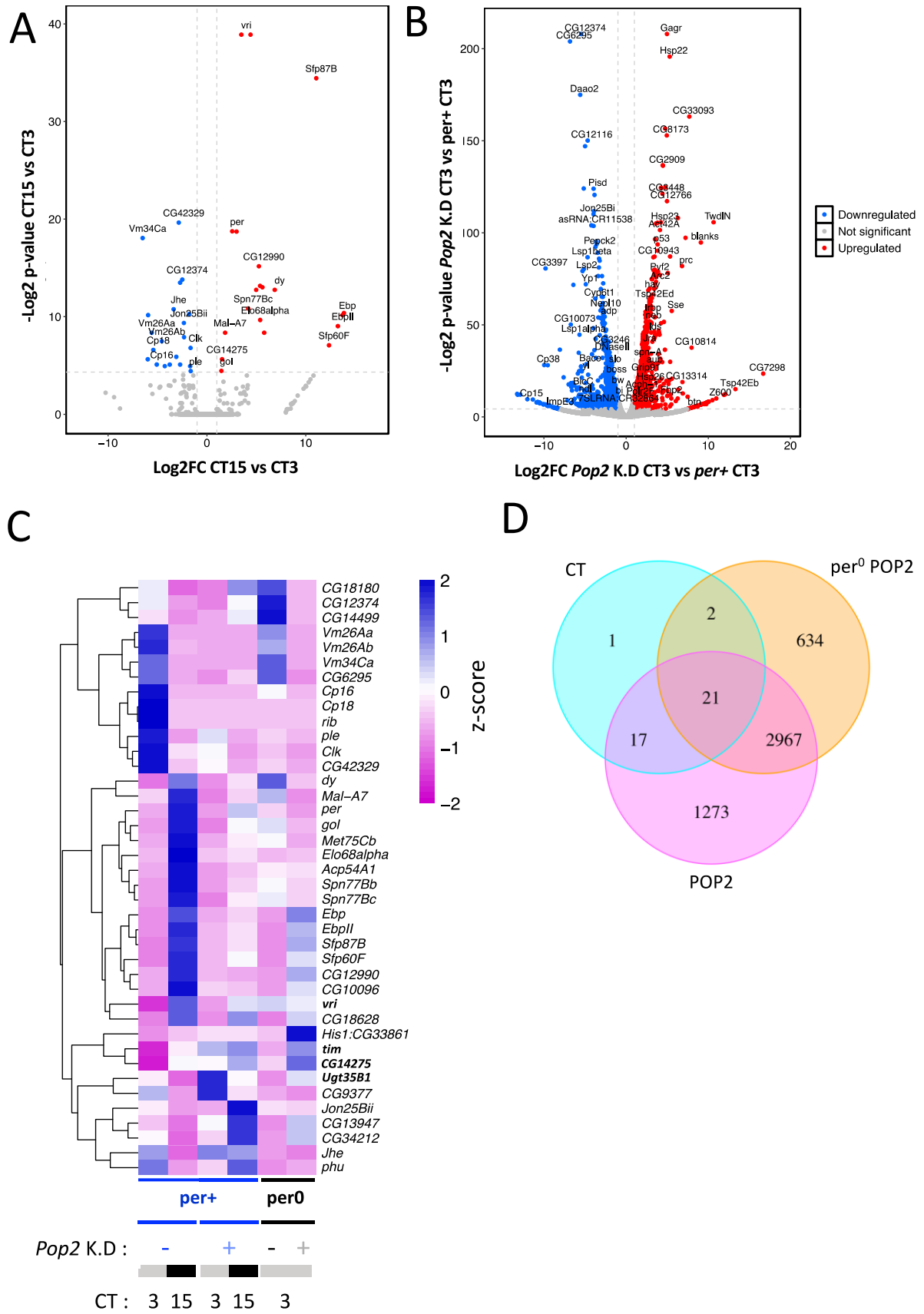




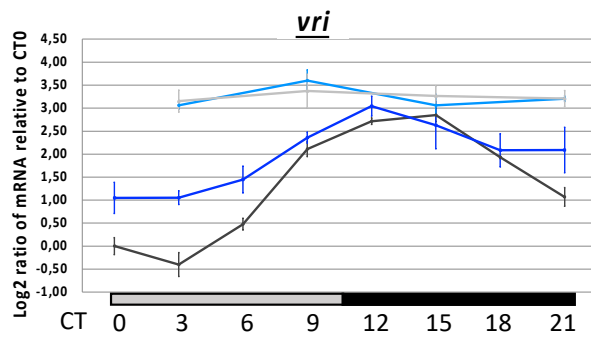
Fig. 3



A

Total mRNA

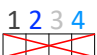
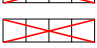
1 2 3 4
 Rhythm  BICW = 0,92
 Mean  BICW = 0,88

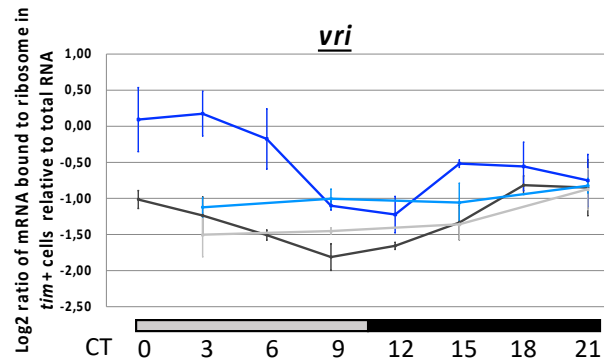


B

1 : *tg4* / + ; *UAS-RPL13AF3* / +
 2 : *tg4* / + ; *UAS-Pop2-RNAi* / *UAS-RPL13AF3*
 3 : *per⁰* ; *tg4* / + ; *UAS-RPL13AF3* / +
 4 : *per⁰* ; *tg4* / + ; *UAS-Pop2-RNAi* / *UAS-RPL13AF3*

Translatability

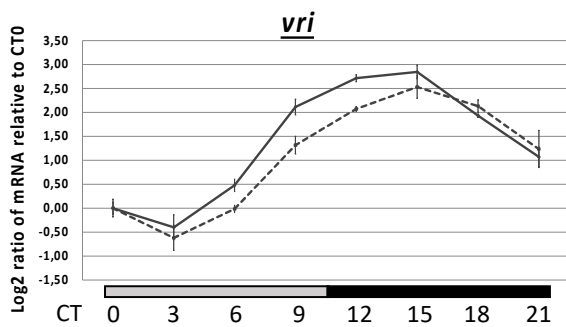
1 2 3 4
 Rhythm  Ambiguous
 Mean  Ambiguous



C

TRAP fractions

—●— Total mRNA
 - -■- Ribosome-bound mRNA



D

Translatability

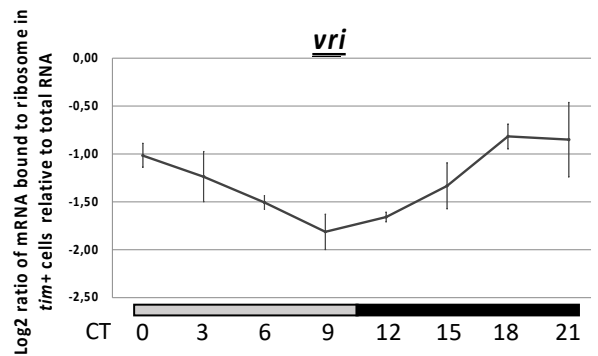


Fig. 5

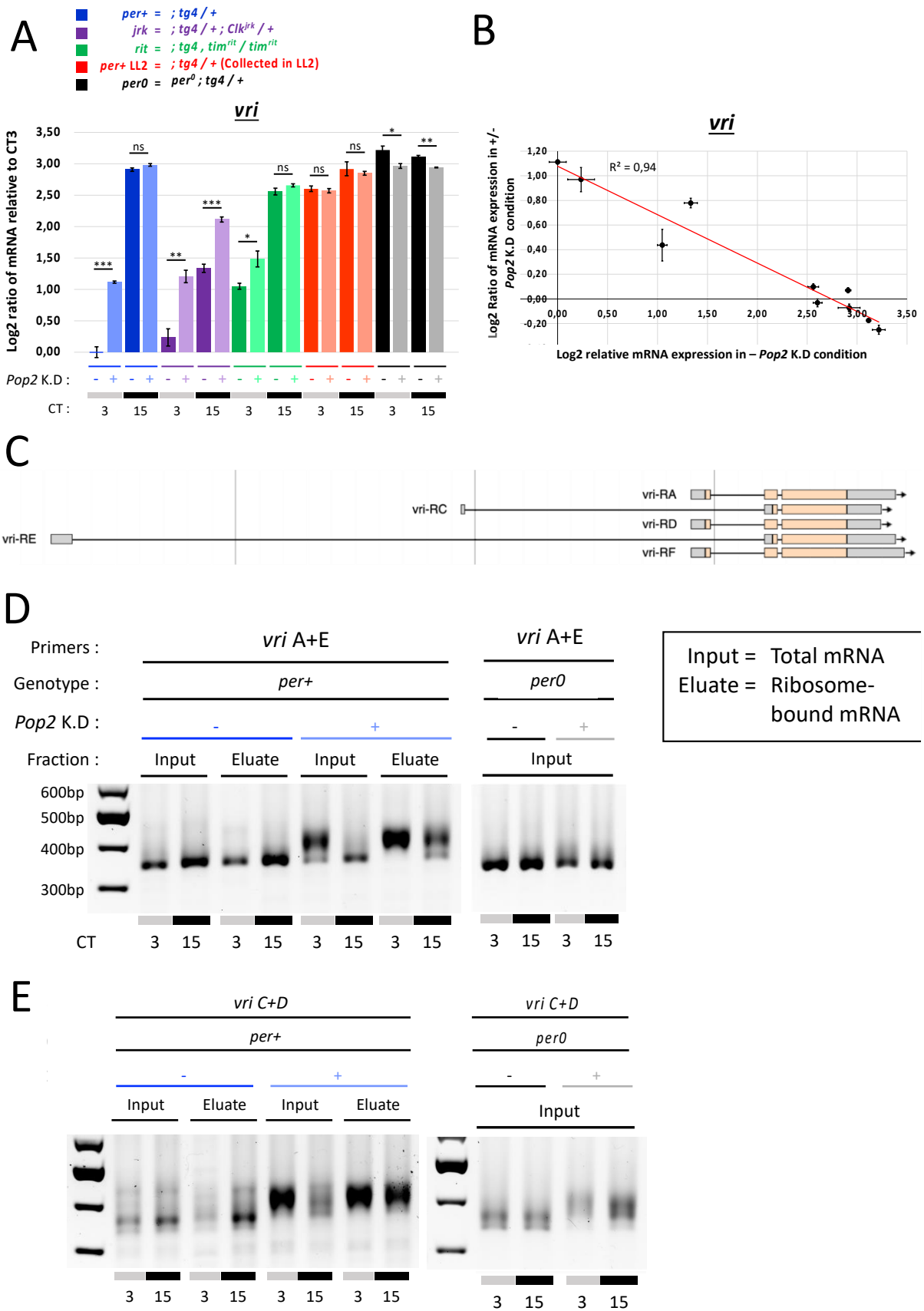


Fig. 6

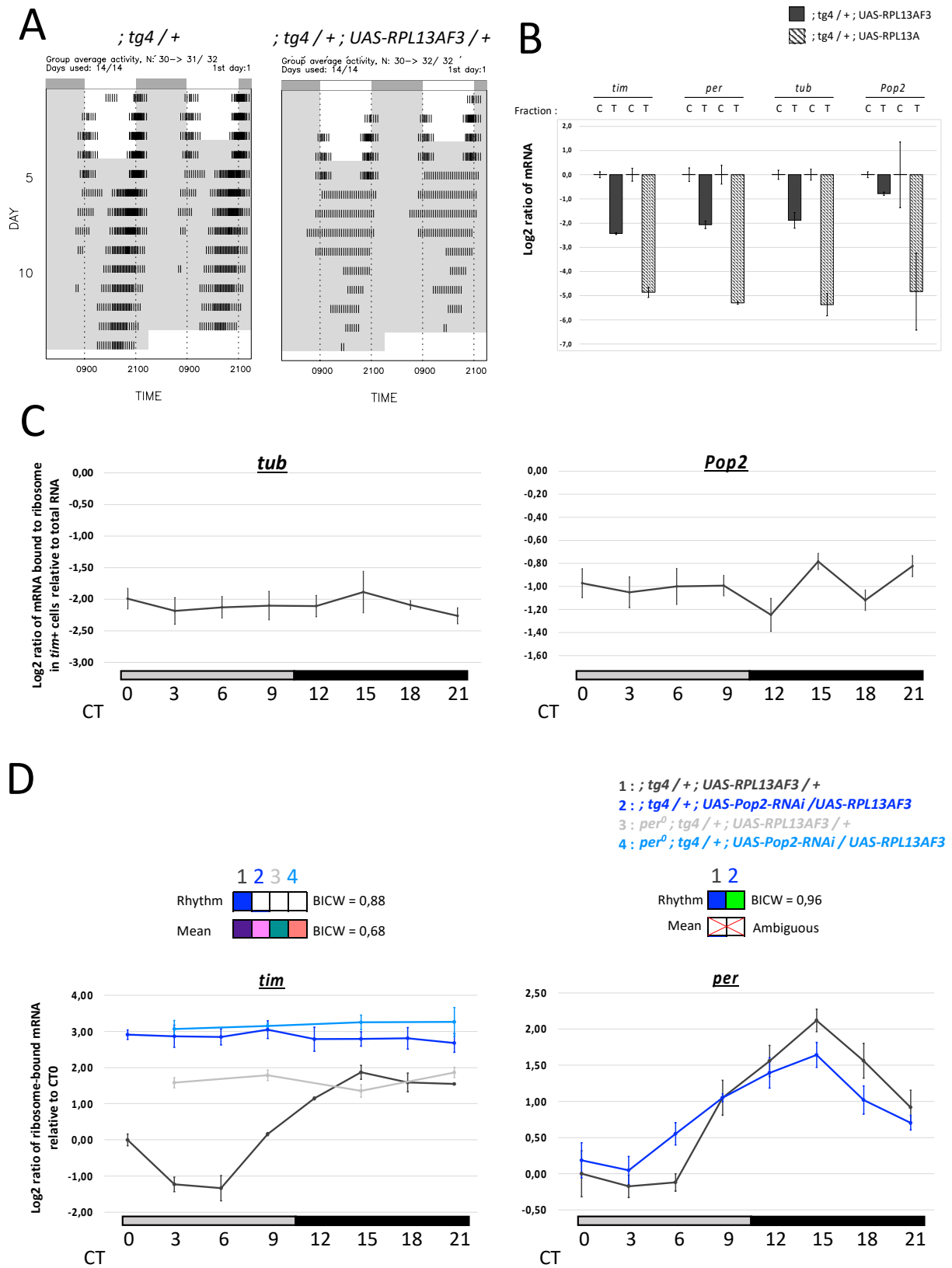


Fig. S1

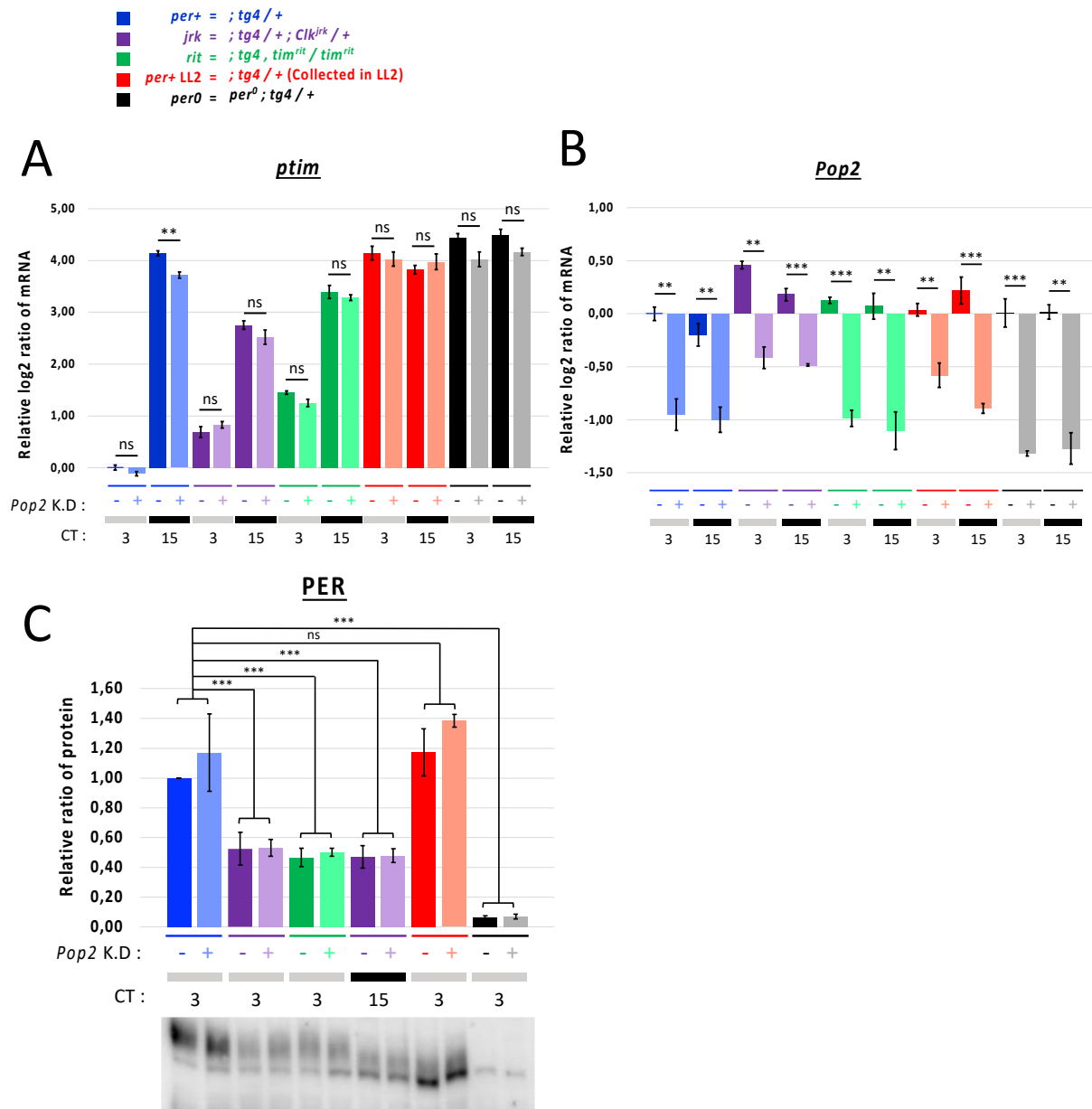


Fig. S2

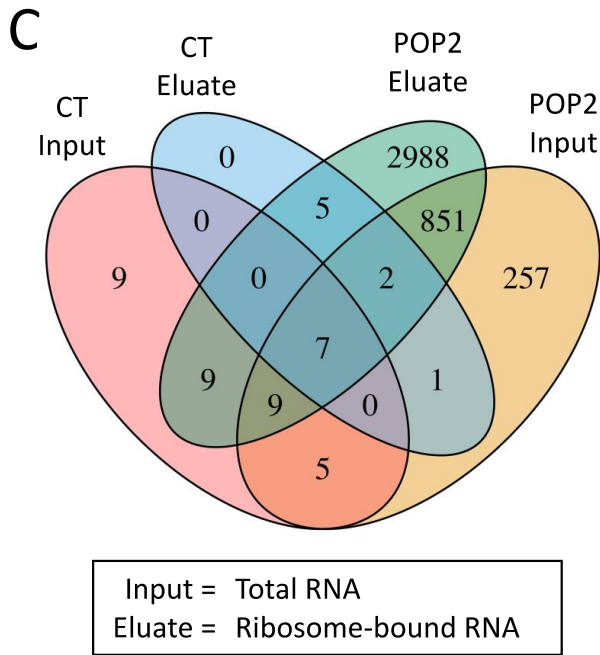
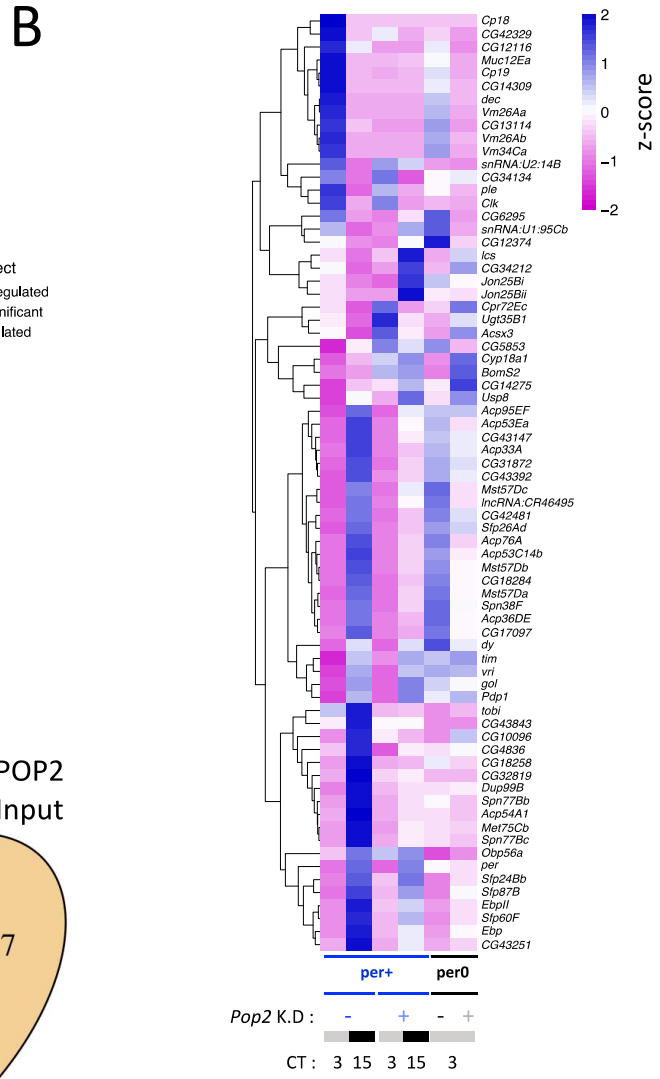
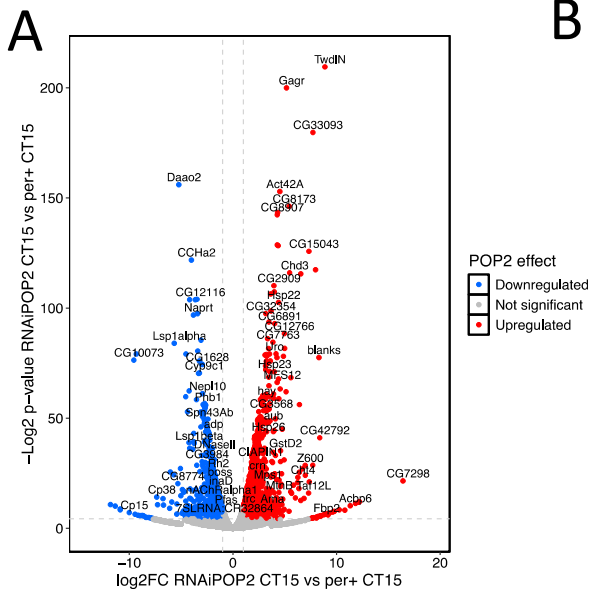


Fig. S3

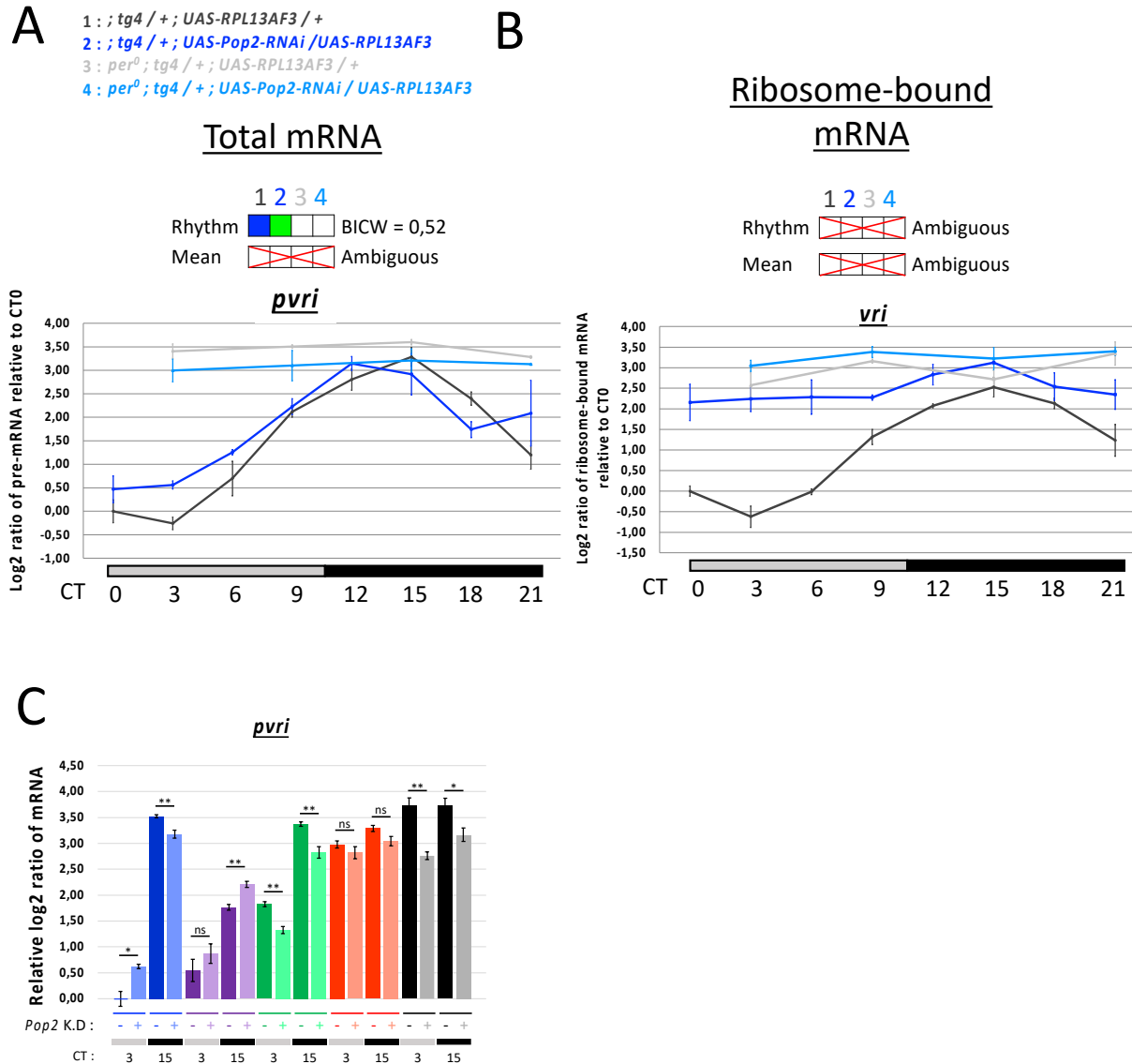


Fig. S4

2. Unpublished data

a. *PER* does not bind *tim* mRNA

In our article figure 2B representing *tim* translatability, we observed a significant decrease of average *tim* translatability in *per⁰* compared to *per⁺* contexts. This made us wonder whether PER itself could regulate the translatability of *tim*, if so, we could expect binding between the PER protein and *tim* mRNA. To test this hypothesis, we use an RNA-IP protocol modified from one communicated to us by Chunghun Lim (KAIST, South Korea).

We carried out this RNA-IP using anti-HA conjugated beads on *per⁰;per-HA* flies, that only express a PER-HA tagged protein through a transgene, and on *per⁺* flies as negative control. In parallel, we carried out an RNA-IP using anti-PER conjugated Sepharose beads on *per⁺* flies, and on *per⁰* flies as negative control. This double

experiment allowed to benefit from the high affinity and specificity of anti-HA antibodies, and also to investigate a physiological condition using the anti-PER antibody. This experiment was carried out at CT3 and 15, in case this potential interaction revealed to be circadian (Fig. 27).

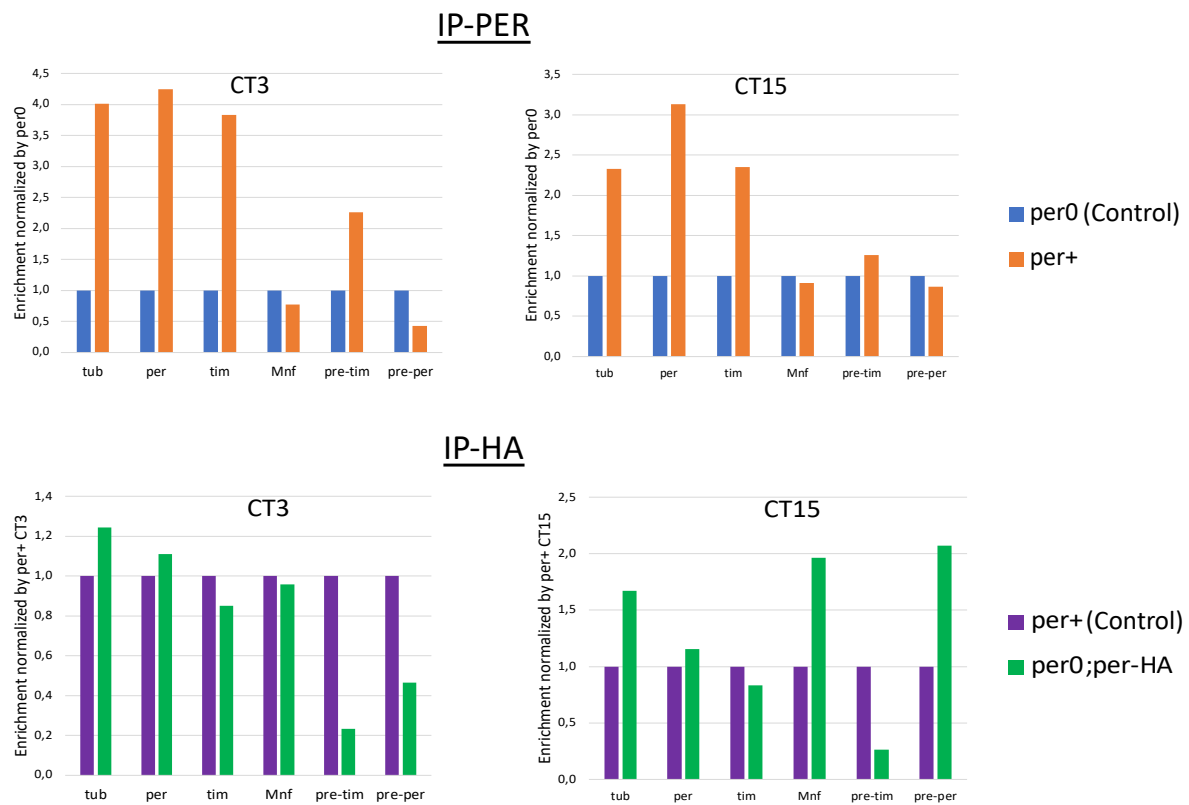


Figure 27 : RT-qPCR quantification of the enrichment of mRNAs bound to PER compared to control background noise. IP-PER was carried out using anti-PER antibodies, IP-HA was carried out using anti-HA antibodies. *Tim* was the gene of interest, *tub*, *per*, *Mnf*, *pre-tim* and *pre-per* were control conditions. Equal volumes of samples were analyzed for all the conditions, as the eluates display total RNA concentrations extremely low, these are normalized by applying a factor to the raw PCR Ct (Cycle threshold) value directly. The values obtained in the eluate fractions are then normalized by their respective input, to account for mRNA cycling levels between CT3 and CT15. Finally, the obtained ratio is divided to its negative control's ratio to give the enrichment of the mRNA relative to both input and negative control condition. No reference genes normalization was applied to avoid potential bias from unknown interactions between this one and the PER protein.

The difficulty of this RNA-IP experiment is the lack of positive control, as PER is not known to display any RNA-binding activity. We thus use *per* mRNA, *pre-tim*, *pre-per* and housekeeping genes *tub* and *Mnf* to estimate the relevance of a potential enrichment of *tim* mRNA precipitated with PER. In the IP-HA experiment, we did not detect any enrichment of *tim* mRNA in *per-HA* expressing flies compared to *per+* control flies, although the anti-HA antibody is more specific than the anti-PER antibody.

In the IP-PER experiment, we can see an enrichment of *tim* potentially bound to PER compared to its *per0* control condition, but similar enrichment is found for *tub* and *per* mRNA. Meaning that there could be an interaction between *tim* mRNA and PER protein, but this one would not be specific. Moreover, *tub* mRNA is also found enriched

with PER in the IP-PER, yet *tub*'s translatability is not impacted by the presence or absence of PER (Fig. S7), further suggesting that this result is not relevant.

b. POP2 isoform-specificity for *tim*

It was previously shown that *tim* is alternatively spliced in function of the temperature (Boothroyd *et al.*, 2007; Shakhmantsir *et al.*, 2018; Foley *et al.*, 2019; Martin Anduaga *et al.*, 2019). And that *tim* isoforms were targeted by AGO1 differentially with miRNAs predicted to target uniquely certain isoforms (Martin Anduaga *et al.*, 2019). It is possible that this isoform -specific targeting of *tim* is applied to POP2's activity as well. Among the 4 described *tim* isoforms, *tim-SC* is found in very low proportions at 25°C, corresponding to the temperature used in our experiments, we will thus focus on the 3 other isoforms : *tim-RL* (canonical), *tim-M* and *tim-C*. (Fig. 28)(Martin Anduaga *et al.*, 2019).

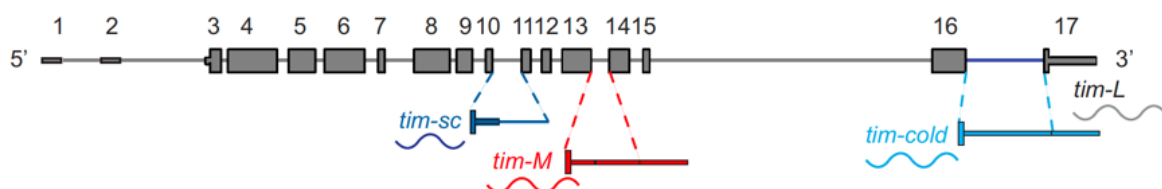


Figure 28 : Representation of the different *tim* isoforms from (Martin Anduaga *et al.*, 2019). The rectangles correspond to coding exons, the thick lines to non-coding exons (example with *tim-M*, *tim-C* and the beginning of *tim-SC*), and the thin lines to introns (end of *tim-SC*). *Tim-L* corresponds to the 5 canonical *tim* isoforms, among which *tim-RL*.

We designed RT-qPCR primers that were specific of each isoforms and measured their levels in control and Pop2 depleted conditions (Fig. 29).

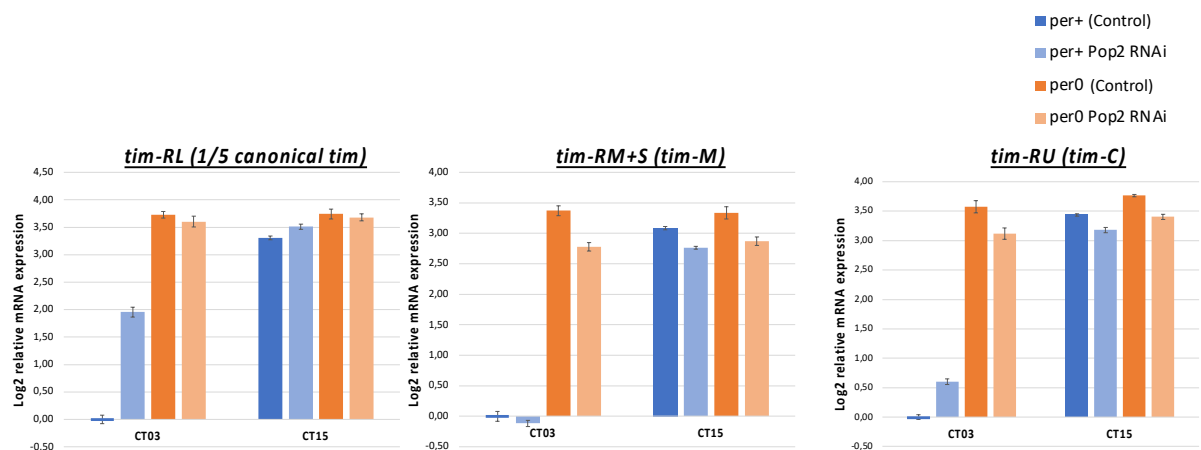


Figure 29 : RT-qPCR quantification of *tim* isoforms at 2 circadian times in *Pop2* K.D context and in presence or absence of PER. N=3 replicates. Experiment done with Éric Jacquet & Naima Nhiri.

In this experiment, we see a strong increase of the canonical *tim-RL* mRNA levels upon *Pop2* depletion, at CT3 and in presence of PER only, in line with our previous results done without considering the different isoforms. Interestingly, we observed no strong differences for *tim-M* and *tim-C* levels upon *Pop2* K.D, for both CT3 and CT15 and in

presence or absence of PER. This result suggests that POP2 acts on *tim* in an isoform-specific manner.

c. POP2-downregulated genes also seem less regulated when highly abundant

In our article, we showed a mild negative correlation between the effect of POP2 for genes significantly upregulated upon *Pop2* K.D and the abundance of these genes in *per+* CT3 conditions for ribosome-bound RNAs (Article fig. 7A). However, our volcano plot figure showing the POP2 significantly-regulated genes at CT3 also displayed numerous downregulated genes upon *Pop2* K.D, in line with previous results in *Drosophila* (Article Fig. 4B) (Zeng *et al.*, 2018; Haugen *et al.*, 2023) . We thus looked whether the genes downregulated by POP2 were also impacted in function of their abundance (Fig. 30)

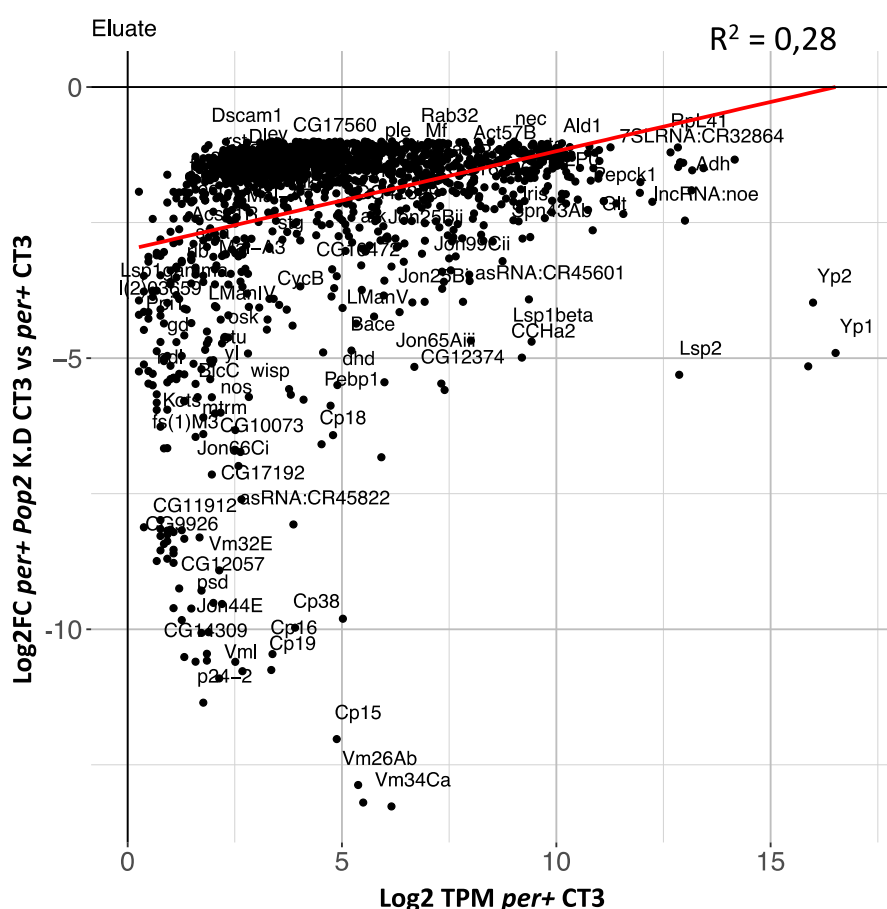


Figure 30 : Scatter plot showing the correlation between log2 normalized TPM values >0 for POP2-targeted genes in *per+* CT3 condition (x-axis) and of significant log2 fold changes between *Pop2* K.D vs *per+* context at CT3 for downregulated genes only (y-axis), red line shows trendline and R-squared determined by Spearman's correlation test.

This correlation yielded a low positive correlation, yet observe a relatively similar phenomenon than when plotting upregulated genes only. This suggests that the effect of POP2 is more visible on low abundance transcripts, for both up and down-regulated genes.

d. Many differentially-regulated genes between CT3 and CT15 are not known cyclers

Furthermore, our analysis was carried out at 2 timepoints only, CT3 and CT15, which is enough to estimate differentially-regulated gene levels between these two timepoints, but not to deduce oscillations, especially for the genes reaching their peak or trough levels in between CT3 and CT15 and that might thus show equal levels of mRNAs at these 2 timepoints. We thus compared our list of differentially-regulated genes to previously published lists of cycling genes in DD in *Drosophila* (Hughes *et al.*, 2012; Huang *et al.*, 2013; Ma and Rosbash, 2020b; Litovchenko *et al.*, 2021). In the table 7 we can see that few of our putative circadianly-regulated genes were also found in other published work, and although these papers present little overlap with each others themselves, this highlights the importance to remain conservative and not propose confidently these differentially-regulated genes as cyclers. Yet, our results are overall consistent with previously found ones, as we retrieved many clock components in this table, particularly *per*, *vri*, *tim*, *Clk*. It was surprising to see *per* and *Clk* as *Pop2* regulated genes, but our RT-qPCR results on ribosome-bound RNAs did show the same results for both *per* (Article fig. S1D) and *Clk* (Data not shown), this suggests a role of POP2 on *per* and *Clk* ribosome-bound mRNA levels, but not on their total mRNA levels, as these genes are not impacted in this fraction.

Name	FlyBase ID	Chromosome	per+ CT15/per+ CT3	per+ Pop2 RNAi CT3/ per+ CT3	per+ Pop2 RNAi CT15/ per+ CT15	per0 Pop2 RNAi/ per0	Found as cyclers				
/	/	/	Log2 FC	FDR p-value	Log2 FC	FDR p-value	Log2 FC	FDR p-value	Log2 FC	FDR p-value	/
<i>per</i>	FBgn0003068	X	2,55	2,3E-06	-0,61	2,4E-01	-1,33	1,0E-03	-1,58	2,7E-08	4
<i>vri</i>	FBgn0016076	2L	3,48	2,0E-12	1,57	8,6E-07	-1,04	6,6E-03	-0,83	2,1E-03	3
<i>tim</i>	FBgn0014396	2L	2,99	2,3E-06	3,05	4,5E-11	0,19	7,4E-01	0,50	1,9E-01	3
<i>Ugt35B1</i>	FBgn0026314	3R	-1,80	8,2E-04	0,77	2,7E-02	1,44	1,9E-05	0,80	5,1E-03	3
<i>Clk</i>	FBgn0023076	3L	-1,66	9,0E-03	-1,69	1,4E-05	-1,70	2,6E-06	-1,42	5,0E-05	2
<i>gol</i>	FBgn0004919	2R	1,46	4,6E-02	-0,72	7,5E-02	-1,30	9,5E-05	-1,28	8,5E-06	1
<i>ple</i>	FBgn0005626	3L	-1,64	4,6E-02	-1,28	1,2E-04	-0,46	2,7E-01	-0,81	3,3E-03	1
<i>CG10096</i>	FBgn0038032	3R	4,41	2,0E-12	1,20	4,0E-01	-3,78	1,1E-13	3,40	2,8E-03	0
<i>Sfp87B</i>	FBgn0259975	3R	11,06	4,3E-11	7,49	5,0E-04	-2,68	3,1E-06	3,01	1,1E-01	0
<i>CG42329</i>	FBgn0259229	2L	-2,85	1,2E-06	-2,44	6,3E-13	-1,68	5,2E-03	-2,90	5,2E-10	0
<i>Vm34Ca</i>	FBgn0003983	2L	-6,50	3,7E-06	-13,27	1,7E-04	-1,62	4,9E-01	-8,46	1,1E-11	0
<i>CG12990</i>	FBgn0030859	X	5,26	2,7E-05	1,56	5,1E-01	-5,06	6,7E-09	4,86	3,3E-03	0
<i>CG12374</i>	FBgn0033774	2R	-2,49	7,0E-05	-5,47	2,4E-63	1,83	1,8E-02	-3,26	9,4E-28	0
<i>CG18180</i>	FBgn0036024	3L	-2,72	8,7E-05	-2,28	2,4E-08	2,65	2,1E-05	-2,32	1,7E-10	0
<i>Spn77Bb</i>	FBgn0036969	3L	5,37	1,1E-04	-1,64	6,0E-01	-3,11	1,2E-05	-1,68	2,9E-01	0
<i>dy</i>	FBgn0004511	X	6,85	1,5E-04	3,15	2,3E-01	-2,11	2,4E-02	-2,53	2,8E-03	0
<i>Acp54A1</i>	FBgn0083936	2R	4,98	1,5E-04	-2,42	3,3E-01	-4,04	1,0E-04	-0,70	5,8E-01	0
<i>Spn77Bc</i>	FBgn0036970	3L	4,17	5,5E-04	-1,70	4,9E-01	-2,49	4,6E-03	-1,56	3,0E-01	0
<i>Jhe</i>	FBgn0010052	2R	-3,37	5,8E-04	-0,41	5,9E-01	2,82	1,1E-04	-1,15	2,5E-01	0
<i>Met75Cb</i>	FBgn0028415	3L	13,86	7,5E-04	6,05	1,7E-01	-3,01	2,8E-06	-4,90	5,9E-08	0
<i>Ebp</i>	FBgn0004181	2R	13,71	8,7E-04	9,76	7,9E-03	-2,87	4,3E-09	3,66	4,9E-02	0
<i>CG14499</i>	FBgn0034317	2R	-5,95	8,7E-04	-1,89	2,5E-01	6,23	5,6E-07	-4,00	1,3E-03	0
<i>Elo68alpha</i>	FBgn0052072	3L	5,38	1,2E-03	1,23	6,8E-01	-3,62	1,6E-03	0,85	7,2E-01	0
<i>Jon25Bii</i>	FBgn0031654	2L	-2,33	1,5E-03	-2,89	3,8E-16	3,83	1,0E-09	-1,25	2,4E-02	0
<i>EbplI</i>	FBgn0011694	2R	13,25	1,9E-03	9,55	8,2E-03	-2,66	2,1E-06	3,29	7,2E-02	0
<i>Vm26Aa</i>	FBgn0003979	2L	-5,58	3,0E-03	-13,19	2,4E-04	-4,35	6,0E-02	-6,74	1,6E-08	0
<i>Mal-A7</i>	FBgn0033296	2R	1,84	3,0E-03	-2,49	2,2E-05	-2,34	8,3E-07	-3,29	5,4E-03	0
<i>His1:CG33861</i>	FBgn0053861	2L	5,79	3,0E-03	5,56	5,9E-07	-0,19	9,2E-01	2,16	8,7E-02	0
<i>phu</i>	FBgn0043791	3R	-2,31	4,2E-03	-2,03	4,3E-05	2,01	5,0E-07	0,35	6,7E-01	0
<i>Vm26Ab</i>	FBgn0003980	2L	-4,57	5,6E-03	-12,87	2,2E-04	-4,51	2,6E-02	-6,74	2,1E-08	0
<i>Sfp60F</i>	FBgn0259968	2R	12,35	7,4E-03	8,69	2,1E-02	-2,25	2,6E-04	2,81	1,3E-01	0
<i>Cp18</i>	FBgn0000357	3L	-5,43	1,0E-02	-6,59	4,7E-05	-6,48	1,2E-01	-1,33	6,3E-01	0
<i>CG34212</i>	FBgn0085241	2R	-3,10	1,7E-02	-1,03	2,2E-01	3,58	2,1E-15	0,95	7,6E-02	0
<i>ndl</i>	FBgn0002926	3L	-5,99	2,0E-02	-5,47	2,3E-04	0,28	9,4E-01	-2,82	3,2E-02	0
<i>CG14275</i>	FBgn0032022	2L	1,53	2,0E-02	0,95	1,2E-02	-0,29	5,0E-01	0,01	9,8E-01	0
<i>Cp16</i>	FBgn0000356	3L	-5,08	2,9E-02	-10,46	5,2E-03	-5,30	2,3E-01	-9,22	1,2E-02	0
<i>CG6295</i>	FBgn0039471	3R	-2,72	2,9E-02	-6,83	4,0E-62	0,40	7,3E-01	-5,19	1,6E-21	0
<i>CG13947</i>	FBgn0031277	2L	-3,77	2,9E-02	0,10	9,4E-01	5,13	2,1E-19	2,08	3,2E-02	0
<i>rib</i>	FBgn0003254	2R	-4,27	3,3E-02	-3,51	5,3E-03	0,68	7,0E-01	-1,16	5,0E-01	0

Table 7 : Summary of the RNA-seq results in the ribosome-bound RNA fractions of genes significantly modified between CT15 vs CT3 and between Pop2 K.D vs Pop2+ at CT3 or CT15, all in per+ context. Results

of each comparison are presented, and the column "Found as cycler" corresponds to the number of articles showing the given gene as cycling in DD conditions.

3. Discussion

The discovery of the POP2 specificity for canonical *tim-RL* isoform and not *tim-M* or *tim-C* revealed in our RT-qPCR experiment is very informative. We could expect that the activity of POP2 on *tim* is due to a sequence present only on *tim-RL* and not on *tim-M* or *tim-C*. Yet, the only sequence we find is the 7 nucleotides extension of the 5'UTR first exon used to amplify this transcript specifically, these 7 nucleotides were aligned to *Drosophila* RNA motif database TomTom (Gupta *et al.*, 2007), and do not align significantly with known RBP motifs. An explanation we could formulate is that : *Tim* mRNA has been shown to be alternatively spliced according to temperature (Martin Anduaga *et al.*, 2019), and at 25°C (our working temperature), only the canonical *tim-L* isoform is found at the protein level, potentially due to translational repression of the other isoforms. The authors also found putative miRNAs predicted to target specifically the *tim-M* and *tim-C* isoforms. which for *tim-M* was expected, as this isoform seems translationally repressed, as no protein signal can be found in WB analysis for this isoform, although it makes up a large part of the *tim* isoforms mix (Shakhmantsir *et al.*, 2018; Martin Anduaga *et al.*, 2019). There could thus be a link between the fact that these isoforms are not impacted in their levels by POP2 and that they are uniquely targeted by miRNAs and show differential binding with AGO1 in IP experiments. Yet this hypothesis is rather unlikely, as miRNAs-related mRNA downregulation/translational repression has been associated to the CCR4-NOT complex via GW182 in *Drosophila* (Chekulaeva *et al.*, 2011), which would suggest that the isoform targeted uniquely by some miRNAs should be the one more likely to be regulated by POP2.

Interestingly however, *tim-M* and *tim-C* 3'UTR sequences are different than the canonical *tim* isoforms ones, but they are all predicted to be polyadenylated at the same location, meaning that our PATassay experiments (Article Fig. 2C, 3B) display all these isoforms' poly(A) tails, so the short poly(A) tailed forms of *tim* observed in total but not ribosome-bound mRNAs in Pop2 K.D context could correspond to *tim-M*, as this isoform is strongly expressed, not impacted by POP2 in its levels, and might not be translated as no proteins are visible in WB, hence this isoform would not be found in the ribosome-bound fraction.

Referring to the polyadenylation of *tim* mRNA, it is still not clear how *per* mRNA presents short poly(A) tail forms in PATassay, indeed POP2 does not impact *per* poly(A) tail (Grima *et al.*, 2019), and this later is short in all conditions, and similarly from *tim*, even if *tim-M* is the isoform presenting lower PATassay signal in total RNA, how does it present a short poly(A) tail while probably not being impacted by POP2 ? Two hypotheses can be easily imagined to answer this question :

Another deadenylase could act on *per* and a subset of *tim* mRNAs, probably not TWIN, as it joins the CCR4-NOT complex by being bound to POP2 (Basquin *et al.*, 2012), and *twin* K.D flies present normal circadian locomotor activity (data not shown). But PAN2-

PAN3 could act as the main deadenylase complex for specific mRNAs, although it was shown in human and yeast that PAN2-PAN3 are more efficiently deadenylating long poly(A) tailed transcripts, due to stimulation of their activity by PABP molecules, they can still shorten transcripts' poly(A) tails down to ~10 adenosines long tails (Uchida, Hoshino and Katada, 2004; Schäfer *et al.*, 2019), yet, no effect were observed in behavior upon K.D of these deadenylases as well (data not shown).

Another hypothesis, although more speculative, could be that the poly(A) tail added by the nuclear poly(A) polymerase upon transcription of per mRNA is shorter than the one of average transcripts, this could also be true for *tim*, where a part of it would be polyadenylated in the cytoplasm before being deadenylated by POP2.

Concluding remarks

During my project, we discovered that POP2 shows circadian deadenylation on *tim* mRNA and its other targets not through cyclic expression of *Pop2* gene products, but in function of POP2's target abundance itself. I consider three main hypotheses to explain such results.

A circadian one, where POP2 could be recruited in a circadian fashion to its targets.

An integrator one, where somehow, POP2 or related factors follow the abundance of specific targets to trigger up- or down-regulation when threshold levels of transcripts are met.

A saturation one, where limited POP2 molecules act on their targets in a stable manner through the time, for POP2 up- or down-regulated targets, but can reach saturation when high levels of transcripts are reached. This action would not be directly circadianly-controlled, but would certainly participate in strengthening or weakening the relative amplitude of cyclically-transcribed RNAs.

So far, we focused on the study of the transcripts that were destabilized by POP2, but many transcripts targeted by POP2 are in fact up-regulated by it. It would be interesting to investigate the control of POP2 on such genes presenting oscillation in mRNA levels. This could reveal a dual role of POP2, increasing the amplitude of cycling of some genes and negating the one of others.

Then, we unfortunately failed at isolating a cis- or trans-regulatory element explaining the specificity of POP2 for *tim*, or *vri* so far. And our vast RNA-seq dataset of POP2 targeted genes might not allow the identification of a specific sequence motif or feature that could trigger POP2 recruitment. Indeed, we expect POP2 to be recruited through diverse pathways, various RBPs, miRNAs, and would likely fail at isolating one explicatory element. Yet, I believe that more thorough comparative bioinformatics analyses targeting *tim* and *vri* sequences could unveil the origin of POP2 specificity for these clock mRNAs. Similarly, the subcellular localizations of *tim* and *vri* vs *per* mRNA could be worth investigating.

The discovery of *vri* as another clock gene targeted by POP2 was made thanks to our RNA-seq analysis from TRAP samples, additionally, several other genes presenting both circadian and POP2 regulations were identified and particularly CG14275, which seems regulated in a very similar way than *tim* and *vri* and has been predicted to play

a role in sleep, further experiments could confirm a role of this gene in the circadian rhythms in a POP2-dependent manner.

Next, we propose a new layer of control in the oscillation of clock gene products, and potentially in the delay observed between transcript and protein levels peak. Studying the quantities of ribosome-bound mRNA levels for *tim*, *per* and *vri* revealed slight delays between total and ribosome-bound mRNA levels in control conditions, suggesting the presence of translational controls in the clock genes oscillations. Yet, translational control in the *Drosophila* clock might be greater than what we found, as our TRAP method is limited to quantify mRNAs bound to any amounts of ribosomes, reducing greatly the resolution of our translation estimate. Additionally, we found that POP2 impacted greatly the ribosome-binding dynamics of *tim* and *vri*. Yet, it is hard to know whether this increased ribosome-binding in *Pop2* K.D context can be attributed to increased translation, or instead to increased ribosome stalling, that would normally be resolved by POP2 through deadenylation-mediated decay. It would therefore be of interest to carry out ribosome profiling in *Drosophila*, to allow more precise determination of translation dynamics around the clock and to discover potential ribosome pause/stall sites in clock genes that could trigger POP2 recruitment and subsequent mRNA decay.

Next, POP2 seems to show preference for some alternatively spliced isoforms of *tim* and *vri*, although the mechanism leading to such preference is not clear (cis-regulatory elements, localization, abundance, ribosome-binding etc...) it would be interesting to exploit our RNA-seq data and investigate the role of POP2 in the regulation of specific isoforms POP2-regulated genes. This could allow us to understand more precisely how POP2 can be specific of one isoform rather than another, and reveal a more extensive role of POP2 in controlling the mix of alternatively spliced isoforms in circadianly-regulated genes.

Finally, two genes were identified as playing a role in the circadian rhythms by altering the molecular clock, namely *lig* and *Mettl3*. It would be interesting to characterize further their role in the clock, although these roles seem unrelated to POP2.

All in all, these results place POP2 as a major regulator of the clock and of circadianly-regulated genes, and this, by acting extensively in the control of the oscillations of certain cycling genes. This control occurs probably at many different steps of the life of the RNA including transcription, translation and degradation making POP2 a highly versatile regulator of the clock.

Material and methods

I. Fly genetics and behavioral assay

1. Balancer chromosomes

Balancer chromosomes are used in two cases :

- To maintain a stock of flies carrying a mutation that would be lethal in the homozygous context.
- To avoid recombination and follow a chromosome through crosses.

This is possible because balancer chromosomes contain recessive lethal or sterile mutations, inversion breakpoints as well as dominant mutations causing visible phenotypes (Kaufman, 2017).

Briefly, the recessive deleterious mutations carried on the balancer chromosome cause homozygous progeny to be not viable, leaving only the possibility to have homozygous progeny for the homolog chromosome, or heterozygous progeny. Which, in the case of stocks carrying other recessive lethal mutations on the homolog chromosome too, makes it only possible to obtain heterozygous progeny.

Nevertheless, these lethal mutations could be lost through recombination, which is also prevented by the inversion breakpoints, that leads to aneuploid gametes upon meiosis. This stock is thus “balanced” with lethal or sterile mutations on the two homologous chromosomes.

In addition, balancer chromosomes are also used to follow a homolog chromosome through crosses thanks to dominant mutations that display visible phenotypes.

A wide variety of balancer chromosomes exist, the ones that I used for my project are presented in the Table 1.

Name	Chromosome	Main dominant marker	Phenotype
Cyo	2	Cy ¹	Wings curled upward and outward.
TM6B	3	Hu	Additional humeral bristles, some shorter than normal.
TM6C	3	Sb ¹	Bristles stout and short.

Table 1 : Balancer chromosomes used in my experiments.

2. UAS-GAL4 system

The UAS-GAL4 system is used to express any transgene under the control of a tissue- or cell- specific promoter (Brand and Perrimon, 1993).

This system is based on the action of the yeast transcriptional activator GAL4 which is inserted downstream of a promoter of interest, limiting its expression to the cells/tissues where the promoter is targeted. Once expressed, the GAL4 factor will bind to the Upstream Activating Sequence (UAS) placed upstream of the element to express and activate its transcription (Fig. 1).

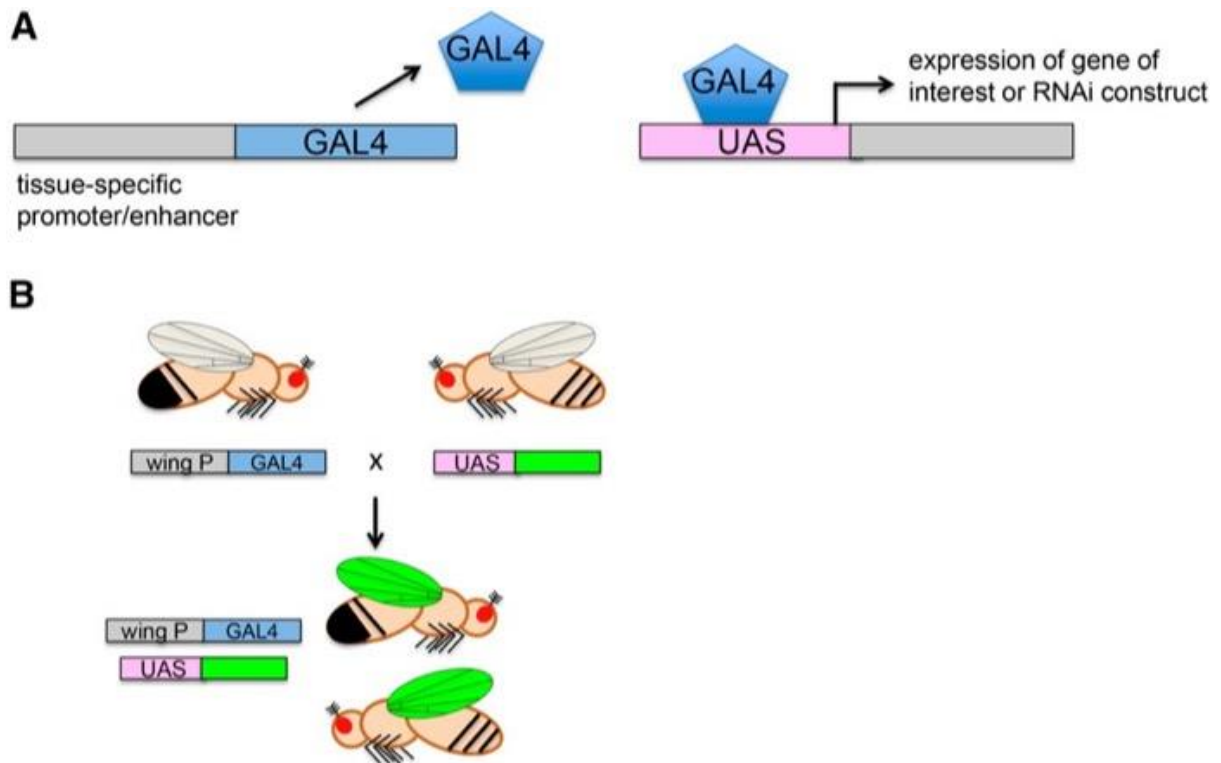


Figure 1: Scheme of the UAS-GAL4 system in *Drosophila*. (A) The GAL4 protein is expressed specifically in the tissue where the promoter is activated, making it the driver. The GAL4 protein will then promote the expression of the construct localized downstream of the UAS sequence. (B) An example of the GAL4 system functioning with parental flies possessing separately the tissue specific driver-GAL4 sequence, here the wings, and the gene of interest, here the GFP, downstream of the UAS sequence, offsprings will thus express the GFP protein in their wings only. Figure from (Hales et al., 2015).

The UAS-GAL4 system can be used to overexpress a gene, or underexpress one with an RNAi, for which the expression strength can be finetuned by keeping the flies at lower/higher temperature.

The GAL4 drivers used for my experiments are :

- *Tim-gal4* (Emery *et al.*, 1998; Kaneko, 1998), which will be appropriate for experiments carried out on head extracts, as it will permit the expression of the transgene of interest in all *tim* expressing cells (essentially the eyes) (Hunter-Ensor, Ousley and Sehgal, 1996a; Stanewsky *et al.*, 1998). Nevertheless, it should not be forgotten that the experiments carried out with this driver do not reflect the molecular state of the clock neurons only, but of a mixture of the few clock neurons with a majority of other cells.
- *Gal1118*, which is expressed mainly in clock cells it will thus be used for behavioral studies, and for immunofluorescence experiments to visualize clock neurons (Blanchardon *et al.*, 2001).

3. *Drosophila* circadian behavior assays

Locomotor activity assay is the most common way to study the fly's circadian clock. Briefly, flies are individually placed in glass tubes containing food at one extremity. The

tubes are then loaded in a monitor where they are crossed by an infrared beam that will be interrupted when the fly moves through it. A phototransistor is placed at the other side of the tube to detect the infrared beam, the beam interruptions are recorded, in order to generate activity profiles of the flies (Fig. 2)

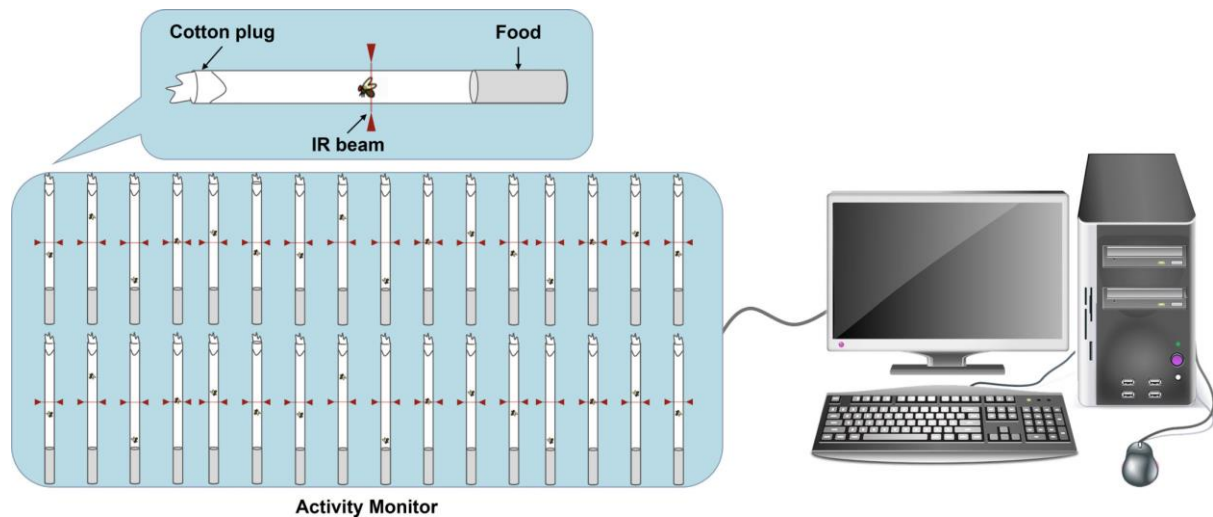


Figure 2: Presentation of the *Drosophila* Activity Monitoring System (DAM System, from TriKinetics) setup.

Once our data extracted, we can generate plots using the FaasX 2 software, such as actograms, educations, tables (summary showing the period, rhythmicity, and flies period statistics).

To control environmental parameters, such as light and temperature, these monitors are placed in incubators with which we can control the temperature, light-on and light-off times, light intensity, light color. The conditions I used in my experiments are presented in the Table 2 and stated in the legend of the figures of experiments if otherwise.

For every experiment, the flies were first synchronized 3 days in 12h:12h light-dark (LD) conditions, after this entrainment phase, they were placed in constant conditions, often in constant darkness (DD).

Experiment type	Light color	Light intensity	Temperature	Entrainment phase	Constant condition
WB, IF, RT-qPCR, TRAP	White	~2350 lux	25°C	12h:12h LD 3 days	First day DD=DD1
Locomotor activity assay	White	~2350 lux	25°C	12h:12h LD 3 days	≥ 7 days DD

Table 2 : Incubator parameters. WB = Western Blot, IF = Immunofluorescence, TRAP = Translating Ribosome Affinity Purification. LD = Light-Dark, DD = Dark-Dark. For biochemistry experiments, the flies are collected during the first day of DD = DD1, unless stated otherwise.

4. Pop2-HA K.I design and screening workflow

The design used is illustrated below (Fig. 3), briefly, embryos expressing the CAS9 protein under the control of the UAS-GAL4 system in their germ lines were microinjected by the BestGene Inc. with donor DNA containing the HA sequence and two gRNAs, one specific of the *Pop2* CDS end, the other for the marker gene *ebony*,

this co-CRISPR strategy (Kane *et al.*, 2017) allows to screen more efficiently for successful knock-in events, as the design used was scarless, it could be recognized for *Pop2* only through PCR. Injected flies (P1) emerging from their pupae were crossed individually with balancer ebony flies, potentially generating K.I events in their gametes. Offsprings (F1) were crossed with each others, after larvae progeny emerged (F2), DNA was extracted from their parents (F1) to carry out PCR screening of K.I events, with particular emphasis put on ebony parents (Jackpot lines).

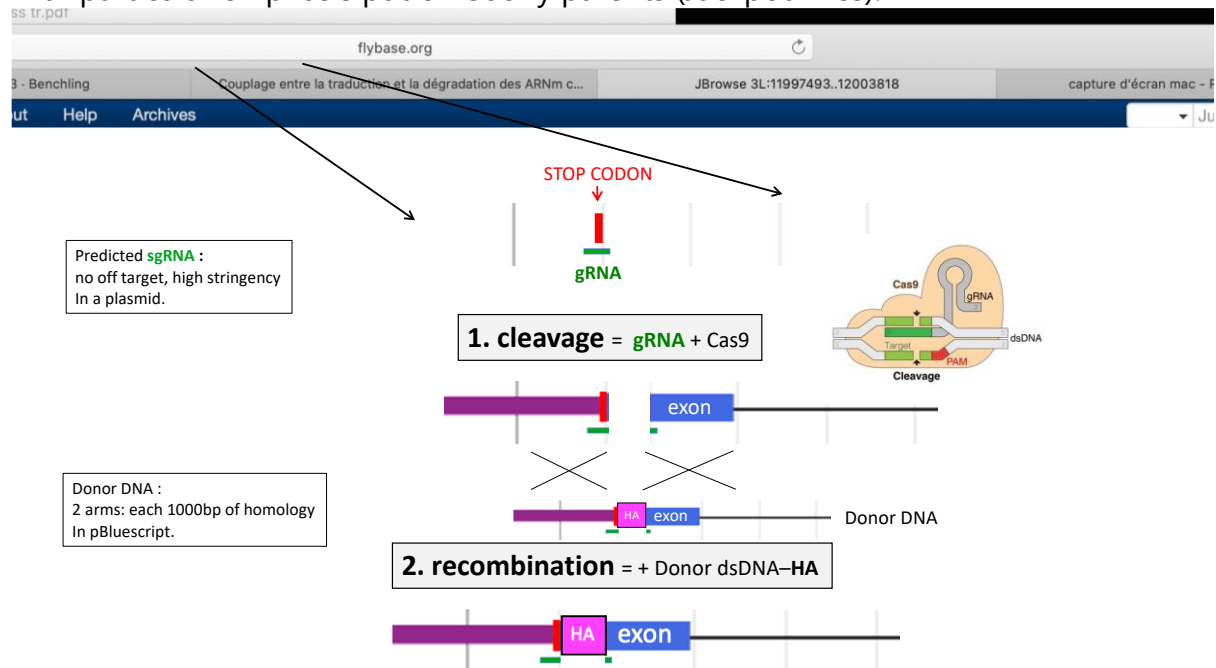


Figure 3 : *Pop2*-HA K.I design. Per attempts ~300 *Drosophila* embryos were microinjected with a vector containing the DNA donor sequence corresponding to the end of the CDS of *Pop2* transcripts with an added HA tag sequence placed just before the stop codon, similarly to the UAS-*Pop2*-HA construct, together with a gRNA (designed on the FlyCRISPR website) targeting the CDS just before the stop codon to induce the cleavage there. Recombination events could integrate the HA sequence from the donor DNA. Design realized by Béatrice Martin.

PCR screening was realized with 2 PCR designs (Fig. 4,5) to ensure optimal screening conditions. Screening attempt n°3+4 yielded one positive K.I event identified after screening a total of 3 224 flies using the Vasa-Cas9 injected line.

Confirmation of the proper integration of the HA-tag was confirmed by sequencing. Once the K.I event identified in the cross n°69, all the progeny from that cross were crossed individually with balancer flies to identify offsprings carrying the K.I event (Fig. 6). The established endogenously tagged *Pop2*-HA line was then outcrossed with 11 crosses to get rid of background genetic polymorphism.

PCR specific of the region of interest = **HA-Spe**

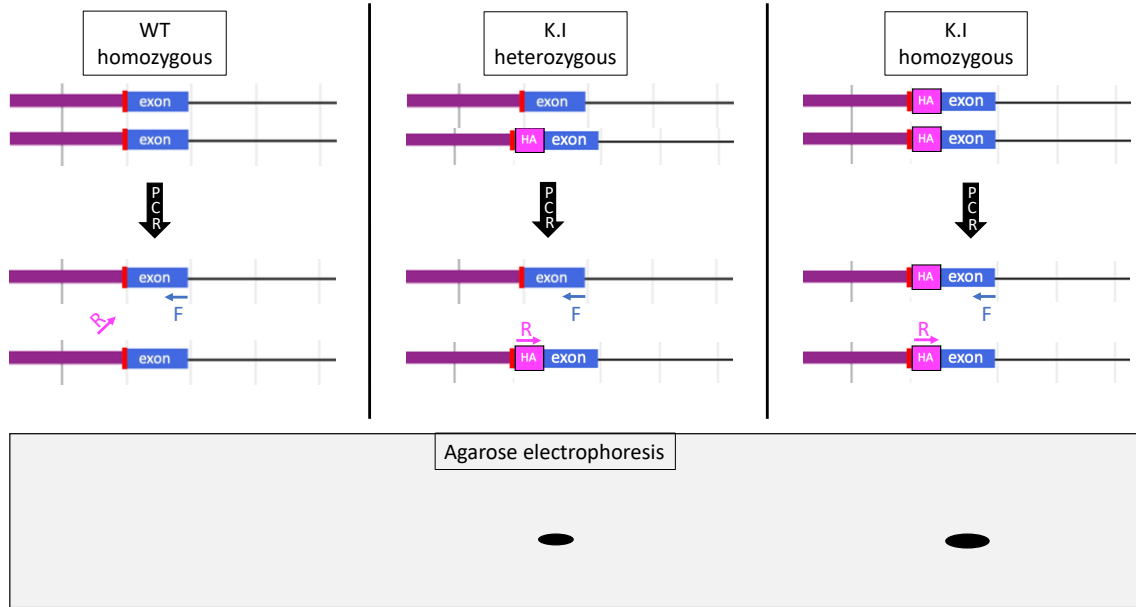


Figure 4 : Specific PCR design. This design allows the detection of K.I event through present/absent signal. This design has the advantage to work robustly even if DNA from several flies is amplified in a single PCR reaction, while its limit is that the absence of signal could be both due to technical issues or absence of K.I in the tested DNA.

PCR surrounding the region of interest = **HA-Flanking**

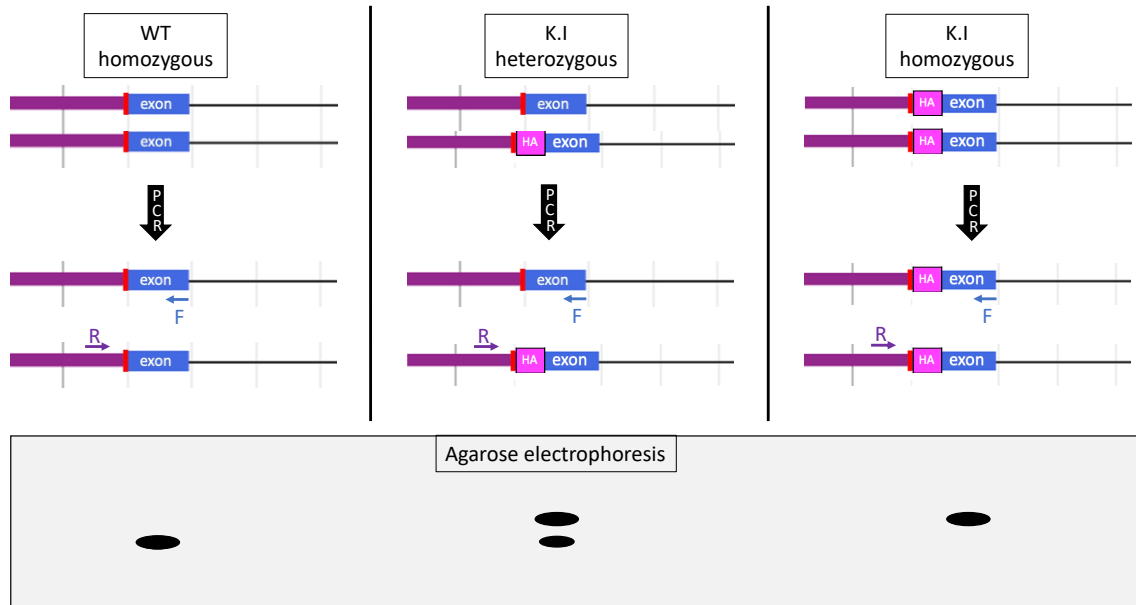


Figure 5 : Flanking PCR design. This design allows the detection of K.I event through a change in signal size. This design has the advantage to always display a signal if the PCR reaction was successful, while being limited by the risk of not amplifying efficiently longer signals (K.I) if they are strongly diluted in WT DNA.

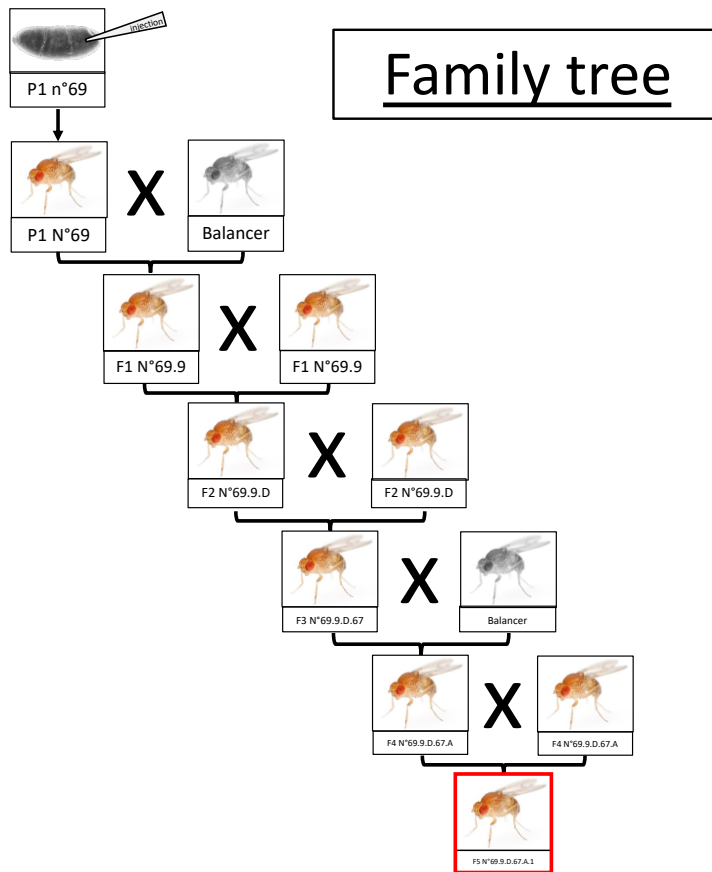


Figure 6 : Family tree leading to the isolation of the *K.I Pop2-HA* flies.

II. Immunofluorescence of POP2-HA

The first imaging experiment realized was done using an epifluorescence microscope with brains squeezed between slide and coverslip (Fig. 7).

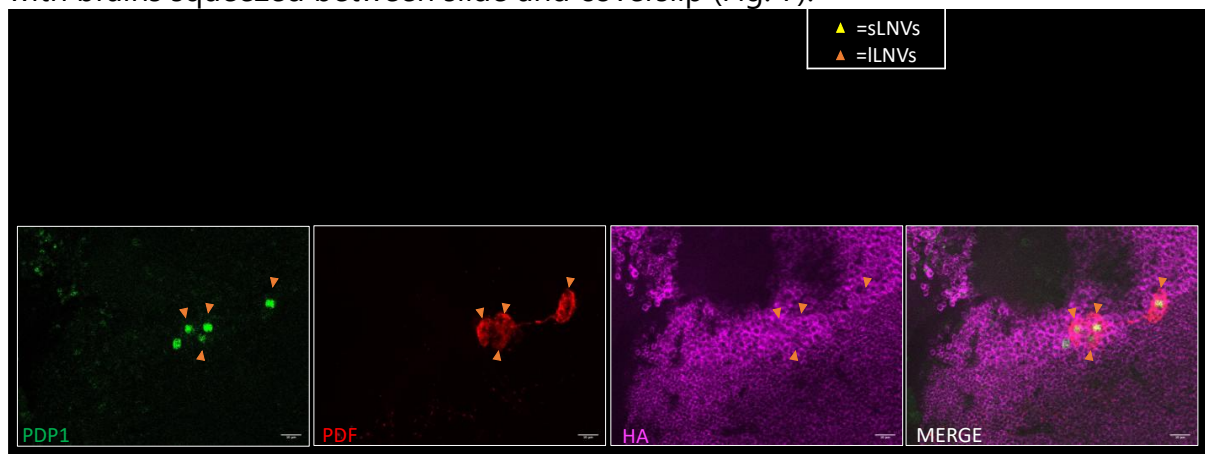


Figure 7 : IF picture of LNvs clock neurons marked with anti-PDF (LNvs marker), HA (POP2), PDP1 (clock cells marker) antibodies of *Pop2-HA* flies dissected at CT21. Images taken using a Zeiss Z1 epifluorescence microscope equipped with an ApoTome 2 optical sectioning device. Realized with Élisabeth Chélot.

In this experiment we could see the POP2-HA signal being present in every cell in our brain, making the quantification of such signal challenging, as the brains are pressed

between slide and coverslip during the mounting step of the protocol, this action brings cells from different focal planes into the same, creating some overlap between cell signals in our image. Yet this step is necessary to use the epifluorescence microscope, as not pressing the brains leads to blurry images when the targeted focal plane is deep in the tissue.

We then decided to carry out this experiment using a confocal SP8 Leica microscope, as the use of confocal microscopes allows to mount brains while preserving the tissue integrity using spacers between slide and coverslip without affecting the imaging quality (Fig. 8).

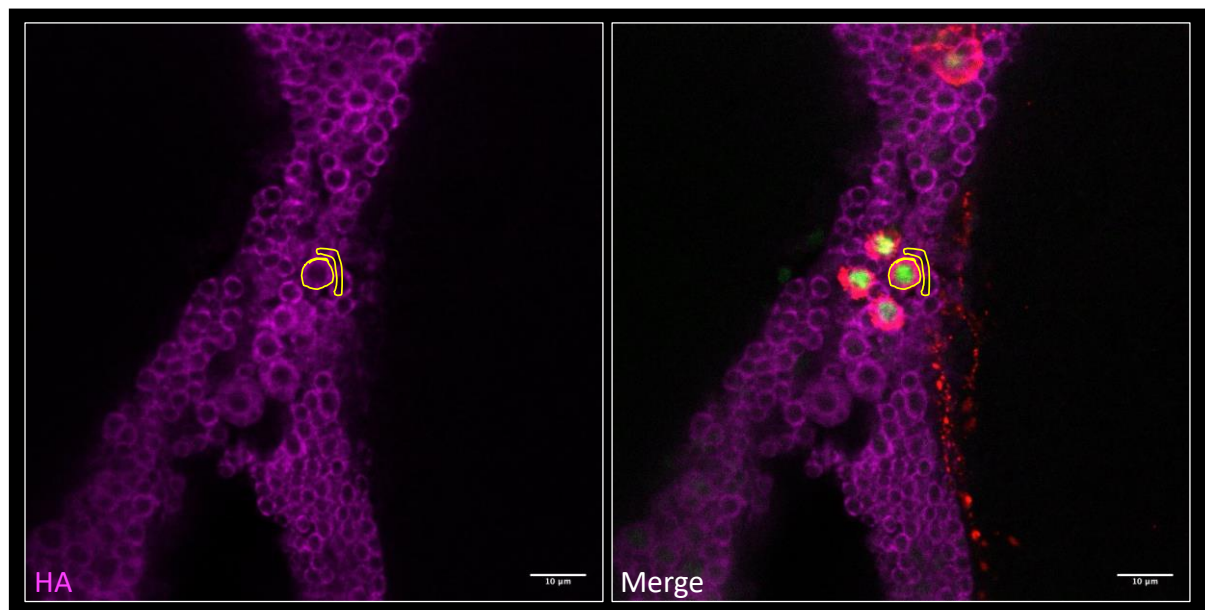


Figure 8 : IF image from confocal microscope showing HA signal only in magenta, as well as merged HA (magenta), PDF (red), PDP1 (green) signals of endogenous Pop2-HA flies. The yellow areas drawn represent : for the circle the Region of Interest to quantify, for the reverse L shaped area we would normally draw for such quantifications.

The use of the confocal microscope led to the acquisition of high quality and resolutive images, allowing us to distinguish each cell in the HA-associated channel. However, another limit needed troubleshooting for proper POP2 quantification. Upon quantification of our signals in the drawn Region Of Interest (ROI), we also quantify an area in the background near our cells of interest, to normalize our signal from the ROI by background noise (Fig. 8). But the ubiquitous expression of POP2 in the brain forces us to select background areas far from our ROI, which are then not representative of the background signal present around the quantified cell anymore. Plus, the presence of neighboring cells around the LNvs is variable, but usually counts tens/hundreds of cells per picture, which could make background subtraction impossible for some images filled with signals from neighboring cells.

We took advantage of our previous results obtained in WB to find a way to normalize our IF ROI signals. Indeed, we knew that the protein levels of endogenous POP2-HA do not oscillate in the heads of *Drosophila*. We thus conjectured that the expression of endogenous POP2-HA likely does not oscillate in most of the brain cells either, so

using the POP2-HA signals from neighboring cells, given their large numbers, could constitute a reliable way to normalize our ROI signal. Carrying out the selection of s-LNv neighboring cells by hands would be tedious and prone to bias, we thus trained the Weka segmentation machine learning algorithm (Arganda-Carreras *et al.*, 2017) to recognize the POP2-HA signal forming cell-shaped objects (Fig. 9), allowing for automatic selection of all neighbor cells with more accuracy than the Fiji thresholding function (Fig. 10).

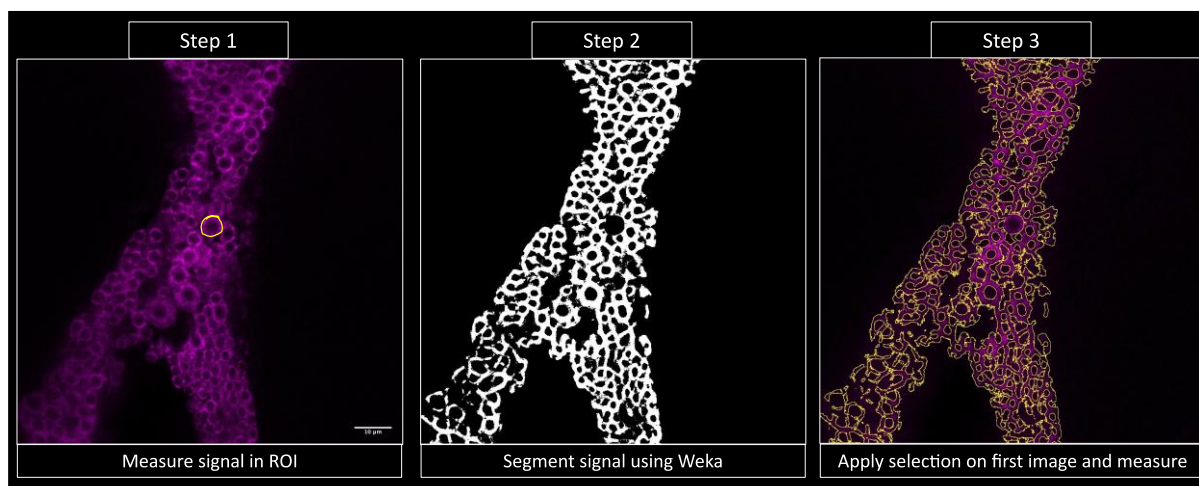


Figure 9: Workflow of the quantification process using Weka segmentation algorithm to automatically recognize cell-shaped objects that was applied to select neighbor cell areas in Fiji (ImageJ software), to which the s-LNv areas (ROI) were removed in Fiji. Signal visible in magenta, selected areas in yellow, in white the segmented part of the image created by Weka.

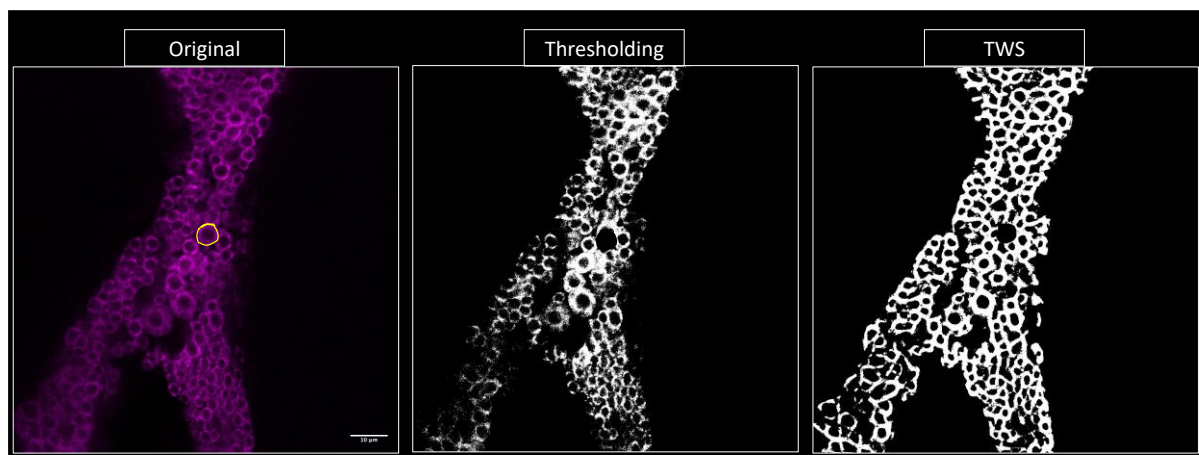


Figure 10: Comparison between Fiji thresholding function (Thresholding) and Weka segmentation algorithm (TWS).

III. POP2-HA IP followed by mass spec

Pop2-HA and *w;stj+* control flies were entrained through 4 pools of CT, as done in 2017, 5 replicates were prepared for each timepoints as this was predicted to reduce greatly our false discovery rate of cycling proteins found bound to POP2-HA (Fig. 11). Immunoprecipitation of POP2-HA was carried out, eluates were then loaded on Tris-Glycine acrylamide gels for electrophoresis, followed by Coomassie blue dye

application on the gels that were then delivered to the proteomics facility (SiCaPS) in I2BC, Gif-sur-Yvette, for mass spec analysis. Our experimental design allows not only to detect POP2 interactors with the enrichment of a protein in *Pop2*-HA flies normalized by *w;stj+* control flies at each timepoint. But also to determine oscillations in the protein enrichment detected through robust regression. Another difference with the 2017 screening is the use of a new component on the mass-spec, the TIMS-TOF module, providing higher sensitivity than the previously used triple-TOF module. This nanoLC MS/MS using the TIMS-TOF module on 5 replicates was expected to yield more POP2 partners that could be found bound to POP2 weakly thanks to better sensitivity (TIMS-TOF), robustness (5 replicates) and physiological conditions (*Pop2*-HA). Data analysis was carried out by David Cornu (SiCaPS).

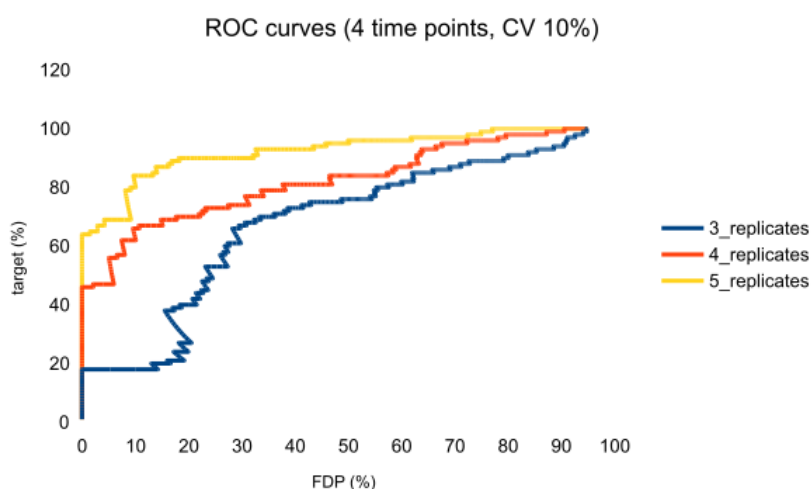


Figure 11 : ROC curves showing the false positive proportion of cycling protein identification over 4 CTs for a model comprising 100 cycling proteins over 2000 stable proteins with a variability of 10% and no outliers for different number of replicates. Analysis realized by David Cornu.

IV. Molecular biology techniques

1. Poly(A) Tail Length assay (PATassay)

PATassay allows to measure the size of the poly(A) tail of a given transcript in the form of smearing band, with increased band corresponding to longer poly(A) tails.

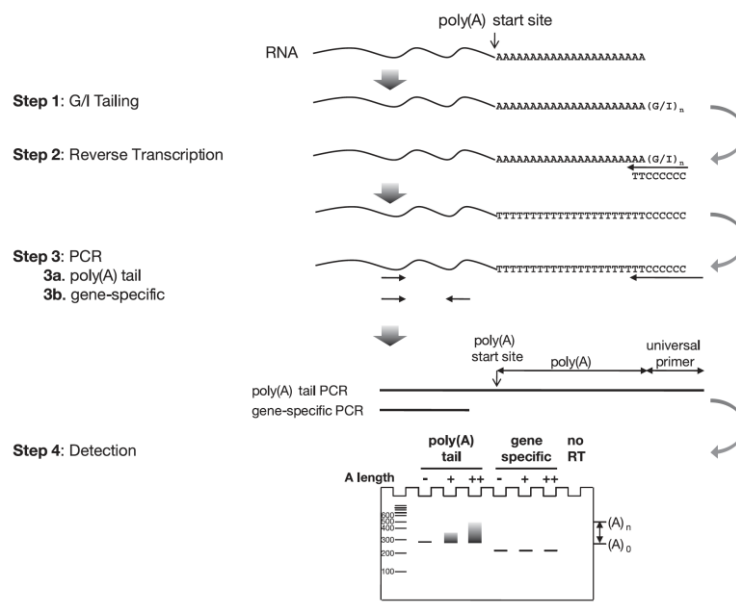


Figure 12 : PATassay protocol from Affymetrix kit. RNAs are tailed at their 3' end by G/I bases, followed by reverse transcription of the tailed RNAs using a primer overlapping the G/I and poly(A) tails. Subsequent PCR amplifies the portion of cDNA starting from a 3'UTR-located forward primer to a reverse primer specific of the gene (*gene spe*) or specific of the poly(A)-G/I tail intersections (*tail*). PCR product is then migrated through electrophoresis, where smearing signal corresponds to longer poly(A) tails of the amplified transcript.

2. Translating Ribosome Affinity Purification (TRAP)

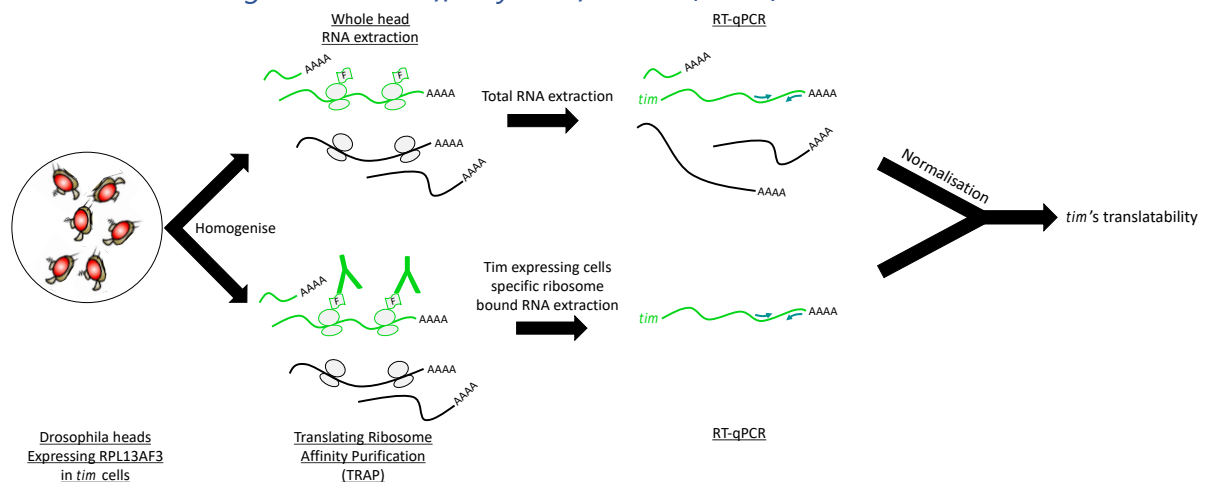


Figure 13 : TRAP protocol carried out on *Drosophila* heads overexpressing a flag-tagged ribosomal protein (RPL13AF3) in the *tim* positive cells. 2 fractions are generated, one containing total RNAs, from the whole heads, and being bound to ribosome or not (total RNAs). The other fraction is the eluate of anti-flag immunoprecipitation and corresponds to ribosome-bound RNAs in the *tim* positive cells only. Normalizing the ribosome-bound RNA levels by the total RNA levels approximates the translatability of a gene, and reflects how specifically this gene is bound to ribosome independently of its total levels.

3. TRAP followed by PATassay

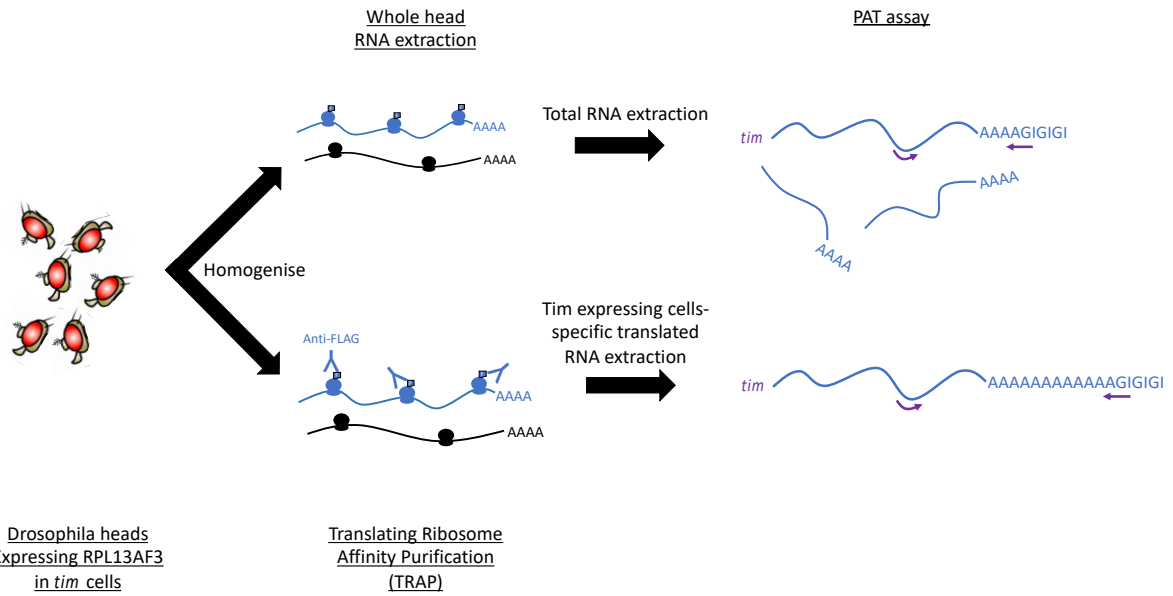


Figure 14 : TRAP fractions used together with PAT assay protocol to follow the poly(A) tail length of RNAs in the whole heads. And the poly(A) tail length of RNA bound to ribosomes in the *tim* positive cells.

V. dryR

dryR is an R package allowing the comparison of differential rhythmic gene expression between 2 and 4 conditions.

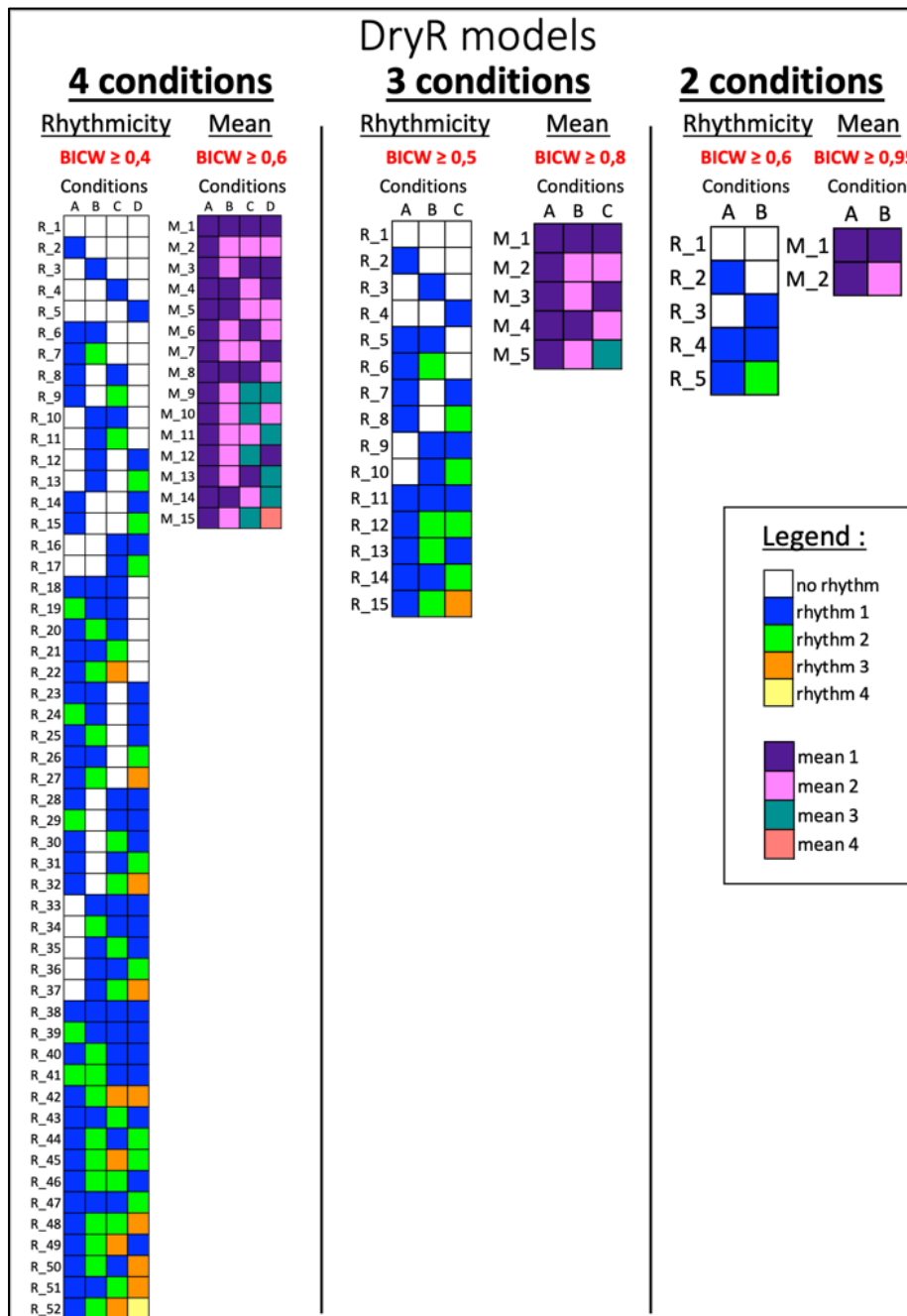


Figure 15 : dryR models presentations, the number of conditions compared to each others defines the number of total possibilities/ Rhythmicity of the data is represented by colored squared in the rhythmicity model lists, different colors between conditions reflect different parameters of oscillations (phase, amplitude). BICW : Bayesian Information Criterion Weight illustrate the plausibility of a chosen model to represent the data the best among all the tested models. Similar comparisons are proposed for the mean levels of a transcript quantity between conditions. Where different colors indicate differences in mean levels.

Annexes

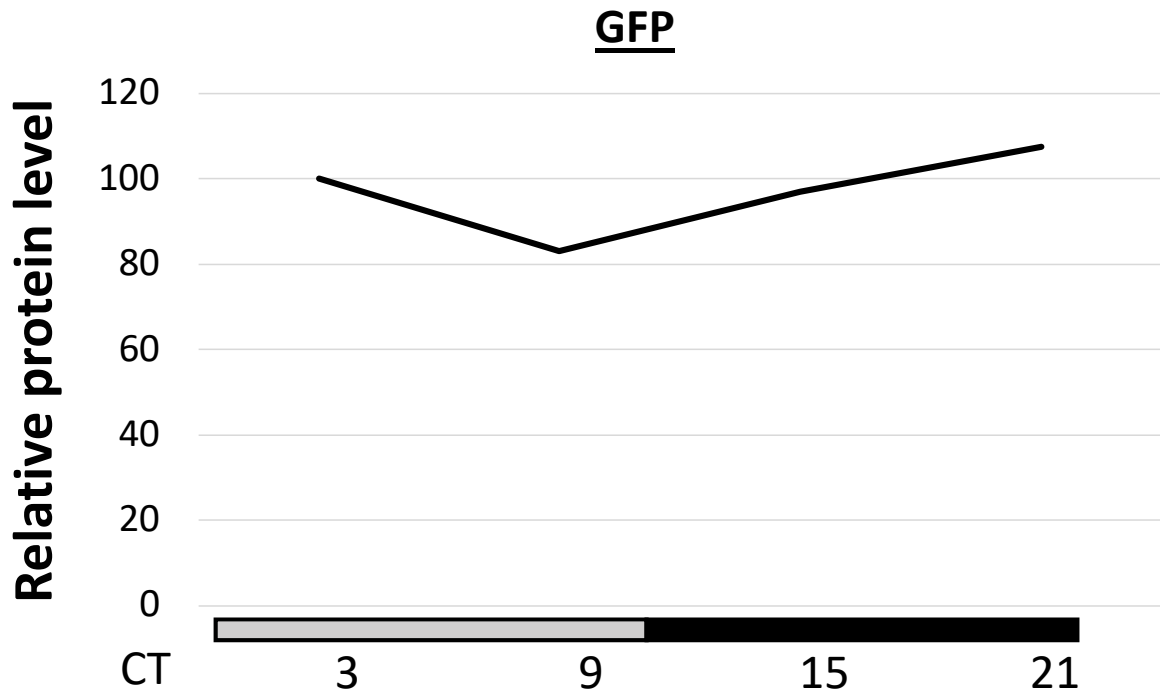


Figure S1 : Quantification of Western Blot analysis of GFP protein using anti-GFP antibodies from UAS-GFP expressing flies under the control of the *tim-gal4* driver in *drosophila* heads. Results from one representative replicate out of the 2 made. Experiment realized by Christian Papin.

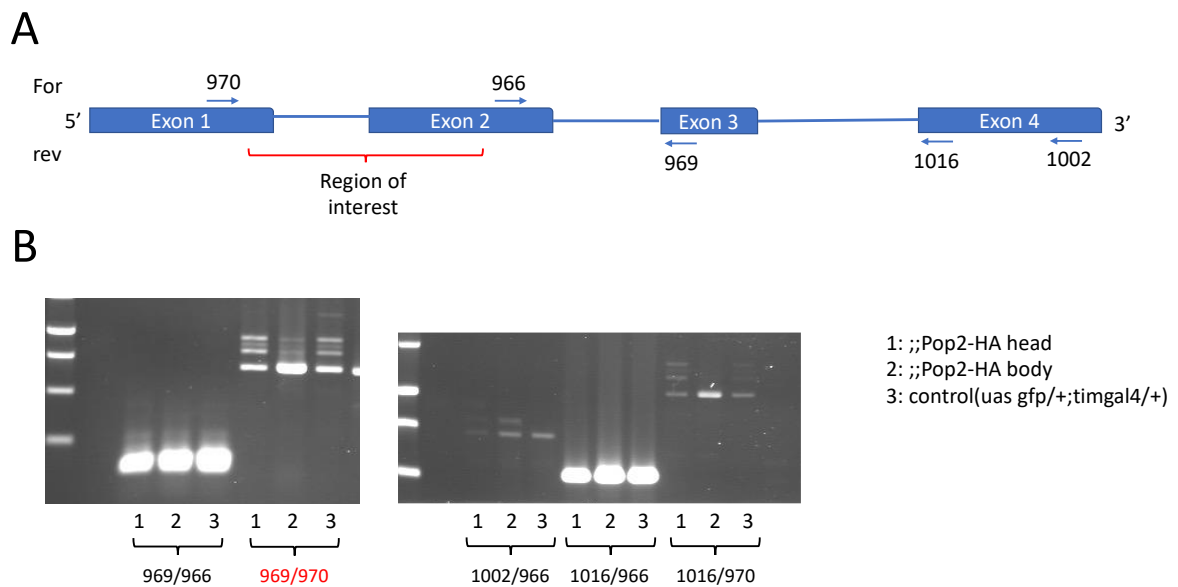


Figure S2 : Pop2-HA isoforms PCR investigations (A) Schematic representation of Pop2-RA isoform with the primers used to localize the differences at the transcript level between heads and bodies of Pop2-HA flies. Blue lines represent introns. Arrows represent the PCR primers, the numbers associated refer to the number of the corresponding primer. **(B)** Agarose gel of Pop2-HA cDNAs amplified using different sets of primers to localize differences between head and body. Experiment realized by Brigitte Grima.

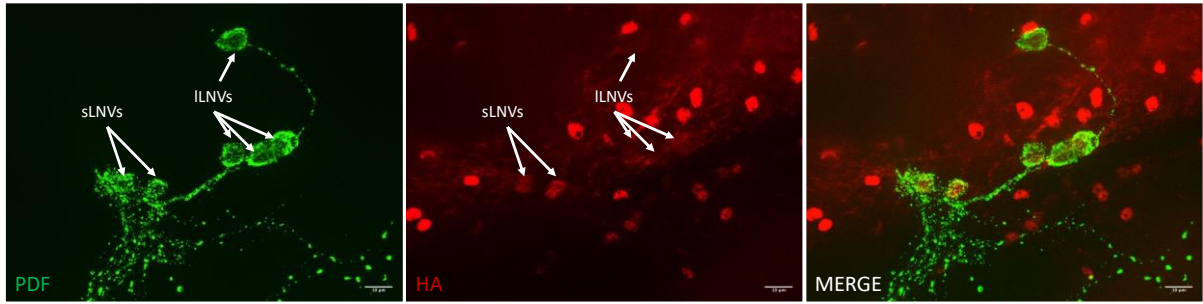


Figure S3 : IF image from showing HA signal in red, as well as PDF (green) signal of exogenous UAS-Pop2-HA flies.



Figure S4 : IF image from confocal microscope showing HA signal only in magenta from endogenous Pop2-HA flies.

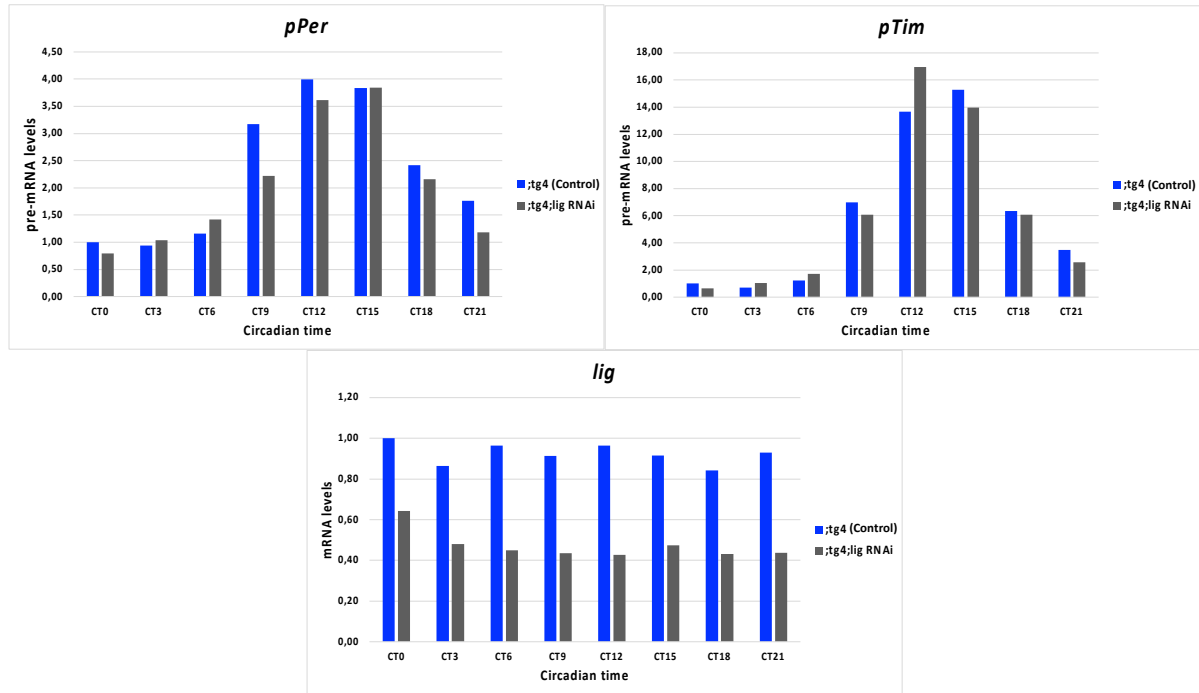


Figure S5 : RT-qPCR quantification of pre-per; pre-tim; lig mRNA at 8 circadian times in presence or absence of lig-RNAi under the control of tim-gal4 driver. N=1 replicate. Experiment done with Christian Papin, Éric Jacquet & Naima Nhiri.

	Stock name	Homolog	Comment
Ctrl line	$\Delta 6144$ Negative CTRL	Alkbh6	Flies negative for mutation after last isogenization cross. Used as control for indicated line.
Ctrl line	$\Delta CG1582$ Negative CTRL	Dhx57	
KO mutant	$\Delta CG6144$ / Cyo GFP	Alkbh6	Demethylase (unknown substrate)
KO mutant	$\Delta CG1582$	Dhx57	Potential m6A reader
catalytic mutant	Mettl3 $\Delta 6'$ TM6C	Mettl3	m6A methyltransferase, C-terminal part containing the catalytic domain removed
KO mutant	lme4 $\Delta 1.7$ / TM6C	Mettl3	m6A methyltransferase, entire coding sequence removed
KO mutant	PusL1-KO	PusL1	Pseudouridine synthases for tRNA
KO mutant	Pus3KO	Pus3	
KO mutant	Pus7 KO	Pus7	

Table S1 : Mutant lines screened for effect on circadian rhythms.

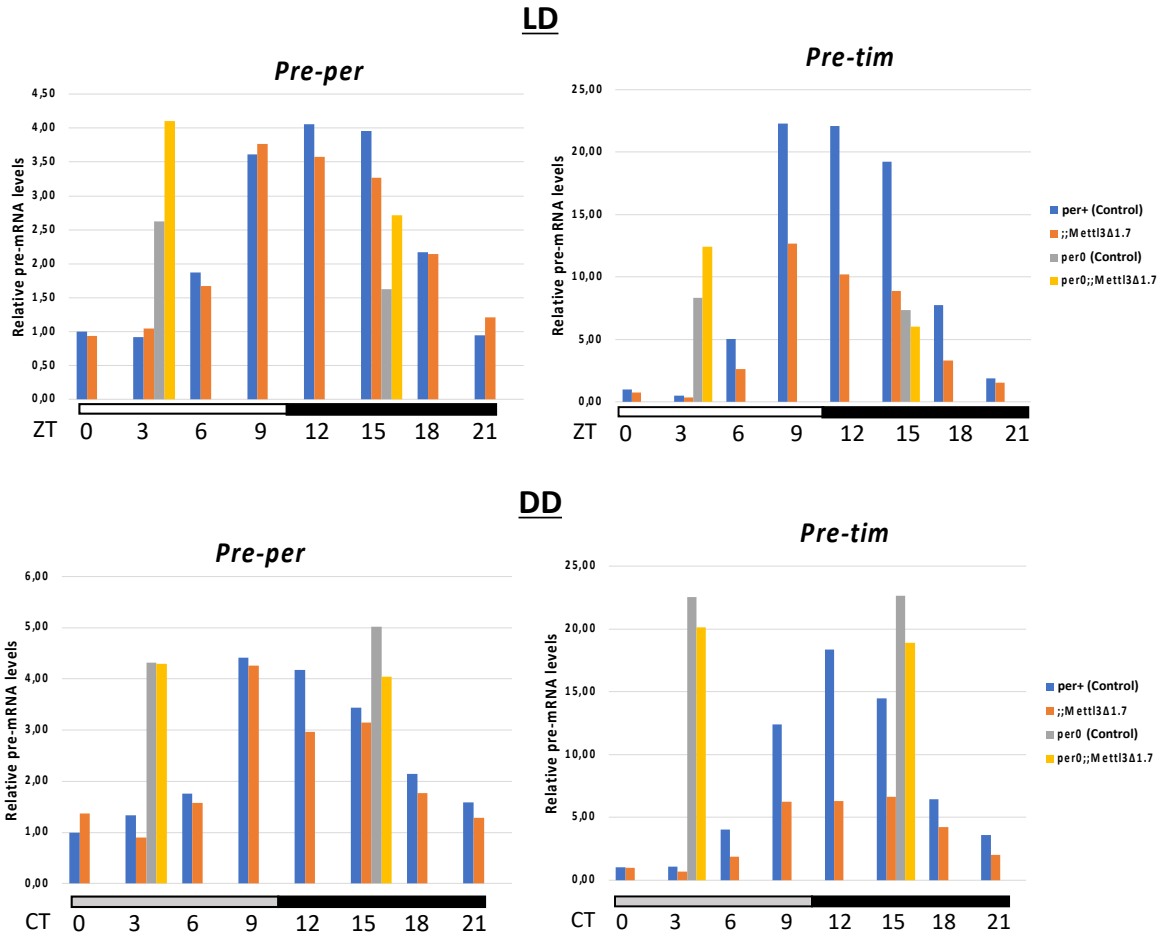


Figure S6 : RT-qPCR quantification of pre-per & pre-tim mRNA at 8 circadian times in presence or absence of *Mett13Δ1.7* null mutant. N=1 replicate. Experiment done with Christian Papin, Éric Jacquet & Naima Nhiri.

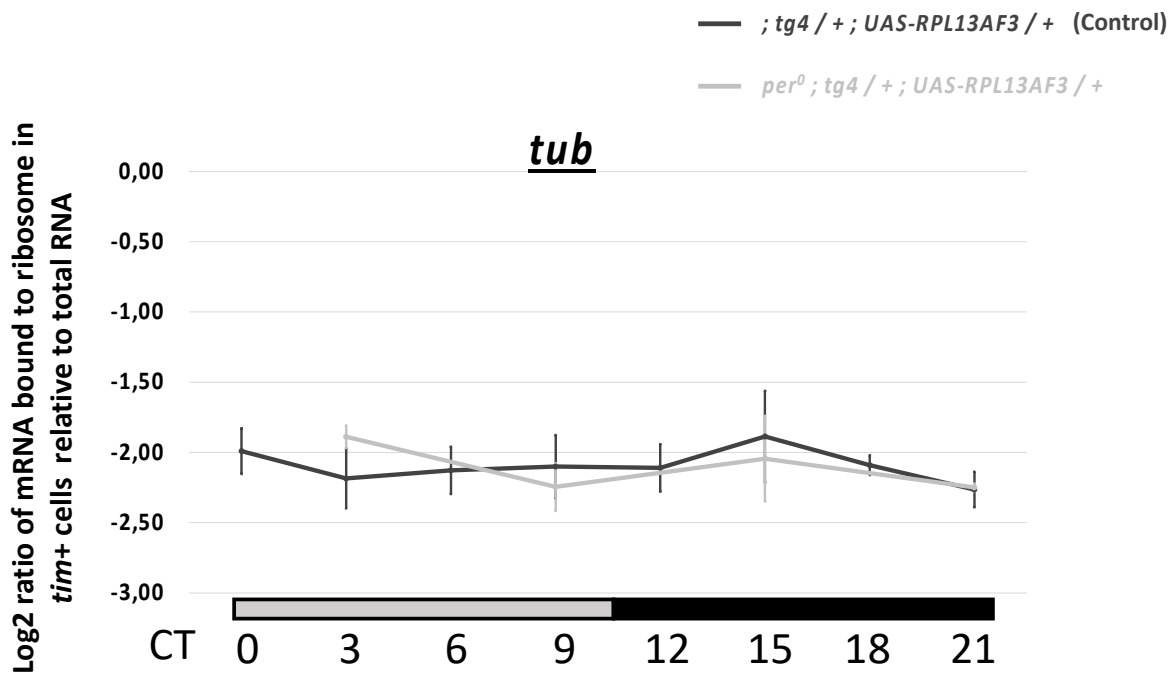


Figure S7 : Log2 ribosome-bound mRNA levels relative to respective total mRNA levels. Error bars indicate SEM of log2 normalized datapoints, $n = 3$ biological replicates, $n = 2$ biological replicates in *per*⁰ conditions CT9 & 21. RT-qPCR realized with *Éric Jacquet* and *Naima Nhiri*.

Synthèse en français

I. Introduction

1. Introduction générale à l'horloge circadienne

Les rythmes circadiens sont des rythmes biologiques retrouvés dans la physiologie et le comportement de la plupart, voire tous les organismes vivants sur Terre, qui se répètent de façon quotidienne. Ces rythmes sont contrôlés à l'échelle de la cellule par des horloges circadiennes. Elles vont permettre non seulement le suivi des cycles jour/nuit, mais surtout leur anticipation, ce qui représente un avantage évolutif (Edery, 2000). Les horloges circadiennes sont des oscillateurs internes qui vont cycler avec une période d'environ 24 heures. Celles-ci intègrent des inputs environnementaux, tels que les changements de lumière et de température, et vont contrôler des outputs. Dans le cas de la drosophile, on retrouve souvent des études s'appuyant sur les rythmes d'éclosion ainsi que les rythmes veille-sommeil, ces derniers étant principalement étudiés via l'activité locomotrice des drosophiles (Muraro et Ceriani, 2014). L'activité locomotrice des drosophiles est suivie en utilisant le système DAM (Drosophila activity monitoring system) (Figure 1A) et peut être représentée sous forme d'actogrammes (Figure 1B). Dans la figure 1B, on peut retrouver 2 des 3 propriétés caractérisant les horloges circadiennes :

- La capacité d'osciller avec une période d'environ 24h en absence d'inputs environnementaux, appelée « free-running », cf figure 1B activité rythmique en obscurité constante.

- La capacité de se synchroniser par des changements d'inputs environnementaux aussi appelée « entraînement », cf figure 1B changement d'heure d'allumage et d'extinction des lumières.
- La capacité de maintenir une rythmicité avec une période d'environ 24h dans une large gamme de températures physiologiques, appelée « compensation de température » (non présentée en figure 1B).

Le suivi de l'activité locomotrice des drosophiles permet d'estimer l'état de l'horloge circadienne. Par exemple, l'étude de l'activité des drosophiles en obscurité constante permet de détecter des altérations dans l'horloge qui vont causer son accélération, ralentissement, ou perte de rythmicité (arythmie).

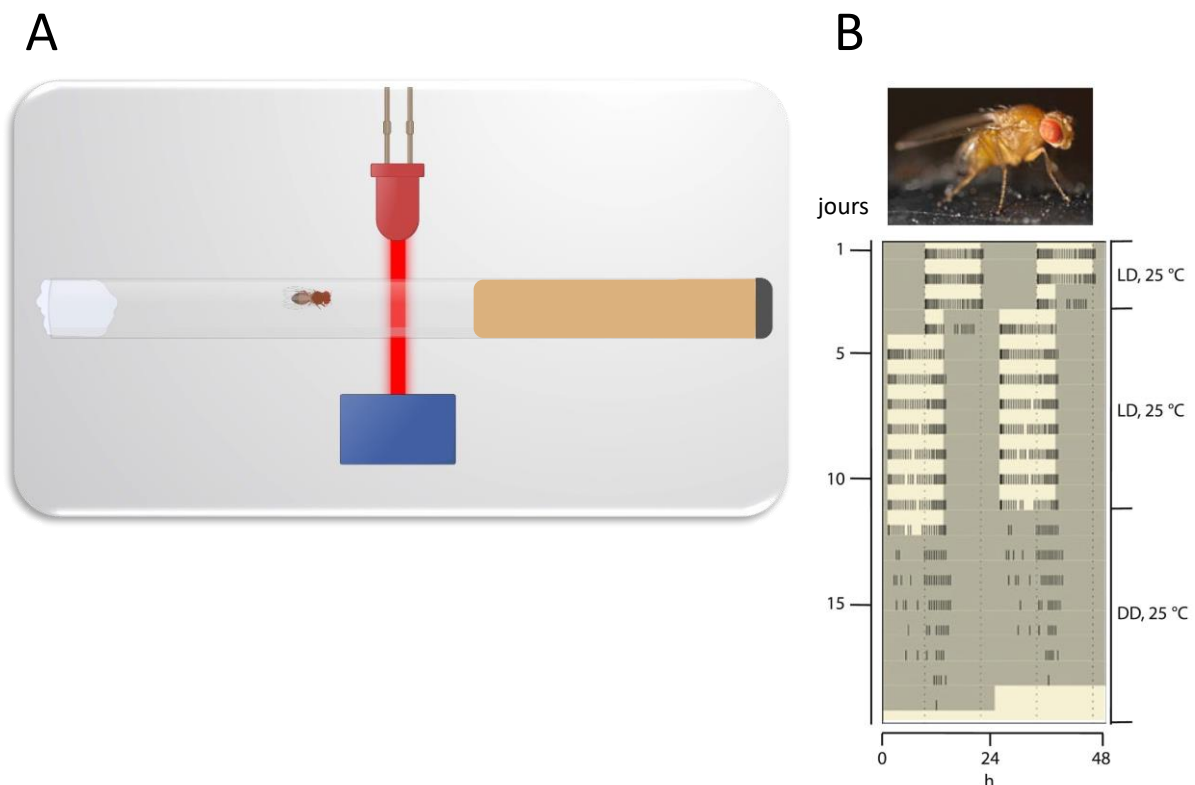


Figure 1: (A) Représentation du fonctionnement de DAM system. Les mouches sont placées individuellement dans des tubes en verre, contenant de la nourriture à une extrémité, et fermés de l'autre. Le tube est traversé par un faisceau infra-rouge détecté de l'autre côté du tube. Lors du passage de la drosophile, le faisceau est interrompu, ce qui est comptabilisé comme une activité locomotrice. Ces activités sont compilées dans un ordinateur et peuvent être représentées sous plusieurs formes. Schéma modifié à partir de (Chiu et al., 2010). **(B)** Actogramme de l'activité locomotrice de drosophiles. L'activité des drosophiles est représentée par les barres noires. La couleur de fond jaune clair correspond à une période de lumière et la couleur sombre à une période d'obscurité. Les actogrammes sont tracés en doubles afin de mieux identifier les motifs d'activité des drosophiles. LD : light-dark, cycle jour/nuit ; DD : dark-dark, obscurité constante. Schéma issu de (Rouyer, 2013).

Les rythmes veille-sommeil sont contrôlés par environ 150 neurones d'horloge retrouvés dans le cerveau de la drosophile. Ceux-ci sont catégorisés en fonction de leur anatomie et rôle dans le rythme. Ces neurones d'horloge co-expriment les composants de l'horloge moléculaire (Figure 2A). Pendant le jour, CLOCK (CLK) et CYCLE (CYC), qui sont des facteurs de transcription, vont se lier au site E-box des régions promotrices de leurs gènes cibles, dont *period* (*per*) et *timeless* (*tim*) et induire

leur expression. Les niveaux d'ARN messagers (ARNm) *tim* et *per* vont croître pendant la journée et atteindre un pic en début de nuit (Figure 2B). Une fois transcrits, les ARNm *per* et *tim* vont être exportés vers le cytoplasme où ils seront traduits en protéines PER et TIM. Celles-ci seront cependant immédiatement dégradées par des mécanismes post-traductionnels bien décrits dans la littérature (Revue dans Mendoza-Viveros *et al.*, 2013) qui les adressent au protéasome. Ainsi, on peut voir un décalage entre les oscillations d'ARNms et de protéines pour TIM et PER. Au début de la nuit, les protéines PER et TIM vont s'accumuler de par la formation d'un complexe hétérodimérique stable, ainsi, leur niveau va atteindre un pic au milieu de la nuit, où ces deux protéines vont rentrer dans le noyau et réprimer l'action de CLK et CYC. Ainsi leur propre expression étant inhibée, on parle donc de boucle de rétro-contrôle négatif. On observe à ce moment une diminution des niveaux d'ARNm *tim* et *per* (Figure 2B). Puis, vers la fin de la nuit, les protéines TIM et PER sont dégradées, ce qui lève l'inhibition opérée sur CLK-CYC, permettant à un nouveau cycle de démarrer. Dans le complexe PER-TIM, on distingue l'action de PER, décrite comme étant à l'origine de la répression de l'activité de CLK et CYC, et celle de TIM, permettant la stabilisation de PER ainsi que son import nucléaire.

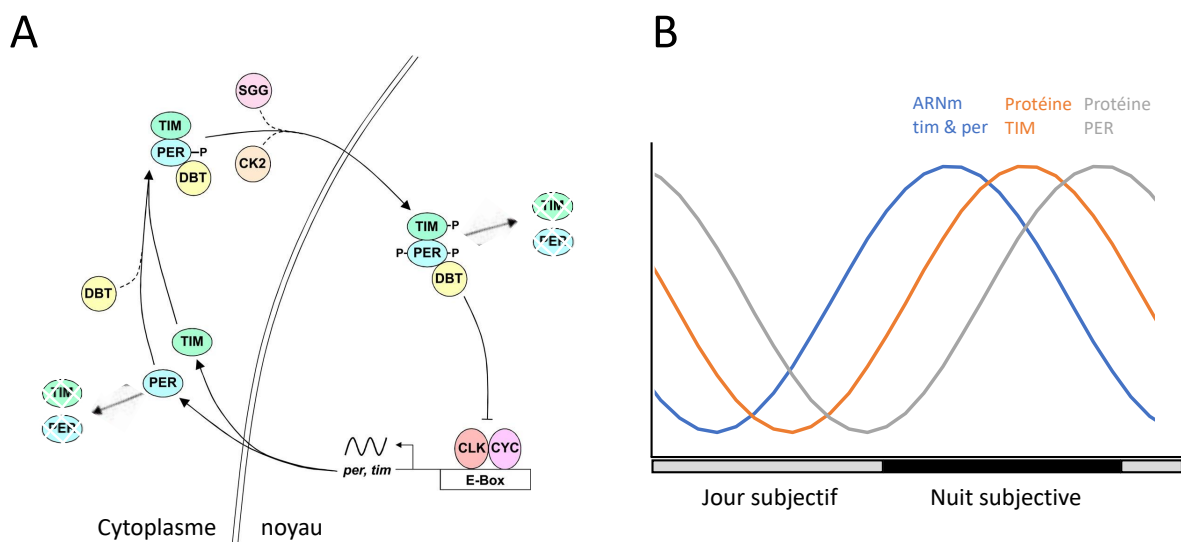


Figure 2: (A) Présentation de l'horloge moléculaire, schéma modifié à partir de (Hardin, 2011) (B) Représentation schématique des oscillations des niveaux d'ARNms et protéines TIM et PER lors d'un cycle d'obscurité constante. Le jour subjective correspond au temps de lumière pendant la phase d'entraînement des drosophiles et la nuit subjective au temps d'obscurité.

Les décalages entre pics d'ARNms et de protéines pour TIM et PER sont essentiels dans le maintien des oscillations de l'horloge moléculaire avec une période proche de 24h. Ceux-ci ont été largement attribués à des mécanismes post-traductionnels qui ont été caractérisés en détails par le passé. Pour citer un exemple, l'expression d'un transgène *per* chez la drosophile, sous le contrôle d'un promoteur activé de façon stable et conduisant donc à une expression stable de l'ARNm *per* pendant les temps circadiens est tout de même associée à des oscillations de la protéine PER dans ce contexte (Cheng & Hardin, 1998). Bien que l'existence d'un tel mécanisme soit moins clair pour *tim* (Yang & Sehgal, 2001 ; Hara *et al.*, 2011), cela suggère un rôle majeur des contrôles

post-traductionnels dans les oscillations des composants de l'horloge moléculaire. Cependant, l'existence de contrôles traductionnels, jusqu'à présent moins caractérisés chez la drosophile (Lim *et al.*, 2011 ; Lim & Allada, 2013 ; Lee *et al.*, 2017), pourrait aussi expliquer les oscillations de protéines cyclantes en absence d'oscillation de leurs ARNm. De plus, des décalages entre niveaux de transcription et de transcrits, pour *per* (So *et al.*, 1997 ; Rodriguez *et al.*, 2013 ; Yu & Rosbash, 2023) comme pour *tim* (So *et al.*, 1997; Yu & Rosbash, 2023), sont observés dans la littérature comme dans nos expériences lorsque l'on suit les niveaux de pré-ARNm vs ARNm pour *per* comme pour *tim* (données non montrées). Ceci indiquant l'existence de mécanismes post-transcriptionnels impliqués dans les retards d'expression des protéines TIM et PER. La caractérisation de contrôle post-transcriptionnel a été exposée pour la première fois dans l'horloge par ma directrice de thèse, Dr. Brigitte Grima, dans un article publié en 2019 (Grima *et al.*, 2019).

2. Résultats antérieurs à la thèse

Plusieurs années précédant mon arrivée, un crible d'ARN interférant (ARNi) (Figure 3) a été mené dans l'équipe afin de découvrir des nouveaux composants de l'horloge. Ce crible a été fait sur la collection ARNi de NIG-fly (Japon) visant ~6000 gènes, causant l'inhibition de leur expression. Le crible a été fait en suivant l'activité locomotrice des mouches en obscurité constante afin de trouver les gènes qui, une fois déplétés dans les neurones d'horloge, causeraient une altération de l'activité locomotrice des drosophiles.

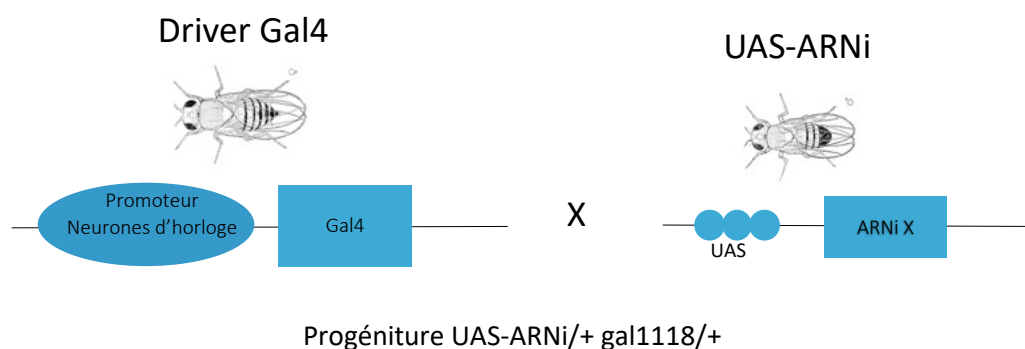


Figure 3 : Présentation du système UAS-Gal4. Le parent 1 exprime la protéine GAL4 sous le contrôle d'un promoteur spécifique d'un tissu (driver), ici des neurones d'horloge. Le parent 2 exprime l'élément de réponse UAS sur lequel la protéine GAL4 peut se fixer afin d'induire l'expression d'un transgène situé en aval de l'élément UAS, dans ce cas un ARNi visant un gène afin d'inhiber son expression. La progéniture F1 de ce croisement va donc inhiber l'expression d'un gène ciblé spécifiquement par l'ARNi qu'elle porte, spécifiquement dans les neurones d'horloge.

Parmi les gènes d'intérêt, le gène *Pop2* a été identifié, les mouches déplétées en POP2 dans les neurones d'horloge devenant arythmiques en obscurité constante. L'impact de POP2 a été confirmé en mesurant les niveaux de protéines TIM qui se trouvaient augmentés dans la tête en condition ARNi *Pop2*, et ce, seulement le jour subjectif. PER, quant à lui, n'était pas affecté dans ses niveaux protéiques par POP2. POP2 est une des deux déadénylases du complexe CCR4-NOT qui est connu pour déadényler les queues poly(A) des ARNm, et ainsi impacter leur stabilité. De plus, ce complexe est aussi

connu pour réprimer la traduction de ses cibles. POP2 étant une déadénylase du complexe CCR4-NOT, les changements circadiens des niveaux de TIM par POP2 ont été attribués à des changements opérés en amont sur les niveaux d'ARNm *tim*, augmentés le jour subjectif en condition ARNi *Pop2*. Cependant, les niveaux de pré-ARNm *tim* ne sont eux, pas impactés par l'ARNi *Pop2* le jour subjectif. Prouvant que POP2 impacte la stabilité de *tim*, et non sa transcription, ce qui indique un contrôle post-transcriptionnel et circadien de POP2 sur *tim*. L'ARNm *per*, quant à lui, n'était pas affecté par POP2 le jour subjectif, indiquant un contrôle spécifique de POP2 sur *tim*. Ensuite, la taille de la queue poly(A) de *tim* a été mesurée en expérience de PATassay afin de savoir si POP2 agissait sur *tim* via son activité de déadénylase. En condition contrôle, *tim* possède une queue poly(A) assez courte, inférieure à 50 nucléotides, en tout temps circadiens. Cependant, l'ARNi *Pop2* conduit à un rallongement de celle-ci, particulièrement le jour subjectif, indiquant que POP2 déstabilise l'ARNm *tim* en le déadénylant.

Enfin, il a été montré qu'en absence de PER, (mouches mutantes *per⁰*), l'effet de l'ARNi *Pop2* était perdu. En effet, les niveaux élevés d'ARNm *tim* observés normalement en contexte *per⁰* n'étaient pas affectés par l'ARNi *Pop2*. De même, la queue poly(A) de *tim* était raccourcie dans ce contexte aussi.

L'équipe a publié ces résultats dans un article rapportant une déadénylation de l'ARNm *tim* par POP2, spécifique, circadienne et dépendante de PER. Les résultats sont résumés ci-dessous (Figure 4).

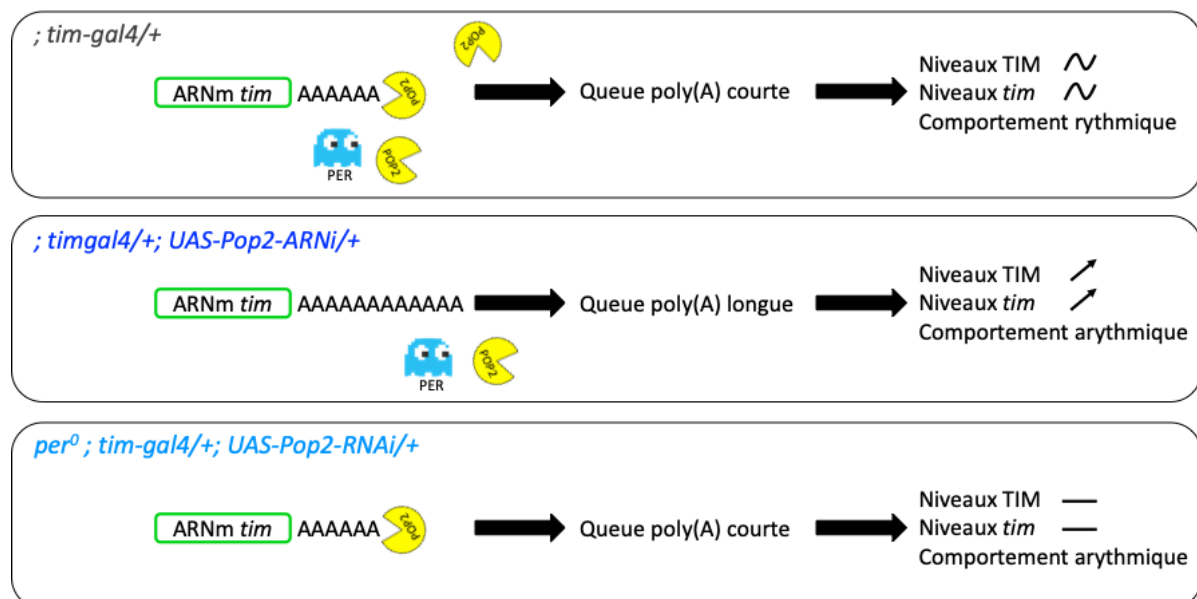


Figure 4 : Résumé des résultats de l'article (Grima et al., 2019).

3. Objectifs de ma thèse

L'objectif de mon projet de thèse était de mieux comprendre le contrôle de POP2 sur l'ARNm *tim*.

L'effet de POP2 sur *tim* est circadien, avec un effet visible le jour subjectif seulement, soutenant l'hypothèse de l'existence de régulations circadiennes de l'activité de POP2. De plus, PER semble contrôler l'activité de POP2, il est donc possible que les niveaux de POP2 oscillent, bien que les niveaux d'ARNm *Pop2* n'oscillent pas (Grima *et al.*, 2019). Des oscillations de la protéine POP2 peuvent tout de même être générées via des mécanismes de contrôles traductionnels/post-traductionnels. La première partie de cette synthèse portera sur l'étude de l'oscillation potentielle de la protéine POP2.

Ensuite, POP2 agit spécifiquement sur l'ARNm *tim*, mais pas *per*. La recherche du facteur expliquant la spécificité de POP2 pour *tim* constitue donc le second chapitre de cette synthèse.

Enfin, le complexe CCR4-NOT est connu non seulement pour déstabiliser ses cibles, mais aussi pour réprimer leur traduction. Nous allons donc voir si POP2 agit sur la traduction de *tim* en utilisant la technique de TRAP (purification affine de ribosome en cours de traduction) couplée à de la RT-qPCR pour mesurer les niveaux d'ARNms, du PATassay pour mesurer la taille de leur queue poly(A) (approches gène spécifique), et à du RNA-seq (approche transcriptome) afin d'observer l'effet de POP2 à l'échelle du transcriptome mais aussi des gènes régulés de façon circadienne. De plus, le rôle de PER sur POP2 sera précisé dans ce chapitre final également.

II. Résultats

1. Action circadienne de POP2 sur *tim*

Le suivi de l'oscillation de la protéine POP2 par Western blot ou Immunomarquage nécessite l'utilisation d'anticorps anti-POP2, cependant, nous ne disposons pas dans l'équipe d'anticorps anti-POP2 présentant une qualité satisfaisante. Il était donc nécessaire de suivre POP2 via un tag ajouté à la protéine POP2 endogène afin d'estimer l'oscillation potentielle de ses niveaux. Nous avons donc généré des lignées de drosophiles présentant un tag-HA intégré dans le gène *Pop2* endogène en utilisant l'outil CRISPR-Cas9. Après avoir criblé 3224 mouches par PCR afin de trouver un transformant ayant intégré le tag-HA à la protéine POP2, nous avons quantifié les niveaux de protéines POP2-HA dans des têtes de drosophiles à plusieurs temps circadiens (CT) le premier jour d'obscurité constante (DD1). Nous n'avons pas vu d'oscillation des niveaux protéiques de POP2-HA, ni pour la bande haute, ni pour la bande basse détectées par notre anticorps et correspondant, toutes deux, à POP2 (Figure 5A). Cependant, cela pourrait indiquer que POP2 n'oscille que dans les cellules d'horloge. En effet, ici, nous mesurons les niveaux de protéines POP2 dans toute la tête de la drosophile. Or, POP2 est exprimée de façon ubiquitaire dans celle-ci, ce qui pourrait masquer des oscillations de POP2 spécifiquement dans les neurones d'horloge, il était donc important de suivre les niveaux de POP2 dans ces neurones. En quantifiant le signal POP2-HA dans les neurones d'horloge à plusieurs temps circadiens (Figure 5B), nous n'observons pas non plus d'oscillation des niveaux de protéines POP2. Indiquant que ni les niveaux d'ARNms, ni les niveaux de protéines

POP2 n'oscillent. De plus, il n'y a pas non plus de variation des niveaux de phosphorylation de POP2 pendant les temps circadiens, qui aurait été détectée en Western blot, ni de variation de sa localisation dans la cellule, qui aurait pu être observée en Immunomarquage.

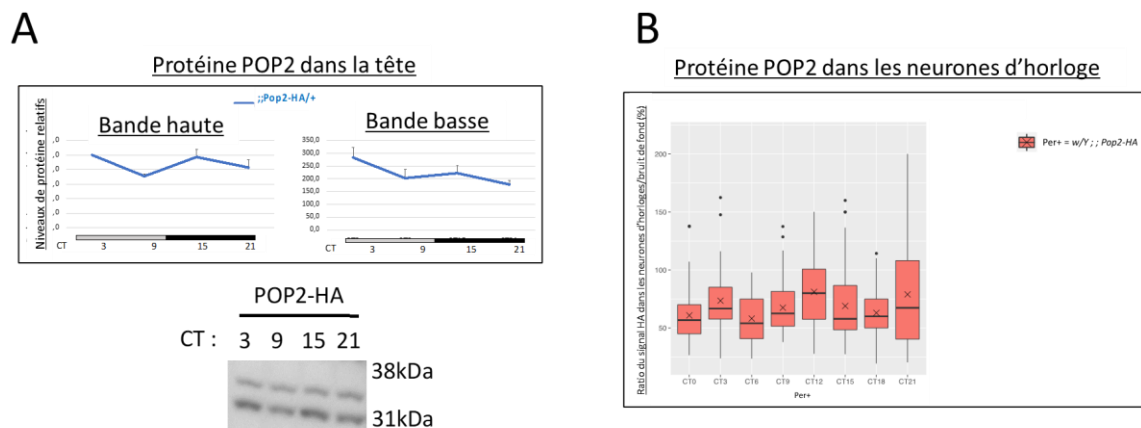


Figure 5 : (A) Quantification des signaux (haut et bas) de POP2-HA en Western blot dans les têtes de drosophiles. Panel inférieur montrant une image de la membrane où les bandes hautes et basses de POP2 sont visibles avec leur poids moléculaire en kDa associé. (B) Quantification de signaux POP2-HA en Immunomarquage dans les neurones d'horloge sLNvs (petits neurones ventro-latéraux, important pour le maintien de la rythmicité de l'activité locomotrice en obscurité constante). Le signal POP2-HA mesuré dans les neurones d'horloge est normalisé par le signal POP2-HA présent dans les cellules voisines, attendues pour présenter une expression de POP2 constitutive comme l'indique le Western blot réalisé dans toute la tête.

Une autre hypothèse expliquant l'action circadienne de POP2 sur *tim* pourrait être l'effet potentiel que PER semble jouer sur POP2. En effet, en absence de PER, nous perdons aussi l'effet de l'ARNi *Pop2*, et PER est régulé de façon circadienne. Nous avons mesuré les niveaux de POP2 par Western blot et Immunomarquage en contexte *per*⁺ et *per*⁰ afin de voir si la présence ou l'absence de PER pouvait affecter les niveaux de POP2. Nous n'avons pas vu d'effet de PER sur les niveaux de POP2 dans la tête (Western blot), ni dans les neurones d'horloge (Immunomarquage). De plus, ni la phosphorylation, ni la localisation de POP2 n'étaient affectées par PER.

2. Spécificité de POP2 pour *tim*

Le complexe CCR4-NOT a été montré à de nombreuses reprises comme étant recruté par des protéines liant l'ARN de façon spécifique (Raisch & Valkov, 2022). Afin de comprendre la raison de la spécificité de POP2 pour *tim* mais pas *per*, une Immunoprécipitation de la protéine POP2 avec ses partenaires protéiques a été effectuée en utilisant les mouches POP2-HA à plusieurs temps circadiens, au cas où cette interaction soit circadienne, ce qui pourrait expliquer en même temps l'effet circadien de POP2 sur *tim*. Les partenaires protéiques de POP2 co-immunoprécipités avec POP2-HA ont été identifiés par spectrométrie de masse. Environ 70 partenaires ont ainsi été identifiés, dont les composants du complexe CCR4-NOT. Sur ces 70 partenaires, ceux présentant des fonctions liées au métabolisme des ARNs ont été criblés en utilisant des ARNi ou des lignées mutées pour ces gènes, afin de chercher un gène présentant le même phénotype qu'en ARNi *Pop2* (Figure 6). Après avoir criblé

les gènes sélectionnés en spectrométrie de masse et dans la littérature, représentant ~80 gènes testés en comportement, dont une quinzaine en Western blot en suivant les niveaux de PER et TIM. Nous n'avons pas retrouvé de candidat présentant un phénotype similaire à POP2.

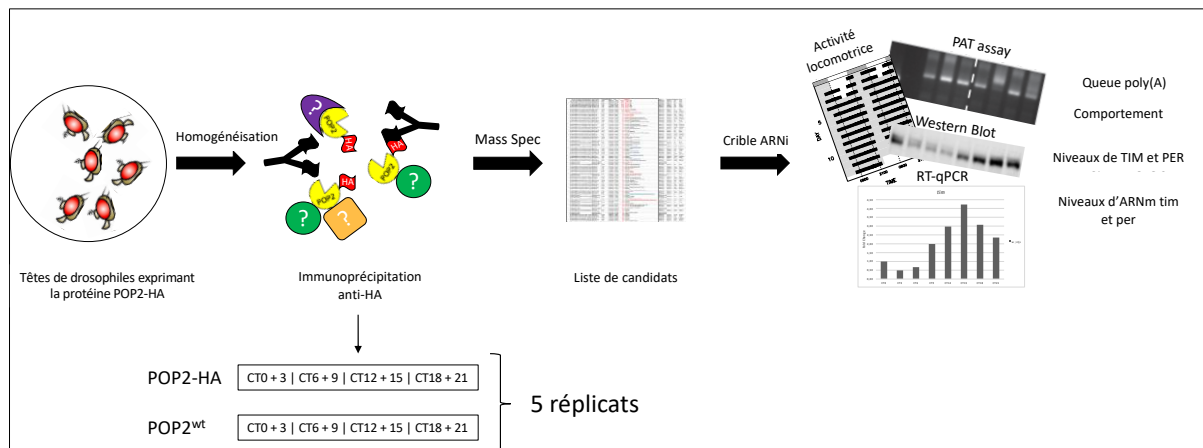


Figure 6 : Procédure de criblage des partenaires protéiques de POP2 identifiés en spectrométrie de masse (Mass Spec).

Une autre hypothèse qui avait été avancée afin d'expliquer la spécificité de POP2 pour *tim* était la présence potentielle de modifications de l'ARNm *tim* qui pourraient être reconnues par des protéines « readers » et causer le recrutement du complexe CCR4-NOT (Du *et al.*, 2016). De plus, des méthylations de l'adénine (m6A) ont été trouvées chez *tim* dans la drosophile (Kan *et al.*, 2021). Nous nous sommes donc associés à l'équipe de Jean-Yves Roignant afin de tester des mutants de modifications de l'ARN pour voir s'ils pouvaient présenter des phénotypes similaires à l'ARNi *Pop2* en comportement et en RT-qPCR mesurant les niveaux d'ARNm *tim*. Cela pourrait indiquer la nécessité de certaines modifications de l'ARNm afin de permettre le recrutement spécifique de POP2. Nous n'avons pas trouvé de résultats similaires à ceux obtenus avec l'ARNi *Pop2* dans les mutants de modifications d'ARN testés.

Ainsi, nous n'avons pas trouvé de protéines ou de modifications de l'ARNm permettant de faire un lien entre POP2 et *tim*.

3. Régulation de la traduction par POP2

a. Approches spécifiques d'un gène

Le complexe CCR4-NOT est non seulement connu pour réguler la stabilité de ses cibles, mais aussi leur traduction. Ainsi, POP2 pourrait aussi agir sur la traduction de *tim*. Afin de répondre à cette question, la technique de TRAP a été utilisée pour suivre la traduction de *tim* et *per* (Figure 7). Une expérience similaire a été réalisée dans l'équipe de Rob Jackson (Huang *et al.*, 2013 ; You *et al.*, 2021), quantifiant les niveaux d'ARNms liés aux ribosomes à plusieurs temps circadiens. Cependant, ces niveaux n'étaient pas normalisés par les niveaux d'ARNms totaux, ne permettant pas de distinguer les régulations transcriptionnelles et traductionnelles. Nous avons procédé à cette normalisation afin d'isoler des contrôles traductionnels potentiels. En condition contrôle (Figure 8), on peut voir une oscillation de la traductibilité de *tim* et de *per*,

avec une amplitude d'environ un fold change 2. Cette oscillation de la traductibilité, lorsque comparée aux niveaux d'ARNm et de protéine TIM et PER (Figure 9), montre un minimum aux temps correspondant à des niveaux élevés d'ARNm totaux, mais minimum pour la protéine PER et encore assez faible pour la protéine TIM. Ainsi, les retards entre pics d'ARNm et de protéine TIM et PER, jusqu'à présent largement attribués à des mécanismes post-traductionnels, semblent aussi régulés par des contrôles de la traduction de *per* et de *tim*, puisqu'on observe des niveaux de traduction plus faibles de *per* et *tim* lorsqu'on a besoin de niveaux de protéines faibles. Nous avons donc découvert un nouveau niveau de régulation de l'expression des protéines TIM et PER dans l'horloge qui contribue probablement au retard entre leurs pics d'ARNm et de protéine.

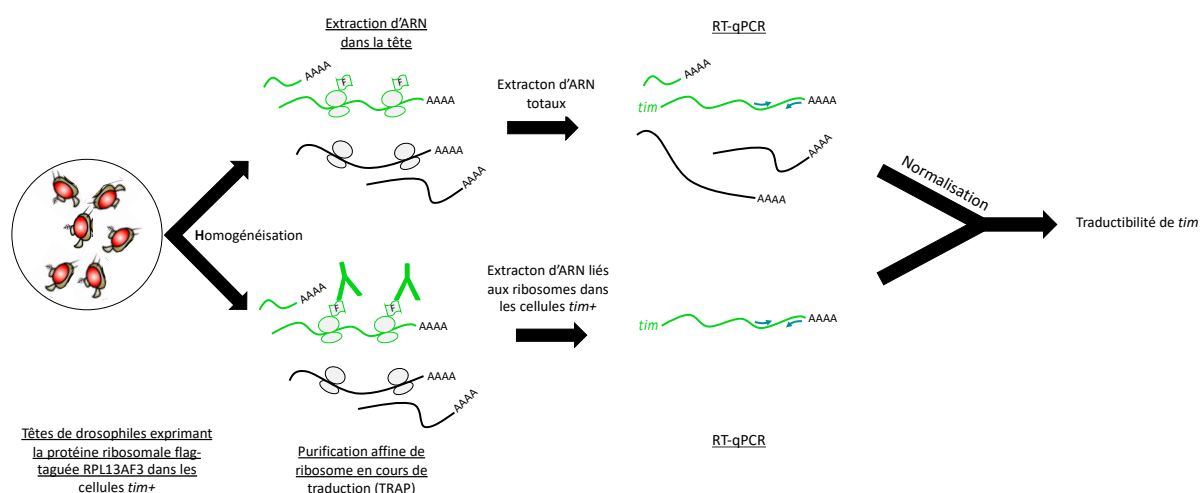


Figure 7 : Procédure de TRAP. La quantité d'ARNm liés aux ribosomes dans les cellules exprimant *tim* est mesurée par qPCR et normalisée par la quantité totale d'ARNm correspondante afin de déterminer la traductibilité de celui-ci, ou, quelle quantité d'ARNm est liée au ribosome, indépendamment de sa quantité totale dans la tête.

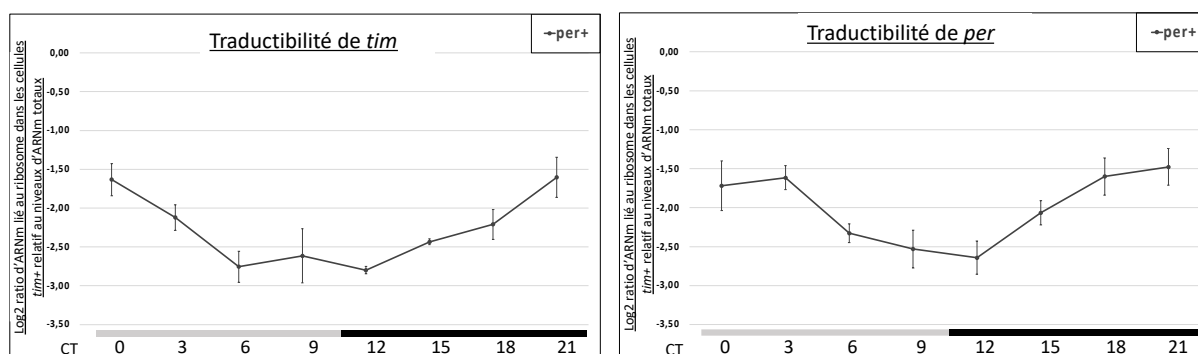


Figure 8 : Niveaux de traductibilité de *tim* et *per*.

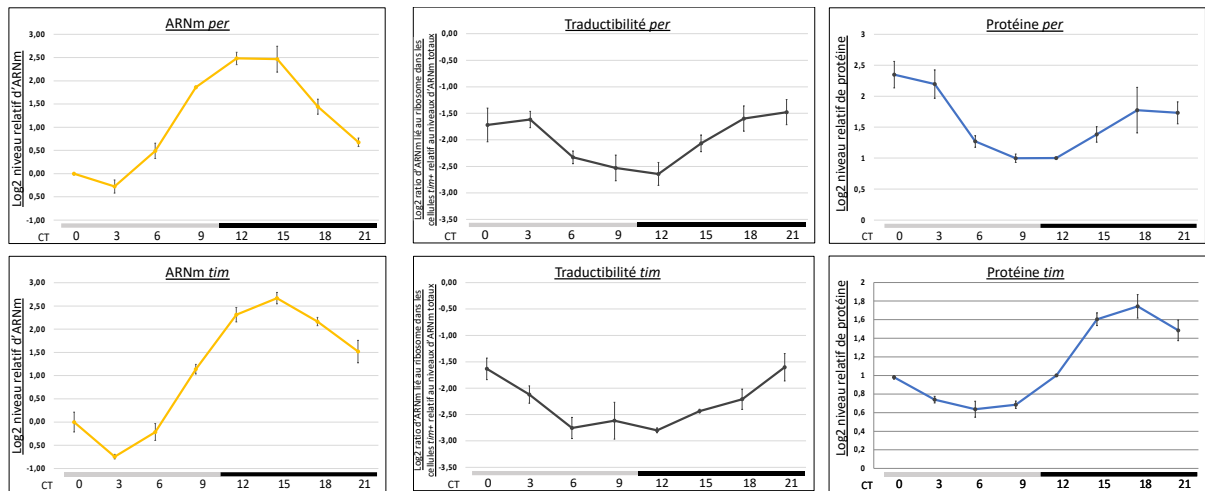


Figure 9 : Comparaison des courbes d'oscillation des ARNm, traductibilité, et protéines PER et TIM.

Nous avons ensuite étudié l'impact de POP2 sur la traductibilité de *tim* et de *per* (Figure 10). L'ARNi *Pop2* augmente spécifiquement la traductibilité de *tim*, et ce à tous les temps circadiens, avec un effet plus fort le jour subjectif que la nuit subjective. *per*, lui, montre juste un léger déphasage de l'oscillation de sa traductibilité en condition ARNi *Pop2*. Ce résultat indique une inhibition forte de la traductibilité de *tim* par POP2, et ce, de façon indépendante de l'effet de POP2 sur la stabilité de *tim*, étant donné que l'augmentation des niveaux d'ARNm *tim* en condition ARNi *Pop2* sont déjà pris en compte dans le calcul de la traductibilité de *tim*. Cela indiquant un contrôle spécifique et fort de la traduction de *tim* par POP2.

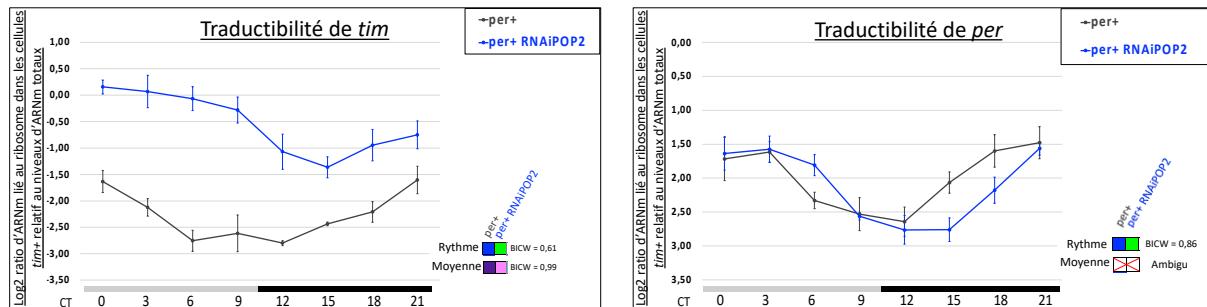


Figure 10 : Traductibilité de *tim* et *per* en condition +/- ARNi *Pop2*. Analyses statistiques des oscillations et des niveaux moyens de traductibilité réalisées avec *dryR* (Weger et al., 2021) BICW : Bayesian Information Criterion Weight.

Le rôle de PER sur le contrôle de la traduction de *tim* par POP2 a ensuite été testé (Figure 11). On peut voir que POP2 régule l'ARNm *tim* total de façon dépendante de PER (pas d'effet de l'ARNi *Pop2* en absence de PER), mais au contraire, régule la traductibilité de *tim*, même en absence de PER. Ainsi, POP2 régule la traductibilité de *tim* de façon indépendante de PER.

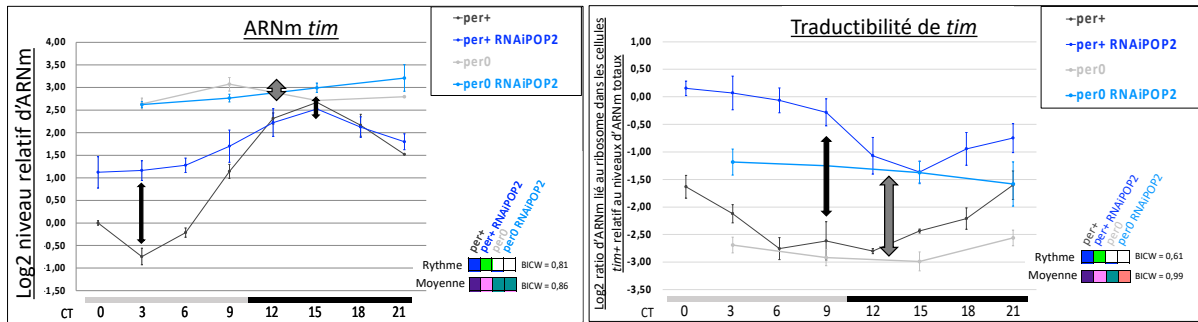


Figure 11 : Niveau d'ARNm *tim* totaux en condition *per+*/*per0* +/- ARNi Pop2. Traductibilité de *tim* en condition *per+*/*per0* +/- ARNi Pop2. Analyses statistiques des oscillations et des niveaux moyens de traductibilité réalisées avec *dryR* (Weger et al., 2021) BICW : Bayesian Information Criterion Weight.

Nous nous sommes ensuite intéressés à l'état de polyadénylation de l'ARNm *tim*, lorsque celui-ci est lié aux ribosomes. Nous avons donc réutilisé nos échantillons de TRAP afin d'effectuer des PATassays dessus pour mesurer la queue poly(A) de *tim* dans les fractions d'ARNs totaux et liés aux ribosomes dans nos différentes conditions (Figure 12). Sur cette expérience, nous retrouvons les mêmes résultats que précédemment publiés dans l'équipe (Grima et al., 2019) dans la fraction totale (Figure 13), montrant des formes polyadénylées de *tim* en condition ARNi Pop2, principalement le jour subjectif, avec un effet moins fort la nuit subjective, ainsi qu'en contexte *per0* ARNi Pop2. De façon intéressante, nous voyons que les formes liées aux ribosomes sont toujours les formes polyadénylées, à partir du moment où celles-ci sont visibles dans la fraction totale. De plus, même si celles-ci sont minoritaires par rapport aux formes déadénylées (comme en condition *per0* et *per+* la nuit subjective), elles sont retrouvées en très grande majorité liées aux ribosomes. Cela indiquant une forte interaction entre formes polyadénylées de *tim* et ribosomes.

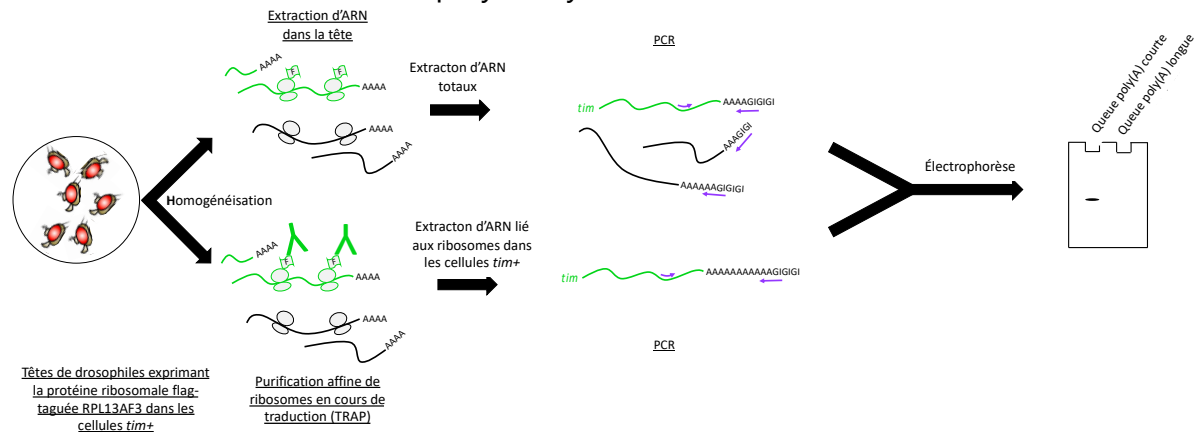


Figure 12 : Procédure de PATassay sur échantillons de TRAP. Les ARNm liés aux ribosomes ou dans la fraction totale sont passés en PATassay afin de mesurer la taille de la queue poly(A) de *tim* dans ces deux différentes fractions. Les produits PCR obtenus sont séparés en fonction de leur taille en électrophorèse en gel d'agarose.

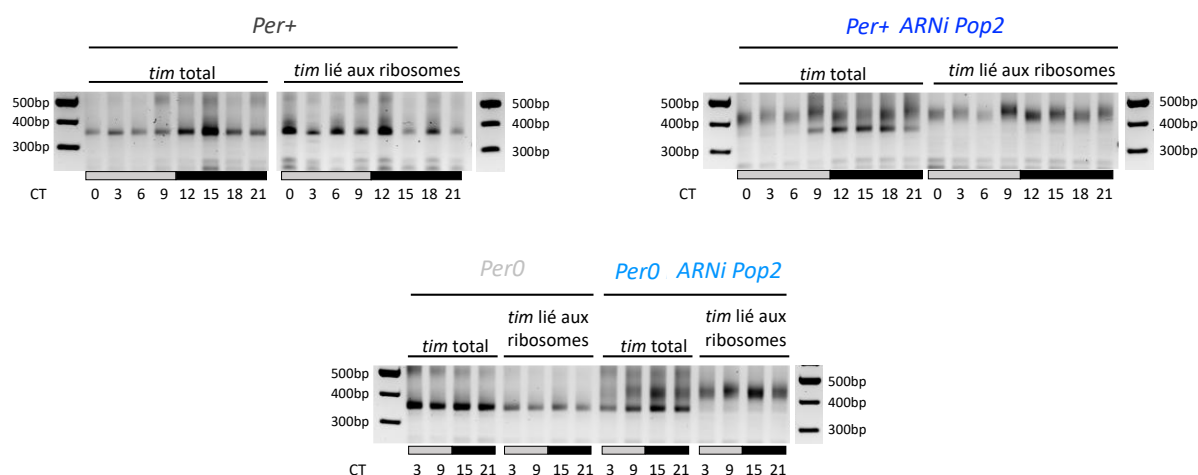
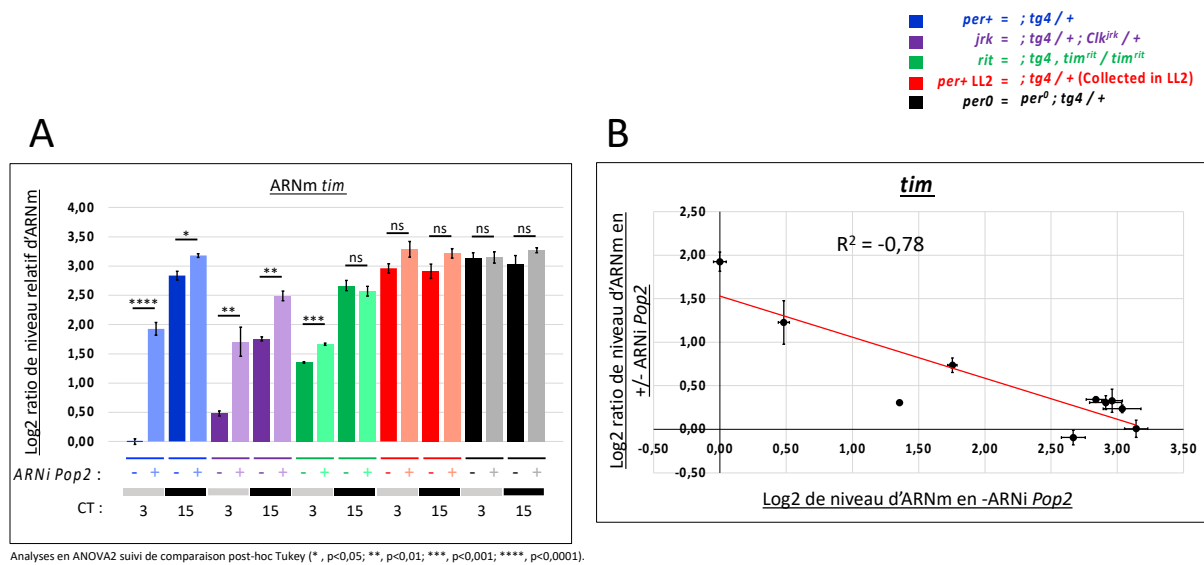


Figure 13 : Résultats de PATassay sur l'ARNm *tim* en fraction totale ou liée aux ribosomes, taille du marqueur de taille en paires de bases (bp).

De plus, ce résultat nous a fait remarquer une contradiction. En effet, la perte d'effet de l'ARNi *Pop2* en condition *per0* est associée à la présence de formes déadénylées de *tim* dans ce contexte dans la fraction d'ARNm totaux. Or, nous observons le même résultat en condition *per+* pendant la nuit subjective, là où les niveaux de PER sont les plus élevés. La présence ou l'absence de PER ne semble donc pas être un bon indicateur de l'activité de POP2. À l'inverse, lorsque l'on s'intéresse aux niveaux d'ARNm *tim* dans ces conditions, on remarque des niveaux élevés de *tim* en condition *per0*, comme en condition *per+* la nuit subjective. Et POP2 n'impacte la stabilité de l'ARNm *tim* que le jour subjectif, lorsque ses niveaux sont très bas. Il est donc possible que l'effet circadien de POP2 sur *tim* le jour subjectif ne soit pas dû à PER lui-même, mais aux niveaux d'ARNm *tim*, qui pourraient causer la saturation de POP2 lorsqu'ils sont trop élevés. Nous avons donc cherché dans la littérature des contextes altérant les niveaux d'ARNm *tim*, que nous avons mesurés en RT-qPCR, en présence et en absence de l'ARNi *Pop2* (Figure 14). Nous pouvons voir sur ces échantillons que les conditions présentant des niveaux élevés d'ARNm *tim* présentent aussi les régulations les plus faibles de *tim* liées à POP2. Inversement, les conditions présentant des niveaux de *tim* faibles montrent de fortes élévations des niveaux de celui-ci en condition ARNi *Pop2*. Cela indiquant que le contrôle de l'action de POP2 sur *tim* n'est probablement pas régulé en fonction de PER directement, mais plutôt en fonction de l'abondance de *tim* dans un contexte donné. Ainsi suggérant un contrôle indirect de PER sur l'action de POP2, étant donné que PER contrôle la transcription de *tim* via son action répressive sur CLK et CYC (Figure 2). De plus, la taille de la queue poly(A) de *tim* a été suivie dans ces différents contextes, et on observe que les conditions présentant une action significative de POP2 sur les niveaux d'ARNm *tim* présentent aussi le plus de formes polyadénylées de *tim* (données non montrées). Ceci, suggérant que POP2 régule *tim* en fonction de son abondance, et ce, via sa queue poly(A).



Analyses en ANOVA2 suivi de comparaison post-hoc Tukey (*, p<0,05; **, p<0,01; ***, p<0,001; ****, p<0,0001).

Figure 14 : (A) Résultats de RT-qPCR quantifiant les niveaux d'ARNm *tim* dans plusieurs contextes mutants connus pour affecter les niveaux d'ARNm *tim*. Ces contextes sont suivis en condition +/- ARNi Pop2. (B) Corrélation entre niveaux d'ARNm *tim* dans une condition donnée, et effet de l'ARNi Pop2 dans cette même condition. De plus, les niveaux de pré-*tim* ont été mesurés pour chaque condition afin de confirmer que l'effet de POP2 sur les niveaux de *tim* n'était pas transcriptionnel. R^2 représentant le coefficient de corrélation de Pearson.

Ces résultats répondent donc aux deux questions posées précédemment. En effet, l'action circadienne de POP2 sur la stabilité de *tim* est ici expliquée par un effet plus ou moins visible de POP2 sur *tim* en fonction de l'abondance de *tim*. Cela suggère donc une action stable de POP2 sur *tim*, qui peut saturer lorsque ses cibles deviennent trop abondantes. De plus, l'effet de PER ne semble pas atteindre directement POP2, mais semble au contraire passer par le contrôle de la transcription de *tim*, ce qui va impacter son abondance, et ainsi causer la saturation de POP2.

b. Approche transcriptomique

Après la découverte du contrôle de la traduction de *tim* par POP2, nous avons décidé de chercher si d'autres gènes d'horloges étaient eux aussi régulés par POP2. Nous avons donc envoyé nos échantillons de TRAP en séquençage ARN en conditions *per+ / 0 +/- ARNi Pop2*, à CT3 et 15 pour les conditions *per+*, et CT3 seulement pour les conditions *per0*, pour lesquelles les temps circadiens ne sont pas pertinents. Cette analyse a été originalement faite sur nos fractions ARN totaux et liés aux ribosomes afin de pouvoir normaliser les quantités d'ARNm liés aux ribosomes par leur niveaux totaux initiaux. Cependant, nous avons découverts de nombreux gènes présentant des expressions de leurs transcrits en dehors des cellules *tim+*, constituant un biais lors de la comparaison entre fractions totale et lié aux ribosomes, qui pour cette dernière, est aussi spécifique des cellules *tim+*. Nous nous sommes donc intéressés principalement à la fraction liée aux ribosomes (Figure 15). Nous voyons qu'environ 40 gènes sont significativement régulés entre CT3 et CT15 (Figure 15A), alors que plusieurs milliers sont régulés par POP2 en condition *per+* et *per0*, indiquant un contrôle important de POP2 à l'échelle du transcriptome. À l'inverse, le faible nombre de gènes régulés de façon circadiennes (CT3 vs CT15) est assez surprenant. Cela peut être dû au faible

nombre de temps testés, ne permettant pas d'identifier de nombreux transcrits via leurs oscillations. Néanmoins, lorsque l'on s'intéresse aux gènes présentant une régulation circadienne (Figure 15B), nous retrouvons plusieurs gènes d'horloges (*tim*, *vri*, *per*, *Clk*). Indiquant que, malgré le faible nombre de temps analysés, nous sommes quand même capables de retrouver des gènes pertinents dans l'horloge avec notre jeu de données. Le clustering hiérarchique nous permet de retrouver des gènes présentant des variations de leurs score-Z similaires entre les différentes conditions testées. Ainsi, nous trouvons le gène CG14275 comme régulé de façon très similaire à *tim*, ce qui constitue une piste intéressante dans la découverte potentielle d'un nouveau gène d'horloge. En effet, le CG14275 est déjà connu comme cyclant dans plusieurs cribles en micro-array (Claridge-Chang *et al.*, 2001 ; Keegan *et al.*, 2005). De plus, ce gène est prédit pour impacter le sommeil de par la présence de domaines Ly6 retrouvés aussi dans le gène *sleepless* (Koh *et al.*, 2008). Ensuite, le gène *vri* est représenté dans la heatmap comme potentiellement régulé par POP2 à CT3, ces résultats ont été confirmés en consultant les données de séquençage ARN.

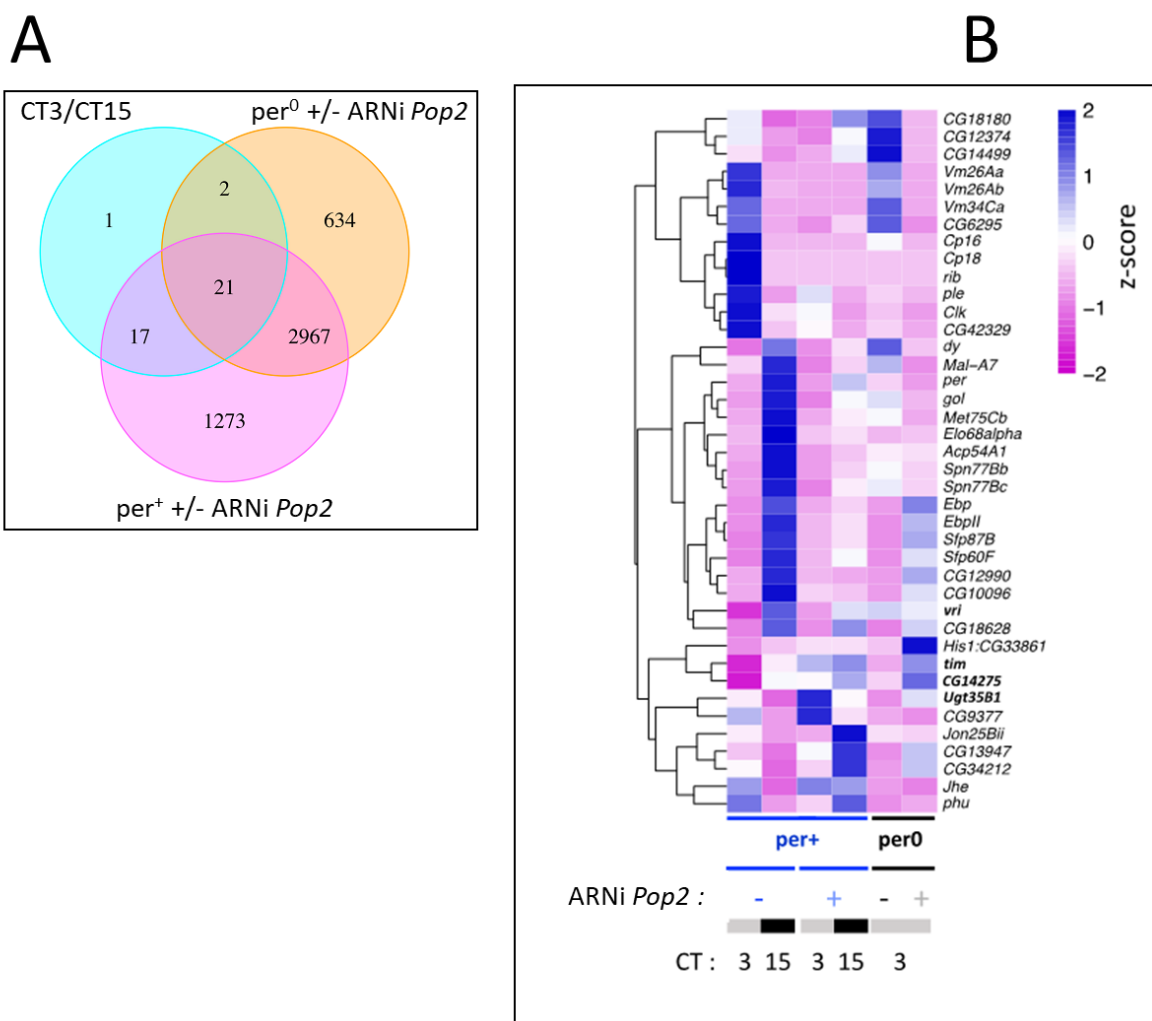


Figure 15 : (A) Diagramme de Venn représentant le nombre de gènes significativement régulés entre CT3 et CT15 en condition per⁺, entre +/- ARNi Pop2 en condition per⁺ ou per⁰. (B) Heatmap avec clustering hiérarchique représentant les scores Z pour les gènes régulés significativement entre CT3 et CT15 en per⁺. Les gènes surlignés en

bleu sont soit des gènes d'horloges, soit des candidats d'intérêt déjà connus pour osciller dans d'autres cribles et qui seront caractérisés plus en détail.

Cette découverte d'un contrôle potentiel de *vri* par POP2 est très intéressante, étant donné que *vri* est un gène d'horloge impliqué dans une seconde boucle de rétrocontrôle négatif qui va contrôler la transcription de *Clk* de façon circadienne, permettant le renforcement des oscillations de l'horloge moléculaire dans son ensemble (Figure 16).

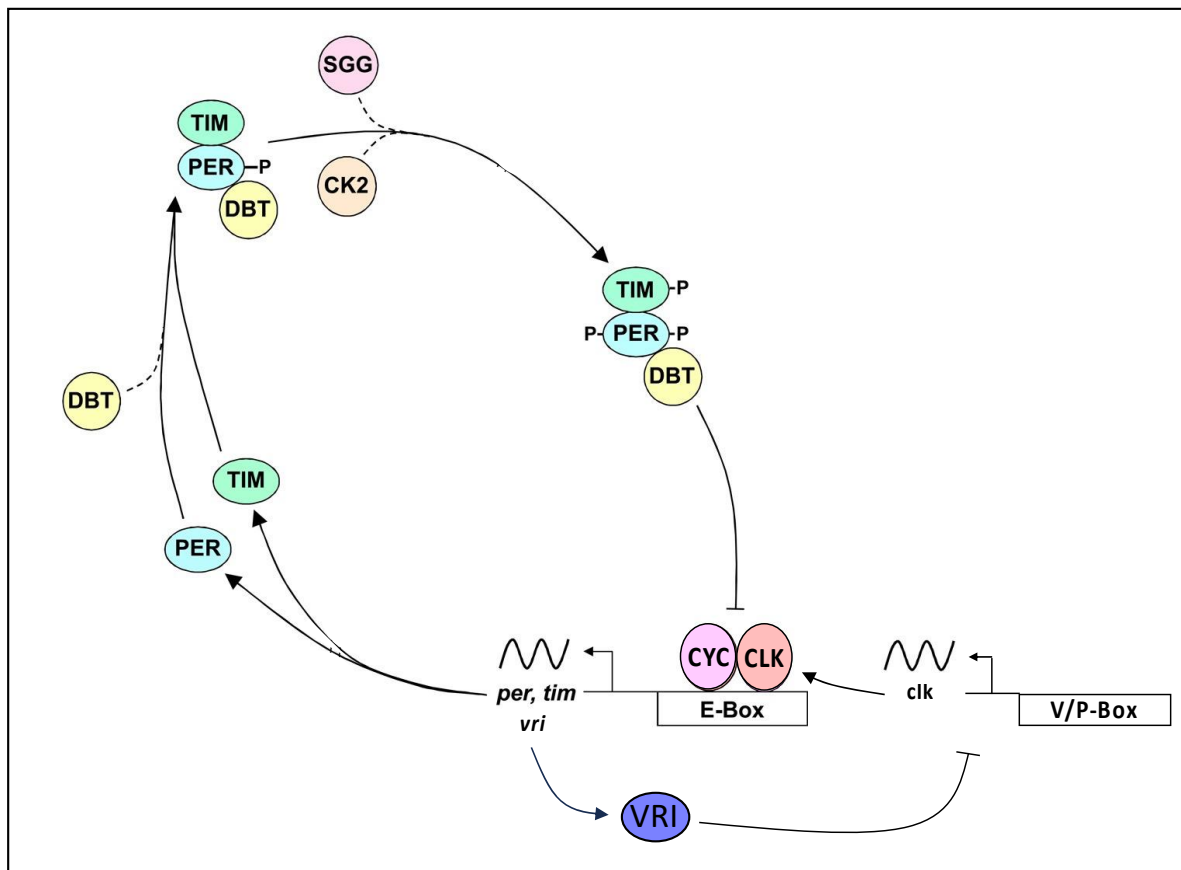


Figure 16 : Schéma de l'action de *vri* dans l'horloge moléculaire présentée en figure 2A. CLK et CYC induisent la transcription de leur gènes cibles, dont *per*, *tim* et *vri*. *vri* est traduit en protéine, qui va agir en tant que répresseur transcriptionnel sur *Clk*, et inhiber son expression de façon circadienne, renforçant les oscillations de l'horloge moléculaires et la stabilisant. Schéma modifié à partir de (Hardin, 2011)

Ainsi, l'impact de POP2 sur la stabilité de l'ARNm *vri* ainsi que sa traductibilité ont été caractérisés (Figure 17). On peut voir tout d'abord que l'ARNm *vri* présente lui aussi une oscillation de sa traductibilité (Figure 17A), avec une amplitude d'environ 2 Fold changes. Cela indiquant l'existence de mécanismes de contrôles traductionnel pour *vri* en plus de *tim* et *per*. Ensuite, les niveaux d'ARNm *vri* sont inhibés par POP2 le jour subjectif en condition *per+* (Figure 17B), mais pas la nuit subjective en condition *per+*, ni en condition *per0*. Ainsi confirmant un contrôle de la stabilité de *vri* par POP2, et ce, de façon très similaire à celui observé pour *tim*. La traductibilité de *vri*, elle aussi, est inhibée par POP2 en condition *per+* (Figure 17C), l'existence de tels contrôles en condition *per0* étant néanmoins plus ambigus. Ainsi, nous savons à présent que l'ARNm *vri* est lui aussi, la cible de POP2, et ce, d'une façon similaire à *tim*. De plus, il

semble que POP2 impacte aussi la stabilité de *vri* de façon plus importante le jour subjectif, lorsque les niveaux d'ARNm *vri* sont les plus faibles.

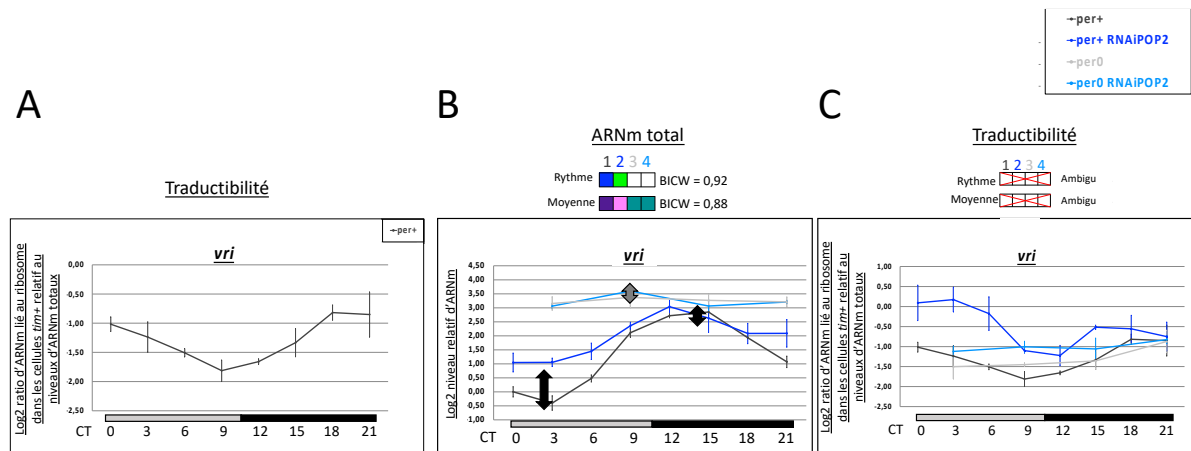


Figure 17 : (A) Niveaux de tractabilité de *vri*. **(B)** Niveau d'ARNm *vri* totaux en condition *per+*/*per0* +/- ARNi Pop2. Tractabilité de *vri* en condition *per+*/*per0* +/- ARNi Pop2. Analyses statistiques des oscillations et des niveaux moyens de tractabilité réalisées avec *dryR* (Weger et al., 2021) BICW : Bayesian Information Criterion Weight.

Nous avons donc reproduit l'expérience précédemment faite sur *tim* pour *vri*. Afin de chercher si POP2 impacte aussi *vri* plus efficacement lorsque ses niveaux sont faibles. Nous avons suivi l'impact de POP2 sur la stabilité de l'ARNm *vri* en fonction de ses niveaux (Figure 18). Nous retrouvons là aussi un effet fort de POP2 sur *vri* lorsque ses niveaux sont faibles, et au contraire un effet faible de POP2 lorsque *vri* est très abondant.

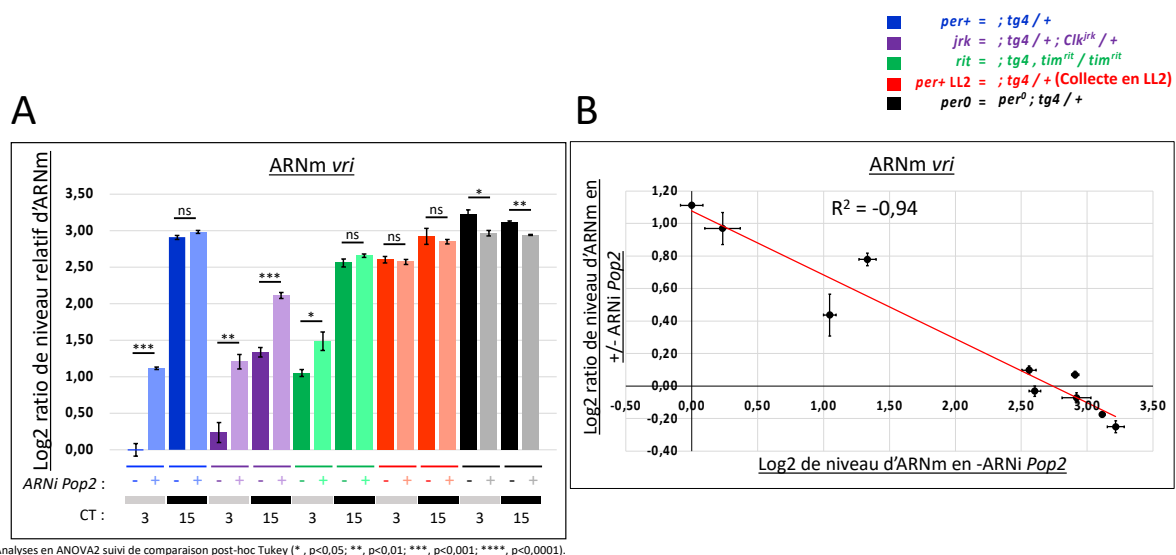


Figure 18 : (A) Résultats de RT-qPCR quantifiant les niveaux d'ARNm *vri* dans plusieurs contextes mutants connus pour affecter les niveaux d'ARNm *vri*. Ces contextes sont suivis en condition +/- ARNi Pop2. **(B)** Corrélation entre niveaux d'ARNm *vri* dans une condition donnée, et effet de l'ARNi Pop2 dans cette même condition. De plus, les niveaux de pré-*vri* ont été mesurés pour chaque condition afin de confirmer que l'effet de POP2 sur les niveaux de *vri* n'était pas transcriptionnel. R^2 représentant le coefficient de corrélation de Pearson.

Ici, nous avons donc caractérisé *vri* comme une autre cible de POP2, de plus, POP2 régule *vri* de façon très proche de *tim*, ouvrant la voie à des études supplémentaires visant à comprendre la spécificité de POP2 pour ses cibles (*tim* et *vri* ici) en recherchant

des similarités présentes dans ces 2 transcrits mais absentes chez *per*, notamment au niveau de leur séquences, fonctions biologiques, localisations, recherche de protéines ou micro-ARN interagissants avec etc...

Nous voulions ensuite exploiter nos données de séquençage ARN afin de mieux comprendre le fonctionnement de POP2 à l'échelle du transcriptome, afin de notamment savoir si POP2 régulait moins fortement les transcrits présentant une abondance élevée dans le transcriptome. Nous avons donc étudié les transcrits présentant des modifications de leur expressions en contexte +/- ARNi *Pop2* (Figure 19A). On remarque immédiatement la présence d'approximativement autant de gènes sur-exprimés que sous-exprimés en condition ARNi *Pop2* à CT3. Ce résultat peut paraître surprenant, puisqu'on attendrait plutôt un effet déstabilisateur de POP2 à l'échelle du transcriptome (Gillen *et al.*, 2021). Cependant plusieurs articles ont déjà présentés des résultats similaires chez la drosophile (Zeng *et al.*, 2018; Haugen *et al.*, 2023), indiquant un rôle différentiel de POP2 selon ses cibles. Ici nous nous concentrons sur la portion de transcrits sur-exprimés en ARNi *Pop2*, ce qui correspond à l'effet observé pour *tim* (Figure 11 – panel gauche) et *vri* (Figure 17B). Lorsque l'on suit l'effet de POP2 sur ses cibles en fonction de leur abondance à l'échelle du transcriptome (Figure 19B), on remarque que les transcrits les moins abondants sont ceux présentant la plus forte régulation par POP2, à l'inverse les transcrits très abondants sont impactés moins fortement par POP2, indiquant qu'à l'échelle du transcriptome aussi, POP2 impacte ses cibles en fonction de leur abondance, suggérant bien un mécanisme de saturation de POP2.

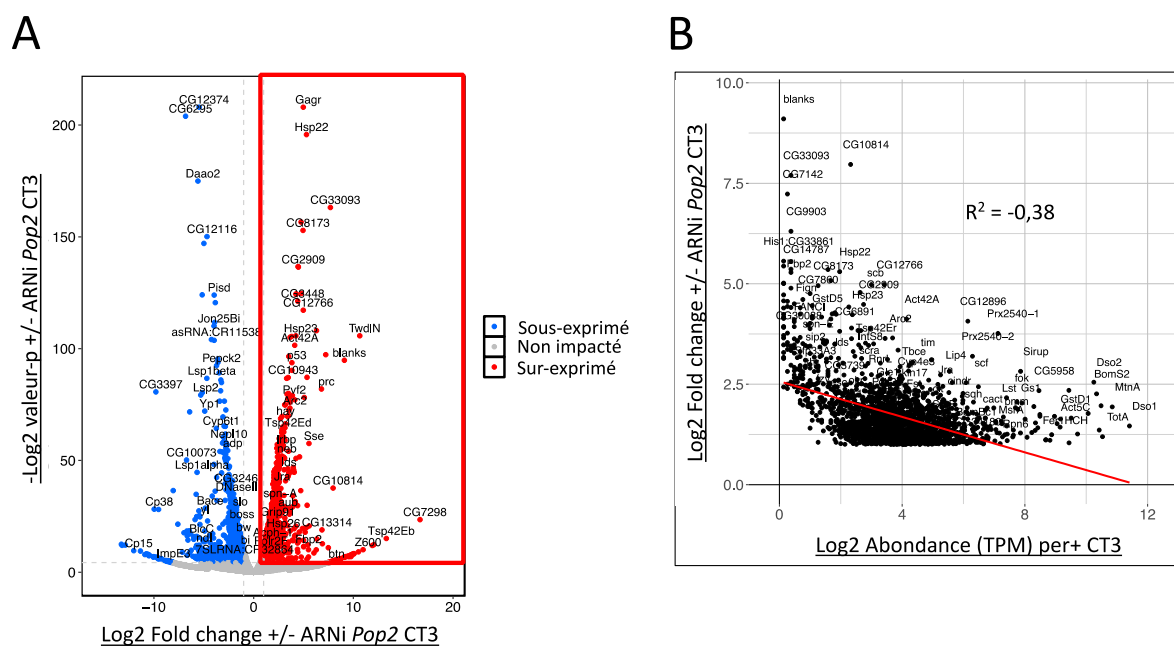


Figure 19 : (A) Volcano plot représentant les gènes significativement régulés par POP2 à CT3, avec les gènes sur-exprimés (rouge) ou sous-exprimés (bleu) en condition ARNi *Pop2*. (B) Les transcrits sur-exprimés en ARNi *Pop2* sont représentés avec leur abondance représentée en abscisse (en transcrits par million) et l'effet de l'ARNi *Pop2* en ordonnée, le tout à CT3. R^2 représentant le coefficient de corrélation de Spearman.

Nous avons ensuite cherché une propriété présente dans les séquences des transcrits qui pourrait expliquer la force de l'effet de POP2 sur ses cibles. L'usage des codons a précédemment été corrélé avec leur optimalité. En effet, certains codons vont correspondre à des ARN de transfert (ARNt) très abondants dans la cellule dans un contexte physiologique donné, ce qui est associé avec une traduction par les ribosomes sur les transcrits riches en ces codons (qu'on appelle optimaux) efficace, ce qui va résulter en une stabilisation de ce transcrit. À l'inverse, des transcrits riches en codons peu optimaux, c'est-à-dire dont les ARNts correspondants sont peu abondants dans la cellule, vont causer des ralentissements de l'élongation de la traduction par les ribosomes, ce qui peut induire le recrutement du complexe CCR4-NOT, qui va déadényler puis dégrader les ARNms en question (Buschauer *et al.*, 2020; Allen *et al.*, 2021 ; Allen *et al.*, 2023 ; revue dans Hanson et Coller 2021). Ainsi l'usage des codons a été montré comme corrélant avec l'effet du complexe CCR4-NOT sur la demi vie des transcrits chez l'Homme (Gillen *et al.*, 2021). De plus, on peut même suivre l'effet de CCR4-NOT sur ses cibles selon l'enrichissement des codons terminant en A/U ou en G/C dans la séquence codante des transcrits, ainsi, les transcrits riches en codons terminant en G/C sont plus déstabilisés par le complexe CCR4-NOT. Nous avons donc reproduit cette représentation sur nos données afin de voir si l'effet du POP2 pouvait aussi être expliqué en fonction de l'usage des codons (Figure 20A). De façon surprenante, nous trouvons un résultat inverse à celui de Gillen *et al.*, 2021. Où, sur notre jeu de données, les gènes les plus inhibés par POP2 sont ceux riches en codons terminant en A/U, montrant la dichotomie de l'optimalité des codons entre les modèles et les conditions physiologiques testées (Burrow *et al.*, 2018). Notre résultat est soutenu par le lien entre abondance d'un transcrit et usage des codons (Figure 20B). En effet, lorsque l'on suit l'effet de l'usage des codons et l'abondance des transcrits en condition contrôle *per+*, on voit que les transcrits riches en codons terminant en A/U sont ceux dont l'abondance est la plus faible en condition contrôle. Ainsi on voit que l'abondance et l'effet de POP2 corrélerent tout deux avec l'usage des codons. Donc, ces résultats suggèrent que les transcrits riches en codons terminant en A/U, qui pourraient donc être moins optimaux, semble causer le recrutement de POP2 afin de les dégrader, entraînant ainsi une diminution de leur abondance.

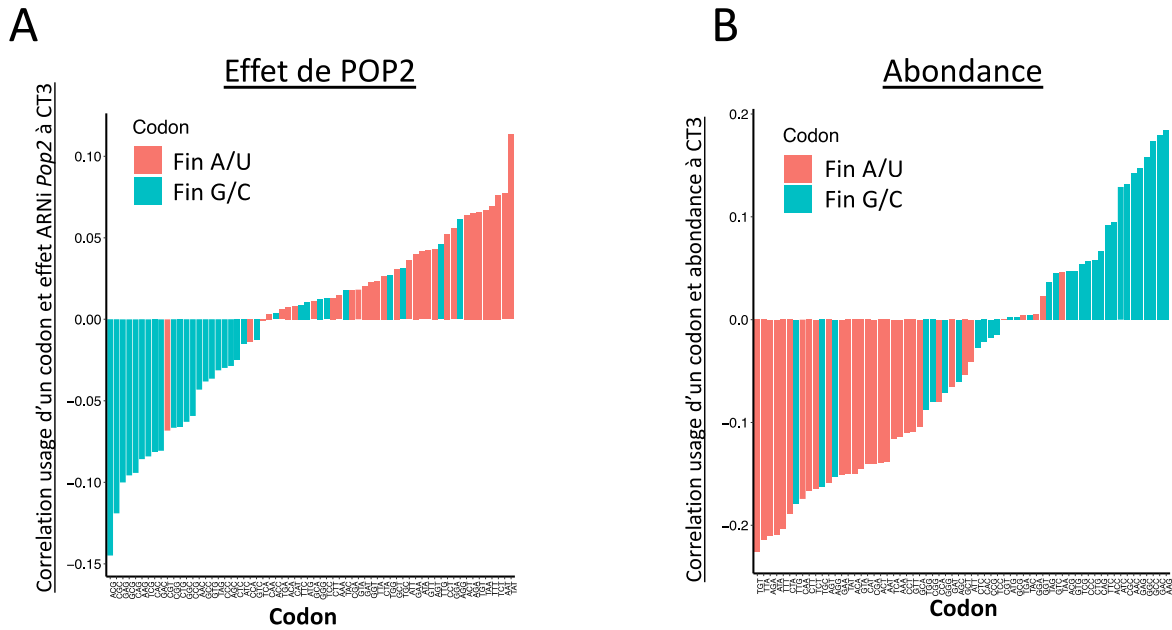


Figure 20 : (A) Corrélations pour chaque codon entre usage de ce codon et effet de l'ARNi Pop2 à CT3 pour les gènes sur-exprimés significativement par ARNi Pop2, les corrélations sont colorées en fonctions de la troisième base du codon. (B) Corrélations pour chaque codon entre usage de ce codon et abondance du transcrit en TPM à CT3 pour les gènes sur-exprimés significativement par ARNi Pop2.

Nous proposons donc un modèle (Figure 21), dans lequel les gènes cibles de POP2 (*tim* et *vri*) pourraient être ciblées par celui-ci en fonction de l'optimalité de leurs codons en tout temps, ce qui serait associé à une dégradation via POP2 stable, qui peut saturer en condition de transcription élevée (*per0*, *per+* la nuit subjective) et ne plus être visible en mesure relatives, bien que toujours présente.

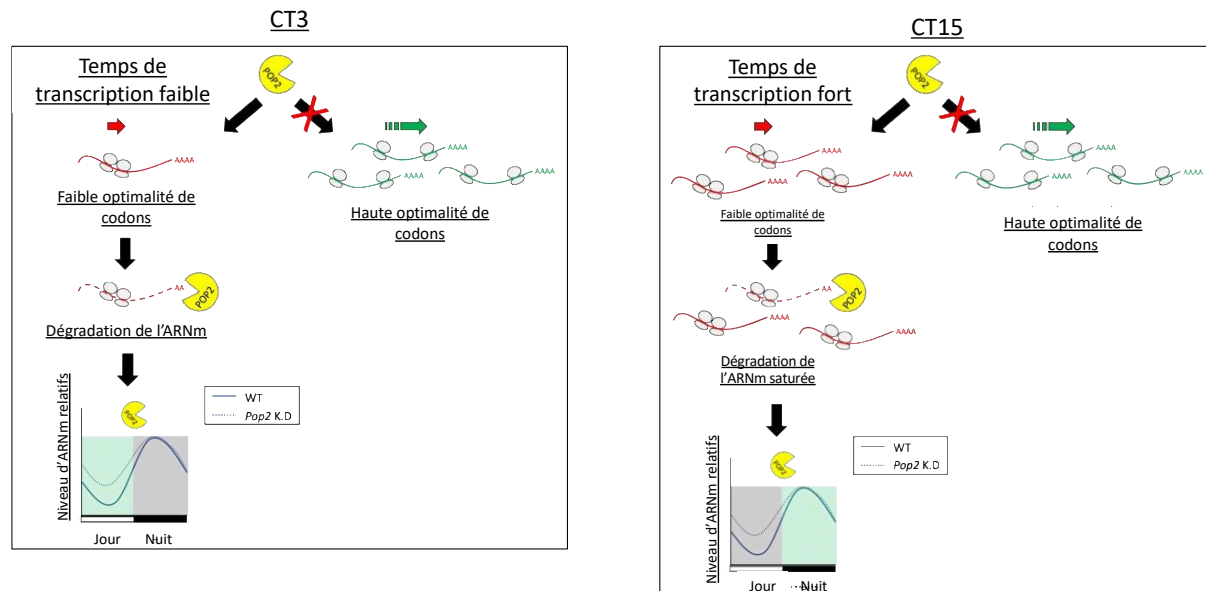


Figure 21 : Modèle intégrant les résultats obtenus en approches spécifiques et transcriptomiques. Aux temps de transcription faible (CT3), les ARNm riches en codons optimaux sont traduits normalement et stabilisés, à l'inverse, les ARNm riches en codons non optimaux (comme pourraient l'être *tim* ou *vri*) causent le ralentissement des ribosomes pendant la traduction, déclenchant le recrutement du complexe CCR4-NOT, qui va déadényler ces transcrits via POP2 et induire leur dégradation. La baisse de niveaux de transcrits étant très visible en mesures relatives de par l'effet de POP2 non saturé sur ses cibles peu abondantes. À l'inverse, au temps de transcription fort (CT15), les cibles étant

transcrites fortement à ces temps déclencheraient toujours le recrutement de CCR4-NOT qui, cette fois, présenterait une saturation de son activité, ne permettant pas de voir l'effet de celui-ci sur ses cibles très abondantes en mesure relatives.

Enfin, nous avons voulu vérifier l'effet de POP2 sur ses cibles présentant des régulations circadiennes significatives. Étant donné que celles-ci ne devraient pas présenter de changement de l'usage de leurs codons en fonction du temps (hormis en cas d'épissages alternatifs). On s'attend donc à isoler l'effet de POP2 sur ses cibles seulement en fonction des temps circadiens (Figure 22A). On découvre en effet que les gènes présentant un temps fort à CT3 vs CT15 voient leurs niveaux augmenter à CT3 grâce à POP2, puisque l'ARNi *Pop2* les diminue. À l'inverse, les transcrits présentant un temps faible à CT3 vs CT15 (comme *tim* et *vri*), sont quant à eux diminués par POP2 à CT3, puisque l'ARNi *Pop2* les augmente. On voit donc que POP2 joue un rôle différentiel dans l'oscillation de ses cibles (Figure 22B), en effet, POP2 va diminuer le temps minimum de certains gènes (comme *tim* et *vri*), dans le cas du « gene 1 », et à l'inverse va augmenter le maximum d'autres, dans le cas « gene 2 ». De plus, on retrouvait déjà cet effet différentiel de POP2 dans notre heatmap de séquençage ARN (Figure 15B). Où l'on peut voir pour le premier grand cluster, qu'en ARNi *Pop2*, les transcrits ne présentent aucun changement entre CT3 et CT15, néanmoins, en condition *per+* sans ARNi *Pop2*, on voit clairement une différence forte entre CT3 et CT15 avec un maximum à CT3. On voit donc non seulement que POP2 peut augmenter les amplitudes d'oscillations de certains gènes (Figure 22A), en augmentant leur maximum, diminuant leur minimum, ou même en créant de l'oscillation (Figure 15B), et ce, de façon spécifique des gènes ciblés (Figure 22B).

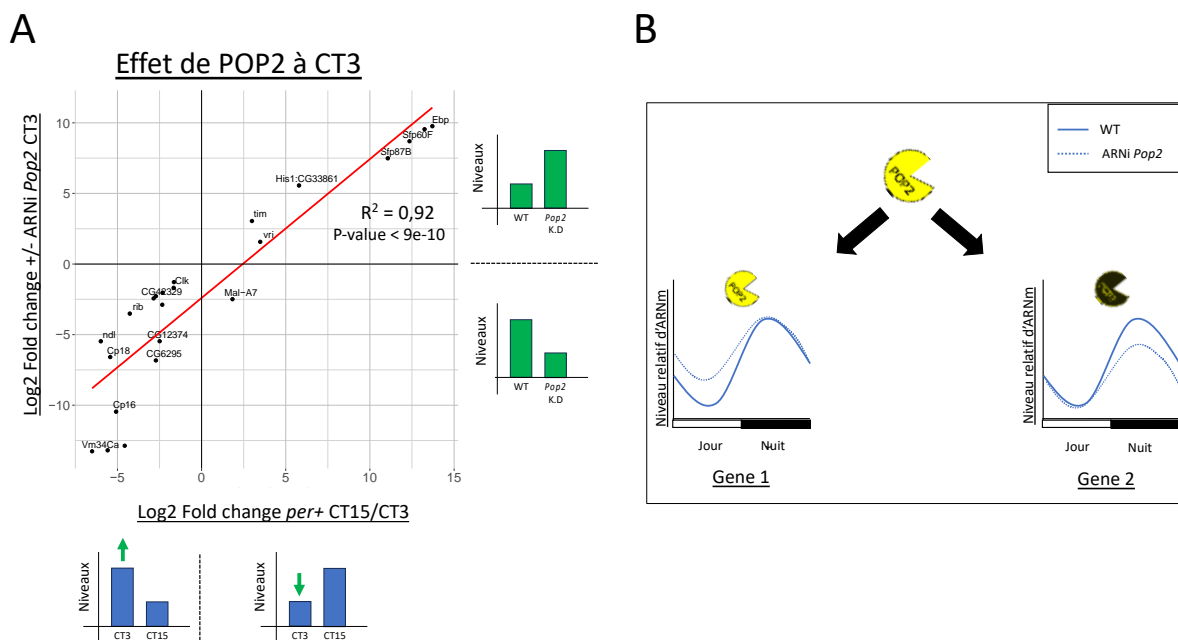


Figure 22 : (A) Les gènes présentant des changements significatifs entre CT3 et CT15 et entre +/- ARNi *Pop2* CT3 sont représentés et corrélés pour voir si les changements de niveaux circadiens sont liés à l'effet de POP2. (B) Modèle de l'action différentielle de POP2 selon sa cible régulée de façon circadienne.

III. Conclusions

Ici nous avons montré que les gènes d'horloge *tim*, *per*, et *vri* présentent des régulations de leur traduction, notamment de par l'oscillation de leur traductibilité détectée en TRAP. Ce contrôle traductionnel contribue probablement au décalage observé entre pics d'ARNms et protéines pour ces gènes et représente un nouveau niveau de régulation de l'oscillation des protéines TIM, PER et VRI, jusqu'à présent attribué principalement à des mécanismes post-traductionnels. Il serait intéressant de poursuivre ces investigations en effectuant des analyses de gradient de polysomes ou de ribosome profiling afin de déterminer si le nombre de ribosomes associés par molécule d'ARNm peut-elle aussi être sous contrôle circadien.

Nos résultats de séquençage nous ont permis de découvrir et caractériser *vri*, comme une nouvelle cible de POP2 impliquée dans l'horloge moléculaire. Ce qui indique un effet de POP2 sur plusieurs gènes circadiens, avec d'autres cibles potentiellement à caractériser dans le futur.

Nous avons découvert que l'effet circadien de POP2 sur *tim* et *vri* était en fait corrélé à l'abondance de ces transcrits, et non à la présence ou absence de PER, ou encore à une régulation circadienne de l'activité de POP2. Ce résultat indique que la saturation de l'activité des enzymes doit être considérée lors de l'étude de celles-ci et que l'abondance des transcrits étudiés est un facteur important à prendre en compte lors du suivi des régulations de ceux-ci en mesures relatives.

Nous avons aussi montré que POP2 inhibe la traductibilité de *tim* et de *vri*, mais pas de *per*, et ce, de façon indépendante de l'abondance de ceux-ci. Ce résultat pourrait être observé soit dans le cas d'un découplage des régulations de la traduction et la stabilisation des transcrits par POP2, comme déjà démontré par le passé (Gillen *et al.*, 2021). Ou par l'enrichissement d'une fraction des ARNms *tim* et *vri* liés aux ribosomes, permettant de mesurer l'effet de POP2, bien que saturé dans la fraction totale et dont les effets sont indétectables en mesures relatives en fraction totale mais deviennent mesurables dans la fraction liée aux ribosomes.

Nos résultats de séquençage ARN nous ont permis d'étudier l'action de POP2 à l'échelle du transcriptome. Où nous voyons que POP2 régule ses cibles en fonction de leur abondance, pour certaines d'entre elles, avec un effet plus fort sur les cibles peu abondantes. De plus, l'effet de POP2 corrèle très bien avec l'usage des codons des transcrits ciblés, avec un effet de POP2 plus fort sur les transcrits riches en codons terminant en A/U dans notre jeu de données, ces transcrits sont aussi retrouvés comme moins abondant en condition contrôle (et donc en présence POP2). Indiquant un rôle probable de l'optimalité des codons dans le recrutement de POP2 dans notre modèle d'étude.

Enfin, lors de l'étude de transcrits régulés de façon circadienne, et dont l'usage des codons est attendu stable d'un temps à l'autre, nous trouvons en effet de POP2 différent selon les cibles. En effet, certaines vont voir leur minimum diminuer par POP2, d'autre au contraire, voient leur maximum augmenter par celui-ci. Certains transcrits semblent même devoir leurs régulations circadiennes entièrement à POP2, ce qui place POP2 comme un élément capable d'amplifier et même de générer de l'oscillation chez les transcrits pendant les temps circadiens. Il serait à présent intéressant de suivre les dynamiques de traduction des transcrits à plusieurs temps circadiens en présence et en absence de POP2, afin de déterminer si POP2 contrôle ces oscillations post-transcriptionnellement, traductionnellement, ou les deux. De plus, l'étude du lien potentielle entre POP2 et résolution des pauses traductionnelles se révélerait intéressante, puisque déjà montré chez l'Homme (Gillen *et al.*, 2021) mais pas dans un contexte circadien, ce qui pourrait constituer un nouveau mécanisme de contrôle de l'expression des gènes oscillants au niveau de la traduction.

References

Abrahamson, E.E. and Moore, R.Y. (2001) 'Suprachiasmatic nucleus in the mouse: retinal innervation, intrinsic organization and efferent projections', *Brain Research*, 916(1–2), pp. 172–191. Available at: [https://doi.org/10.1016/S0006-8993\(01\)02890-6](https://doi.org/10.1016/S0006-8993(01)02890-6).

Allada, R. *et al.* (1998) 'A Mutant *Drosophila* Homolog of Mammalian Clock Disrupts Circadian Rhythms and Transcription of period and timeless', *Cell*, 93(5), pp. 791–804. Available at: [https://doi.org/10.1016/S0092-8674\(00\)81440-3](https://doi.org/10.1016/S0092-8674(00)81440-3).

Allen, G.E. *et al.* (2021) 'Not4 and Not5 modulate translation elongation by Rps7A ubiquitination, Rli1 moonlighting, and condensates that exclude eIF5A', *Cell Reports*, 36(9), p. 109633. Available at: <https://doi.org/10.1016/j.celrep.2021.109633>.

Arganda-Carreras, I. *et al.* (2017) 'Trainable Weka Segmentation: a machine learning tool for microscopy pixel classification', *Bioinformatics*. Edited by R. Murphy, 33(15), pp. 2424–2426. Available at: <https://doi.org/10.1093/bioinformatics/btx180>.

Bae, H. and Coller, J. (2022) 'Codon optimality-mediated mRNA degradation: Linking translational elongation to mRNA stability', *Molecular Cell*, 82(8), pp. 1467–1476. Available at: <https://doi.org/10.1016/j.molcel.2022.03.032>.

Barnes, J.W. *et al.* (2003) 'Requirement of Mammalian *Timeless* for Circadian Rhythmicity', *Science*, 302(5644), pp. 439–442. Available at: <https://doi.org/10.1126/science.1086593>.

Basquin, J. *et al.* (2012) 'Architecture of the Nuclease Module of the Yeast Ccr4-Not Complex: the Not1-Caf1-Ccr4 Interaction', *Molecular Cell*, 48(2), pp. 207–218. Available at: <https://doi.org/10.1016/j.molcel.2012.08.014>.

Baumgartner, R., Stocker, H. and Hafen, E. (2013) 'The RNA-binding Proteins FMR1, Rasputin and Caprin Act Together with the UBA Protein Lingerer to Restrict Tissue Growth in *Drosophila melanogaster*', *PLoS Genetics*. Edited by N. Tapon, 9(7), p. e1003598. Available at: <https://doi.org/10.1371/journal.pgen.1003598>.

Benna, C. *et al.* (2010) 'Drosophila timeless2 Is Required for Chromosome Stability and Circadian Photoreception', *Current Biology*, 20(4), pp. 346–352. Available at: <https://doi.org/10.1016/j.cub.2009.12.048>.

Bhaskar, V. *et al.* (2013) 'Structure and RNA-binding properties of the Not1–Not2–Not5 module of the yeast Ccr4–Not complex', *Nature Structural & Molecular Biology*, 20(11), pp. 1281–1288. Available at: <https://doi.org/10.1038/nsmb.2686>.

Blanchardon, E. *et al.* (2001) 'Defining the role of *Drosophila* lateral neurons in the control of circadian rhythms in motor activity and eclosion by targeted genetic ablation and PERIOD protein overexpression: Control of circadian rhythms in the *Drosophila* brain', *European Journal of Neuroscience*, 13(5), pp. 871–888. Available at: <https://doi.org/10.1046/j.0953-816x.2000.01450.x>.

Blau, J. and Young, M.W. (1999) 'Cycling vrilE Expression Is Required for a Functional *Drosophila* Clock', *Cell*, 99(6), pp. 661–671. Available at: [https://doi.org/10.1016/S0092-8674\(00\)81554-8](https://doi.org/10.1016/S0092-8674(00)81554-8).

Boothroyd, C.E. *et al.* (2007) 'Integration of Light and Temperature in the Regulation of Circadian Gene Expression in *Drosophila*', *PLoS Genetics*. Edited by G. Gibson, 3(4), p. e54. Available at: <https://doi.org/10.1371/journal.pgen.0030054>.

Brand, A.H. and Perrimon, N. (1993) 'Targeted gene expression as a means of altering cell fates and generating dominant phenotypes', *Development*, 118(2), pp. 401–415. Available at: <https://doi.org/10.1242/dev.118.2.401>.

Brenner, S., Jacob, F. and Meselson, M. (1961) 'An Unstable Intermediate Carrying Information from Genes to Ribosomes for Protein Synthesis', *Nature*, 190(4776), pp. 576–581. Available at: <https://doi.org/10.1038/190576a0>.

Buchan, J.R. (2014) 'mRNP granules: Assembly, function, and connections with disease', *RNA Biology*, 11(8), pp. 1019–1030. Available at: <https://doi.org/10.4161/15476286.2014.972208>.

Buschauer, R. *et al.* (2020) 'The Ccr4-Not complex monitors the translating ribosome for codon optimality', *Science (New York, N.Y.)*, 368(6488), p. eaay6912. Available at: <https://doi.org/10.1126/science.aay6912>.

Busza, A. *et al.* (2004) 'Roles of the Two *Drosophila* CRYPTOCHROME Structural Domains in Circadian Photoreception', *Science*, 304(5676), pp. 1503–1506. Available at: <https://doi.org/10.1126/science.1096973>.

Carrasco, J. *et al.* (2020) 'ELAV and FNE Determine Neuronal Transcript Signatures through EXon-Activated Rescue', *Molecular Cell*, 80(1), pp. 156–163.e6. Available at: <https://doi.org/10.1016/j.molcel.2020.09.011>.

Castelo-Szekely, V. *et al.* (2017) 'Translational contributions to tissue specificity in rhythmic and constitutive gene expression', *Genome Biology*, 18(1), p. 116. Available at: <https://doi.org/10.1186/s13059-017-1222-2>.

Chang, D.C. and Reppert, S.M. (2003) 'A Novel C-Terminal Domain of *Drosophila* PERIOD Inhibits dCLOCK:CYCLE-Mediated Transcription', *Current Biology*, 13(9), pp. 758–762. Available at: [https://doi.org/10.1016/S0960-9822\(03\)00286-0](https://doi.org/10.1016/S0960-9822(03)00286-0).

Chang, H. *et al.* (2014) 'TAIL-seq: Genome-wide Determination of Poly(A) Tail Length and 3' End Modifications', *Molecular Cell*, 53(6), pp. 1044–1052. Available at: <https://doi.org/10.1016/j.molcel.2014.02.007>.

Chapat, C. *et al.* (2017) 'Alternative splicing of CNOT7 diversifies CCR4–NOT functions', *Nucleic Acids Research*, 45(14), pp. 8508–8523. Available at: <https://doi.org/10.1093/nar/gkx506>.

Chekulaeva, M. *et al.* (2011) 'miRNA repression involves GW182-mediated recruitment of CCR4–NOT through conserved W-containing motifs', *Nature Structural & Molecular Biology*, 18(11), pp. 1218–1226. Available at: <https://doi.org/10.1038/nsmb.2166>.

Chen, C.-Y.A. and Shyu, A.-B. (2011) 'Mechanisms of deadenylation-dependent decay', *Wiley interdisciplinary reviews. RNA*, 2(2), pp. 167–183. Available at: <https://doi.org/10.1002/wrna.40>.

Chen, Y. *et al.* (2021) 'Crystal structure and functional properties of the human CCR4-CAF1 deadenylase complex', *Nucleic Acids Research*, 49(11), pp. 6489–6510. Available at: <https://doi.org/10.1093/nar/gkab414>.

Cheng, Y. and Hardin, P.E. (1998) '*Drosophila* Photoreceptors Contain an Autonomous Circadian Oscillator That Can Function without *period* mRNA Cycling', *The Journal of Neuroscience*, 18(2), pp. 741–750. Available at: <https://doi.org/10.1523/JNEUROSCI.18-02-00741.1998>.

Chiu, J.C. *et al.* (2010) 'Assaying Locomotor Activity to Study Circadian Rhythms and Sleep Parameters in *Drosophila*', *Journal of Visualized Experiments*, (43), p. 2157. Available at: <https://doi.org/10.3791/2157>.

Chiu, J.C., Ko, H.W. and Edery, I. (2011) 'NEMO/NLK Phosphorylates PERIOD to Initiate a Time-Delay Phosphorylation Circuit that Sets Circadian Clock Speed', *Cell*, 145(3), pp. 357–370. Available at: <https://doi.org/10.1016/j.cell.2011.04.002>.

Collart, M.A. (2016) 'The Ccr4-Not complex is a key regulator of eukaryotic gene expression', *WIREs RNA*, 7(4), pp. 438–454. Available at: <https://doi.org/10.1002/wrna.1332>.

Cooke, A., Prigge, A. and Wickens, M. (2010) 'Translational Repression by Deadenylation', *Journal of Biological Chemistry*, 285(37), pp. 28506–28513. Available at: <https://doi.org/10.1074/jbc.M110.150763>.

Crick, F. (1970) 'Central Dogma of Molecular Biology', *Nature*, 227(5258), pp. 561–563. Available at: <https://doi.org/10.1038/227561a0>.

Crick, F.H. (1958) 'On protein synthesis', *Symposia of the Society for Experimental Biology*, 12, pp. 138–163.

Curtin, K.D., Huang, Z.J. and Rosbash, M. (1995) 'Temporally regulated nuclear entry of the *Drosophila* period protein contributes to the circadian clock', *Neuron*, 14(2), pp. 365–372. Available at: [https://doi.org/10.1016/0896-6273\(95\)90292-9](https://doi.org/10.1016/0896-6273(95)90292-9).

Cyran, S.A. *et al.* (2003) 'vrille, Pdp1, and dClock Form a Second Feedback Loop in the *Drosophila* Circadian Clock', *Cell*, 112(3), pp. 329–341. Available at: [https://doi.org/10.1016/S0092-8674\(03\)00074-6](https://doi.org/10.1016/S0092-8674(03)00074-6).

Darlington, T.K. *et al.* (1998) 'Closing the Circadian Loop: CLOCK-Induced Transcription of Its Own Inhibitors *per* and *tim*', *Science*, 280(5369), pp. 1599–1603. Available at: <https://doi.org/10.1126/science.280.5369.1599>.

Deng, S. *et al.* (2022) 'RNA m6A regulates transcription via DNA demethylation and chromatin accessibility', *Nature Genetics*, 54(9), pp. 1427–1437. Available at: <https://doi.org/10.1038/s41588-022-01173-1>.

Du, H. *et al.* (2016) 'YTHDF2 destabilizes m6A-containing RNA through direct recruitment of the CCR4–NOT deadenylase complex', *Nature Communications*, 7(1), p. 12626. Available at: <https://doi.org/10.1038/ncomms12626>.

Dubowy, C. and Sehgal, A. (2017) 'Circadian Rhythms and Sleep in *Drosophila melanogaster*', *Genetics*, 205(4), pp. 1373–1397. Available at: <https://doi.org/10.1534/genetics.115.185157>.

Dufourt, J. *et al.* (2021) 'Imaging translation dynamics in live embryos reveals spatial heterogeneities', *Science*, 372(6544), pp. 840–844. Available at: <https://doi.org/10.1126/science.abc3483>.

Edery, I. (2000) 'Circadian rhythms in a nutshell', *Physiological Genomics*, 3(2), pp. 59–74. Available at: <https://doi.org/10.1152/physiolgenomics.2000.3.2.59>.

Emery, P. *et al.* (1998) 'CRY, a Drosophila Clock and Light-Regulated Cryptochrome, Is a Major Contributor to Circadian Rhythm Resetting and Photosensitivity', *Cell*, 95(5), pp. 669–679. Available at: [https://doi.org/10.1016/S0092-8674\(00\)81637-2](https://doi.org/10.1016/S0092-8674(00)81637-2).

Emery, P. *et al.* (2000) 'Drosophila CRY Is a Deep Brain Circadian Photoreceptor', *Neuron*, 26(2), pp. 493–504. Available at: [https://doi.org/10.1016/S0896-6273\(00\)81181-2](https://doi.org/10.1016/S0896-6273(00)81181-2).

Ewer, J. *et al.* (1992) 'Expression of the period clock gene within different cell types in the brain of Drosophila adults and mosaic analysis of these cells' influence on circadian behavioral rhythms', *The Journal of Neuroscience*, 12(9), pp. 3321–3349. Available at: <https://doi.org/10.1523/JNEUROSCI.12-09-03321.1992>.

Fabian, M.R. *et al.* (2011) 'miRNA-mediated deadenylation is orchestrated by GW182 through two conserved motifs that interact with CCR4–NOT', *Nature Structural & Molecular Biology*, 18(11), pp. 1211–1217. Available at: <https://doi.org/10.1038/nsmb.2149>.

Fang, Y., Sathyanarayanan, S. and Sehgal, A. (2007) 'Post-translational regulation of the *Drosophila* circadian clock requires protein phosphatase 1 (PP1)', *Genes & Development*, 21(12), pp. 1506–1518. Available at: <https://doi.org/10.1101/gad.1541607>.

Foley, L.E. *et al.* (2019) 'Drosophila PSI controls circadian period and the phase of circadian behavior under temperature cycle via tim splicing', *eLife*, 8, p. e50063. Available at: <https://doi.org/10.7554/eLife.50063>.

Formicola, N. *et al.* (2021) 'Tyramine induces dynamic RNP granule remodeling and translation activation in the Drosophila brain', *eLife*, 10, p. e65742. Available at: <https://doi.org/10.7554/eLife.65742>.

Fu, J. *et al.* (2016) 'Codon usage affects the structure and function of the *Drosophila* circadian clock protein PERIOD', *Genes & Development*, 30(15), pp. 1761–1775. Available at: <https://doi.org/10.1101/gad.281030.116>.

Furuichi, Y. (2015) 'Discovery of m⁷G-cap in eukaryotic mRNAs', *Proceedings of the Japan Academy, Series B*, 91(8), pp. 394–409. Available at: <https://doi.org/10.2183/pjab.91.394>.

Gekakis, N. *et al.* (1995) 'Isolation of *timeless* by PER Protein Interaction: Defective Interaction Between *timeless* Protein and Long-Period Mutant PER^L', *Science*, 270(5237), pp. 811–815. Available at: <https://doi.org/10.1126/science.270.5237.811>.

Gekakis, N. *et al.* (1998) 'Role of the CLOCK protein in the mammalian circadian mechanism', *Science (New York, N.Y.)*, 280(5369), pp. 1564–1569. Available at: <https://doi.org/10.1126/science.280.5369.1564>.

Gilbert, W.V., Bell, T.A. and Schaening, C. (2016) 'Messenger RNA modifications: Form, distribution, and function', *Science*, 352(6292), pp. 1408–1412. Available at: <https://doi.org/10.1126/science.aad8711>.

Gillen, S.L. *et al.* (2021) 'Differential regulation of mRNA fate by the human Ccr4-Not complex is driven by coding sequence composition and mRNA localization', *Genome Biology*, 22(1), p. 284. Available at: <https://doi.org/10.1186/s13059-021-02494-w>.

Glossop, N.R.J. *et al.* (2003) 'VRILLE Feeds Back to Control Circadian Transcription of Clock in the Drosophila Circadian Oscillator', *Neuron*, 37(2), pp. 249–261. Available at: [https://doi.org/10.1016/S0896-6273\(03\)00002-3](https://doi.org/10.1016/S0896-6273(03)00002-3).

Goldbeter, A. (1995) 'A model for circadian oscillations in the *Drosophila* period protein (PER)', *Proceedings of the Royal Society of London. Series B: Biological Sciences*, 261(1362), pp. 319–324. Available at: <https://doi.org/10.1098/rspb.1995.0153>.

Graveley, B.R. *et al.* (2011) 'The developmental transcriptome of *Drosophila melanogaster*', *Nature*, 471(7339), pp. 473–479. Available at: <https://doi.org/10.1038/nature09715>.

Grima, B. *et al.* (2002) 'The F-box protein Slimb controls the levels of clock proteins Period and Timeless', *Nature*, 420(6912), pp. 178–182. Available at: <https://doi.org/10.1038/nature01122>.

Grima, B. *et al.* (2004) 'Morning and evening peaks of activity rely on different clock neurons of the *Drosophila* brain', *Nature*, 431(7010), pp. 869–873. Available at: <https://doi.org/10.1038/nature02935>.

Grima, B. *et al.* (2012) 'CULLIN-3 Controls TIMELESS Oscillations in the *Drosophila* Circadian Clock', *PLOS Biology*, 10(8), p. e1001367. Available at: <https://doi.org/10.1371/journal.pbio.1001367>.

Grima, B. *et al.* (2019) 'PERIOD-controlled deadenylation of the timeless transcript in the *Drosophila* circadian clock', *Proceedings of the National Academy of Sciences*, 116(12), pp. 5721–5726. Available at: <https://doi.org/10.1073/pnas.1814418116>.

Gros, F. *et al.* (1961) 'Unstable Ribonucleic Acid Revealed by Pulse Labelling of *Escherichia Coli*', *Nature*, 190(4776), pp. 581–585. Available at: <https://doi.org/10.1038/190581a0>.

Gunawardhana, K.L. and Hardin, P.E. (2017) 'VRILLE Controls PDF Neuropeptide Accumulation and Arborization Rhythms in Small Ventrolateral Neurons to Drive

Rhythmic Behavior in *Drosophila*', *Current Biology*, 27(22), pp. 3442–3453.e4. Available at: <https://doi.org/10.1016/j.cub.2017.10.010>.

Guo, F. *et al.* (2014) 'PDF neuron firing phase-shifts key circadian activity neurons in *Drosophila*', *eLife*, 3, p. e02780. Available at: <https://doi.org/10.7554/eLife.02780>.

Gupta, S. *et al.* (2007) 'Quantifying similarity between motifs', *Genome Biology*, 8(2), p. R24. Available at: <https://doi.org/10.1186/gb-2007-8-2-r24>.

Haberle, V. and Stark, A. (2018) 'Eukaryotic core promoters and the functional basis of transcription initiation', *Nature Reviews Molecular Cell Biology*, 19(10), pp. 621–637. Available at: <https://doi.org/10.1038/s41580-018-0028-8>.

Hales, K.G. *et al.* (2015) 'Genetics on the Fly: A Primer on the *Drosophila* Model System', *Genetics*, 201(3), pp. 815–842. Available at: <https://doi.org/10.1534/genetics.115.183392>.

Handler, A.M. and Konopka, R.J. (1979) 'Transplantation of a circadian pacemaker in *Drosophila*', *Nature*, 279(5710), pp. 236–238. Available at: <https://doi.org/10.1038/279236a0>.

Hara, T. *et al.* (2011) 'Post-Translational Regulation and Nuclear Entry of TIMELESS and PERIOD Are Affected in New timeless Mutant', *Journal of Neuroscience*, 31(27), pp. 9982–9990. Available at: <https://doi.org/10.1523/JNEUROSCI.0993-11.2011>.

Hardin, P.E. (2011) 'Molecular Genetic Analysis of Circadian Timekeeping in *Drosophila*', in *Advances in Genetics*. Elsevier, pp. 141–173. Available at: <https://doi.org/10.1016/B978-0-12-387690-4.00005-2>.

Haugen, R.J. *et al.* (2023) *Regulation of the Drosophila transcriptome by Pumilio and CCR4-NOT deadenylase*. preprint. Molecular Biology. Available at: <https://doi.org/10.1101/2023.08.29.555372>.

Hellen, C.U.T. (2018) 'Translation Termination and Ribosome Recycling in Eukaryotes', *Cold Spring Harbor Perspectives in Biology*, 10(10), p. a032656. Available at: <https://doi.org/10.1101/cshperspect.a032656>.

Huang, Y. *et al.* (2013) 'Translational Profiling of Clock Cells Reveals Circadianly Synchronized Protein Synthesis', *PLOS Biology*, 11(11), p. e1001703. Available at: <https://doi.org/10.1371/journal.pbio.1001703>.

Hughes, M.E. *et al.* (2012) 'Deep sequencing the circadian and diurnal transcriptome of *Drosophila* brain', *Genome Research*, 22(7), pp. 1266–1281. Available at: <https://doi.org/10.1101/gr.128876.111>.

Hunter-Ensor, M., Ousley, A. and Sehgal, A. (1996a) 'Regulation of the *Drosophila* Protein Timeless Suggests a Mechanism for Resetting the Circadian Clock by Light', *Cell*, 84(5), pp. 677–685. Available at: [https://doi.org/10.1016/S0092-8674\(00\)81046-6](https://doi.org/10.1016/S0092-8674(00)81046-6).

Hunter-Ensor, M., Ousley, A. and Sehgal, A. (1996b) 'Regulation of the *Drosophila* Protein Timeless Suggests a Mechanism for Resetting the Circadian Clock by Light', *Cell*, 84(5), pp. 677–685. Available at: [https://doi.org/10.1016/S0092-8674\(00\)81046-6](https://doi.org/10.1016/S0092-8674(00)81046-6).

Jang, C. *et al.* (2015) 'Ribosome profiling reveals an important role for translational control in circadian gene expression', *Genome Research*, 25(12), pp. 1836–1847. Available at: <https://doi.org/10.1101/gr.191296.115>.

Jeske, M. *et al.* (2006) 'Rapid ATP-dependent Deadenylation of nanos mRNA in a Cell-free System from *Drosophila* Embryos', *Journal of Biological Chemistry*, 281(35), pp. 25124–25133. Available at: <https://doi.org/10.1074/jbc.M604802200>.

Joly, W. *et al.* (2013) 'The CCR4 Deadenylation Acts with Nanos and Pumilio in the Fine-Tuning of Mei-P26 Expression to Promote Germline Stem Cell Self-Renewal', *Stem Cell Reports*, 1(5), pp. 411–424. Available at: <https://doi.org/10.1016/j.stemcr.2013.09.007>.

Juge, F. *et al.* (2002) 'Control of poly(A) polymerase level is essential to cytoplasmic polyadenylation and early development in *Drosophila*', *The EMBO journal*, 21(23), pp. 6603–6613. Available at: <https://doi.org/10.1093/emboj/cdf633>.

Kan, L. *et al.* (2021) 'A neural m6A/Ythdf pathway is required for learning and memory in *Drosophila*', *Nature Communications*, 12(1), p. 1458. Available at: <https://doi.org/10.1038/s41467-021-21537-1>.

Kane, N.S. *et al.* (2017) 'Efficient Screening of CRISPR/Cas9-Induced Events in *Drosophila* Using a Co-CRISPR Strategy', *Genes|Genomes|Genetics*, 7(1), pp. 87–93. Available at: <https://doi.org/10.1534/g3.116.036723>.

Kaneko, M. (1998) 'Neural substrates of *Drosophila* rhythms revealed by mutants and molecular manipulations', *Current Opinion in Neurobiology*, 8(5), pp. 652–658. Available at: [https://doi.org/10.1016/S0959-4388\(98\)80095-0](https://doi.org/10.1016/S0959-4388(98)80095-0).

Kaufman, T.C. (2017) 'A Short History and Description of *Drosophila melanogaster* Classical Genetics: Chromosome Aberrations, Forward Genetic Screens, and the Nature of Mutations', *Genetics*, 206(2), pp. 665–689. Available at: <https://doi.org/10.1534/genetics.117.199950>.

Kedersha, N. *et al.* (2005) 'Stress granules and processing bodies are dynamically linked sites of mRNP remodeling', *The Journal of Cell Biology*, 169(6), pp. 871–884. Available at: <https://doi.org/10.1083/jcb.200502088>.

- Kiebler, M.A. and Bassell, G.J. (2006) 'Neuronal RNA Granules: Movers and Makers', *Neuron*, 51(6), pp. 685–690. Available at: <https://doi.org/10.1016/j.neuron.2006.08.021>.
- Kim, E.Y. *et al.* (2007) 'A DOUBLETIME Kinase Binding Domain on the *Drosophila* PERIOD Protein Is Essential for Its Hyperphosphorylation, Transcriptional Repression, and Circadian Clock Function', *Molecular and Cellular Biology*, 27(13), pp. 5014–5028. Available at: <https://doi.org/10.1128/MCB.02339-06>.
- Kim, E.Y. *et al.* (2012) 'A role for O -GlcNAcylation in setting circadian clock speed', *Genes & Development*, 26(5), pp. 490–502. Available at: <https://doi.org/10.1101/gad.182378.111>.
- Kim, T.H. *et al.* (2019) 'Phospho-dependent phase separation of FMRP and CAPRIN1 recapitulates regulation of translation and deadenylation', *Science*, 365(6455), pp. 825–829. Available at: <https://doi.org/10.1126/science.aax4240>.
- Kimura, S. *et al.* (2015) 'The *Drosophila* lingerer protein cooperates with Orb2 in long-term memory formation', *Journal of Neurogenetics*, 29(1), pp. 8–17. Available at: <https://doi.org/10.3109/01677063.2014.917644>.
- Kinoshita, E. *et al.* (2006) 'Phosphate-binding Tag, a New Tool to Visualize Phosphorylated Proteins', *Molecular & Cellular Proteomics*, 5(4), pp. 749–757. Available at: <https://doi.org/10.1074/mcp.T500024-MCP200>.
- Kloss, B. *et al.* (1998) 'The *Drosophila* Clock Gene double-time Encodes a Protein Closely Related to Human Casein Kinase I ϵ ', *Cell*, 94(1), pp. 97–107. Available at: [https://doi.org/10.1016/S0092-8674\(00\)81225-8](https://doi.org/10.1016/S0092-8674(00)81225-8).
- Knowles, T.P.J. *et al.* (2009) 'An Analytical Solution to the Kinetics of Breakable Filament Assembly', *Science*, 326(5959), pp. 1533–1537. Available at: <https://doi.org/10.1126/science.1178250>.
- Koh, K., Zheng, X. and Sehgal, A. (2006) 'JETLAG Resets the *Drosophila* Circadian Clock by Promoting Light-Induced Degradation of TIMELESS', *Science*, 312(5781), pp. 1809–1812. Available at: <https://doi.org/10.1126/science.1124951>.
- Kojima, S., Sher-Chen, E.L. and Green, C.B. (2012) 'Circadian control of mRNA polyadenylation dynamics regulates rhythmic protein expression', *Genes & Development*, 26(24), pp. 2724–2736. Available at: <https://doi.org/10.1101/gad.208306.112>.
- Komar, A.A., Lesnik, T. and Reiss, C. (1999) 'Synonymous codon substitutions affect ribosome traffic and protein folding during in vitro translation', *FEBS letters*, 462(3), pp. 387–391. Available at: [https://doi.org/10.1016/s0014-5793\(99\)01566-5](https://doi.org/10.1016/s0014-5793(99)01566-5).

Konopka, R., Wells, S. and Lee, T. (1983) 'Mosaic analysis of a *Drosophila* clock mutant', *Molecular and General Genetics MGG*, 190(2), pp. 284–288. Available at: <https://doi.org/10.1007/BF00330652>.

Krause, S.A. *et al.* (2022) 'FlyAtlas 2 in 2022: enhancements to the *Drosophila melanogaster* expression atlas', *Nucleic Acids Research*, 50(D1), pp. D1010–D1015. Available at: <https://doi.org/10.1093/nar/gkab971>.

Kume, K. *et al.* (1999) 'mCRY1 and mCRY2 Are Essential Components of the Negative Limb of the Circadian Clock Feedback Loop', *Cell*, 98(2), pp. 193–205. Available at: [https://doi.org/10.1016/S0092-8674\(00\)81014-4](https://doi.org/10.1016/S0092-8674(00)81014-4).

Lamaze, A. *et al.* (2022) 'A natural timeless polymorphism allowing circadian clock synchronization in "white nights"', *Nature Communications*, 13(1), p. 1724. Available at: <https://doi.org/10.1038/s41467-022-29293-6>.

Larkin, A. *et al.* (2021) 'FlyBase: updates to the *Drosophila melanogaster* knowledge base', *Nucleic Acids Research*, 49(D1), pp. D899–D907. Available at: <https://doi.org/10.1093/nar/gkaa1026>.

Lee, C. *et al.* (1996) 'Resetting the *Drosophila* Clock by Photic Regulation of PER and a PER-TIM Complex', *Science*, 271(5256), pp. 1740–1744. Available at: <https://doi.org/10.1126/science.271.5256.1740>.

Lee, H. *et al.* (2009) 'Essential roles of CK1 δ and CK1 ϵ in the mammalian circadian clock', *Proceedings of the National Academy of Sciences*, 106(50), pp. 21359–21364. Available at: <https://doi.org/10.1073/pnas.0906651106>.

Lee, J. *et al.* (2017) 'LSM12 and ME31B/DDX6 Define Distinct Modes of Posttranscriptional Regulation by ATAXIN-2 Protein Complex in *Drosophila* Circadian Pacemaker Neurons', *Molecular Cell*, 66(1), pp. 129–140.e7. Available at: <https://doi.org/10.1016/j.molcel.2017.03.004>.

Li, Y. and Kiledjian, M. (2010) 'Regulation of mRNA decapping', *WIREs RNA*, 1(2), pp. 253–265. Available at: <https://doi.org/10.1002/wrna.15>.

Li, Y.H. *et al.* (2019) 'O-GlcNAcylation of PERIOD regulates its interaction with CLOCK and timing of circadian transcriptional repression', *PLOS Genetics*. Edited by P.H. Taghert, 15(1), p. e1007953. Available at: <https://doi.org/10.1371/journal.pgen.1007953>.

Lim, C. *et al.* (2011) 'The novel gene twenty-four defines a critical translational step in the *Drosophila* clock', *Nature*, 470(7334), pp. 399–403. Available at: <https://doi.org/10.1038/nature09728>.

Lim, C. and Allada, R. (2013) 'ATAXIN-2 Activates PERIOD Translation to Sustain Circadian Rhythms in *Drosophila*', *Science*, 340(6134), pp. 875–879. Available at: <https://doi.org/10.1126/science.1234785>.

Lim, J. *et al.* (2016) 'mTAIL-seq reveals dynamic poly(A) tail regulation in oocyte-to-embryo development', *Genes & Development*, 30(14), pp. 1671–1682. Available at: <https://doi.org/10.1101/gad.284802.116>.

Lima, S.A. *et al.* (2017) 'Short poly(A) tails are a conserved feature of highly expressed genes', *Nature Structural & Molecular Biology*, 24(12), pp. 1057–1063. Available at: <https://doi.org/10.1038/nsmb.3499>.

Lin, Y., Stormo, G.D. and Taghert, P.H. (2004) 'The Neuropeptide Pigment-Dispersing Factor Coordinates Pacemaker Interactions in the *Drosophila* Circadian System', *The Journal of Neuroscience*, 24(36), pp. 7951–7957. Available at: <https://doi.org/10.1523/JNEUROSCI.2370-04.2004>.

Litovchenko, M. *et al.* (2021) 'Extensive tissue-specific expression variation and novel regulators underlying circadian behavior', *Science Advances*, 7(5), p. eabc3781. Available at: <https://doi.org/10.1126/sciadv.abc3781>.

Liu, J. *et al.* (2020) ' N^6 -methyladenosine of chromosome-associated regulatory RNA regulates chromatin state and transcription', *Science*, 367(6477), pp. 580–586. Available at: <https://doi.org/10.1126/science.aay6018>.

Ma, D. and Rosbash, M. (2020a) 'A transcriptomic taxonomy of *Drosophila* circadian neurons around the clock'.

Ma, D. and Rosbash, M. (2020b) 'A transcriptomic taxonomy of *Drosophila* circadian neurons around the clock'.

Mao, Y. *et al.* (2013) 'Potential cancer-related role of circadian gene TIMELESS suggested by expression profiling and in vitro analyses', *BMC Cancer*, 13(1), p. 498. Available at: <https://doi.org/10.1186/1471-2407-13-498>.

Marrus, S.B., Zeng, H. and Rosbash, M. (1996) 'Effect of constant light and circadian entrainment of *perS* flies: evidence for light-mediated delay of the negative feedback loop in *Drosophila*', *The EMBO journal*, 15(24), pp. 6877–6886.

Martin Anduaga, A. *et al.* (2019) 'Thermosensitive alternative splicing senses and mediates temperature adaptation in *Drosophila*', *eLife*, 8, p. e44642. Available at: <https://doi.org/10.7554/eLife.44642>.

Martinek, S. *et al.* (2001) 'A Role for the Segment Polarity Gene shaggy/GSK-3 in the *Drosophila* Circadian Clock', *Cell*, 105(6), pp. 769–779. Available at: [https://doi.org/10.1016/S0092-8674\(01\)00383-X](https://doi.org/10.1016/S0092-8674(01)00383-X).

Mendoza-Viveros, L. *et al.* (2017) 'Molecular modulators of the circadian clock: lessons from flies and mice', *Cellular and Molecular Life Sciences*, 74(6), pp. 1035–1059. Available at: <https://doi.org/10.1007/s00018-016-2378-8>.

Meyer, P., Saez, L. and Young, M.W. (2006) 'PER-TIM Interactions in Living *Drosophila* Cells: An Interval Timer for the Circadian Clock', *Science*, 311(5758), pp. 226–229. Available at: <https://doi.org/10.1126/science.1118126>.

Mohawk, J.A., Green, C.B. and Takahashi, J.S. (2012) 'Central and Peripheral Circadian Clocks in Mammals', *Annual Review of Neuroscience*, 35(1), pp. 445–462. Available at: <https://doi.org/10.1146/annurev-neuro-060909-153128>.

Monaghan, L., Longman, D. and Cáceres, J.F. (2023) 'Translation-coupled mRNA quality control mechanisms', *The EMBO Journal*, 42(19), p. e114378. Available at: <https://doi.org/10.15252/emj.2023114378>.

Morgan, T.H. (1910) 'Sex Limited Inheritance in *Drosophila*', *Science*, 32(812), pp. 120–122. Available at: <https://doi.org/10.1126/science.32.812.120>.

Muraro, N.I. and Fernanda Ceriani, M. (2014) 'Circadian rhythms', in J. Dubnau (ed.) *Behavioral Genetics of the Fly (Drosophila Melanogaster)*. Cambridge University Press, pp. 104–115. Available at: <https://doi.org/10.1017/CBO9780511920585.009>.

Myers, M.P. *et al.* (1996) 'Light-Induced Degradation of TIMELESS and Entrainment of the *Drosophila* Circadian Clock', *Science*, 271(5256), pp. 1736–1740. Available at: <https://doi.org/10.1126/science.271.5256.1736>.

Naidoo, N. *et al.* (1999) 'A Role for the Proteasome in the Light Response of the Timeless Clock Protein', *Science*, 285(5434), pp. 1737–1741. Available at: <https://doi.org/10.1126/science.285.5434.1737>.

Nakajima, M. *et al.* (2005) 'Reconstitution of Circadian Oscillation of Cyanobacterial KaiC Phosphorylation in Vitro', *Science*, 308(5720), pp. 414–415. Available at: <https://doi.org/10.1126/science.1108451>.

Nawathean, P. and Rosbash, M. (2004) 'The Doubletime and CKII Kinases Collaborate to Potentiate *Drosophila* PER Transcriptional Repressor Activity', *Molecular Cell*, 13(2), pp. 213–223. Available at: [https://doi.org/10.1016/S1097-2765\(03\)00503-3](https://doi.org/10.1016/S1097-2765(03)00503-3).

Noda, M. *et al.* (2019) 'Role of Per3, a circadian clock gene, in embryonic development of mouse cerebral cortex', *Scientific Reports*, 9(1), p. 5874. Available at: <https://doi.org/10.1038/s41598-019-42390-9>.

O'Neill, J.S. and Reddy, A.B. (2011) 'Circadian clocks in human red blood cells', *Nature*, 469(7331), pp. 498–503. Available at: <https://doi.org/10.1038/nature09702>.

Panasenko, O.O. *et al.* (2019) 'Co-translational assembly of proteasome subunits in NOT1-containing assemblysomes', *Nature Structural & Molecular Biology*, 26(2), pp. 110–120. Available at: <https://doi.org/10.1038/s41594-018-0179-5>.

Park, J.-E. *et al.* (2016) 'Regulation of Poly(A) Tail and Translation during the Somatic Cell Cycle', *Molecular Cell*, 62(3), pp. 462–471. Available at: <https://doi.org/10.1016/j.molcel.2016.04.007>.

Patil, D.P. *et al.* (2016) 'm6A RNA methylation promotes XIST-mediated transcriptional repression', *Nature*, 537(7620), pp. 369–373. Available at: <https://doi.org/10.1038/nature19342>.

Peschel, N. *et al.* (2009) 'Light-Dependent Interactions between the Drosophila Circadian Clock Factors Cryptochrome, Jetlag, and Timeless', *Current Biology*, 19(3), pp. 241–247. Available at: <https://doi.org/10.1016/j.cub.2008.12.042>.

Peschel, N., Veleri, S. and Stanewsky, R. (2006) 'Veela defines a molecular link between Cryptochrome and Timeless in the light-input pathway to *Drosophila*'s circadian clock', *Proceedings of the National Academy of Sciences*, 103(46), pp. 17313–17318. Available at: <https://doi.org/10.1073/pnas.0606675103>.

Pichon, X. *et al.* (2016) 'Visualization of single endogenous polysomes reveals the dynamics of translation in live human cells', *Journal of Cell Biology*, 214(6), pp. 769–781. Available at: <https://doi.org/10.1083/jcb.201605024>.

Pittendrigh, C.S. (1954) 'ON TEMPERATURE INDEPENDENCE IN THE CLOCK SYSTEM CONTROLLING EMERGENCE TIME IN DROSOPHILA', *Proceedings of the National Academy of Sciences*, 40(10), pp. 1018–1029. Available at: <https://doi.org/10.1073/pnas.40.10.1018>.

Pittendrigh, C.S. and Daan, S. (1974) 'Circadian Oscillations in Rodents: A Systematic Increase of Their Frequency with Age', *Science*, 186(4163), pp. 548–550. Available at: <https://doi.org/10.1126/science.186.4163.548>.

Presnyak, V. *et al.* (2015) 'Codon Optimality Is a Major Determinant of mRNA Stability', *Cell*, 160(6), pp. 1111–1124. Available at: <https://doi.org/10.1016/j.cell.2015.02.029>.

Price, J.L. *et al.* (1995) 'Suppression of PERIOD protein abundance and circadian cycling by the Drosophila clock mutation timeless.', *The EMBO Journal*, 14(16), pp. 4044–4049. Available at: <https://doi.org/10.1002/j.1460-2075.1995.tb00075.x>.

Price, J.L. *et al.* (1998) 'double-time Is a Novel Drosophila Clock Gene that Regulates PERIOD Protein Accumulation', *Cell*, 94(1), pp. 83–95. Available at: [https://doi.org/10.1016/S0092-8674\(00\)81224-6](https://doi.org/10.1016/S0092-8674(00)81224-6).

- Raisch, T. *et al.* (2019) 'Reconstitution of recombinant human CCR4-NOT reveals molecular insights into regulated deadenylation', *Nature Communications*, 10(1), p. 3173. Available at: <https://doi.org/10.1038/s41467-019-11094-z>.
- Raisch, T. and Valkov, E. (2022) 'Regulation of the multisubunit CCR4-NOT deadenylase in the initiation of mRNA degradation', *Current Opinion in Structural Biology*, 77, p. 102460. Available at: <https://doi.org/10.1016/j.sbi.2022.102460>.
- Reddy, A.B. *et al.* (2006) 'Circadian Orchestration of the Hepatic Proteome', *Current Biology*, 16(11), pp. 1107–1115. Available at: <https://doi.org/10.1016/j.cub.2006.04.026>.
- Reinhard, N. *et al.* (2022) 'The Neuronal Circuit of the Dorsal Circadian Clock Neurons in *Drosophila melanogaster*', *Frontiers in Physiology*, 13, p. 886432. Available at: <https://doi.org/10.3389/fphys.2022.886432>.
- Reiter, L.T. *et al.* (2001) 'A Systematic Analysis of Human Disease-Associated Gene Sequences In *Drosophila melanogaster*', *Genome Research*, 11(6), pp. 1114–1125. Available at: <https://doi.org/10.1101/gr.169101>.
- Rodriguez, J. *et al.* (2013) 'Nascent-Seq analysis of *Drosophila* cycling gene expression', *Proceedings of the National Academy of Sciences*, 110(4), pp. E275–E284. Available at: <https://doi.org/10.1073/pnas.1219969110>.
- Rodríguez-Molina, J.B., West, S. and Passmore, L.A. (2023) 'Knowing when to stop: Transcription termination on protein-coding genes by eukaryotic RNAPII', *Molecular Cell*, 83(3), pp. 404–415. Available at: <https://doi.org/10.1016/j.molcel.2022.12.021>.
- Roote, J. and Prokop, A. (2013) 'How to Design a Genetic Mating Scheme: A Basic Training Package for *Drosophila* Genetics'. Available at: <http://g3journal.org/lookup/doi/10.1534/g3.112.004820> (Accessed: 13 August 2020).
- Rothenfluh, A., Young, M.W. and Saez, L. (2000) 'A TIMELESS-Independent Function for PERIOD Proteins in the *Drosophila* Clock', *Neuron*, 26(2), pp. 505–514. Available at: [https://doi.org/10.1016/S0896-6273\(00\)81182-4](https://doi.org/10.1016/S0896-6273(00)81182-4).
- Rouyer, F. (2013) 'Circadian Timing', in C.G. Galizia and P.-M. Lledo (eds) *Neurosciences - From Molecule to Behavior: a university textbook*. Berlin, Heidelberg: Springer Berlin Heidelberg, pp. 609–627. Available at: https://doi.org/10.1007/978-3-642-10769-6_27.
- Saez, L. and Young, M.W. (1996) 'Regulation of Nuclear Entry of the *Drosophila* Clock Proteins Period and Timeless', *Neuron*, 17(5), pp. 911–920. Available at: [https://doi.org/10.1016/S0896-6273\(00\)80222-6](https://doi.org/10.1016/S0896-6273(00)80222-6).
- Sanchez, R. and Grau, R. (2005) 'A NOVEL ALGEBRAIC STRUCTURE OF THE GENETIC CODE OVER THE GALOIS FIELD OF FOUR DNA BASES', *R. SA* [Preprint].

Sandrelli, F. *et al.* (2007) 'A Molecular Basis for Natural Selection at the *timeless* Locus in *Drosophila melanogaster*', *Science*, 316(5833), pp. 1898–1900. Available at: <https://doi.org/10.1126/science.1138426>.

Sathyanarayanan, S. *et al.* (2004) 'Posttranslational Regulation of Drosophila PERIOD Protein by Protein Phosphatase 2A', *Cell*, 116(4), pp. 603–615. Available at: [https://doi.org/10.1016/S0092-8674\(04\)00128-X](https://doi.org/10.1016/S0092-8674(04)00128-X).

Schäfer, I.B. *et al.* (2019) 'Molecular Basis for poly(A) RNP Architecture and Recognition by the Pan2-Pan3 Deadenylase', *Cell*, 177(6), pp. 1619–1631.e21. Available at: <https://doi.org/10.1016/j.cell.2019.04.013>.

Sehgal, A. *et al.* (1995) 'Rhythmic Expression of timeless: A Basis for Promoting Circadian Cycles in period Gene Autoregulation', *Science*, 270(5237), pp. 808–810. Available at: <https://doi.org/10.1126/science.270.5237.808>.

Shafer, O.T. *et al.* (2022) 'Connectomic analysis of the Drosophila lateral neuron clock cells reveals the synaptic basis of functional pacemaker classes', *eLife*, 11, p. e79139. Available at: <https://doi.org/10.7554/eLife.79139>.

Shakhmantsir, I. *et al.* (2018) 'Spliceosome factors target timeless (tim) mRNA to control clock protein accumulation and circadian behavior in Drosophila', *eLife*, 7, p. e39821. Available at: <https://doi.org/10.7554/eLife.39821>.

Shearman, L.P. *et al.* (2000) 'Targeted Disruption of the *mPer3* Gene: Subtle Effects on Circadian Clock Function', *Molecular and Cellular Biology*, 20(17), pp. 6269–6275. Available at: <https://doi.org/10.1128/MCB.20.17.6269-6275.2000>.

Sheth, U. and Parker, R. (2003) 'Decapping and Decay of Messenger RNA Occur in Cytoplasmic Processing Bodies', *Science*, 300(5620), pp. 805–808. Available at: <https://doi.org/10.1126/science.1082320>.

Shirokikh, N.E. and Preiss, T. (2018) 'Translation initiation by cap-dependent ribosome recruitment: Recent insights and open questions', *Wiley interdisciplinary reviews. RNA*, 9(4), p. e1473. Available at: <https://doi.org/10.1002/wrna.1473>.

So, W.V. (1997) 'Post-transcriptional regulation contributes to Drosophila clock gene mRNA cycling', *The EMBO Journal*, 16(23), pp. 7146–7155. Available at: <https://doi.org/10.1093/emboj/16.23.7146>.

Stanewsky, R. *et al.* (1998) 'The cryb Mutation Identifies Cryptochrome as a Circadian Photoreceptor in Drosophila', *Cell*, 95(5), pp. 681–692. Available at: [https://doi.org/10.1016/S0092-8674\(00\)81638-4](https://doi.org/10.1016/S0092-8674(00)81638-4).

Stoleru, D. *et al.* (2004) 'Coupled oscillators control morning and evening locomotor behaviour of *Drosophila*', *Nature*, 431(7010), pp. 862–868. Available at: <https://doi.org/10.1038/nature02926>.

Subtelny, A.O. *et al.* (2014) 'Poly(A)-tail profiling reveals an embryonic switch in translational control', *Nature*, 508(7494), pp. 66–71. Available at: <https://doi.org/10.1038/nature13007>.

Suri, V., Hall, J.C. and Rosbash, M. (2000) 'Two Novel *doubletime* Mutants Alter Circadian Properties and Eliminate the Delay between RNA and Protein in *Drosophila*', *The Journal of Neuroscience*, 20(20), pp. 7547–7555. Available at: <https://doi.org/10.1523/JNEUROSCI.20-20-07547.2000>.

Szklarczyk, D. *et al.* (2023) 'The STRING database in 2023: protein–protein association networks and functional enrichment analyses for any sequenced genome of interest', *Nucleic Acids Research*, 51(D1), pp. D638–D646. Available at: <https://doi.org/10.1093/nar/gkac1000>.

Tauber, E. *et al.* (2007) 'Natural Selection Favors a Newly Derived *timeless* Allele in *Drosophila melanogaster*', *Science*, 316(5833), pp. 1895–1898. Available at: <https://doi.org/10.1126/science.1138412>.

Temme, C. *et al.* (2004) 'A complex containing the CCR4 and CAF1 proteins is involved in mRNA deadenylation in *Drosophila*', *The EMBO Journal*, 23(14), pp. 2862–2871. Available at: <https://doi.org/10.1038/sj.emboj.7600273>.

Temme, C. *et al.* (2010) 'Subunits of the *Drosophila* CCR4-NOT complex and their roles in mRNA deadenylation', *RNA*, 16(7), pp. 1356–1370. Available at: <https://doi.org/10.1261/rna.2145110>.

Top, D. *et al.* (2016) 'GSK-3 and CK2 Kinases Converge on Timeless to Regulate the Master Clock', *Cell Reports*, 16(2), pp. 357–367. Available at: <https://doi.org/10.1016/j.celrep.2016.06.005>.

Uchida, N., Hoshino, S. and Katada, T. (2004) 'Identification of a Human Cytoplasmic Poly(A) Nuclease Complex Stimulated by Poly(A)-binding Protein', *Journal of Biological Chemistry*, 279(2), pp. 1383–1391. Available at: <https://doi.org/10.1074/jbc.M309125200>.

Van Etten, J. *et al.* (2012) 'Human Pumilio Proteins Recruit Multiple Deadenylases to Efficiently Repress Messenger RNAs', *Journal of Biological Chemistry*, 287(43), pp. 36370–36383. Available at: <https://doi.org/10.1074/jbc.M112.373522>.

Wang, Q. *et al.* (2018) 'Striking circadian neuron diversity and cycling of *Drosophila* alternative splicing', *eLife*, 7, p. e35618. Available at: <https://doi.org/10.7554/eLife.35618>.

Webster, M.W. *et al.* (2018) 'mRNA Deadenylation Is Coupled to Translation Rates by the Differential Activities of Ccr4-Not Nucleases', *Molecular Cell*, 70(6), pp. 1089-1100.e8. Available at: <https://doi.org/10.1016/j.molcel.2018.05.033>.

Wheeler, D.A. *et al.* (1993) 'Behavior in Light-Dark Cycles of *Drosophila* Mutants That Are Arrhythmic, Blind, or Both', *Journal of Biological Rhythms*, 8(1), pp. 67–94. Available at: <https://doi.org/10.1177/074873049300800106>.

Will, C.L. and Luhrmann, R. (2011) 'Spliceosome Structure and Function', *Cold Spring Harbor Perspectives in Biology*, 3(7), pp. a003707–a003707. Available at: <https://doi.org/10.1101/cshperspect.a003707>.

Wippich, F. and Ephrussi, A. (2019) 'Transcript specific mRNP capture from *Drosophila* egg-chambers for proteomic analysis', *Methods* [Preprint]. Available at: <https://doi.org/10.1016/j.ymeth.2019.09.001>.

Wu, Q. and Bazzini, A.A. (2023) 'Translation and mRNA Stability Control', *Annual Review of Biochemistry*, 92(1), pp. 227–245. Available at: <https://doi.org/10.1146/annurev-biochem-052621-091808>.

Yang, Z. and Sehgal, A. (2001) 'Role of Molecular Oscillations in Generating Behavioral Rhythms in *Drosophila*', *Neuron*, 29(2), pp. 453–467. Available at: [https://doi.org/10.1016/S0896-6273\(01\)00218-5](https://doi.org/10.1016/S0896-6273(01)00218-5).

Yi, H. *et al.* (2018) 'PABP Cooperates with the CCR4-NOT Complex to Promote mRNA Deadenylation and Block Precocious Decay', *Molecular Cell*, 70(6), pp. 1081-1088.e5. Available at: <https://doi.org/10.1016/j.molcel.2018.05.009>.

Yoo, S.-H. *et al.* (2005) 'A noncanonical E-box enhancer drives mouse Period2 circadian oscillations in vivo', *Proceedings of the National Academy of Sciences of the United States of America*, 102(7), pp. 2608–2613. Available at: <https://doi.org/10.1073/pnas.0409763102>.

Yoshida, K. *et al.* (2013) 'TIMELESS is overexpressed in lung cancer and its expression correlates with poor patient survival', *Cancer Science*, 104(2), pp. 171–177. Available at: <https://doi.org/10.1111/cas.12068>.

You, S. *et al.* (2021) 'Circadian regulation of the *Drosophila* astrocyte transcriptome', *PLOS Genetics*. Edited by J. Ewer, 17(9), p. e1009790. Available at: <https://doi.org/10.1371/journal.pgen.1009790>.

Yu, A.D. and Rosbash, M. (2023) 'Butt-seq: a new method for facile profiling of transcription', *Genes & Development*, p. genesdev;gad.350434.123v1. Available at: <https://doi.org/10.1101/gad.350434.123>.

Yu, W. *et al.* (2009) 'DOUBLETIME Plays a Noncatalytic Role To Mediate CLOCK Phosphorylation and Repress CLOCK-Dependent Transcription within the Drosophila Circadian Clock', *Molecular and Cellular Biology*, 29(6), pp. 1452–1458. Available at: <https://doi.org/10.1128/MCB.01777-08>.

Zeng, H. *et al.* (1996) 'A light-entrainment mechanism for the Drosophila circadian clock', *Nature*, 380(6570), pp. 129–135. Available at: <https://doi.org/10.1038/380129a0>.

Zeng, J. *et al.* (2018) 'The Drosophila CCR4-NOT complex is required for cholesterol homeostasis and steroid hormone synthesis', *Developmental Biology*, 443(1), pp. 10–18. Available at: <https://doi.org/10.1016/j.ydbio.2018.08.012>.

Zhang, Y. *et al.* (2013) 'A Role for Drosophila ATX2 in Activation of PER Translation and Circadian Behavior', *Science*, 340(6134), pp. 879–882. Available at: <https://doi.org/10.1126/science.1234746>.

Zheng, B. *et al.* (2001) 'Nonredundant Roles of the mPer1 and mPer2 Genes in the Mammalian Circadian Clock', *Cell*, 105(5), pp. 683–694. Available at: [https://doi.org/10.1016/S0092-8674\(01\)00380-4](https://doi.org/10.1016/S0092-8674(01)00380-4).

Zonato, V. *et al.* (2018) 'Inverse European Latitudinal Cline at the *timeless* Locus of *Drosophila melanogaster* Reveals Selection on a Clock Gene: Population Genetics of *Is-tim*', *Journal of Biological Rhythms*, 33(1), pp. 15–23. Available at: <https://doi.org/10.1177/0748730417742309>.